Predicting the Mechanical Properties of Animal Glue Thin Films

W. de Zeeuw

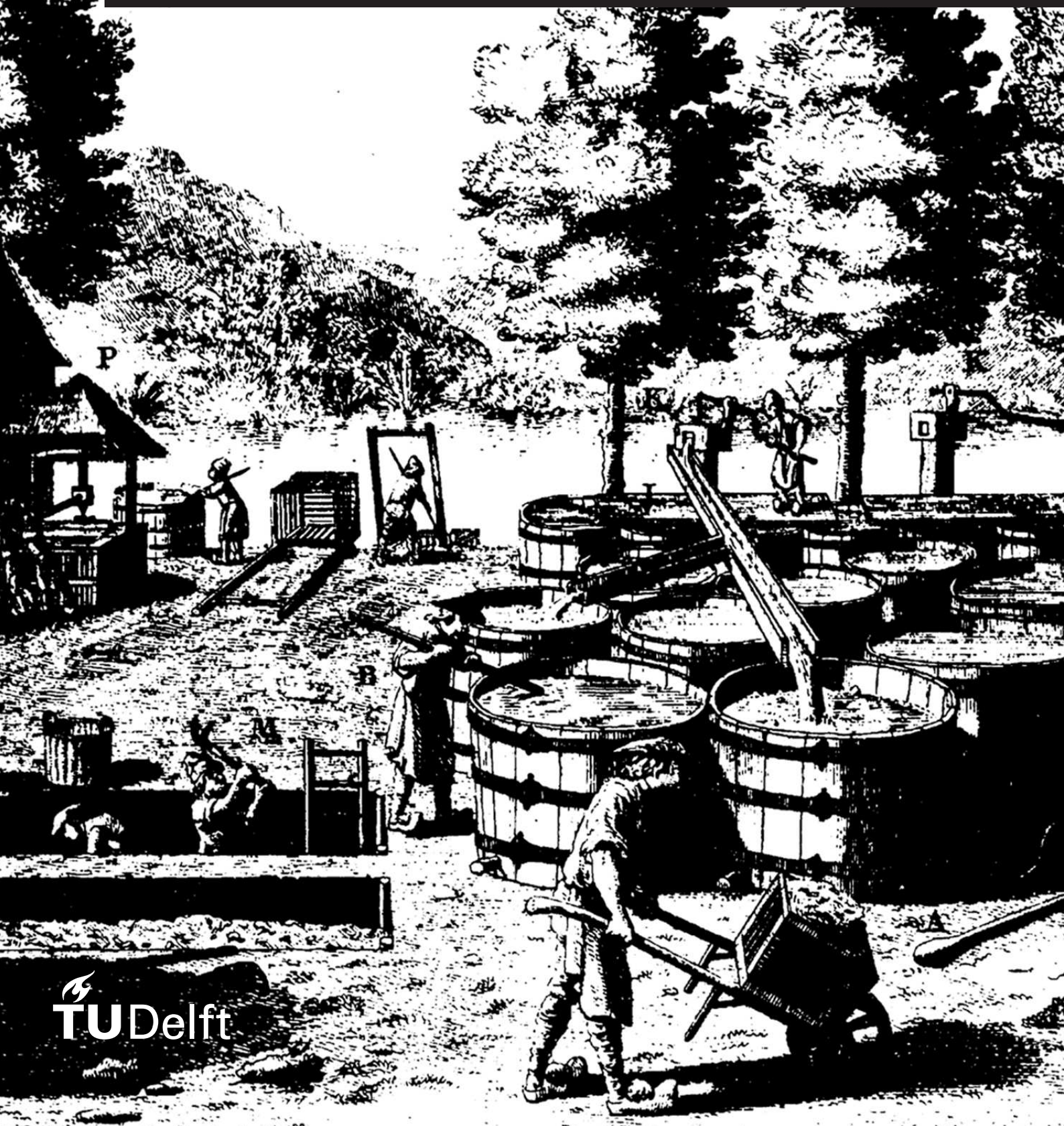

TU Delft

MASTER THESIS

Predicting the Mechanical Properties of Animal Glue Thin Films

by

W. de Zeeuw

to obtain the degree of Master of Science in Aerospace Engineering
at the Delft University of Technology,
to be defended publicly on Tuesday September 26, 2017 at 09:00 AM.

Student number:	4221230	
Project duration:	December 5, 2016 – September 26, 2017	
Thesis committee:	Dr. R. M. Groves,	TU Delft, chair
	Dr. J. A. Poulis,	TU Delft
	Dr. J. C. Bijleveld,	TU Delft
	P. van Duin,	Rijksmuseum Amsterdam

An electronic version of this thesis is available at `http://repository.tudelft.nl/`.
Cover image taken from [23]

TU Delft

Preface

This thesis was made as the final assignment in completing my MSc degree in Aerospace Engineering at the TU Delft. I am grateful for the many exiting opportunities this thesis offered me. Not the least among those opportunities was the possibility to do my internship at the furniture conservation department of the Rijksmuseum Amsterdam.

Many people have contributed in their own way to the work presented in this thesis. First of all, I would like to thank my supervisors, Hans Poulis and Johan Bijleveld, for their constructive feedback and invaluable guidance. A special word of thanks is due to Paul van Duin, head of furniture conservation at the Rijksmuseum and supervisor of my internship, for the help he has given and the many surprising things he showed me about art and art conservation.

I would also like to thank Iskander Breebaart, Jan Dorscheid, and Davina Kuh Jakobi, conservators at the furniture conservation department, for all the help they have offered each and every time I ran into new challenges; you have been wonderful colleagues. Many thanks are due to the DASML technicians, for their help in carrying out all the experiments.

Another word of appreciation is due to Ton Dirks and Wil Dankers for inviting me to Trobas Gelatine B.V. and providing me with all the information and sample material I needed.

Finally I would like to thank my family and friends for supporting me during this period and providing their honest feedback.

W. de Zeeuw
Delft, September 2017

Summary

In recent years, climate change has become an increasingly important topic in the world of art conservation. In order to reduce the carbon footprint of musea, one promising approach would be to lower the extend of climate control. However, to convince the conservation community that risks associated to such an approach are acceptable, more needs to be known about the behaviour of art exposed to climate fluctuations.

An earlier research program, Climate for Wood, found that in wooden panels, climate fluctuations generally lead to glue joint failure. The glue joints under consideration were all animal glue joints. So in order to really understand the behaviour of wooden panels exposed to climate fluctuations it is important to investigate the properties of animal glue itself. Unfortunately, not a lot of research has been done regarding the mechanical characteristics of pure animal glue.

Therefore this thesis aims to investigate (1) the mechanical characteristics of a pure animal glue film without additives and (2) how the quality of this film can be predicted using non-destructive or micro-destructive techniques.

Samples of animal glue were made by casting dilute animal glue solutions on flat moulds. Five types of glue were used, and out of each glue four sample series were made. Each sample series was characterised by ten tensile tests, and at least one analysis by each of the three selected film quality assessment techniques.

The chosen quality assessment techniques were Differential Scanning Calorimetry (DSC), Fourier Transform Infrared Spectroscopy (FTIR), and X-Ray Diffraction (XRD). These were chosen as they measure the amount of renaturation in the animal glue. Renaturation is the process of the animal glue proteins partially regaining the structure they had in the native collagen they were derived from. Additionally, creep tests and polarised light experiments were conducted. The latter was used to investigate internal stresses resulting from the casting process.

The experimental results showed that the maximum tensile strength is linearly related to the bloom strength. As the renaturation level of the glue is linearly related to the bloom strength too, this leads to the conclusion that the maximum tensile strength is linearly related to the renaturation level of the animal glue. Besides that, it was shown that the E-modulus is constant with bloom strength, provided that the animal glue is in the glassy state.

From the three investigated analysis techniques, only XRD proved to give a reliable measure of the mechanical properties, though it is believed that DSC would be able to do even better once small improvements are made to the set-up. This is due to the fact that the DSC curves showed an event related to internal stresses, which cannot be measured by XRD.

Contents

Glossary

Term	Description
AG	Atelier Gebouw
AMW	Average Molecular Weight
ATR	Attenuated Total Reflectance
C4W	Climate for Wood
DMA	Dynamic Mechanical Analysis
DSC	Differential Scanning Calorimetry
FTIR	Fourier Transform Infra-red Spectroscopy
Gly	Glycine
Hyp	Hydroxiproline
IEP	Iso-Electric Point
MWD	Molecular Weight Distribution
Pro	Proline
RCE	Rijksdienst Cultureel Erfgoed
Repeatability	The degree of agreement between two measurements when repeated using the same equipment, working at the same location, etc.
Reproducibility	The degree of agreement between two measurements when repeated using different equipment, working at a different location, etc.
RH	Relative Humidity
RH/T-Logger	Relative Humidity/Temperature-Logger
RMA	Rijksmuseum Amsterdam
TGA	Thermogravimetric Analysis
UATR	Universal Attenuated Total Reflectance
XRD	X-ray Diffraction

List of Symbols

Symbol	Description	Units
ΔH_m	Denaturation enthalpy	J
E	Young's modulus of elasticity	GPa
$\epsilon_{F\max}$	Strain at maximum force	%
$F_{\max}$	Maximum force	N
K_{vq}	Factor of Visual Quality	-
M	Mass	kg
R_{break}	Breaking factor	N/mm
ρ	Density	mg/mm^3
$\sigma_{\max}$	Maximum strength	MPa
t_{avg}	Average thickness	mm
T_g	Glass transition temperature	K
T_m	Melt temperature	K
V	Volume	mm^3

List of Figures

List of Tables

Chapter 1

Introduction

This chapter introduces the background of the research in section 1.1. The research questions are presented in Section 1.2. Finally, Section 1.3 shows a short overview of the structure of the report.

1.1 Background of the Research Question

Climate change and art conservation, two topics not generally associated by most people, show a worrying relation. As climate change progresses, the weather will show more and larger fluctuations and thus indoor climates of musea will experience more and larger fluctuations too. As the museum indoor climate is usually required to be as stable as possible, this will require increasingly extensive climate control, which will come at the price of increasing energy consumption. However, to stop climate change, energy consumption should decrease rather than increase. This negative relation emphasises the need to reduce the museums' energy consumption.

One promising approach would be to allow more variation of the indoor climate, which would lead to less energy intensive climate conditioning. However, the conservation community fears that such a policy would damage irreplaceable works of art. In order to be able to weigh the risks, research into the effects of such a policy should be conducted.

The Climate for Wood (C4W)-project therefore addressed the effect of climate fluctuations on wooden panels, as used in cabinet doors and in paintings. One of the preliminary findings was that climate induced damage mostly appears as failure of glue joints [15].

This result indicated the necessity of studying the behaviour of animal glues as a function of climatic fluctuations, as these glue joints were made using animal glue. However, as the baseline behaviour of animal glues is not yet fully characterised, this should be addressed first.

1.2 Research Questions

The aim of this thesis is to present the results of the thesis-project that was carried out at the Faculty of Aerospace Engineering of the TU Delft, in collaboration with the Rijksmuseum Amsterdam. The thesis project addressed the following research questions:

What are (1) the mechanical characteristics (e.g. maximum strength and E-modulus) of a pure animal glue film without additives and (2) how can the quality of this film be predicted using non-destructive or micro-destructive techniques.

This research question on the one hand defines the properties of pristine animal glue. This will be important to study the influence of additives in further research. On the other hand, additional techniques are used to evaluate the quality of the animal glue film, mostly related to homogeneity and reproducibility of the film, in order to get a measure of the properties of a film without carrying out a destructive test. This is important in research that requires identical samples at the start of a test or experiment.

1.3 Report Overview

This report starts with an overview of the history of animal glues in Chapter 2 embedding the thesis in its context of art conservation. The material research context is explained by a literature review in Chapter 3. An account of the used materials and processes can be found in Chapter 4, while the methodology is explained in Chapter 5. Sample Production is the topic of Chapter 6. Chapter 7 covers the results of the tensile tests, followed by the Chapters 8, and 9 on the results of film quality assessment using Differential Scanning Calorimetry (DSC), and X-ray Diffraction (XRD) respectively. Chapter 10 discusses the creep tests, Fourier Transform Infra-red Spectroscopy (FTIR) analyses and polarised light experiments. The connection between aforementioned techniques and the tensile tests is analysed in Chapter 11. Finally, the conclusions and recommendations are dealt with in Chapter 12 and Chapter 13.

Chapter 2

The History of Animal Glues

As explained in the introduction, Chapter 1, this research is embedded in the larger effort of understanding the influence of indoor climate fluctuations on works of art and their preservation. This chapter aims to connect the worlds of art conservation and material research by showing how a simple product as animal glue has a rich history spanning millennia, and how a thorough understanding of its history influences the choice of materials described in later chapters. Sections 2.1 through 2.3 will split this long history in several eras of interest, ranging from medieval to modern times. Section 2.4 discusses a final aspect of historical animal glue production, while Section 2.5 discusses the relevance of this chapter as a part of the larger thesis work.

2.1 Medieval Age

The sources from medieval times are not the first to mention animal glue. Older accounts can be found from Grecian and Roman authors, while the oldest known account of animal glue is a painting in an Egyptian tomb dating back to 1500 B.C. [8, 17, 27].

The best known sources from the Middle Ages are *Schedula Diversarum Artium* and *Il Libro dell'Arte*. The first is written by a German monk, Theophilus Presbyter, living around the 10^{th} or 12^{th} century [8, 17, 26]. The latter is written at the end of the 14^{th} or the beginning of the 15^{th} century by Cennino Cennini [7]. Both mention glues made from animal hides, but also glues made from parchment scrapings and clippings. It appears that the glue production at that time was a small scale activity carried out mostly by the user himself.

However, it should be noted that serious doubts exist with respect to the authenticity of the recipes and information described in these medieval handbooks. Only one aspect of which is that the authors may have had no experience at all with the processes described.

2.2 The 18^{th} and 19^{th} Century

In 1694, the first known picture of a glue manufacturing site was made [8, 17]. This first glue factory was situated in the Netherlands, but by the year 1771 the industry was present in various countries, including France, where its practices were recorded in the book *L'Art de Faire Différentes Sortes de Colles*, written by M. Duhamel du Monceau. This book was published by l'Académie Royale des Sciences and can be regarded as the first peer reviewed account of the animal glue industry [23].

The most important information in this book is that 'strong glue' or 'English glue', which is used by cabinet makers, can vary in composition. It can be made from horse, sheep, and ox hide, or from hare, rabbit, and beaver hide. It seems that these glues are more or less equivalent to modern day hide and rabbit glues.

That this 'strong glue' was the main furniture makers glue is confirmed by other authors from that period such as Diderot and Dawidosky [9, 21].

Another important observation is that Duhamel mentions bone glue production as a new procedure. His choice of words seems to indicate that this glue was not yet used on large scale, but that people were improving the procedure to make it [23]. This would be in line with sources that mention that bone glue was taken into use around 1814 [6] or even later [32].

2.3 Modern Times

From approximately 1900 onwards, books and articles describing animal glue production are readily available (e.g. [17, 27]). However, this literature describes the late industrial animal glue production. As, after the second world war, animal glue became increasingly obsolete, sources later then 1990 mostly describe how animal glue was produced in the past. Consequently a lot of information is lost about specific applications of certain glues.

This loss is for example visible by the fact that these modern sources talk about animal glue mostly as a single product, while Cennini mentions a goat hide glue [7], Presbyter writes about hide glue mixed with antler [26], Duhamel describes English glue, Flanders glue, glove glue etcetera [23].

Besides the mentioned loss of variety in types of glue, also a gap exist in our knowledge of possible additives that were used in the past.

2.4 Final Remarks on Historic Glues

One final element should be added to this discussion, which is the pretreatment of the tissue that provides the collagen. Duhamel describes that the hides were pretreated with lime water, which is an alkali [23]. The medieval sources do not mention any conditioning, but as their source material was mostly parchment or leather, their material would have had a treatment with lime water too. Today, alkali pretreatment is the less used process, most gelatin is of the acid pretreated type.

2.5 Relevance of the History of Animal Glues

The goal of this chapter was to elucidate the relation between art conservation and material research. It was shown that animal glues have a rich tradition which was mostly lost following the rise of synthetic glues. This tradition covers such areas as production techniques, raw material selection, additive utilisation and so forth.

In short, the loss of information described in Section 2.3 shows that modelling glues used in old works of art faces a serious limitation regarding the representativeness of a selected glue for the range of glues used in pre-modern times. This implies that whether a modern glue is used or an old recipe is carried out, a careful and well argued choice should be made.

Chapter 3

Literature Review

This chapter focusses on the state of the art in the mechanical characterisation of animal glue. First of all a description of animal glue and its production is given in Sections 3.1 and 3.2. Following that, an overview is given of the parameters that are known to influence the mechanical properties of gelatin in Section 3.3. Finally, Section 3.4 addresses which techniques can be used to evaluate the quality of a gelatin film.

3.1 The Working Principle of Animal Glue

Figure 3.1: Schematic showing how three alpha chains combine into one large triple-helix. Adapted from [3].

Animal glue can be described as an impure form of gelatin. Were food grade gelatin is a very pure protein, animal glue generally contains more impurities such as ashes, fats and other compounds that result from the production process. Though these impurities can be used to change the properties of the animal glue, the working principle of the animal glue depends upon the gelatin protein. Consequently, gelatin and animal glue will be used mostly as interchangeable terms in this thesis.

Gelatin is the product of the hydrolysis of collagen. Figure 3.1 shows a basic building block of collagen, the triple-helix. As can be seen, three so called alpha-chains combine into a larger structure. These alpha-chains are polypeptides weighing approximately $100,000$ u [30]. The figure clearly shows that each of these alpha chains forms a left handed helix itself. These left handed helices are the secondary structure of the protein. The combination of these helices into a right handed super-helix is known as the tertiary structure. This triple-helix has a length of about 300 nm and weights approximately $300,000$ u [22, 31]. These triple-helices in their turn combine to form collagen fibrils which are known as the quaternary structure of the protein. This latter structure is not shown in Figure 3.1 but can be seen in part (1) of figure 3.2.

Though it may seem as if collagen is a single protein it is in fact a family of proteins. At least 29 types of collagen exist, of which only the types I, II and III can be found in larger quantities [29, 30]. Gelatin is usually produced from type I animal collagen [30].

The alpha-chains making up the triple-helix consist of 334 repetative units of the general sequence Glycine (Gly)-X-Y, only the terminals of the polypeptides are different. Gly thus amounts to almost 33% of the total amino acids composition of gelatin. For mammalian collagen Proline (Pro) and Hydroxiproline (Hyp) form another 22% [30]. These latter two amino acids limit the

rotation of the peptide backbone of the protein and thus create the secondary structure of the protein.

Moreover, the hydroxyl group of the Hyp stabilises the triple-helix structure. For marine collagen the situation is different; cold water fish collagen has less Pro and Hyp content and therefore shows less helical stability and consequently has worse gelling properties compared to mammalian collagen [28, 30].

Up until 2008 it was unclear whether the stabilising effect of Hyp was mediated by hydrogen bonding or stereoelectronic effects forcing the secondary structure of the alpha-chains. In 2008 evidence was found for the latter and it was claimed that water even had a detrimental effect on helical stability [19].

The reason why gelatin is a convenient glue is shown in Figure 3.2. (1) Shows how collagen is composed of multiple triple-helices (2), which are turned into gelatin by heating (3). The left picture in (3) shows the gelatin in random coil formation, in which the glue is liquid and can be applied to the adherents. Then, upon cooling, renaturation takes place and the triple helices are restored. As the gelatin cannot go back to the highly ordered collagen state, the renaturation is only partial, and peptides may contribute to multiple triple-helices. In this way a highly intertwined network is obtained that gives the glue its strength. At a certain point, the gelatin is no longer liquid but forms a gel locking the adherent together, after which point drying progresses until the gelatin is in solid state again.

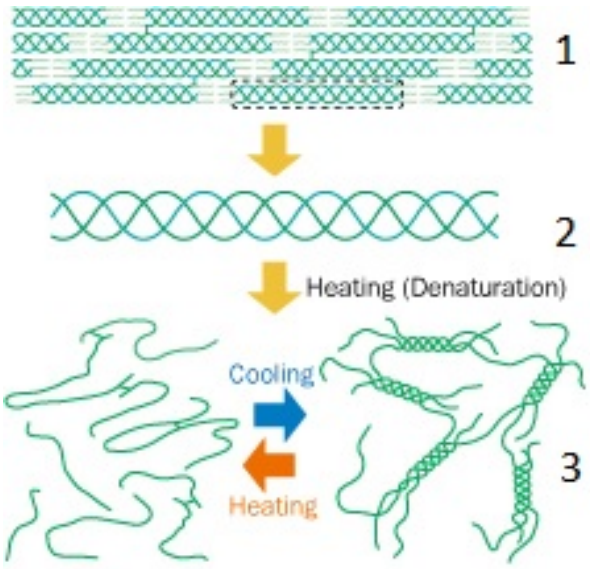

Figure 3.2: Schematic representing how collagen is processed into gelatin. It also shows the thermally reversible process of gelatin gelling. Adapted from [25].

These triple-helices act in a way like cross-links just as seen in modern epoxy glues. However, contrary to epoxy glues, the cross-links in gelatin are just a configuration of the protein and do not form by means of chemical reactions; the process is in principle fully reversible. Reheating of the gel will lead to denaturation of the triple-helices in the gelatin and the glue will change to the sol state again. Though in principle this reversibility is unlimited, ongoing thermal and biological degradation of the polymer chains will eventually lead to a loss of gelling properties.

3.2 The Production of Animal Glue

Animal glue can be produced from a wide range of tissues. However, only the tissue of very young animals or some specific fish tissue, such as the swim bladder of the sturgeon, allows for collagen extraction without or with very mild pretreatment [29]. This is due to the fact that the collagen triple-helices in collagen fibrils form covalent bonds in between as the animal ages. This locks the structure to such an extend that the collagen becomes insoluble in water. In order to extract the collagen from older animals these cross-links need to be broken.

Three common methods for collagen pretreatment exist. The most common are acidic and alkaline pretreatments, in which the collagen source is exposed to a dilute acid or alkali, which leads to chemical hydrolysis of the collagen, breaking both cross-links between triple-helices as well as peptide bonds in the alpha-chains. The alkali and acid processes can be enhanced or

replaced by enzymatic hydrolyses, though only a few very specific enzymes can break down the insoluble native collagen.

After this pretreatment the collagen can be dissolved in warm water. During this step additional thermal hydrolysis takes place [30]. Usually multiple extractions are done, increasing in severity of pretreatment and extraction temperature. Each successive extraction results in gelatin with lower Average Molecular Weight (AMW) [24, 29].

There are two important differences that result from the choice for acidic or alkaline pretreatment. Firstly, alkali pretreated gelatin (also called type B gelatin) has an Iso-Electric Point (IEP) of $8-9$, while acid pretreated gelatin (also called type A gelatin) has an IEP of $4.8-5.5$ [24, 30]. This difference occurs as, during alkaline pretreatment, all the asparagine and glutamine in the peptide chains is converted to aspartic and glutamic acid respectively, resulting in a different charge on the molecule [30]. This difference in IEP influences the spatial configuration of gelatin in a solution with given pH value. Consequently the viscosity of gelatin in a solution depends on the type of gelatin and the solution pH. In case the solution has a pH equal to the IEP, the gelatine forms a random coil structure and has minimum viscosity.

The second important difference is related to the molecular weight distribution of type A and type B gelatin. In Figure 3.3 a typical distribution is given for both types of gelatin. Type B gelatin shows a distinct peak around 10^5 u, while type A gelatin has a broader maximum at that point. The gelling power of a given gelatin mainly depends upon the molecular weight fraction around 10^5 u, while the higher molecular weight fractions mainly result in a higher viscosity.

It should be pointed out that as a general rule each subsequent extraction will have a molecular weight distribution that has a lower fraction of the molecular weight at 10^5 u and higher. This is due to ongoing thermal and chemical hydrolysis combined with the increasing severity of each extraction.

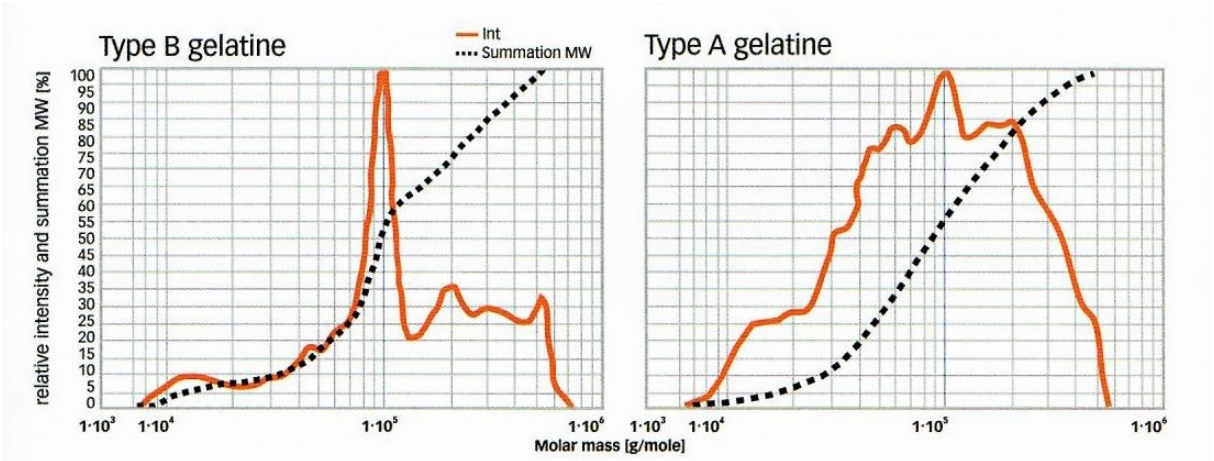

Figure 3.3: Typical molecular weight distribution of high-quality type A and type B gelatin. Note that the fractions of 10^5 u are responsible for the gelling properties while the fractions of higher weight mainly contribute to viscosity [30]. The dotted line represents the integral of the mass fraction. Taken from [30]

3.3 Parameters Influencing the Mechanical Characteristics of Gelatin

Research into the mechanical characteristics of animal glue is limited and usually not fully documented. Most often, standard deviations are large and sample sizes small, leading to a

claims based on analyses with relatively low statistical power. Still, there is valuable information from previous experiments which will be discussed in the following sections.

3.3.1 Gelatin Water Content

In general, four stages of water are known in gelatin. In stage one, water is bound to high energy sorption centres. This stage is the first to form, at a Relative Humidity (RH) between 0 and 10%. This corresponds to a gelatin water content of 0 to 5.5% as a fraction of dry gelatin mass. The second stage is water bound to the protein chains. It occurs at a RH of 10 to 40%, leading to a water content of 5.5 to 14%. The next stage is a polymolecular water layer, formed in stage three. The corresponding RH ranges from 40 to 90%, with a water content range of 14 to 37%. Finally, stage four water forms at an RH above 90%, when more then 37% of water is present in the gelatin. This last stage presents itself as free water [20, 33]. In musea, stage three is most likely to occur as humidities are usually close to 50-55% [5, 14].

It should be noted that the studies referred to in the cited papers are not clear on whether or not the fourth stage does exist for gelatin. In fact, an older source acknowledges the four stages for collagen, but only the first three for gelatin [18].

With respect to the mechanical properties of the animal glue it was found that the stress and strain at break were highest for gelatin with stage two water. Also, measurements of the melting enthalpy pointed out that this region was characterised by the highest triple-helix content. According to Yakimets et al. this is caused by the function of water as a stabiliser of the triple-helices [33]. However, according to the earlier cited article by Kotch et al., water has no stabilising effects [19].

Both conclusions follow directly from the experimental data and it is therefore most likely that both conclusions are correct. This means that both conclusions should have a explanation in a larger theoretical framework.

Considering the fact that water is a small molecule compared to gelatin, and that gelatin is hygroscopic, it is most likely to assume that water will interact with the gelatin stability. The following proposed framework allows both phenomena to take place: Stereoelectronic effects limit backbone rotation of the alpha-chains, thus stabilising triple-helices by providing an optimal spatial configuration. Still, a minimum amount of water is beneficial to the structure by forming additional hydrogen bonds. Once a certain limit is passed (probably stage three water), water becomes deleterious to helix stability. Within this framework the data obtained from Yakimets et al. can easily be explained, while the data by Kotch et al. can be interpreted too, as they do not mention the effect of dehydration on helical stability.

3.3.2 Gelatin Film Casting Conditions

Just like the water content determines gelatin renaturation, so do casting conditions. Important aspects are drying temperature, drying time, initial concentration of the gelatin solution, and the presence of (cross-linking) additives.

From inspection of gelatin films it was found that films dried at room temperature, or at even lower temperatures, had predominantly a triple-helix structure. However, films dried at temperatures above 35 °C showed no signs of molecular order and all gelatin had a random coil configuration [20].

The drying time is an important factor too. Triple-helix formation is a kinetic process and thus requires some time to reach a maximum. The fact that it was found that ageing gels before casting films from them improved triple-helix content is in line with this [20]. Consequently, as gelatin solutions gel after being cast, the time between gelling and becoming a dried film, determines the time given for the process of renaturation. Thus a longer drying time could result in a higher triple-helix content.

With regard to initial concentration of the gelatin solution it was found that as the drying temperature came closer to the gelling temperature, a higher gelatin concentration was required to reach the same level of renaturation. Finally, the effect of (cross-linking) additives is dependent on the specific additive and might either promote or hinder triple-helix formation [20].

3.3.3 Gelatin Bloom Number

In Sections 3.3.1 and 3.3.2 it was pointed out that the mechanical properties of gelatin are related to the renaturation level. However, the most important aspect in tripe-helix formation has not yet been discussed: the gelatin quality. For the present discussion the general notion of gelatin quality will be adopted. The general notion of gelatin quality is related to thermal and chemical degradation of the polymer chains. An ideal gelatin would solely consist of the unwound polypeptide chains of $100,000$ u. However, real gelatins always consist of mixtures of chains with various lengths, as shown before in Figure 3.3. A high quality gelatin is therefore a gelatin with a high fraction of chains around $100,000$ u.

The most important measure of the gelatin quality is the bloom strength. This is a standard and generally adapted measure of the stiffness of a gelled gelatin sample. It has been shown that a linear relationship exists between bloom strength and renaturation level[1] [4].

3.4 Gelatin Film Quality Assessment

Various methods can be adopted in order to determine the quality of a gelatin film. As the mechanical properties are believed to depend mostly on the triple-helix content of the gelatin film, three methods to evaluate this helicity will be presented in this section. The fourth method mainly allows to estimate the extend of internal stresses in the samples.

3.4.1 Differential Scanning Calorimetry

DSC evaluates the heat capacity of a sample as a function of temperature. Changes in the heat capacity occur at phase changes such as the T_g (glass transition temperature) and T_m (melting temperature). The position of these phenomena as well as their associated energy contain valuable information on the properties of the sample. Also, information on the structure of the sample can be retrieved as the T_g is associated with the amorphous part of a material while the T_m represents the crystalline part.

In the specific case of gelatin, the position of the T_g and T_m is expected to shift in the various glues, as their Molecular Weight Distribution (MWD) varies. However, the important information is not contained in the position of the T_g or T_m, but in the energy associated to the T_m. As the triple-helix is a crystaline configuration of gelatin, it will show up in the melting peak. By comparing the melting enthalpy (ΔH_m) of the gelatin sample with that of collagen (100% crystaline gelatin) the degree of renaturation can be evaluated [4, 33].

3.4.2 X-Ray Diffraction

Another way to analyse the renaturation uses XRD. The evenly spaced molecules in a triple-helix give rise to constructive interference. The angles under which such constructive interference happens holds information about the underlying structure.

The triple-helix formed by gelatin has an inner diameter of 1.1 nm. Constructive interference related to this structure should be expected to show up at 8 $^\circ 2\vartheta$, for a X-ray source of CuKα radiation [4, 33].

[1] For bloom strengths between 80 g and 270 g

3.4.3 Fourier Transform Infra-red Spectroscopy

FTIR evaluates which energies are absorbed by molecular, organic bonds in the sample of interest. Specific bonds absorb specific energies and by analysing the energies that are absorbed, an overview can be made of the types of bonds that are present in a sample. However, the energy of a bond not only depends on the two molecules linked, but also, to some degree, on the surrounding molecules. Therefore, shifts in bond energy can indicate that the surroundings of the chemical structure under investigation has changed.

The use of FTIR as a means of evaluating the helicity of gelatin depends on this peak shift. It has been shown that the peak corresponding to the amide-I band shifts depending on the fact whether or not the gelatin is in helical configuration. Coiled gelatin, which is the amorphous fraction, will show this amide-I peak at 1633 cm^{-1}, while helical gelatin will show it at 1660 cm^{-1} [33].

3.4.4 Polarised Light Experiments

Gelatin is an optically active medium, meaning that it changes the rotation of an incident, polarised light beam [13]. This property allows to visualise internal stresses in the material, as varying stress states will create regions of varying optical rotation.

Chapter 4

Experimental

This chapter provides an overview of the materials and processes used during the experiments in the Sections 4.1 and 4.2 respectively.

4.1 Materials

Glues: The experiments were carried out on type A gelatin made from food grade porcine skins. The animal glues are produced by Trobas Gelatine B.V. situated in Dongen. Table 4.1 shows the gelatin labels, their bloom strengths and their batch numbers.

Pesticides: Additionally Mergal KM90 was used as a pesticide. This pesticide is produced by Troy Chemical Company B.V. situated in Maassluis. Additional information can be found in Appendix A.

Table 4.1: Properties of the animal glues. The labels show the type of glue (G for food grade gelatin and L for technical gelatins) while the number corresponds with the reported (double) bloom strength.

Label	Bloom Strength [g]		Batch
G240	240	(6.67%)	6024020.00.0030
G180	180	(6.67%)	6018020.00.0060
G120	120	(6.67%)	6012030.00.0014
L330	330	(12.5%)	62330120.00.0034
L180	180	(12.5%)	6218060.00.0030

4.2 Processes

This section lists various processes used in this thesis. It starts with processes related to sample production in Section 4.2.1, followed by sample conditioning processes in Section 4.2.2. Finally , the processes related to mechanical tests and film quality assessment are listed in Sections 4.2.3 and 4.2.4.

4.2.1 Sample Production Processes

Sample production procedures involve three parts, film casting, film drying, and sample cutting.

Table 4.2: Comparison of the two film casting methods.

	Method 1	Method 2
Mould	I	II
Size	1.0x1.0 m	0.49x0.49 m
Materials	MDF, Perspex, Teflon	MDF, Perspex, Polyethylene
Glue	75 g	30 g
Water	1500 ml	300 ml
Preservatives	None	0.1 v%
Soaking time	>1 h	>1 h
Casting temperature	55-60 °C	55-60 °C

4.2.1.1 Film Casting

Two methods were used for film casting and a summary of the methods can be found in Table 4.2. Method one used a mould with a 1.0x1.0 m inner area, composed of a 15 mm thick MDF board with a 4 mm thick perspex board on top, covered by a thin Teflon film. The edges of the mould were made of two layers of 4 mm perspex stacked on top of each other to provide an 8 mm high boundary. This mould was kept together by screws that were located at 15 cm intervals on this edge (See Figure 4.1a). This mould will be referred to as a type I mould.

The gelatin solution used for casting in this mould was made by soaking 75 g of animal glue in 1500 ml of demi-water for at least an hour. This mixtures was mixed by hand on some occasions to prevent lumps of dry animal glue to form. After soaking, the glue and unabsorbed water were poured into a metal cooking pan and heated up to a temperature between 55 °C and 60 °C using a heating plate and a continuous magnetic stirrer.

Finally, the gelatin solution was poured on the mould and mechanically spread out over the mould surface.

The second method used a mould with an inner area of 0.49x0.49 m. They were made of a 15 mm MDF board with a 4 mm perspex board on top. Again, the edges were made by stacking 4 mm perspex strips, now using 4 layers. All these elements were adhered using double sided tape (See Figure 4.1b). Finally, a polyethylene film was adhered to the inner area on the mould using double sided tape. Cuts were made in this film to allow it to cover the corners of the mould. The resulting slits in the film were covered using masking tape. This type of mould will hereafter be called type II.

The gelatin solution used for casting in these smaller moulds was made by soaking 30 g of animal glue in 300 ml of boiled demi-water containing 0.1 v% Mergal KM90. After soaking for at least an hour (in which stirring was applied as described for the first procedure), the animal glue and remaining water were poured into a metal cooking pan. The heating and casting procedure was equal to that used in method one.

4.2.1.2 Film Drying

Film drying was carried out following three methods, a summary of which is given in Table 4.3. The first method used two type I moulds, placed in an isolated room in the Atelier Gebouw (AG) in Amsterdam. The moulds were placed level and were protected from the dust by a plastic film enclosure as can be seen in Figure 4.2a. A Relative Humidity/Temperature-Logger (RH/T-Logger) (EL-USB-2 Multi datalogger, Lascar Electronics) was placed inside this enclosure to log the climate. The position of the RH/T-Logger can be seen in Figure 4.2b. The moulds were left there until the animal glue had dried.

(a) Type I mould consisting of a MDF board backing and perspex surface, which is covered by a stretched teflon film acting as non-stick surface. The inner dimensions are 1.0x1.0 m.

(b) Type II mould consisting of a MDF board backing and perspex surface, which is covered by a polyethylene film (not shown), adhered to the perspex with double sided tape. The inner dimensions are 0.49x0.49 m.

Figure 4.1: The two types of moulds.

The second method used two type II moulds in the same isolated room in the AG. These moulds were placed in the same enclosure, with the RH/T-Logger in the same position. This time, 200 g of consumer desiccant was placed at the other end of the room. After approximately 48 hours, the moulds were relocated to the furniture conservation studio of the Rijksmuseum Amsterdam (RMA), situated in the AG too. The RH/T-Logger was placed close to the moulds. The RH in the studio is kept around 55%, and the temperature arround 21 °C.

The third method used two type II moulds placed in a *Weiss SB11 300 40* climate chamber. The climate chambers program was kept at a RH of 70% for 48 hours while a temperature of 18 °C was maintained, followed by 24 hour period at a RH of 55% and a temperature of 21 °C.

4.2.1.3 Sample Cutting

After drying all curled edges were removed and the remaining film was cut in four quarters. These quarters were inspected to select the regions with the least visible flaws and the highest homogeneity in thickness.

From these regions, a total of ten tensile samples was cut using a perspex template and a scalpel. The sample dimensions were 175x20 mm with varying thickness. These dimensions were dictated by the ASTM D882-12 standard. The dimensions of the samples used in the creep test were 150x20 mm.

Table 4.3: Comparison of the three film drying methods.

	Method 1	Method 2	Method 3
Mould	2xI	2xII	2xII
Location	Isolated room AG	(1) Isolated room AG (2) Conservation studio AG	*Weiss SB11 300 40* Delft
Dessicants	None	200 g	None
Climate	Logged	(1) Logged (2) 55% RH & 21 °C	(1) 48h 70% RH & 18 °C (2) 24h 55% RH & 21 °C

(a) Two type I moulds inside an isolated room at the Atelier Gebouw. An enclosure made from plastic film keeps dust from contaminating the gelatin solution.

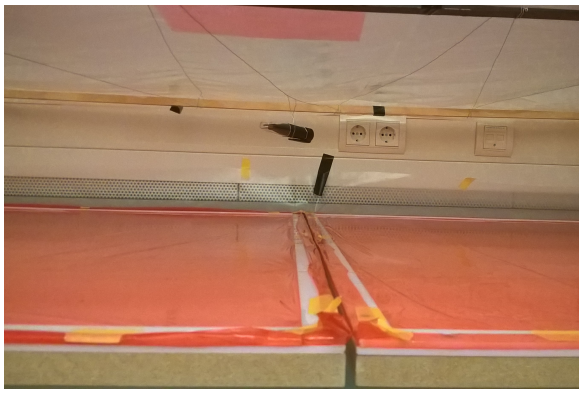

(b) Position of the Relative Humidity/Temperature-Logger inside the enclosure.

Figure 4.2: Set-up of the first moulds at the Atelier Gebouw

The thickness of the samples was measured at three points along their length using an analogue micrometer. According to ASTM D882-12 the thickness was not allowed to vary more then 10% over the length of the specimen.

Besides that, an assessment was made of the number of visible flaws. This was expressed as K_{vq}, a factor with an integer value between 1 and 4, with 1 denoting no visible flaws and 4 denoting extensive visible flaws.

Samples and remaining sheet material were stored in plastic pockets to prevent them from sticking to one another. These separate pockets were then gathered in cardboard file-folders and stored at the Vliegtuighal in Delft without particular measures for climate control.

4.2.2 Sample Conditioning

Sample pretreatment was carried out by storing the samples for at least 40 hours at a RH of 55% and a temperature of 23 °C. The minimum period of 40 hours followed from the ASTM D882-12 standard. The climate chamber used for conditioning was a *Weiss WK111 340*.

4.2.3 Mechanical Tests

Two types of mechanical tests were carried out: tensile tests and creep tests.

4.2.3.1 Tensile Tests

The tensile tests were developed along the ASTM-D882-12 standard. As the elongation of the samples was expected to be lower than 20%, based on the results obtained by Nijhuis [24], the initial grip separation was set to 125 mm, with a rate of grip separation of 12.5 mm/min, leading to an initial strain rate of 0.1 mm/(mm·min).

Modulus of elasticity measurements were made on the same samples as used for determining the other tensile properties. According to ASTM D882-12 this is not optimal as, due to the short length of the specimen, slipping effects may have a profound impact on the measurement of the E-modulus.

The testing apparatus was a *Zwick 20kN* using a 1 kN loadcell with an accuracy of at least 0.5% between 2 N and 1000 N. The grips were flat and lined with rubber which had been adhered using a cyanoacrylate adhesive.

The strain was registered using a longstroke extensometer having a 5 µm accuracy, set to have a gage length of 100 mm. At some point during the tests it was noticed that the extensometer slipped regularly, from then on the lower jaw was covered with some rubber to prevent slipping.

To minimise the effect of the test environment's climate during testing, only 20 till 40 samples were taken out of the climate chamber at the same time.

4.2.3.2 Creep Tests

Creep tests were carried out on a small creep bench designed to fit in a climate chamber. The utilised climate chamber was a *Weiss WK111 340*. Figure 4.3 shows the test set-up. The creep bench used a laser to measure the distance to a reflective surface connected to the end of the sample. The configuration used during the test allowed two samples to be tested simultaneously. The force required for straining the sample was delivered by weights. The clamps were lined with rubber to ensure grip on the specimen. Each 30 seconds, a measurement was made.

Figure 4.3: Creep bench in the climate chamber. The reflective surfaces are not present, as the samples are not yet mounted.

The first creep test method adhered the rubber lining with tape, and strained the sample with normal weights. The force was 30% of the maximum force.

The second method used rubber lining adhered with a cyanoacrylate adhesive. The sample was strained using variable weights of own design. These variable weights were made using an empty paint can which could be filled with small pieces of metal to give the desired weight. The force used was 30% of the maximum force.

The third method was equal to method two, only applying 40% of the maximum load of the sample instead of 30%.

4.2.4 Quality Assessment Tests

Four types of techniques were used for film quality assessment: DSC, XRD, FTIR, and polarised light.

4.2.4.1 Differential Scanning Calorimetry

DSC tests were carried out using a *Perkin Elmer 8000* with 30 µl aluminium pans. To prevent deformation of the pans due to thermal expansion of the contained air, three holes were made in the cover along its diameter.

The program consisted of three steps. (1) Cooling the sample to 0 °C and holding it for 5 min. (2) Heating it to 250 °C at a rate of 50 °C/min. (3) Holding it at 250 °C for 1 minute. 20 ml/min Nitrogen was used as a purge gas.

The limit of 250 °C was determined with Thermogravimetric Analysis (TGA) using a *Perkin Elmer TGA 4000*.

4.2.4.2 X-ray Diffraction

The XRD analysis was performed using the *Rigaku MiniFlex 600* with a NaI scintillator detector and a CuKα radiation source at maximum power (I=15 mA, U=40 kV). The samples were kept at the correct height in the sample holders by a grey gummy of unknown composition. Its diffractogram can be found in Appendix F.

Most analyses were carried out in the domain ranging from 5-12 °2ϑ. They were collected with a step size of 0.1 °2ϑ and a speed of 0.5 °2ϑ/min. For the two analyses in the domain of 3-90 °2ϑ the same step size was used. However, the speed was increased to 1.0 °2ϑ/min.

4.2.4.3 Fourier Transform Infrared Spectroscopy

The machine used to carry out the FTIR was the *Perkin-Elmer Spectrum 100* using the Universal Attenuated Total Reflectance (UATR)-device. The analysed wavenumbers ranged from 4000 cm^{-1} to 600 cm^{-1} with an interval of 1 cm^{-1}. Each transmittance spectrum was an accumulation of 27 measurements. The clamping force used was 80±1% of the maximum force.

Unconditioned samples were analysed at three locations on the surface, while conditioned samples were analysed at two locations.

4.2.4.4 Polarised Light Experiments

The polarised light experiment was carried out using the *Zwick 20kN* with 1 kN loadcell. A standard tensile sample was tested using the same conditions as the tensile tests, while a polariser and led lamp provided polarised light from behind the sample, and a second polariser in front of the sample allowed visualisation of the fringes resulting from the stresses.

Chapter 5

Methodology

This chapter presents the argumentation backing the key decisions made in designing the experimental approach towards answering the research question (See Section 1.2). The chapter starts with an analysis of previous experiments in Section 5.1. These experiments show partially overlapping research questions and are used to define areas of special attention. Then, each experimental phase, namely sample production, mechanical testing, and film quality assessment, is discussed in turn in the Sections 5.2 until 5.4.

5.1 Analysis of Previous Experiments

When looking at previous experiments regarding the mechanical properties of animal glue, two important observations can be made.

First of all, a significant part of the published research lacks crucial information, such as number of samples made (e.g. [1, 4, 33]).

Secondly, most research either investigates one type of animal glue (e.g. [33]) or a wide array of different animal glues (e.g. [24]). In the former case, the results are generally well established, with a sufficiently high number of samples measured. However, it is hardly possible to assess the validity of the results for slightly different glues (e.g. different source material, bloom strength etc.). The latter situation on the other hand, usually leads to problems with the statistical analysis of the results. As a lot of glues have to be tested, the amount of samples per type of glue is decreased. The resulting uncertainty in the results hinders strong conclusions to be made.

These problems are partially due to the fact that most research into (animal) glues used in conservation is embedded in a case study. Once the problem at hand is solved, no further scientific understanding of the material properties is pursued. This approach is illustrated by [10], though they use synthetic glues rather then animal glues.

The observations mentioned in the preceding paragraph greatly hinder attempts to unify various experiments, as it cannot be easily guaranteed that samples from various experiments are comparable to each other. Therefore these observations emphasise the importance of careful selection of materials and procedures, and they show the relevance of presenting the logic behind those choices.

Another general observation comes from experiments on the production of gelatin films or animal glue joints. As explained in Section 3.1, the renaturation level of animal glue plays an important role in the mechanical behaviour of animal glue. And, as discussed in Section 3.3, renaturation itself is influenced by water content and drying conditions; the latter including temperature, humidity, and linked to that, drying time. Contrary to the importance they have, the drying conditions are seldom mentioned or monitored (e.g. [24, 34]). This omission might implicate that most experiments have not ensured equal drying conditions for their samples.

Summarising the above, previous experiments indicate that close attention should be paid to ensure that a sufficiently large number of samples is made, from a carefully chosen array of glues and that these samples are produced using a method that accounts for the importance of water content and drying history.

5.2 Sample Design

Based on the above conditions, sample design covers three topics. Section 5.2.1 covers the selection of the glues, Section 5.2.2 discusses the production method, and finally, Section 5.2.3 addresses the need for a well defined drying history.

5.2.1 Choice of Materials

The first major decision to be made concerns the types of glue to be researched. As explained earlier, glues can differ by source, bloom strength, production method, additives and so forth. Judicious choices should be made in order to prevent that either too little or too many different glues are selected, quickly leading to the problems discussed at the beginning of this chapter.

The first decision was to choose glues without additives, as it is important to understand the properties of pure gelatin before trying to address any changes made by additives. This is especially important regarding the large number of different additives known from historic recipes. This approach immediately influenced the range of glues available, as animal glue retailers always add preservatives and other chemicals to their glues.

Secondly, it was decided to use glues that had known source materials, as this might affect any comparisons made between glues. This meant that even less glues were available as it has been shown that the collagen source of commercially available animal glue is usually not unambigious [28].

Therefore, it was decided to contact a food-grade gelatin manufacturer in order to obtain sample material, because they need to keep precise track of their source materials and are capable of providing high purity gelatin. This decision practically determined the gelatin source, as the largest share of current food-grade gelatin production uses porcine hides as raw material. The production process was set in the same way, as porcine collagen is nowadays always obtained via an acidic process (type A gelatin). It is important to realise that this may be an important difference with historic animal glue which seem to have been mostly type B (See Section 2.4).

Production method and source material being set, the major remaining parameter was the bloom strength. Therefore, a selection of pure, porcine gelatins with varying bloom strengths was made. It is important to realise that the bloom strengths of food grade gelatin and animal glue differ in magnitude. The industries practice is to calculate bloom strength of food grade gelatin as single bloom strength, and that of glues as double bloom strength. The single bloom strengths are calculated using a gelled sample of a 6.67 w% gelatin solution, while the double bloom strength is calculated using a sample of a gelled 12.5 w% gelatin solution [16]. According to the manufacturer, the single bloom strength is approximately one third of the double bloom strength [11].

Finally, during sample production it turned out that at least one additive had to be added to stop biological degradation of the gelatin. Therefore the final materials list, presented in section 4.1 comprises five gelatins and one pesticide. Unfortunately this means that the glues are no longer pure, however, without the pesticide moulding would change the observed properties too.

5.2.2 Sample Production

Once the glues had been selected, a method had to be defined for sample production. The main problem to address in sample production was how to produce homogeneous thin films, not only with respect to thickness, but also with regard to thermal history.

The adopted solution was to create a large film from which the samples for both tensile testing and film quality control could be obtained. In this way, all samples from one film would have the same drying history.

The easiest way to obtain a large and thin film is by casting it from a dilute gelatin solution. This method allows for a relatively long renaturation period and is easy to carry out, as it only requires pouring a warm, dilute gelatin solution on a large mould. Of course this mould should be placed level to produce a film of homogeneous thickness.

5.2.3 Sample Drying Method

The most important feature of the drying method is that is should be reproducible and repeatable. The common notion of repeatability will be used, namely: The degree of agreement between two measurements when repeated using the same equipment, working at the same location, etc. For reproducibility the following definition is adopted: The degree of agreement between two measurements when repeated using different equipment, working at a different location, etc. This is a slightly modified definition of the common notion, while usually the person carrying out the reproducibility measurements should not be the same person as the one doing the original measurements. Nor should he do it in the same period of time. However, for the sake of the thesis, these definitions will suffice, while allowing validation of the results obtained.

In order to test both repeatability and reproducibility, four films were made of each glue. Two films were made in the mentioned climate chamber in Delft, while two others were made at the AG. By comparing the two films made at the same location, for which the same equipment was used, a measure of repeatability is obtained. On the other hand, by comparing the films made at different locations, for which different equipment was used, a measure of reproducibility is obtained.

The final drying profile mainly resulted from a trail-and-error process which will be explained in more detail in Chapter 6

5.3 Analysis of Mechanical Properties

Once the samples had been produced, a tensile test procedure suitable for this task had to be identified. In order to allow comparison with other materials and profit from the existing knowledge on testing thin films, the ASTM D882-12 standard was used as much as possible. As gelatin is a biopolymer, this standard for determining the tensile properties of thin plastic films seemed most applicable to this experiment. Most importantly, the thickness of the gelatin films was well within the range set for thin plastics [2].

5.4 Analysis of Gelatin Film Quality

The final phase of the experiments focussed on gelatin film quality control. Film quality control can be used in a variety of ways. It can be used to evaluate the results found from the mechanical tests and improve the analysis. However, if a method proofs to correlate to the quality of the glue film, it can be used to ensure homogeneous quality of the samples at the start of an experiment too.

Various important parameters such as thickness, weight, and density are 'easily' determined. The most important parameter, triple-helix content, is harder to measure. Three techniques may show a relation to the helix content of a gelatin sample, namely DSC, XRD, and FTIR. The principles of these methods have been explained in Section 3.4.

While performing these measurements it should be kept in mind that gelatin is a hygroscopic material. Besides influencing the weight, volume, and density, the water content may influence the helix content in a gelatin sample too. The water content in turn follows the environmental

humidity fluctuations. By performing analysis on both conditioned and unconditioned samples, it is possible to see the extend to which the water content should be controlled before assessing the film quality.

Chapter 6

Sample Production

This chapter details the design of the sample production process. Section 6.1 describes the first casting procedure, followed by a description of the updated, second procedure in Section 6.2. The final procedure that was used to create the samples for the mechanical and film quality tests is presented in Section 6.3. An overview of the casting and drying procedures mentioned in this chapter, can be found in Appendix B.

6.1 First Sample Production Procedure

This section explains the first casting method used in the first sample production procedure in Section 6.1.1. It then describes the results of this first procedure in Section 6.1.2.

6.1.1 First Casting Procedure

The first mould design was based on the principles presented in Section 5.2.2. It was designed to have a large and flat surface, allowing the production of large and thin gelatin films.

The construction consisted of various layers, each with a specific function. The MDF board provided the required rigidity to prevent twisting or curving of the mould. The second layer, a perspex board, provided the smooth surface required for a high quality film. A thin Teflon film was stretched over this assembly to act as a silicon-free, hydrophobic surface. The reason to go for a silicon-free film was to keep contamination of the glue minimal, as silicon might change the DSC results.

Finally, the Teflon passed under the edges of the mould and was folded upward and fixated in that position to prevent any glue from leaking, even when it would seep under the edges of the mould.

The drying site was chosen based on the principles of Section 5.2.3. To improve repeatability of the drying history the influence of the external climate had to be minimised. It turned out that the Rijksdienst Cultureel Erfgoed (RCE) had a climate chamber in the basement of the building, which was out of order. This room was chosen as the drying site, as it was isolated, providing a stable climate.

As explained in Section 4.2.1.2 two moulds were placed in this room, inside a plastic enclosure, and equipped with a RH/T-Logger to log the climate.

Casting proceeded as described in Section 4.2.1.1. As two moulds were present in the isolated room this procedure was carried out twice. Usually between 15 and 30 minutes elapsed between casting the first and the second glue solution.

Between heating casting solution one and two no cleaning of the cooking pan was performed. As all animal glues contain the same material, only differing by MWD, no real contamination

takes place when a few remains of a dilute solution of a different animal glue remain in the cooking pan.

6.1.2 First Casting Procedure Results

The results of this first procedure were unsatisfactory. The film drying time was approximately 14 days and the resulting films moulded. The first batch, a sheet of G240 and G180, only showed mild signs of moulding. However, the second batch made with the same glues showed very extensive moulding (within a week time).

A quick tensile test confirmed that the extensively moulded G240 film was so weak that an extensometer could not even be attached to measure its elongation. Applying the extensometer would lead to film failure. The extensively moulded sheet of G180 was even weaker, it could not be taken from the mould in strips longer then 15 cm.

These results clearly proved that the first procedure was not suited to produce the required samples as on the one hand the drying time was too long compared to the available time, while on the other hand the films degraded already too much before use.

The logged humidity data showed the cause of this problem. As can be seen in Figure 6.1, the humidity quickly rose upon casting and remained high for more than a week. Observation of the films during drying proved that gelling occurred within a hour after casting. However, drying from a gel to a solid film took much longer. Most likely the high humidity slowed down the evaporation of the water in the gel leading to long drying times. This long, wet period then led to the growth of mould. It was observed that mould growth stopped once the animal glue film was fully dry. The drying temperature was less of a concern in this respect. As the climate chamber was in the basement, the temperature was stable around 18±1 °C. Note that the apparent reduction in noise during the last three days has no clear explanation. It was observed in other logs too, though no special events happened and the sampling frequency was the same. Probably it relates to a change in sensor placement.

A number of small modifications were tested in order to improve the casting procedure.

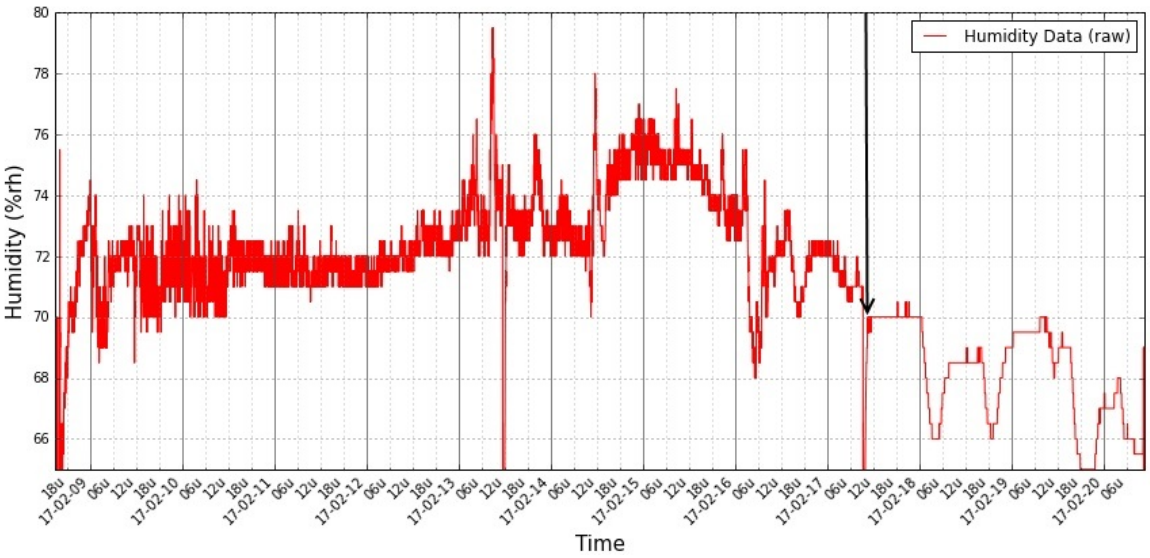

Figure 6.1: Logged humidity for the first batch of gelatin films produced according to the first sample production procedure. The two minima occurring close to 12.00h at 13-02-17 and 17-02-17 were caused by removing the logger from the enclosure to read out the memory and start it again. The black arrow indicates the moment of desiccant application.

These includes measures such as adding some consumer desiccant[1] (at 17-02-17, indicated by the black arrow in Figure 6.1). And though this did lower the RH, the second batch made with this method still showed moulding.

Besides the problems with the samples, also some problems with the moulds showed up. The first was the problem of residual air trapped underneath the Teflon film. Though care was exercised to remove any air when the film was stretched over the mould, some air was still there. When the hot glue solution was poured on the mould, the air expanded, creating air bubbles between the perspex and the Teflon. These air pockets caused thickness variations and even gabs to form in the glue film.

The second problem was the fact that the Teflon film was very thin. As such that it was easily punctured when trying to remove air bubbles. These holes then allowed animal glue to get between the perspex and the Teflon, and form glue pockets that could not be removed.

The third problem was that glue got under the edges of the mould and into the cavity between the outer edge of the borders and the Teflon film that was folded upward. As water could not readily evaporate from there, the glue did not dry, but started to degrade and smell strongly.

Finally, there was one last problem which was an interaction between a problem with the samples and the mould. It turned out that the used amount of dilute gelatin did not give a film with homogeneous thickness. However, additional water could not be added without the risk of spilling it over the edges. The interaction between an uneven surface and slightly too little glue forced to spread over the entire surface, resulted in a film with some very thin sections. As can be expected, these thin sections dried much faster, so in practice this mould facilitated non-homogeneous drying.

6.2 Second Sample Production Procedure

This section describes the use of the second casting method as part of the second sample production procedure in Section 6.2.1. The results of this second procedure are presented in Section 6.2.2.

6.2.1 Second Casting Procedure

The first casting method suffered various problems, therefore the second casting procedure was developed. It combined the second casting method and the second drying method discussed in Sections 4.2.1.1 and 4.2.1.2. The main difference between the moulds was the use of a polyethylene film instead of the Teflon film. This new film was more resistant to puncturing and by taping it to the mould, the problem of residual air was reduced. Also by passing the film over the edges of the mould, no glue could get trapped.

A disadvantage was that the glue film would adhere to the polyethylene film and peel it off the mould after drying. Consequently, the mould had to be repaired after each cast.

Another important improvement was made in the casting solution. By increasing the concentration of the solution and decreasing the size of the mould, less water had to evaporate in the isolated room, reducing the drying time. Also the addition of Mergal KM90 prevented any moulding.

6.2.2 Second Casting Procedure Results

It turned out that the results with the new moulds were better. Even when left to dry in the climate chamber, the drying time was less then seven days and no moulding was formed. Also,

[1] Vochtopnemer Gamma

the entire mould was filled with the glue film. In order to improve the drying speed even more, it was decided to remove the moulds from the isolated room 48 hours after casting. They were then placed in the furniture conservation studio where the RH was only 55% (at a temperature of 21 °C). This adaptation reduced the remaining drying time to 1 day, leading to a total drying time of 3 days.

Removing the film from the polyethylene turned out to be rather easy, as the masking tape covering the slits in the polyethylene film provided starting points for peeling the films apart.

The damage to the mould, caused by the use of polyethylene, was a small disadvantage. Each time a new film was made the mould would get a little more damaged, but except for a few small repairs, not much could be done about it. It was decided that the damage was small, and allowed to make all required glue sheets using the same moulds.

Another problem was that the tape used to adhere the polyethylene had thin wires in it. These wires created a thin indentation pattern on the glue film.

Despite the new setbacks, the glue films produced with type II moulds were much better in quality than those produced with the type I moulds. It was decided that the obtained quality would suffice for the purpose of this thesis.

6.3 Final Sample Production Procedure

This section describes the final sample production procedure. The design of this procedure is the subject of Section 6.3.1. Section 6.3.2 introduces an indexing system for the glue films in order to allow easier identification of the various glue films. Finally, the results are discussed in Section 6.3.3.

6.3.1 Final Casting Procedure

To produce the required amount of samples and investigate the reproducibility and repeatability of the sample production process, the final casting procedure was developed. This included the use of casting method two combined with both drying method two and three. In short this means that both at the AG and in Delft two type II moulds were used. A more detailed overview of the methods can be found in Appendix B or in Chapter 4.

The films that were dried in the climate chamber in Delft followed a climate program mimicking the climate experienced in the AG, allowing reproducibility to be tested. Figure 6.2 shows one of the graphs made at the AG overlayed with the profile set for the climate chamber in Delft. The program of the climate chamber was: 48 hours at a RH of 70% and a temperature of 18 °C, and then 24 hours at a RH of 55% and a temperature of 21 °C.

It is clearly visible that the agreement between the logged data and the set profile is quite good. Especially when factoring in the possible variations between the actual climate in the climate chamber in Delft and the set profile. The climate logs of the other films made in the AG can be found in Appendix C. The actual climate in the climate chamber in Delft has not been logged, though the climate in the climate chamber was checked several times using a thermometer and a hygrometer.

6.3.2 Sample Index Definition

In order to identify the different glue films, the following index convention was used. The first part of the name identifies the type of animal glue, for example G240. The second part identifies the casting location; either RMA, short for Rijksmuseum Amsterdam, for sheets cast at the AG, or D, for sheets cast in Delft. Then follows a number identifying whether it is the first or second sheet made. Each of the 20 sheets thus has an unique index. G240RMA1 is the first sheet of G240 made at the AG, while L330D2 is the second sheet of L330 made in Delft.

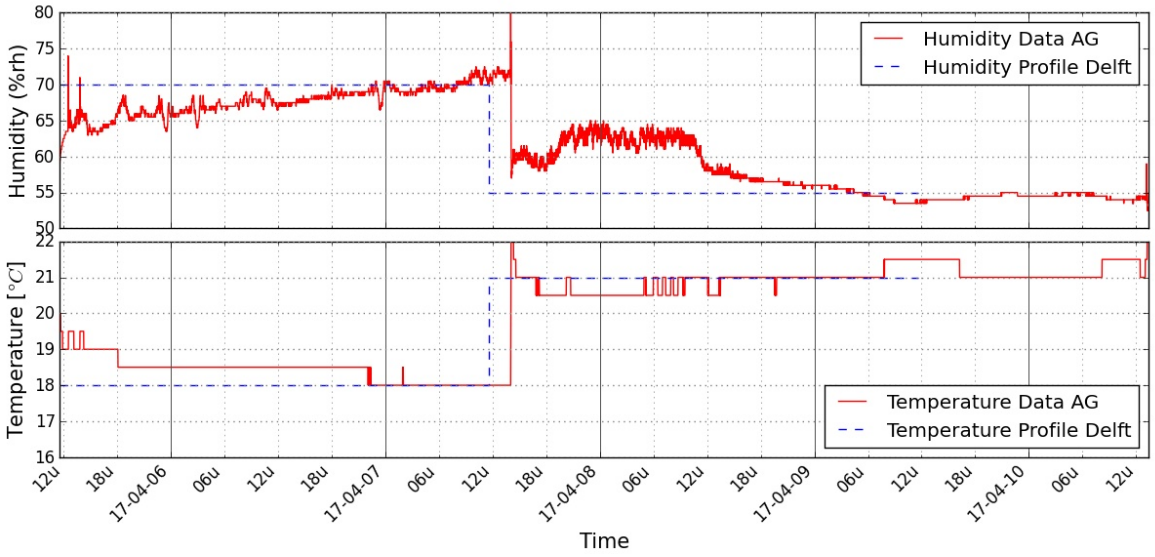

Figure 6.2: Logged humidity and temperature for G240RMA1 and G180RMA1 compared to the profile used in the climate chamber in Delft.

This difference in type of glue and production site has another terminology as well. Especially while discussing the results of various measurements. The term 'types' will refer to all samples from the same type of glue, the term 'series' on the other hand refers to all samples from a specific sheet. Thus the results can generally be evaluated for 5 types or 20 series.

6.3.3 Final Casting Procedure Results

After making the last adaptations to the process, sample production begun. The process was as described above and the production went on without much trouble. Only G120D1 and L330D1 had to be cast again, as during the first try the moulds were not level, which led to a very inhomogeneous film. Another mistake was made with G120D2 and L330D1. They were not taken from the climate chamber after four days, and when the program was finished the RH went up to 90-100% This condition lasted several days.

Normally, when the sheets were dry, they were taken from the moulds. Whether or not a film is dry can be checked by gently touching its surface. If the surface feels sticky, the film is not dry enough.

Due to internal stresses resulting from shrinkage upon drying, all films had curled edges. These were removed and samples were cut according to the method described in section 4.2.1.3

Apart from the two casts that went wrong, there were two other aspects that should be kept in mind. The first is the aforementioned degradation of the moulds, leading to a slight decrease in sample quality between the first sheet of G240 and the last sheet of L180. Secondly, the time that passed between casting the first and last sheet was more than a month, while all tensile tests were done on three days within two weeks time. So the storage time is very different for the various glues.

Chapter 7

Mechanical Properties Found in Tensile Testing

The current chapter deals with the mechanical properties of animal glue as determined via tensile tests. The chapter starts with a description of the hypothesis, in Section 7.1. Section 7.2 presents and discusses the obtained results leading to several conclusions in Section 7.3.

7.1 Hypothesis

As argued in Section 3.3, the mechanical characteristics of animal glue are related to the renaturation of the glue. This renaturation is influenced not only by the drying conditions, but also by the water content.

It has been shown that the bloom strength and renaturation are linearly related. Also it was shown that stress and strain at break, as well as the stiffness, increased with bloom strength [4]. As stress and strain at break are usually close to the maximum stress and strain for brittle materials, it is assumed that the same trend will show up for these parameters.

As all sample films were created using the same method and procedure, casting conditions should not lead to large variations between different films. Furthermore, conditioning of the samples should prevent large variation due to water content. These measures should lead to a situation in which bloom strength is the main differentiator between the films.

The hypothesis therefore is that the tests will show increasing mechanical properties with increasing bloom strength.

7.2 Results and Discussion of the Tensile Tests

This section treats the various results found from the tensile tests. Most results will be presented as a graphical summary. The original data, including those tests later discarded, can be found in Appendix D. This Section will first discus the climate during testing in Section 7.2.1. It will then continue to explain which data had to be discarded. This can be found in Section 7.2.2. Section 7.2.3 presents the results of the remaining data. The final section, Section 7.2.5, is dedicated to showing the type of relation that was found.

7.2.1 The Climate During the Tensile Tests

Completing the tensile tests took three days. At 08-05-17 a total of 90 samples was tested. These were all G240 samples, all G180 samples except G180RMA2, and L180RMA1 and L180D1. The temperature during testing started at 21.6 °C and rose during the day to 23.2 °C. The RH was stable at around 44-45%.

The second day of testing was on 09-05-17, starting around noon. 50 samples were tested: all G120 samples except G120RMA2, and L330RMA1 and L330D1. The temperature was around 22.5 °C and the RH around 47%.

The final day of testing was on 17-05-17. The remaining 60 samples were tested. They belonged to the series G180RMA2, G120RMA2, L330RMA2, L330D2, L180RMA2, and L180D2. The climate was slightly different then. The temperature was around 23.5 °C and the RH varied between 50% and 55%

Though the variations were small, the difference in humidity between the first two days and the last day could imply that the water content in the films differed during testing. In that case, a lower E-modulus would be expected for the samples tested at the third day, due to the properties of water as a plasticiser. Based on the results by Yakimets et al. this decrease could be in the order of 100-200 MPa [33].

7.2.2 Discarded Data

The data presented in Appendix D shows the results for al 200 tensile tests. Before analysis, invalid data should be removed from the dataset in order to exclude incorrect measurement values. Data can be invalid for several reasons, this is not trivial and requires careful selection of criteria. The ASTM D882-12 standard dictates that samples that failed due to obvious flaws should be discarded. However, many samples had flaws that acted as stress raisers, and those samples that failed at obvious flaws did not always perform lower than expected.

Therefore the following criterion was adopted: samples that failed at obvious flaws and had a strength lower than one standard deviation below the mean of their series were discarded. This additional requirement reduces the risk of discarding a sample that failed at a weak point which is representative for the general quality of all the samples. The maximum strength rather than the maximum load was evaluated as the former has been corrected for thickness variations. The ASTM D882-12 warns that for very thin samples, less than 0.13 mm, the maximum load is not proportional to cross-sectional area. However, checking against the breaking factor rather than the maximum stress resulted in the same discarded samples, except for one.

The second criterion listed in ASTM D882-12 is that the thickness variation over the length of a sample should not exceed 10%. To compensate for the fact that the thickness measurement was not as accurate as the one required by the standard, a slightly less strict criterion was adopted. A sample was discarded when any one of its three thickness measurements was more than 10% higher or lower than its average thickness.

Except for the samples discarded by applying this criteria, one other sample was removed. This was G240RMA1-6, as during this test the extensometer was not connected leading to an important loss of data.

The discarded data is presented in Table 7.1. With these data discarded, all series still have the minimum of five samples required for statistical analysis. The data has not yet been corrected for the extensometer slippage, which was mentioned in Section 4.2.3. This is because this slippage only influences the strain measurements, which will be presented later. The measurements of E are correct, as the slippage only occurred at loads higher then those used for calculating E.

7.2.3 Results

The results of the tensile tests can be presented per type and per series. Both offer an interesting perspective on the data. Were the first focusses on differences in between the types of glue, the second allows to inspect differences between the various films too.

Figure 7.1 shows a summary of the measured results. Where $F_{\max}$, $\epsilon_{F\max}$, and E have been measured by the tensile tester. t_{avg} has been measured with an analogue micrometer and is the average of three measurements. Finally, K_{vq} is a factor describing the quality of the film under inspection with the bare eye as explained in Section 4.2.1.3.

Table 7.1: List of samples discarded on basis of the criteria mentioned in ASTM D882-12

Sample ID					
G240RMA1-6	G180D2-8	G120RMA2-2	L330RMA1-8	L330D2-9	L180D1-4
G240D2-4	G180D2-10	G120RMA2-3	L330RMA2-1	L180RMA1-4	L180D1-5
G180RMA2-4	G120RMA1-2	G120RMA2-4	L330RMA2-2	L180RMA2-1	L180D1-6
G180RMA2-5	G120RMA1-6	G120RMA2-10	L330RMA2-3	L180RMA2-3	L180D2-8
G180D1-3	G120RMA1-10	G120D2-2	L330RMA2-4	L180RMA2-7	L180D2-9
G180D2-6	G120RMA2-1	G120D2-6	L330D2-2	L180D1-2	

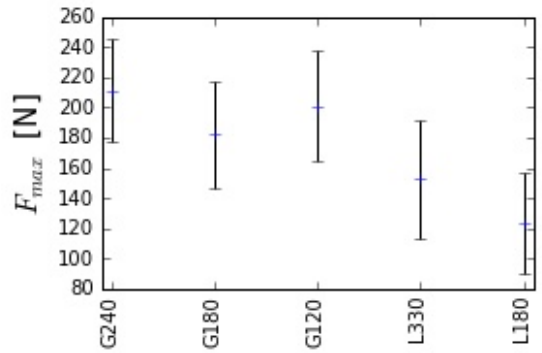

(a) Maximum load per type of animal glue

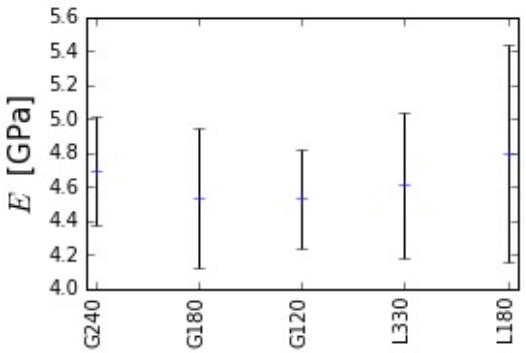

(b) E-modulus per type of animal glue

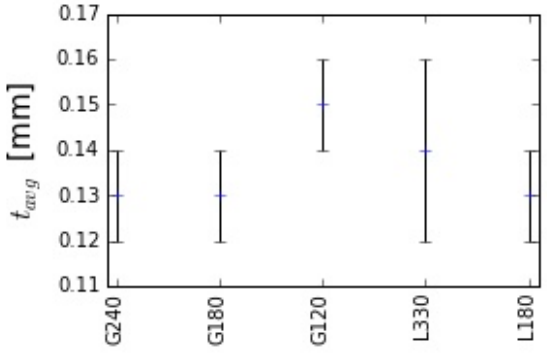

(c) Average thickness per type of animal glue

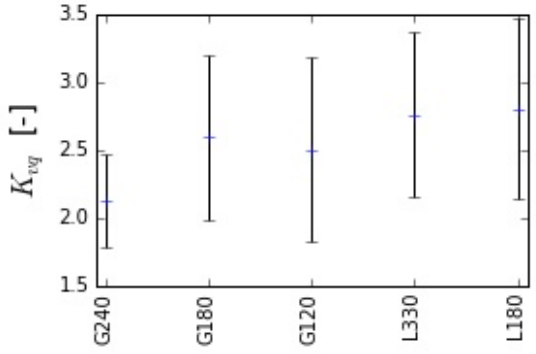

(d) Factor of visual quality per type of animal glue

Figure 7.1: Summary of the measured tensile test results per type of animal glue.

A few interesting results follow directly from Figure 7.1. First of all, the mean of $F_{\max}$ shows a gradual decrease in magnitude as one would expect for films with decreasing helicity. Only the value G120 seem to show a mismatch. This cannot be explained by a possible uncertainty in determining the bloom strength, as the standard deviation for the determination of bloom strength is around 1.5% within one laboratory or no more than 3.0% between laboratories [12].

Secondly, the standard deviation for $F_{\max}$ is rather constant at 35-40 N. With normal stress raisers one would expect the standard deviation to be a certain percentage of the maximum force rather then a near constant value. Neither is there a clear relation between the increasing standard deviation and the increasing K_{vq}. This shows that the standard deviation in the results is not one to one related to visible stress raisers, as the deviation does not change with obviously changing values of K_{vq}. This is interesting, as it reminds of the problem addressed in Section 7.2.2, that clearly damaged samples did not necessarily show worse results compared to other samples, neither when using $\sigma_{\max}$ or R_{break}. The best explanation is that an unknown factor creates a 30-40 N uncertainty in the maximum strength of the samples. A possible candidate would be the internal stresses resulting from drying, as samples taken from different parts of the film will have different internal stress states, which would lead to somewhat different results between samples.

Thirdly, different from the hypothesis, E shows an approximately constant value for all types of animal glue. This is a rather unexpected result based on the article by Bigi et al. [4]. They found an approximately linear relationship between the bloom strength and the E-modulus. This difference cannot be attributed to the fact that several strain measurements are inaccurate, as the extensometer slippage happened at strains past the point used for calculating E. Consequently, the observed difference must either reside in the materials used or in the sample conditioning applied. As the materials used by Bigi et al. are very comparable, it has to be the conditioning. In the article, the gelatin was equilibrated at a RH of 75% [4]. This difference might explain the disagreement in material characteristics. Water is known to lower the T_g of gelatin, and at a RH of 75%, the T_g is around room temperature [24]. It is known that in the glassy state, cross-linking has a limited effect on the E-modulus. Above the T_g, however, the effect is pronounced. Another observation backing this explanation is that Bigi et al. report very high values of strain at break, not consistent with the glassy behaviour of the gelatin in the current experiment.

Finally, Figures 7.1c and 7.1d show data not measured by the tensile tester, but collected right before the start of the tensile tests. As can be seen in 7.1c, the mean of the sample average thickness did not vary a lot between the different types, however, within the types and series, still significant differences occurred. The quality of the films, represented by K_{vq}, shows a gradual decrease, consistent with ongoing damage to the moulds, but no unexpected outliers.

Besides the measured values, some calculated and estimated values have been determined. These are presented in Table 7.2. Most interesting is of course $\sigma_{\max}$, the maximum stress (Also shown

Table 7.2: Summary of calculated tensile test results per type of animal glue

Sample ID	$\boldsymbol{\sigma_{\max}}$ [MPa]	$\mathbf{R_{break}}$ [N/mm]	$\boldsymbol{\rho}$ $[\frac{\text{mg}}{\text{mm}^3}]$	**V** $[\text{mm}^3]$
G240 (n=38)	83 ± 10	11 ± 1.7	1.3 ± 0.03	$4.4{\cdot}10^2$ ± 53
G180 (n=34)	71 ± 15	9.1 ± 1.8	1.3 ± 0.04	$4.6{\cdot}10^2$ ± 37
G120 (n=30)	69 ± 12	10 ± 1.8	1.3 ± 0.04	$5.1{\cdot}10^2$ ± 42
L330 (n=33)	53 ± 11	7.6 ± 2.0	1.2 ± 0.06	$5.0{\cdot}10^2$ ± 56
L180 (n=30)	49 ± 12	6.2 ± 1.7	1.3 ± 0.05	$4.4{\cdot}10^2$ ± 33

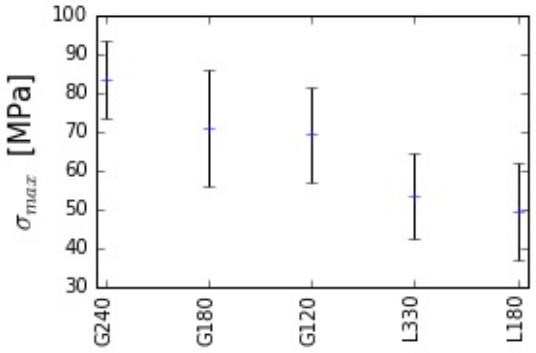

(a) Maximum strength per type of animal glue

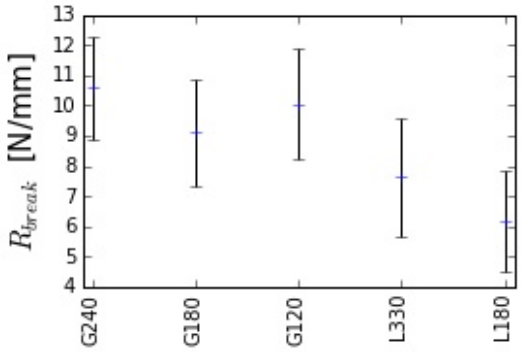

(b) Breaking factor per type of animal glue

in Figure 7.2a). Though the same pattern shows as for $F_{\max}$, namely an overall decrease of $\sigma_{\max}$ with bloom strength, the values for G180 and G120 are much closer here.

R_{break} again shows the pattern reported for $F_{\max}$ (See Figure 7.2b). According to ASTM D882-12 R_{break} is a beneficial way of reporting strengths for thin films if the thickness is reported. However, as previously reported, just mentioning the mean of the average thickness may be slightly misleading, as variation between samples was significant.

The last two columns of Table 7.2 show a density and volume estimate. The measured variables used for the estimation are of course the weight and thickness of the samples. However, in stead of showing those, these estimates are shown as they provide a nice illustration of the variation between samples. The volume has been estimated using the three measured thicknesses along the length of each sample. The formula used for this estimation can be found in Appendix D. The variation in the volume thus provides a better idea of the homogeneity of the samples with respect to thickness along their length and thickness variation between them. On the other hand, the density ρ shows that the variation in weight is mostly related to the variation in volume, so no undetected thin spots altered the results.

Considering the results per type, the most interesting variables are E, and $\sigma_{\max}$. These are shown in Figures 7.3 and 7.4. The graph for $\epsilon_{F\max}$ is omitted as the measurements of $\epsilon_{F\max}$ are not reliable.

As can be seen, the general trends from the summary per type are still visible: E is constant and $\sigma_{\max}$ decreases with bloom strength. One interesting result is that for most series their results are well within one standard deviation of each other. Only for G180RMA2 and G180D2 this is not the case. This is likely related to the fact that their values for K_{vq} are relatively high compared to those of the other G-type animal glues.

As mentioned in Section 7.2.1, five series have been tested under slightly different climatic conditions, but the corresponding effect is smaller than the reported standard deviations on E, so no conclusion can be drawn regarding the influence of the change in climate.

The reason to inspect the reported values per type and per series was to investigate the repeatability and reproducibility of the casting process. High repeatability would result in nearly equal results for RMA1 and RMA2, or for D1 and D2 films. High reproducibility, according to the definitions provided in Section 5.2.3, would show from very equal results between the RMA and D films. Of course these films should be compared per type of animal glue.

Inspection of Figures 7.3 and 7.4 shows that the repeatability could have been better, but that the reproducibility is quite good. The differences between the series are in the same order between the two films made in Delft and those made in the AG. This means that the carefully selected casting and drying process did work as the same results could be obtained by films made at the AG and by those made in Delft.

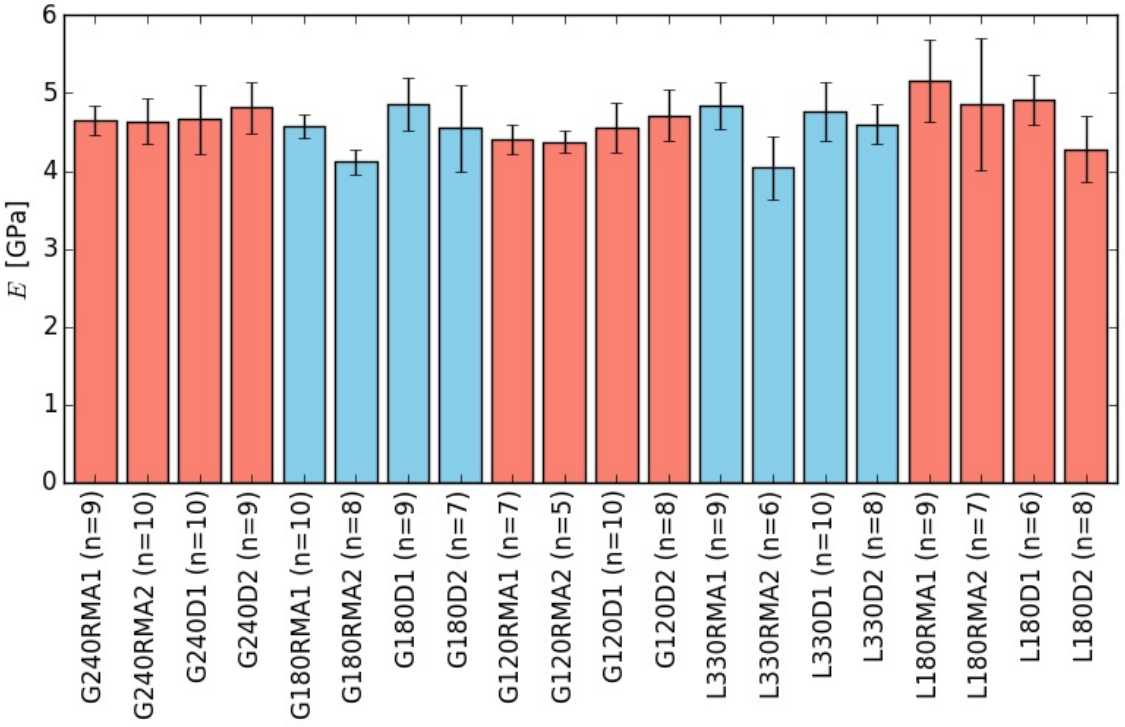

Figure 7.3: Bar plot of E shown per series of animal glue

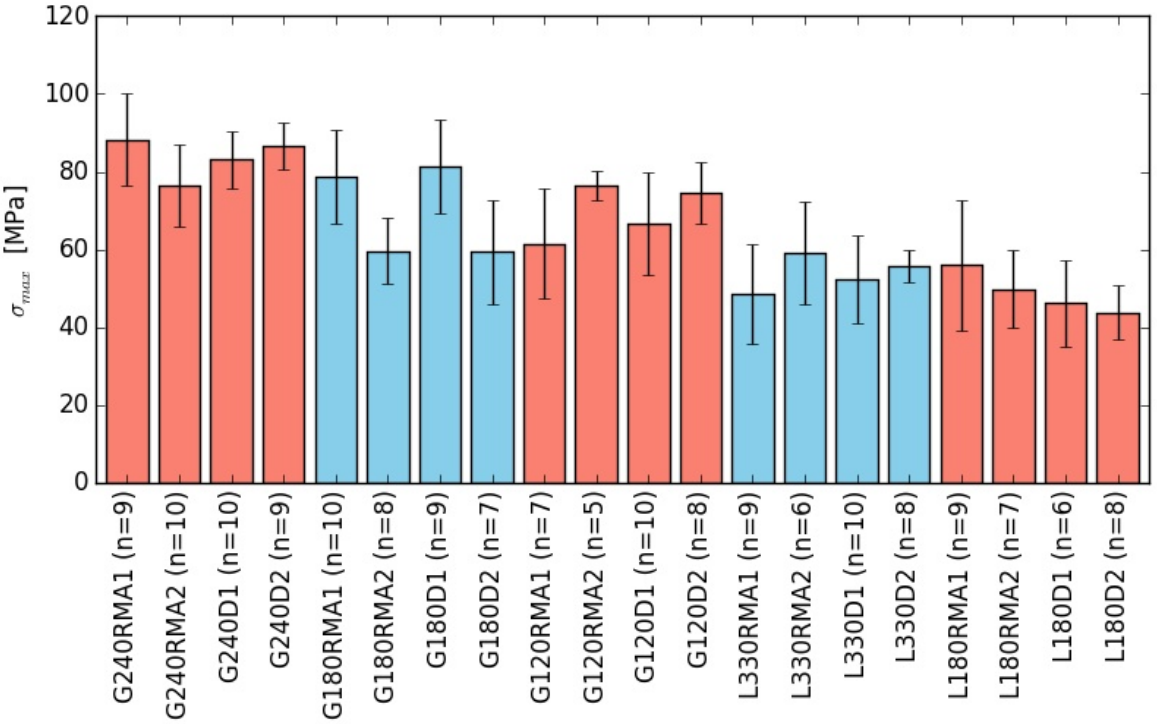

Figure 7.4: Bar plot of $\sigma_{\max}$ shown per series of animal glue

Table 7.3: List of samples discarded on basis of obvious extensometer slippage.

Sample ID				
G240RMA2-3	G180RMA1-3	G180D1-4	G120RMA1-3	L180RMA1-7
G240RMA2-4	G180RMA1-6	G180D1-6	G120RMA1-5	L180RMA1-8
G240RMA2-5	G180RMA1-9	G180D1-7	G120RMA1-8	L180RMA1-9
G240D1-5	G180RMA1-10	G180D2-1	L180RMA1-3	L180D1-3
G240D2-7	G180D1-1	G180D2-9	L180RMA1-6	L180D1-7

7.2.4 Results Corrected for Extensometer Slippage

In the previous results, $\epsilon_{F\max}$ was not reported, as large errors were present in these measurements. By visual inspection of the force-strain curves presented in Appendix D the erroneous results were identified. Note that the samples discarded based on the errors in the strain measurement are added to those removed before. The discarded samples are presented in 7.3

The results of this data selection step can be seen in Table 7.4. The standard deviation does not change much, only the mean goes up slightly, as the discarded data showed lower $\epsilon_{F\max}$ than actually occurred.

Still this is an important step to ensure that the reported decrease in $\epsilon_{F\max}$ with bloom strength is an actual trend. Again G120 is an exception to the trend.

7.2.5 The Relation between Renaturation and Mechanical Properties

The final remaining question is: what type of relation exists between renaturation and the mechanical properties of the animal glue. To allow evaluation of this relation, the double bloom strength of technical gelatins should be converted to single bloom strengths. According to the manufacturer, as a rule of thumb, dividing by a factor three should convert double bloom strengths to single bloom strengths [11].

As can be seen from Figure 7.5, the data strongly suggests a linear relation between bloom strength and $\sigma_{\max}$, and thus between renaturation and $\sigma_{\max}$. This is backed by the results found in Bigi et al. that show an approximately linear relation between the breaking stress and the bloom strength, though the author did not report this trend [4].

Again G120 has a higher strength than expected on basis of its bloom strength. As L330 shows some deviation too, this might be related to the fact that their average thickness was different from that of the other types of glue, as said before for thin films strength no longer scales linearly with cross-sectional area.

As G120 was clearly off, it was decided to exclude it from the linear fit. The formula describing the linear fit in Figure 7.5 is $\sigma_{\max} = 0.20 \cdot \mathrm{x} + 35$ were x is the bloom strength in

Table 7.4: Comparison of the $\varepsilon_{\mathrm{F}_{\max}}$ for an uncorrected (left) and corrected (right) dataset.

Sample ID	$\boldsymbol{\varepsilon_{\mathrm{F}_{\max}}}$	**Sample ID**	$\boldsymbol{\varepsilon_{\mathrm{F}_{\max}}}$
G240 (n=39)	2.6 ± 0.93	**G240 (n=33)**	2.7 ± 0.94
G180 (n=37)	1.7 ± 0.64	**G180 (n=24)**	1.9 ± 0.68
G120 (n=38)	1.8 ± 0.52	**G120 (n=27)**	1.9 ± 0.52
L330 (n=37)	1.2 ± 0.28	**L330 (n=33)**	1.2 ± 0.28
L180 (n=38)	0.93 ± 0.35	**L180 (n=23)**	1.0 ± 0.27

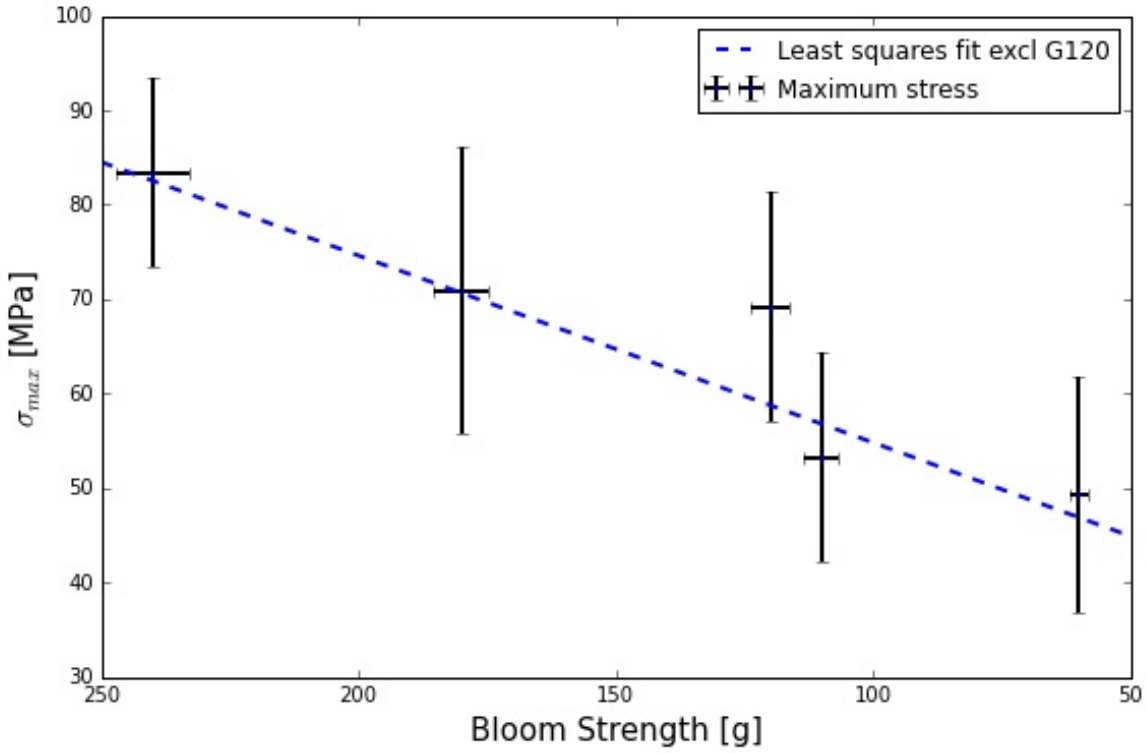

Figure 7.5: Graph of $\sigma_{\max}$ versus bloom strength. It can be clearly seen that the glue at 120 g bloom, G120, performs above average. The standard deviation in bloom strength is taken to be 3%, the maximum deviations found between laboratories [12].

grams. Using this formula, a theoretical strength can be calculated for pure glues[1] between 240 g and 60 g bloom.

Though the formula can be used for higher and lower bloom strengths, a limit might exist. Some very low bloom strength glues exhibit no gelling during drying, indicating that no significant degree of helicity is obtained. For such a case this formula might not work.

Neither is this formula representative for glues made from different collagen sources. Though most mammalian glues might be rather comparable, fish glues will definitively not adhere to this trend as their Pro and Hyp content is markedly lower and Hyp plays an important role in helix formation.

Finally, the formula may be limited to gelatin films of comparable thickness to the films used in this experiment.

7.3 Conclusions on the Tensile Tests

After close inspection of the data and correcting for the most important factors, the initial observation still holds. The E-modulus is approximately constant for all samples while $\sigma_{\max}$ decreases with bloom strength. According to Hook's law this implies that $\epsilon_{F\max}$ decreases with bloom strength too. This trend is indeed visible in the means of $\epsilon_{F\max}$, though the standard deviation inhibits strong conclusions.

Returning to the hypothesis (Section 7.1), the following can be concluded. Though stress and strain at break have not been investigated, it seems acceptable to expect the same relationship for the stress and strain at maximum load. The stress and strain at maximum load indeed show

[1] With small amounts of Mergal KM90

an increase with bloom strength, the former more evidently then the latter. Based on the current experiments, and backed by data from literature [4], a linear relation is proposed between bloom strength and maximum stress. The formula describing this linear fit is $\sigma_{\max} = 0.20 \cdot \mathrm{x} + 35$ were x is the bloom strength in grams.

It turned out that E did not follow the expected behaviour. Instead of increasing with bloom strength, it remained constant at approximately 4.6 GPa. Based on a thorough comparison of the tests, the most likely explanation is that E is constant in glassy gelatin and gets approximately linear to bloom strength in the rubbery domain. This means that the effect of renaturation on E is best described by a cross-linking model.

The results gave an indication of the repeatability and reproducibility too. It turned out that the repeatability can still be improved as quite some differences between the films existed. The repeatability, however, was good, showing the effect of the carefully execution of the drying step.

Chapter 8

Film Quality Assessment using Differential Scanning Calorimetry

Following the discussion on the mechanical tests in Chapter 7, it is time to shift attention to film quality assessment using DSC. The hypothesis, describing the expected results, can be found in Section 8.1. Section 8.2 shows the results obtained, leading to the conclusions presented in Section 8.3

8.1 Hypothesis

The principle of using DSC in gelatin film quality assessment had been explained in Section 3.4.1. The enthalpy of melting of the gelatin should provide a measure of the triple-helix content of the sample. This renaturation level is expected to decrease linearly with bloom strength [4].

Also, as the MWD of the glue decreases, the T_m is expected to shift to lower temperatures.

8.2 Results and Discussion of the DSC Analysis

This section presents the DSC results. All DSC curves can be found in Appendix E. This section first discusses which DSC analyses are usable, in Section 8.2.1, before analysing the various curves in Section 8.2.2.

8.2.1 Discarded Data

The DSC data turned out to be hard to reproduce. Figure 8.1 shows the four curves that were measured on the four sheets of G240. As can be seen, the curves of the sheets made in Delft, reasonably agree up to approximately 170 °C. The first sheet made in the AG has a different melting trajectory and a different melting temperature, while the second sheet made at the AG does not show any signs of being the same material. It is even hard to detect an approximate onset of the melting peak with any certainty.

Curves like G240RMA2 have to be discarded from the data set. Inspection of the curves presented in Appendix E shows that the curves listed in Table 8.1 have to be discarded.

Table 8.1: List of discarded Differential Scanning Calorimetry curves.

Sample ID			
G240RMA2	G180D1	G120D2	L180D2

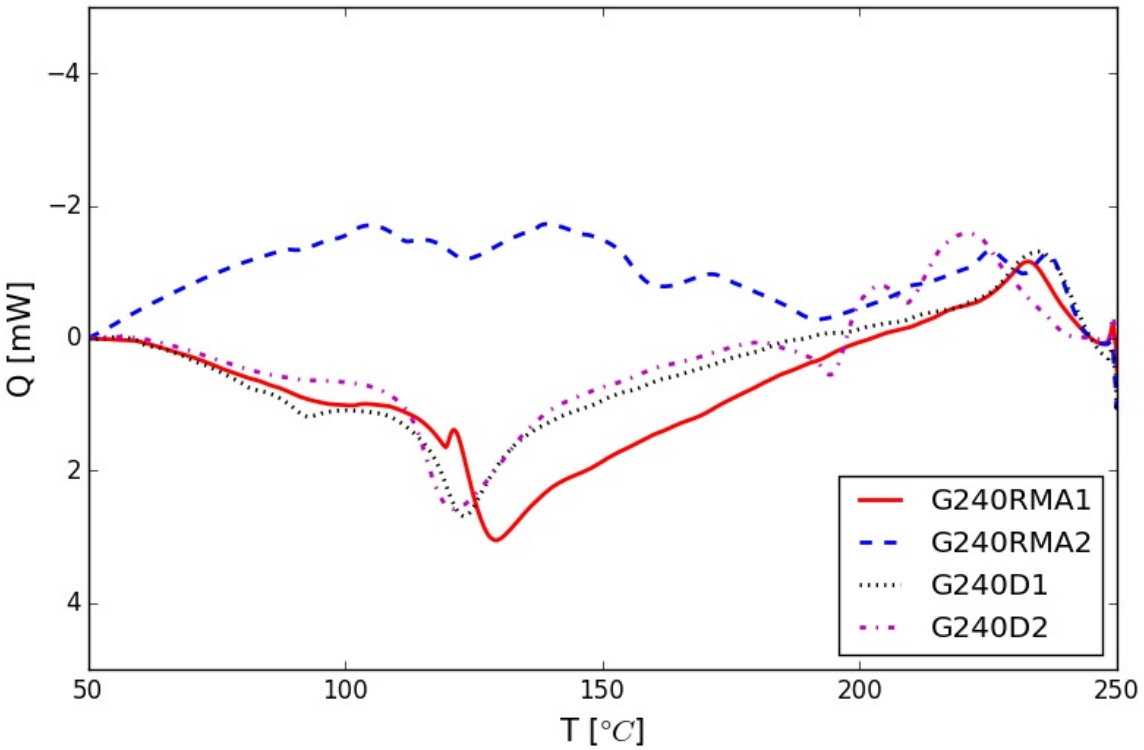

Figure 8.1: DSC curves of the sheets of G240. Note how the curves of the sheets made in Delft seem comparable, and how the first sheet made in the Atelier Gebouw shows the same trends. However, G240RMA2 shows a behaviour that does not allow useful information to be extracted, and has to be removed.

8.2.2 Results

It is hard to identify all events on the DSC curves. Sometimes events do not seem to match between comparable films. A clear example is shown in Figure 8.2, where G180RMA1 seems to have a double melting peak as the baseline seems to remain approximately at the same level, however, the other two graphs show a clear jump in baseline, which can be associated with the release of internal stresses. As mentioned in Section 6.3.3, all sheets showed signs of internal stresses. It is therefore likely that a relaxation event associated to that shows up in the DSC curve.

These stresses result from the gelling of gelatin. During gelling triple-helices more or less lock the molecules' relative positions before shrinking due to a loss of water. The position of the relaxation in the DSC curves corresponds with such a theory, as the relaxation happens once the triple-helices have melted.

Based on this theory, the interpretation of the DSC results gets easier. Though quantitative information cannot be obtained, it reveals that all curves show the same three regions (See Figure 8.2), namely T_g, T_m, and the relaxation event. The confidence that this is a correct interpretation is not so much based on each curve following the same reproducible pattern, but mostly on each curve showing approximately the same type of events as a few very clear curves (e.g. G180RMA2, G180D2, and the conditioned sample of L180RMA1).

With this theory in mind it is interesting to see that L330D1 (Figure E.8) shows no relaxation at all. This sheet has been exposed to a humidity of 90-100% for multiple days, just after drying (See Section 6.3.3). This means that the sheet has been kept at temperatures above its T_g for several days. This might explain the lack of remaining internal stresses.

The quantitative information that could be extracted from all remaining graphs was the

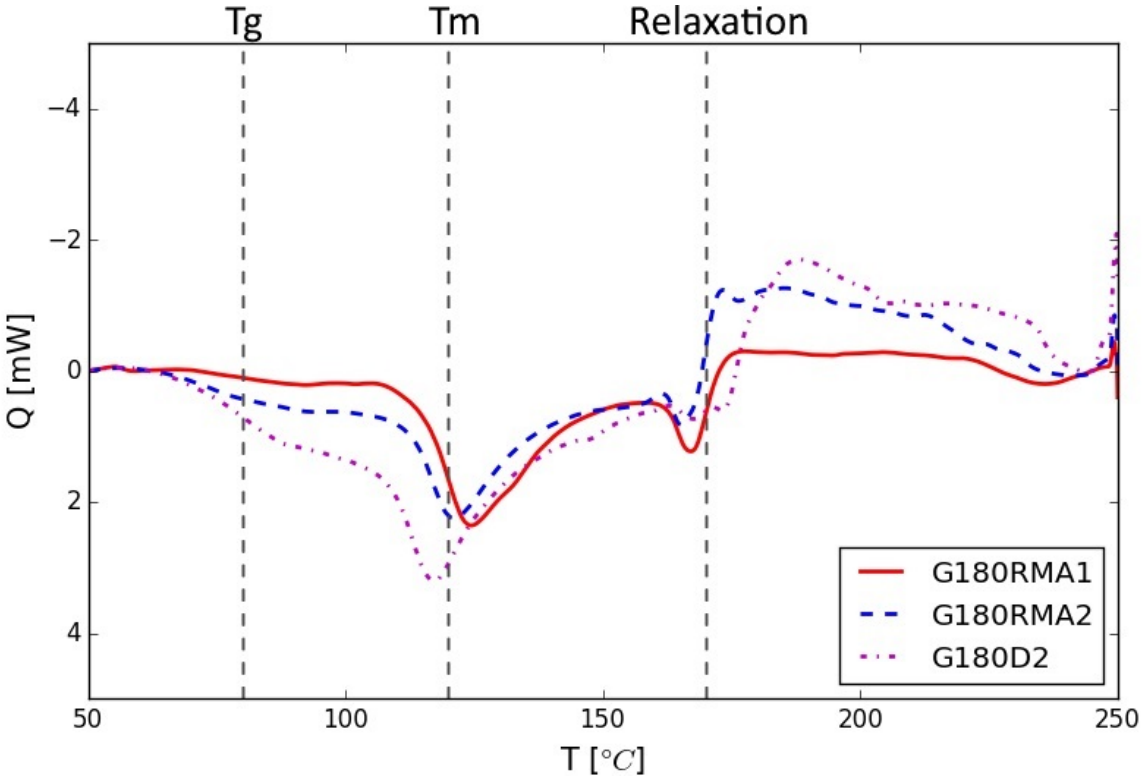

Figure 8.2: DSC curves of the sheets of G180 showing the three regions identifiable in all DSC curves. The first vertical line shows the region of the T_g, which is very faint in G180RMA1. The second line shows the region of the melting peaks. The last vertical line indicates the region of the relaxation event.

onset of the melting peak. Or at least an approximation, as the peak was not always well defined. This onset is reported as T_m in Table 8.2.

Table 8.2 shows no clear trend in T_m. The variations between the values may result from various factors including inhomogeneities in sheets, both in thickness and in thermal history, and varying levels of internal stresses.

The curves shown up to now were unconditioned. The curves for the conditioned samples show better defined peaks. For each curve the onset and offset of the melting curve has been determined. Also the area of the peak was determined as the area between the curve and the line formed by connecting the onset and the offset (See Figure 8.3). The following areas were found: 24.09, 36.72, 22.30, 39.77, 11.98. Clearly there is no direct relation between the measured peak area and the type of glue. The onset of the melting peak was determined to be 123.7, 114.3, 110.2, 111.5, 104.1, and though they show an overall decrease with bloom strength, no conclusion can be drawn, especially as the data reported in Table 8.2 did not show such a relation.

Table 8.2: T_m reported as the onset of the melting peak.

	G240	**G180**	**G120**	**L330**	**L180**
RMA1	121.1	114.8	115.6	103.7	105.0
RMA2		112.6	104.2	100.7	107.5
D1	114.8		105.8	107.7	96.3
D2	111.8	108.9		104.0	

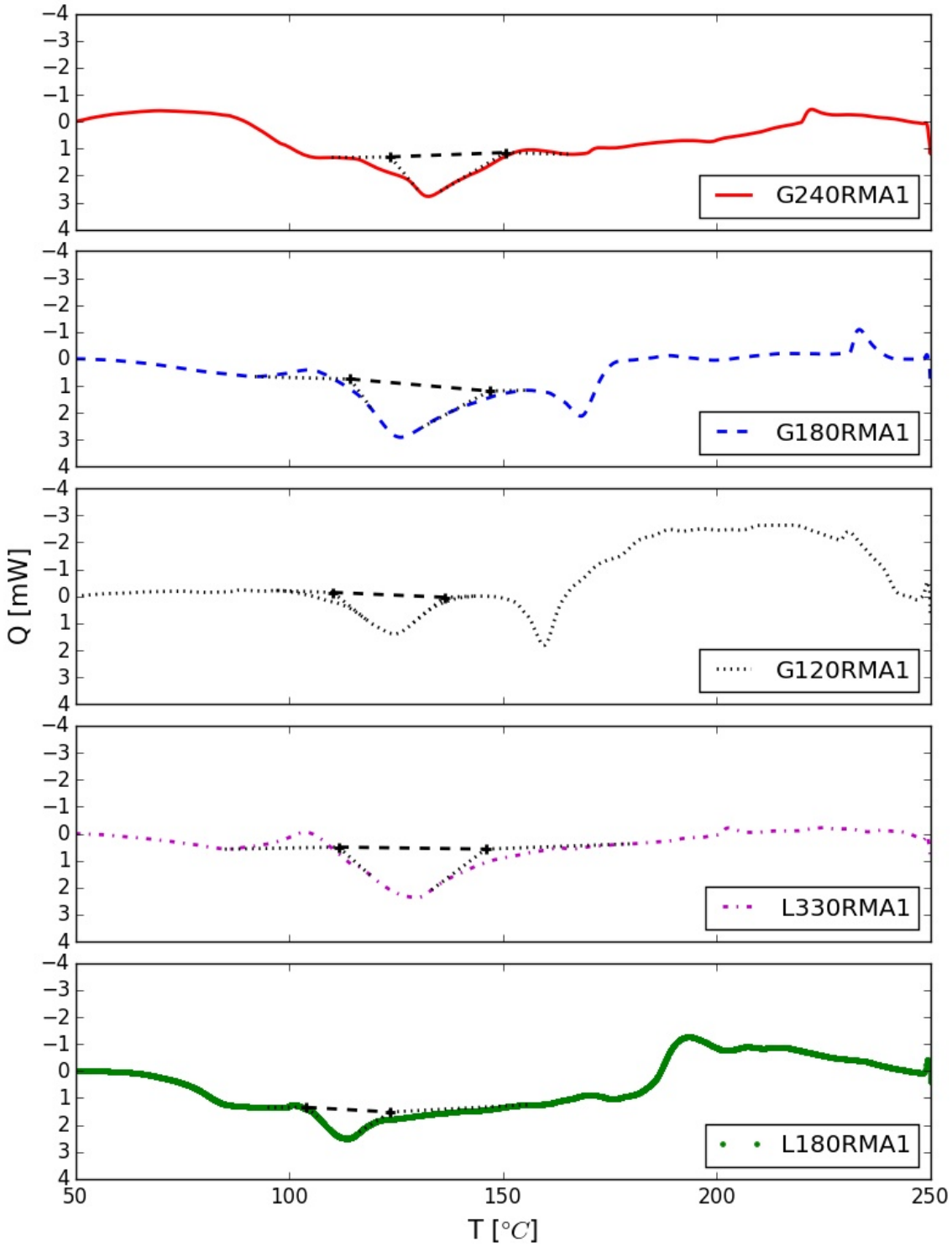

Figure 8.3: DSC curves of the RMA1 sheets after conditioning. The dotted lines show how the onset and offset were determined, while the dashed line shows the approximated baseline using in calculating the peak area.

The failure to produce reproducible DSC curves may have several causes. Of course there is the effect of the glues being mixtures, though this has not posed to be a problem in the experiments of Yakimets et al., Bigi et al., and Kotch et al. [4, 19, 33].

Another factor, which might be important, is the variation in internal stresses. Though the glues were dried under comparable conditions, within a sheet the internal stresses vary, leading to differences in internal stresses for samples cut from various parts of the sheet.

However, the most important factor might be the use of common aluminium pans instead of pressure pans or hermetically sealed pans.The loss of water during the test can be considerable. A TGA test (See Figure 8.4) shows that even unconditioned samples loose up to 10% of water when heated to 250 °C. This loss of water could not be prevented by using high heating rates though it could be delayed.

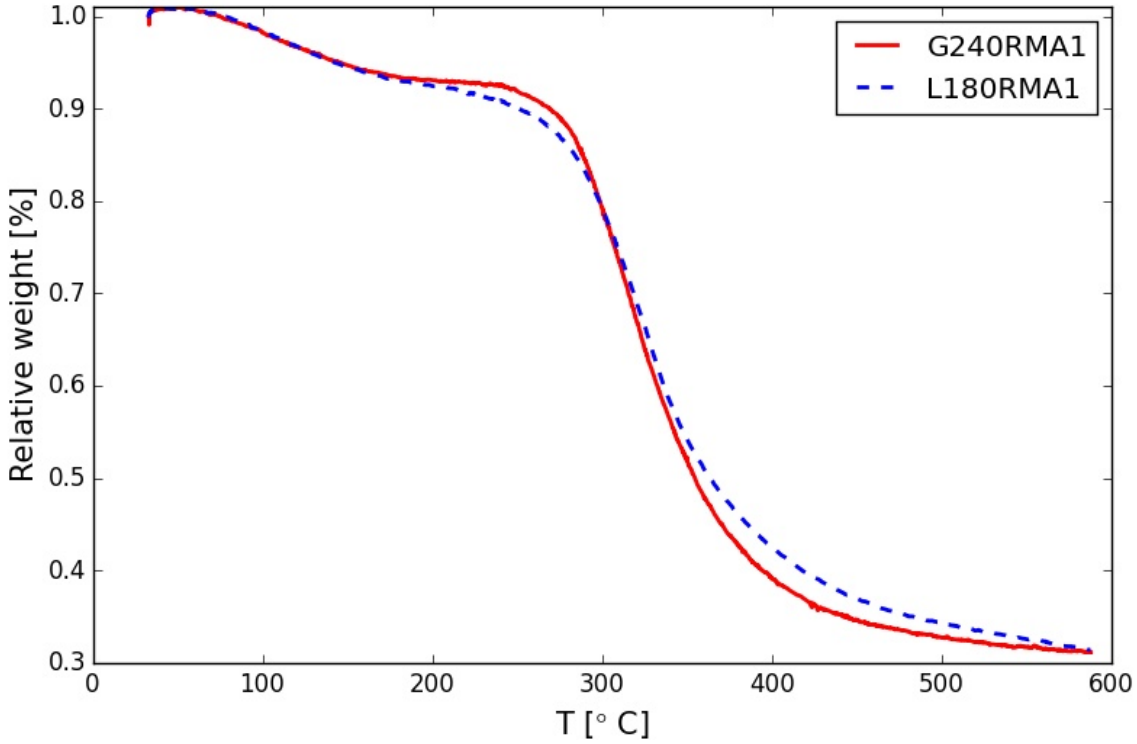

Figure 8.4: TGA curve of two unconditioned glues, showing water evaporation and thermal degradation.

8.3 Conclusions on the DSC Analysis

Based on the discussion in the previous section it can be concluded that the DSC results did not confirm the hypothesis. It proved very hard to create an useful and reproducible DSC-curve.

The hypothesis had been derived based on literature. However, those experiments used hermetically sealed pans, preventing the loss of water which can be significant in gelatin. This water evaporation might partially explain the broad and ill-defined peaks in the current DSC curves.

Despite the unsatisfactory quantitative results, a qualitative analysis of the curves showed that three main events were present in all curves, namely T_g, T_m, and a relaxation related to internal stresses. This shows that an improved test set-up might not only provide an answer to questions regarding renaturation levels, but also present additional information on the internal stress, giving more insight into the quality of the sample production. Thus, though its current value is limited, DSC is believed to be a valuable tool in assessing the animal glue film quality.

Chapter 9

Film Quality Assessment using X-Ray Diffraction

Like Chapter 8 this chapter treats film quality assessment. This time the investigated method is XRD. The hypothesis is presented in Section 9.1. Then the results and discussion follow in Section 9.2. The final section, Section 9.3, presents the conclusions.

9.1 Hypothesis

The principles of using XRD in film quality assessment have been laid out in Section 3.4.2. As explained, the repeating pattern giving rise to constructive interference is the inner diameter of the triple-helix, measuring 1.1 nm. This distance should give a peak at 8 °2ϑ, for a X-ray source of CuKα radiation.

The samples differ by bloom strength and thus, as shown in Section 3.3.3, by renaturation level. A higher renaturation level should result in a higher peak in the XRD diffractogram.

9.2 Results and Discussion of the XRD Analysis

This section presents the results found during XRD analysis of the animal glue samples. All diffractograms can be found in Appendix F. This section starts of with a discussion regarding the validity of the XRD data in Section 9.2.1, before analysing the various diffractograms in Section 9.2.2.

9.2.1 Reproducibility of the XRD Analysis

XRD measures angles with respect to the sample. Therefore, it is important that the sample is in the same location each consecutive measurement. To ensure this, a grey gummy was applied in the sample holder to keep all gelatin samples at the correct height and level with the rim of the sample holder.

In highly crystalline materials, the detected X-rays result from crystals up to a couple of angstroms below the surface. In such a case thickness nor gummy has an influence on the results.

However, as can be seen from the comparison of Figure 9.1a with 9.1b, signals of the gummy were detected through the animal glue samples. The reason is that the gelatin is mostly amorphous and only scatters a part of the X-rays and let the remainder pass. This is backed up by the rather low intensities measured.

On the other hand, the response of the gummy under the animal glue is dampened compared to the response of the pure gummy, so a significant part of detected the X-rays must still result from the animal glue.

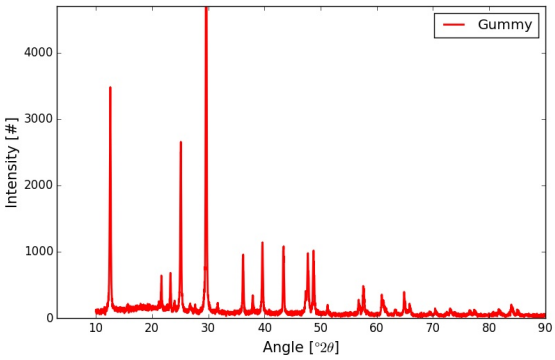

(a) Diffractogram of the gummy used in sample positioning. The peak at 29.62 °2ϑ has an intensity of 7630.

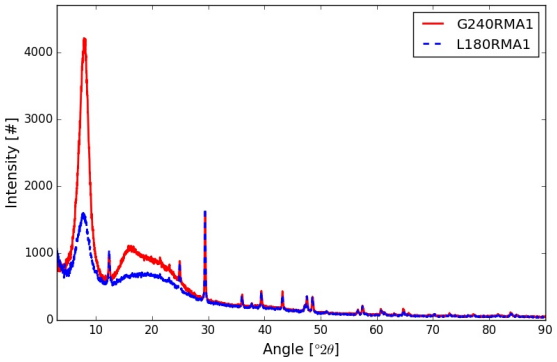

(b) Diffractogram of G240RMA1 and L180RMA1 over a larger domain.

Figure 9.1: XRD diffractograms showing the response of the gummy and its effect on the animal glue diffractograms.

This leads to an intricate problem, as the thickness of the gelatin is now a factor in the resulting diffractograms. The question is whether the influence of small variations in thickness have a significant influence on the test results. Two factors play contradicting roles. As gelatin scatters only small amounts of the X-rays, additional thickness influences the results. On the other hand, the additional gelatin will still only scatter a small part of the incoming radiation. As the gummy fully scatters the remaining X-rays, no radiation will reflect back trough the material further limiting the influence of the additional thickness.

The best way to determine whether significant thickness effects play a role, is by comparing independent analyses. As peak intensity may be influenced by more than one factor, not the absolute peak intensity but the ratio between peak intensities was investigated.

To do so, the ratio between the peak intensity of G240RMA1 and the other RMA1 sheets was determined and compared. This was done separately for the conditioned and unconditioned samples. The results are shown in Table 9.1.

Comparison of the peak intensity ratios shows variation up to 3.7%. However, besides the thickness, also the conditioning is a variable. Furthermore, machine accuracy may play a role. To get a better idea of the possible influence of the latter two effects, the ratio between the conditioned samples of G240RMA1 and L180RMA1 were compared for the XRD analysis over the short and the longer domain. These two analyses were performed on the same sample only several hours apart. This should give an idea about the combination of machine accuracy and the effect of (possible) water loss.

Table 9.1: Ratios between the diffractogram peaks of the types of animal glue for the unconditioned and conditioned films. G240RMA is taken as a baseline. The final column shows the agreement between the ratios.

Ratio	**Unconditioned**	**Conditioned**	**Agreement [%]**
G240RMA1	1	1	100
G180RMA1	0.916	0.944	97.1
G120RMA1	0.626	0.646	96.9
L330RMA1	0.437	0.454	96.3
L180RMA1	0.371	0.378	98.3

The peak intensity ratio of the conditioned sample measured over a short domain was presented in the table and equalled 0.378. For the longer domain the ratio turned out to be 0.385. The difference between the two was 2.0%. This difference is very comparable to the difference between the same ratio for the conditioned and unconditioned samples.

Therefore, based on the results, there is no need to believe that the XRD analyses are inherently invalid to use, though care should be exercised as small differences between the diffractograms may fall within this possible uncertainty.

9.2.2 Results

The main result to obtain from the XRD diffractograms is a measure of the renaturation of the animal glue. There are two possible approaches. One is to compare peak intensities, the other is to compare the integrated peak intensities. As the peaks are not sharply defined, and even less so with decreasing bloom strength, integrated intensity may prove the better measure. Figure 9.2 shows the integrated intensities for the unconditioned samples, while Figure 9.3 shows them for the conditioned ones.

The integrated intensities are decreasing with bloom strength both for the conditioned and unconditioned samples. Of course, when comparing the series, some individual series within one type may have higher or lower integrated intensities, however, the mean clearly decreases with bloom strength.

Figure 9.2 backs the conclusion made in Chapter 7 that the reproducibility of the films was good. It even seems to indicate that the the repeatability was high for the films made at the AG. However, the latter conclusion is based on results that have been determined using one sample per film.

As indicated before, the large difference between G120 and L330 cannot be explained purely on basis of the bloom strength, as their bloom strengths are close together.

Therefore it is interesting to evaluate whether the integrated intensities give a linear relation

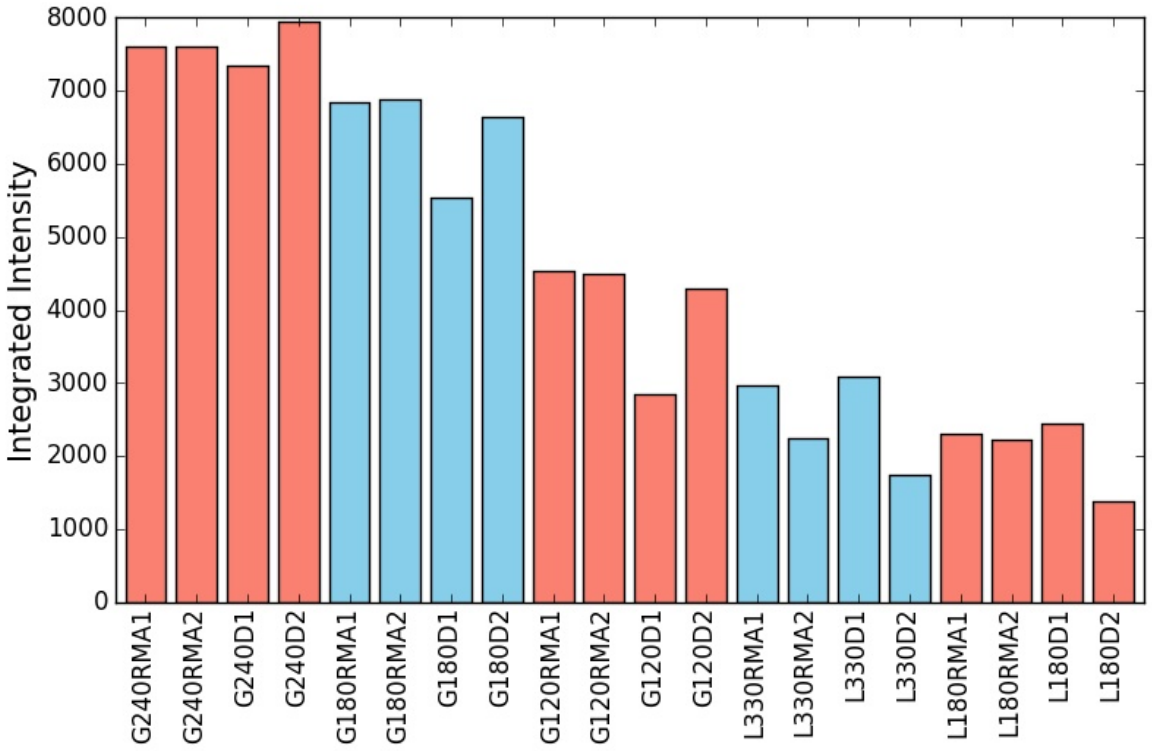

Figure 9.2: Integrated intensity of the XRD diffractograms of the unconditioned samples.

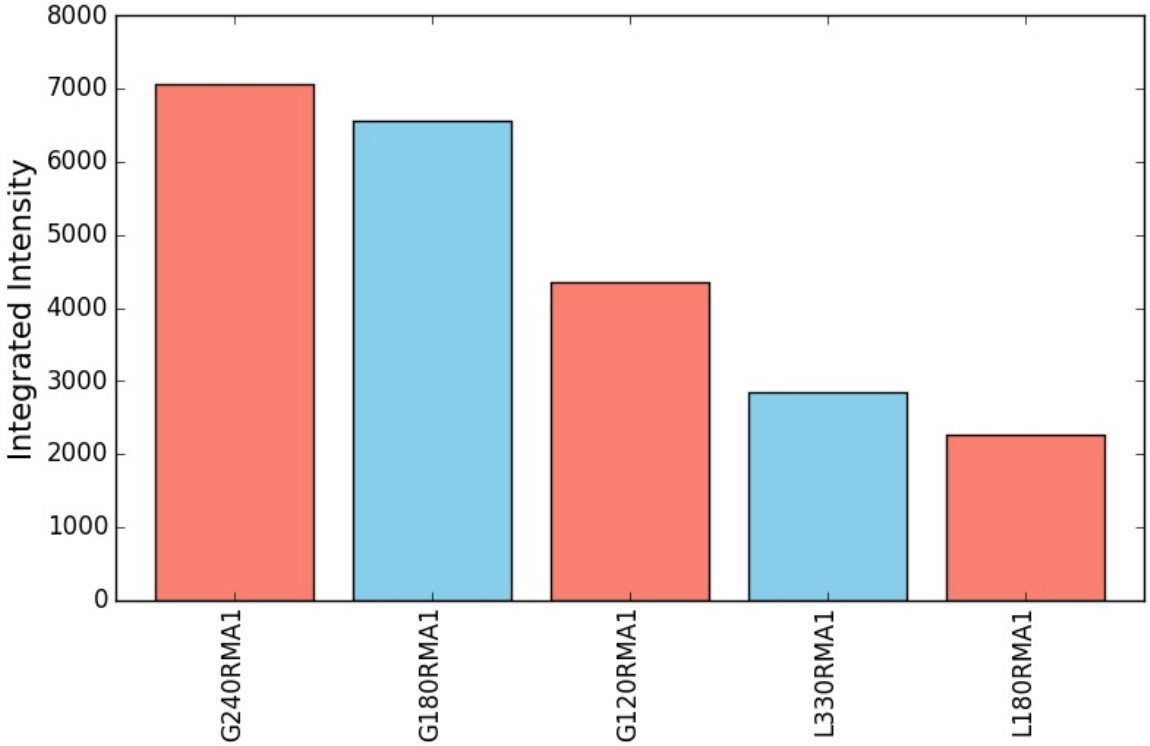

Figure 9.3: Integrated intensity of the XRD diffractograms of the conditioned samples

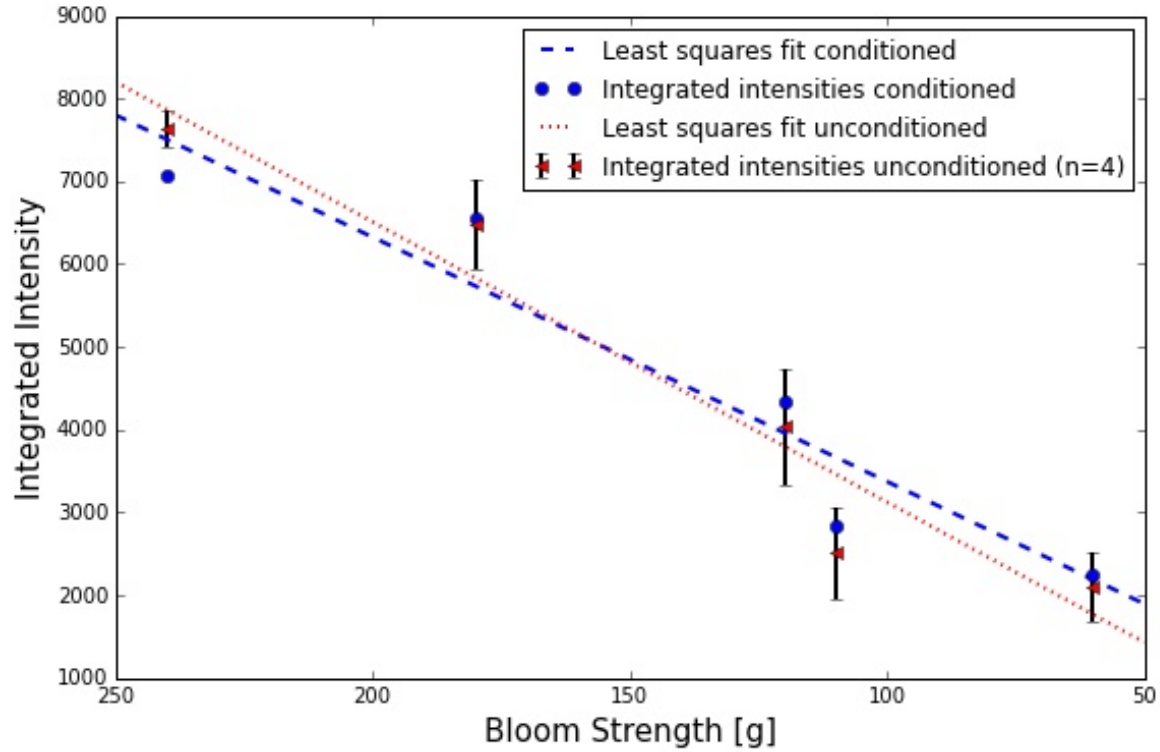

Figure 9.4: Integrated intensity of the XRD diffractograms of the conditioned and unconditioned samples versus their single bloom strength.

with bloom strength. Figure 9.4 shows a linear approximation for both the conditioned and unconditioned samples. As can be seen, both show a linear relation, though water does affect the behaviour a bit. However, for all but G240RMA1 the change is within one standard deviation. In this analysis it shows that L330 and G180 conform the least to the linear relation.

9.3 Conclusions on the XRD Analysis

The results that were presented confirmed the hypothesis. The XRD diffractograms showed a peak around 8 °2ϑ, with its integrated intensity decreasing linearly with bloom strength.

Thus it can be concluded that XRD is a good technique to check for renaturation in gelatin. It should be said though, that further research should take care of the issues described in Section 9.2.1. Possible solutions could include stacking multiple layers of gelatin, carefully tracking thickness. This would not only solve uncertainty due to thickness variations, but also improve the signal strength.

Besides confirming the hypothesis, the results showed information on repeatability and reproducibility too. It turned out that reproducibility is good, though the relations between the films are not the same as those found in Chapter 7. This may indicate that the helix content in a film is not homogeneous.

Chapter 10

Additionally Investigated Techniques

This chapter describes a series of additional experiments that have been carried out, but did not yield sufficient data to treat them in separate chapters. It starts with the creep test in Section 10.1, followed by the FTIR analyses in Section 10.2. The chapter closes by describing the polarised light experiments in Section 10.3.

10.1 Creep Tests

This section treats the creep experiment. It starts with describing the problems that were encountered during the start-up phase of the experiment and the improvements that were made to solve them in Section 10.1.1. Secondly, the results are shown in Section 10.1.2, followed by an evaluation of the test in Section 10.1.3.

10.1.1 Creep Method Development

The first creep test method, as described in Section 4.2.3.2 used the creep bench mostly as it was provided. The only addition was to tape rubber to the clamps, to prevent the animal glue films from early failure. However, the first trail tests showed that the tape was pulled out of the clamps, as the tape started to creep. On top of that, the weights that were used to strain the sample, were difficult to use, as the smallest step in weight was nearly 1 kg. Besides, none of the weights was actually identical, leading to different weights on the first and second sample in the creep bench.

In order to improve the creep bench, two modifications were made. The first one was to glue the rubber lining to the clamps, using a cyanoacrylate adhesive, a solution that had proven advantageous in the tensile tests. The second modification was to make a better weight application system. This was done using variable weights, basically hollow containers that could be filled with heavy particles up to the desired weight, allowing better control over total weight and reducing the differences between the weights applied to the first and second sample in the creep bench.

This defined the second creep test method, and after a test run it turned out that the initial problems were solved. However, when a new test was started, it turned out that at some point during the test the reflective surfaces started to tilt due to the fact that the load application was slightly off the sample axis. This required a few small modifications in the positioning of the pulleys used for the load application. Meanwhile it turned out that the maximum number of measurements was reached before the sample had failed, so it was decided to increase the force on the samples.

This led to creep test method three, the final method that was put to use. Its results are subject of Section 10.1.2.

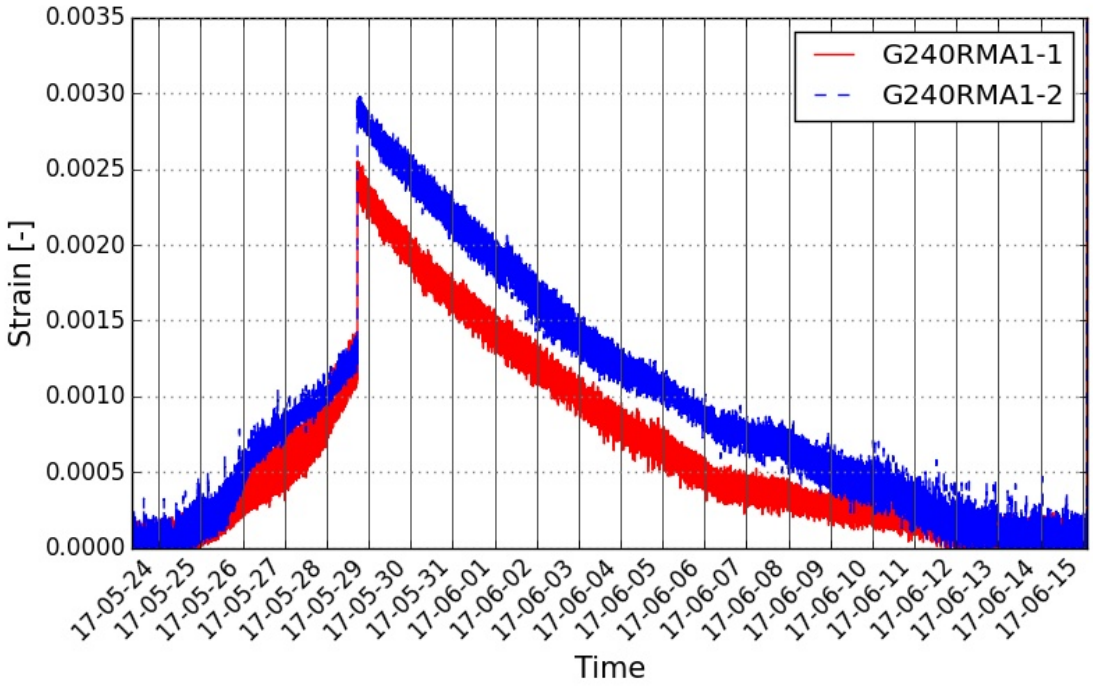

Figure 10.1: Results of the creep tests carried out according to method three.

10.1.2 Creep Test Results

The results of this final creep test are shown in Figure 10.1. The high levels of noise partially result from the climate chambers ventilation system, as it causes movement of the reflecting surfaces.

As can be seen, the first five days show a normal creep pattern. The sixth day, however, shows an sudden event that is not a material response. The further development of the curve is unexpected too, as right after the event, the strain decreases again, until it reaches near zero. Though relaxation can cause the material to contract again, the fact that the contraction exceeds the elongation measured before the event is strange.

Inspection of the samples at the end of the test showed no failure of the specimen, nor any problems with the set-up, leaving the cause of the sudden event unclear.

10.1.3 Evaluation of the Creep Test

It turned out that due to the long runtime of a creep test, no additional creep tests could be performed within the allocated time for this thesis.

As mentioned, the available data is hard to interpret due to an unexpected event. Furthermore, only two measurements were available, rendering statistics on the first five days of the test invalid. Therefore, no use can be made from the results of the creep test.

The main reason that insufficient tests have been carried out is that the creep bench had never before been used to test gelatin samples. It therefore required several modifications and test runs, leaving little time for the real experiments.

10.2 Film Quality Assessment using Fourier Transform Infrared Spectroscopy

Film quality assessment was the subject of Chapters 8, and 9. This section treats the use of FTIR in film quality assessment. Section 10.2.1 presents the research question. The results

and discussion are subject of Section 10.2.2. Finally, the section closes with an overview of the conclusions, as presented in Section 10.2.3.

10.2.1 Research Question

A short explanation of the relevance of FTIR in the context of gelatin film quality evaluation has been given in Section 3.4.3. The article by Yakimets et al. shows the described phenomenon for FTIR in transmission mode [33]. However, due to availability of scientific facilities, transmission FTIR could not be used, therefore the following research question was formulated: Can the relation between an increase in the triple-helix content and a respective increase and decrease of the 1660 cm^{-1} and 1633 cm^{-1} peaks, as described by Yakimets et al., be found using FTIR in Attenuated Total Reflectance (ATR)-mode?

The use of ATR greatly reduces the effort required to perform the measurement, as virtually no preparation of the sample is required. This is an advantage when put to use in predicting mechanical properties of samples, as the measurements can be made faster and easier.

10.2.2 Results and Discussion of the FTIR Analysis

This section discusses the results found during FTIR analysis of the animal glue samples. The original data, including the discarded spectra, can be found in Appendix G. This section starts by discussing the data that should be discarded in Section 10.2.2.1, followed by a discussion of the results in Section 10.2.2.2.

10.2.2.1 Discarded Data

As all samples were A type porcine hide gelatins, all spectra were expected to look more or less equal. All did, but two. Those were the second analysis of the conditioned sample of G240RMA1 (see Figure G.1), and the the second analysis of the conditioned sample of L330RMA1 (see Figure G.4). Because their behaviour was so different from the other measurements, it was decided to discard them. The deviation of this analysis of L330RMA1 had been observed during the measurements, so a third analysis had been made to replace it.

In further analyses of the data, these two measurements of the samples will not be considered. For L330RMA1 no problems will occur, as an additional measurement had been made. For G240RMA1 this means that more noise will be present in the signal as only one analysis is available for this sample instead of two.

10.2.2.2 Results

In order to analyse the differences between the spectra they should be made as comparable as possible. The first step is to reduce noise by calculating the mean of the two or three spectra made from the same sample at different locations on its surface (See Chapter 4). The second step is to normalise the data. This is done by setting the transmittance value at 2100 cm^{-1} equal to 100%, and the value at 1627 cm^{-1} equal to 0%.

The results of this transformation on the spectra of the unconditioned samples can be found in Figure 10.2. The results of the spectra of the conditioned samples are comparable.

As can be seen, the spectra are nearly the same and differences are hard to tell. Therefore, a differential spectrum has been made. The mean of the five types was subtracted from each spectrum to allow small differences to become more obvious. As specifically the data of the conditioned samples was noisy, a rolling mean with an window of 8 was used to reduce noise. A detail of the differential spectra is presented in Figure 10.3a and 10.3b.

Looking at the 1660 cm^{-1} mark, associated to helical gelatin, it is strange to see that G180RMA1 and L330RMA1 have the same value, while G120RMA1 and L330RMA1, which have approximately the same bloom strength, are very different. Or that L180RMA1 is very

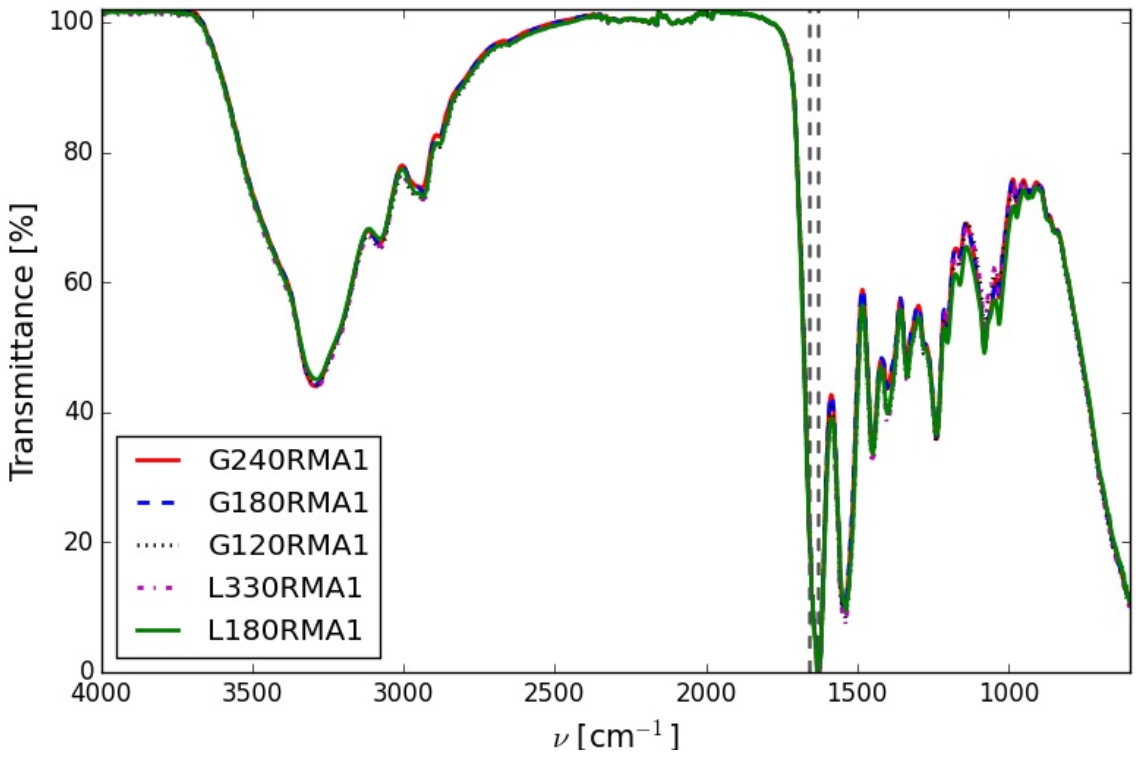

Figure 10.2: Normalised spectra of the unconditioned samples. The dotted lines indicate the location of 1633 cm^{-1} and 1660 cm^{-1}.

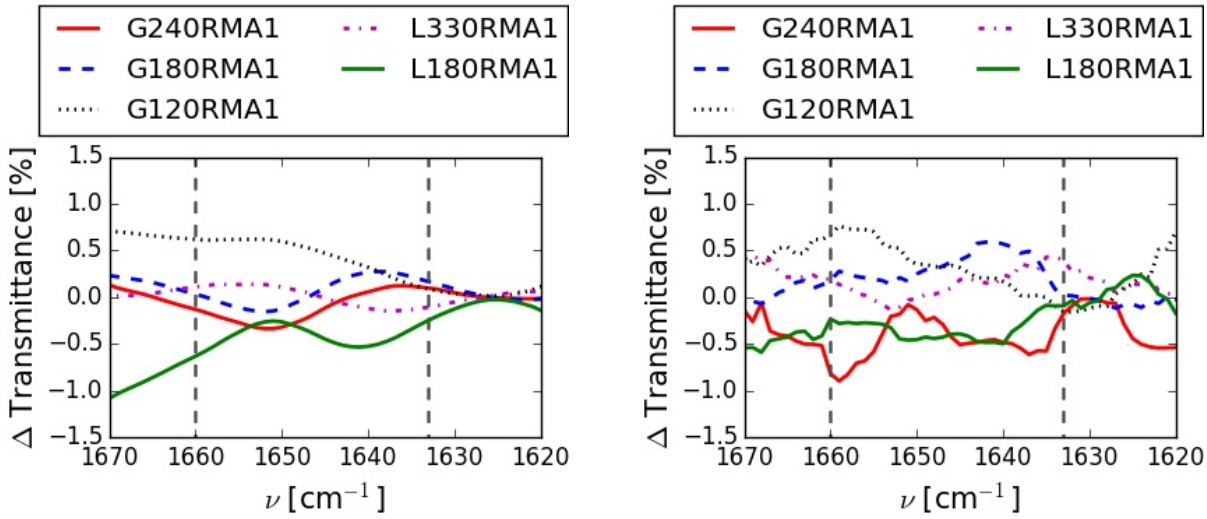

(a) Spectra of the unconditioned samples.

(b) Spectra of the conditioned samples.

Figure 10.3: Detail of the smoothened differential spectra. The dotted lines indicate the location of 1633 cm^{-1} and 1660 cm^{-1}.

close to G240RMA1. These remarks hold for both graphs. Looking at the 1633 cm^{-1} mark, there is no consistent pattern either. More helical gelatin would imply less coiled gelatin, however the relative position changes do not correspond with such a theory.

Care should be taken in the analysis, however, as the relative positions are sensitive to the transformation described earlier. Differences of 3 percent will show in all relevant varieties of the transformation, but differences around one percent may change when a slightly different value is set at 0% transmittance. This means that the observed difference may be to small to detect them given the noise levels present in the signal.

It is important to note that the fact that the relative positions change between the peaks, implies that the spectra of the various animal glues differ. However, it seems not possible to use these changes for film quality control.

The presented results are unsatisfactory. In order to investigate whether this is due to the use of ATR a differential spectrum is created of the conditioned and unconditioned samples. This is done because Yakimets et al. demonstrated the use of FTIR using measurements of films with changing water content [33]. This differential spectrum can be found in Figure 10.4

As can be seen, changes occur around the 1633 cm^{-1} and 1660 cm^{-1} marks. However, they do not reproduce the differences found in the article. The peaks around 1150 cm^{-1} and 1670 cm^{-1} result from hydrogen bonds with **C-O** and **C=O**. The latter is very interesting, as this carbonyl group is part of the peptide backbone of the alpha-chains and has an important influence on the secondary structure of the peptide. However, even when checking versus the corrected tensile results of the RMA1 sheets, the order of the carbonyl peaks is not in line with the expected renaturation, as neither an increase or a decrease of the carbonyl peak with bloom strength is observed. Rather, the order of the peaks seems random.

A final remark that could be made regards the region between 1600 cm^{-1} and 900 cm^{-1}. A very broad peak is visible, that shows a clear distinction between the food grade and technical gelatins. The problem is however, that this pattern cannot relate to the helix content, as in such a case, the spectra of G120RMA1 and L330RMA1 would be close together, as shown in Section 7.2.5. Rather, this pattern shows some difference in composition between the food grade and technical gelatins. Unfortunately not enough information is present to link this peak to specific actors.

Summarising the results, it is clear that no direct link has been found between the FTIR-spectra obtained using ATR and the expected renaturation values, even when taking the tensile test results into account.

It turned out that the difference spectra found by Yakimets et al. could not be reproduced either. This can be explained by the fact that contrary to FTIR in transmission mode, ATR only penetrates a few microns into the sample. For a sample of 130 μm, this is only the surface layer. As the surface layer of a cast gelatin film might be different from its centre, these two methods will give different results. On top of that, differences may exist between the surface that was exposed to air and the surface that was in contact with the plastic during casting. These sides have not been tracked during the tests, so its effect remains unknown.

10.2.3 Conclusions on the FTIR Analysis

In conclusion, it turns out that ATR is unable to yield comparable results to transmission FTIR in analysing gelatin thin films. This likely results from the fact that ATR only analyses the surface layer of the samples.

Therefore, further research into the use of FTIR in animal glue film quality assessment should use FTIR in transmission mode, or device ways to ensure that the bulk of the gelatin film is measured rather then the surface.

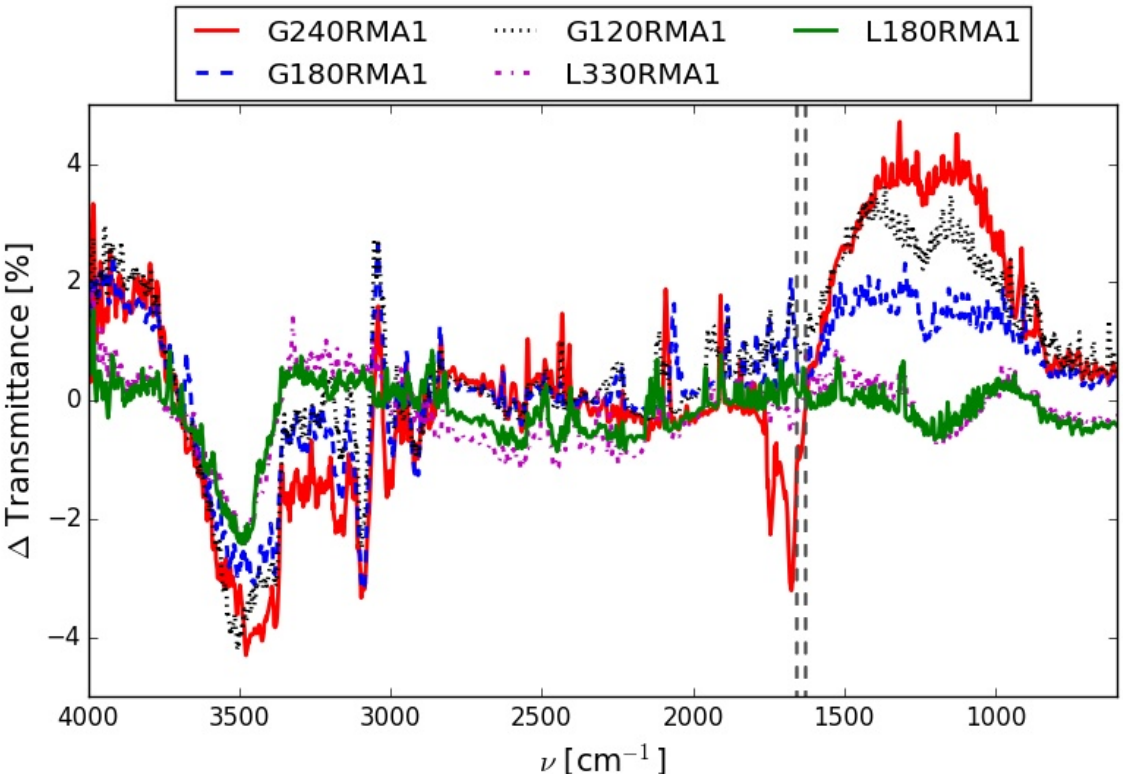

Figure 10.4: Smoothened spectra of the difference between the conditioned and unconditioned samples. The dotted lines indicate the location of 1633 cm^{-1} and 1660 cm^{-1}.

10.3 Polarised Light Experiments

The final experiments used polarised light. A tensile test sample was loaded as described in Section 4.2.4.4 and examined using polarised light. However, no signs of birefringence showed.

Chapter 11

Combined Analysis of the Mechanical Tests and the Quality Control Tests

This chapter aims to combine the information obtained in the previous chapters to investigate the possibilities of using an analysis technique to determine the mechanical properties of a gelatin film in advance. The chapter starts in section 11.1 by showing which techniques should be evaluated. It then continues to this evaluation in Section 11.2. The chapter closes with Section 11.3, presenting the conclusions obtained from the evaluation.

11.1 Relevant Analyses

In Chapter 7 the tensile test data were analysed. The results were mostly in line with the expectation that mechanical properties would increase with bloom strength, except for the behaviour of the E-modulus. This was, however, solved by further analysis of the experiments. The attempts to analyse the triple-helix content of the film were less succesful; out of three tested methods only one yielded a direct quantifiable result.

This chapter will therefore focus on the relation between the results of the XRD analysis and the tensile tests. This decision does not reflect any inherent disability of DSC or FTIR to provide information on the mechanical properties of a gelatin film either by improved set-up or different analysis, but rather the fact that the scope of this thesis is limited to the approach of assessing renaturation.

The potential of DSC to predict strength data once the set-up is improved, is shown by plotting the T_m versus $\sigma_{\max}$, as shown in Figure 11.1. As can be seen, there is a trend, however, the spread in the results is too large to obtain any valid prediction of maximum strength for a gelatin sample. The conditioned samples are closer to a linear trend than the unconditioned ones. Still, one of the conditioned samples is far off the linear trend (at T_m is 111 celsius).

The reason that XRD shows better results is mainly due to a combination of two factors. First, XRD provides a direct measure of helix-content. Second, XRD is independent of water content. DSC for example measures the helix content directly too, but for DSC, water is a notorious problem. FTIR on the other hand does not do a direct measurement, it measures energies and only through comparison of several measurements, a possible measure of renaturation can be made. On top of that, the water content is a major factor in FTIR too.

Seen in the light of the above discussion, it is not surprising that XRD ends up as the best predictor method, followed by DSC, leaving FTIR last.

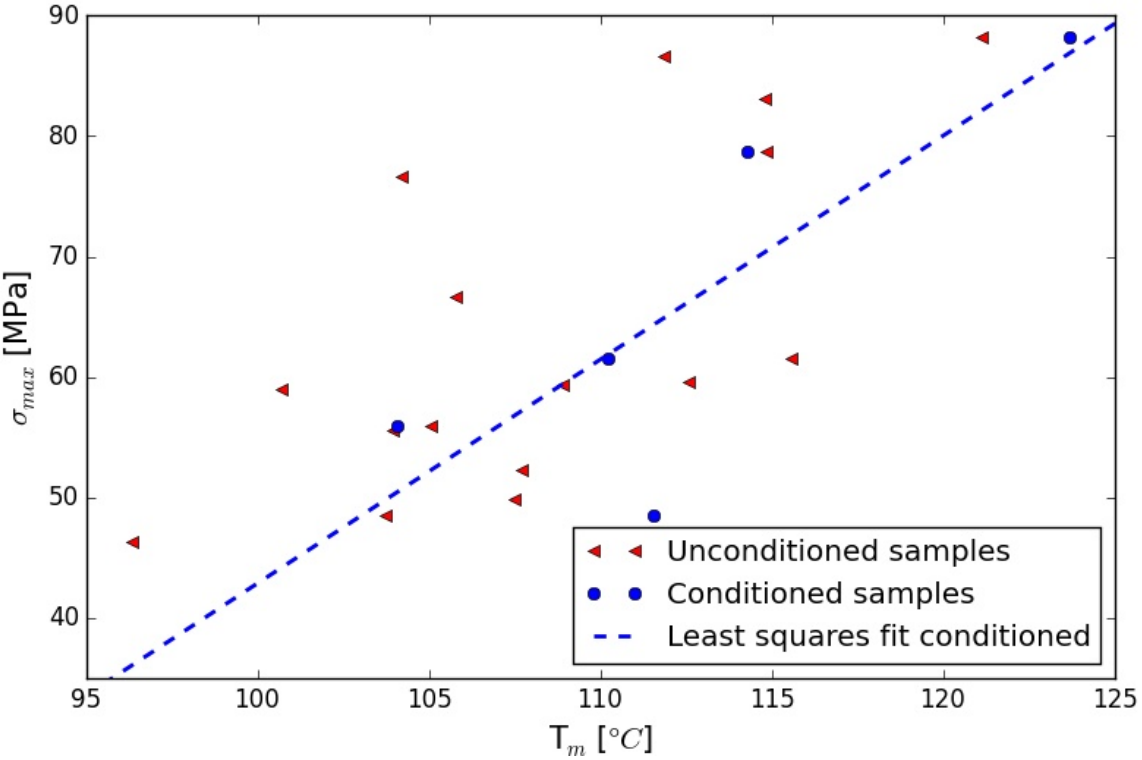

Figure 11.1: Graph showing the mean strength of each series versus T_m.

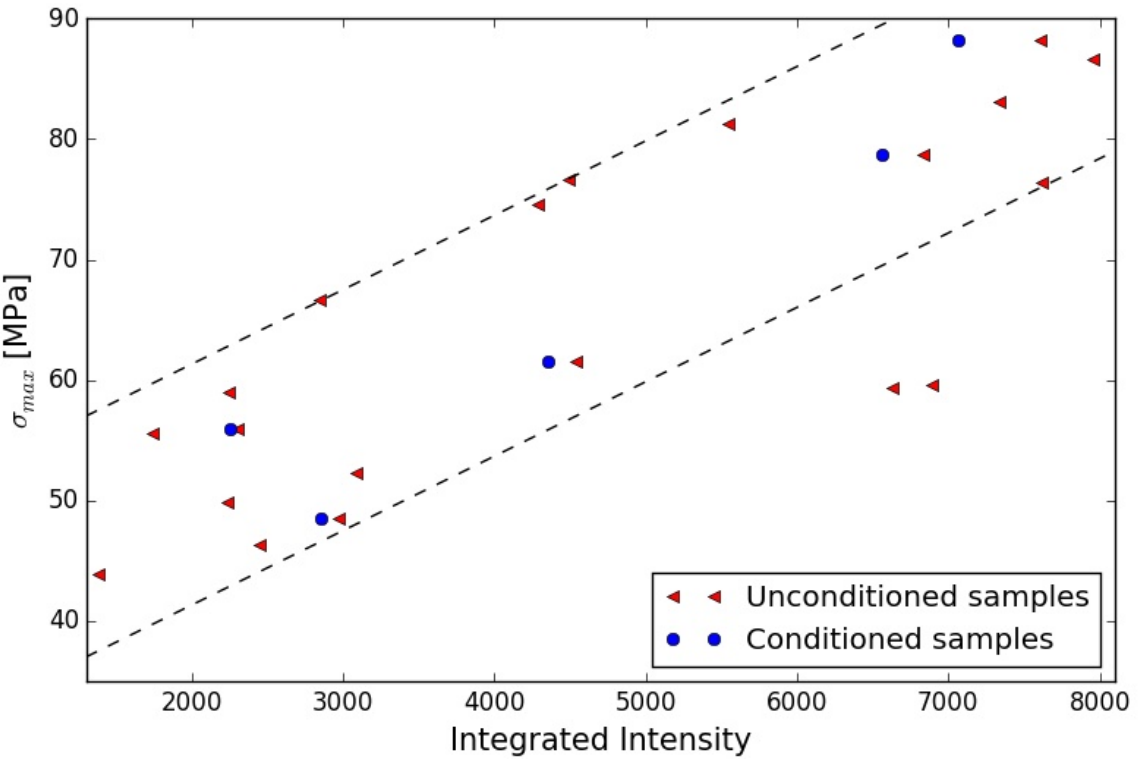

Figure 11.2: Graph showing the mean strength of each series versus the integrated intensity of the triple-helix peak found by XRD.

11.2 XRD in Tensile Strength Prediction

The probability to use XRD as a means of evaluating the quality of gelatin films seems to be successful. Both the tensile tests and the XRD diffractograms, showed a linear relation between bloom strength and the measured parameter. Therefore, it seems reasonable to expect good agreement between the integrated intensities obtained from the XRD diffractograms and the measured maximum tensile strength.

A plot of these variables is shown in Figure 11.2. As can be seen, the agreement is better than that obtained by using the DSC data. Still quite some spread exists. For example, at an integrated intensity of approximately 7000, two samples have a strength of 60 MPa. These are G180RMA2 and G180D2, two series that showed unexpected low maximum strength in the tensile tests. This immediately points out the reason for most of the spread. The XRD measures the helix-content only, while the tensile results follow from a combination of the helix content and geometrical factors, such as stress-raisers and weak spots.

11.3 Conclusions

In conclusion it has been shown that XRD proves a good predictor of tensile strength in gelatin samples. Both from considering the technique as from investigating the relation between the data. However, one should keep in mind that this prediction will only work as long as the mechanical properties of the material dictate the sample behaviour. Once all kind of defects change the behaviour of the sample, the prediction starts to deviate from the observed behaviour.

Chapter 12

Conclusions

The goal of this thesis was to (1) investigate the mechanical properties of a pure animal glue (e.g. maximum strength and E-modulus) and (2) investigate methods to predict the film quality using non-destructive or micro-destructive tests.

Based on the literature study presented in Chapter 3, the triple-helix content or renaturation level of the glue was shown to be key in understanding the mechanical behaviour of the animal glue.

Chapter 7 showed that a linear relation exists between bloom strength and maximum tensile strength with the formula $\sigma_{\max} = 0.20 \cdot \mathrm{x} + 35$ were x is the bloom strength in grams. On top of that, it was shown that a model of the stiffness of gelatin should be based on models describing the effect of cross-linking, as at temperatures lower than the T_g the stiffness was constant at around 4.63 GPa, while experiments from literature report an approximately linear relation with bloom strength at temperatures higher than T_g [4]. In conjunction with Chapters 4 and 5, Chapter 7 showed the merits of using a carefully designed casting process, as this resulted in good reproducibility and sufficient repeatability.

The various techniques to analyse the film quality were presented in Chapters 8, 9, and Section 10.2. The final conclusion arrived at in Chapter 11 is that XRD showed the best relation with the tensile test results, as it directly measured the helix content without being influenced by the water content. The relation between the helix content and the bloom strength found by XRD was a linear one. It was shown that in a different set-up, capable of handling high water contents, DSC would prove useful too. It might even provide more information than XRD as the DSC showed clear relaxation events that can be related to internal stresses. Finally, Section 10.2 showed that FTIR using ATR was unable to provide results, likely hindered by the fact that ATR only measures the surface layer of the gelatin film.

In short, the research question has been fully answered. The mechanical properties of the gelatin have been presented above and it has been proven that XRD is a good and fast method to analyse the film quality. On top of that, the potential of DSC has been shown to exceed XRD in predictive powers by incorporating a measure of internal stress in its results.

It should, however, be noted that the mechanical properties belong to type A porcine hide gelatin. Though the results may prove to be approximately extendible to most mammalian hide glues, they will definitively fall short to describe fish glues and liquid hide glues.

The analyses techniques should work equally for all types of gelatin, as XRD and DSC measure the helices directly, while FTIR relies on the carbonyl group present in the peptide backbone of all collagen types.

Chapter 13

Recommendations

As a final step, several recommendations for future research are presented. The recommendations are grouped by chapter, to allow easier comparison of the obtained results in each chapter and the accompanying recommendations.

The sample production was discussed in Chapter 6. Though casting from dilute solutions turned out to be reproducible, the repeatability likely suffered from small defects in the films. By using a technique which spreads a gelatin gel over a glass plate using a metal knife, more consistent results should be possible, especially regarding thickness homogeneity. As this technique requires a higher viscosity, a more concentrated gelatin solution, or even a gelatin gel should be used. this would reduce the drying time, but could lead to different renaturation levels compared to the samples made with the casting technique.

The mechanical tests presented in Chapter 7 showed that ASTM D882-12 is useful for thin gelatin films. To improve the results obtained in this thesis, a better analysis of sample quality should be used, leading to a more homogeneous sample set. Reducing thickness variations and visible damage will of course be an important factor in this endeavour.

In order to succeed in the use of DSC (Chapter 8) in film quality analysis, the influence of water should be controlled. The most obvious improvement would be the use of pressure pans or hermetically sealed pans. Another improvement could be made by determining the water content of the samples that are analysed using DSC.

The improvement of the XRD results of Chapter 9 could be obtained by monitoring the sample thickness and stacking several samples on top of each other to improve the resulting signal. Increasing the power of the radiation source and decreasing the measurement speed would improve the signal too.

The use of FTIR in ATR-mode, presented in Chapter 10, could be improved by removing the surface layers of the films in order to measure the bulk material. An interesting research question would be whether differences can be found between the centre and either of the surfaces of the gelatin films, this would put the low penetration depth of the ATR-mode to use.

Finally, several questions are still open to discussion. One regards the real effect of water content on helix stability. A possible approach would be to use XRD on samples that have been conditioned in the entire range of humidities ranging from 0% until 90%

Another question is the effect of temperature on the E-modulus, Dynamic Mechanical Analysis (DMA) could prove useful here. It could show whether the proposed explanation of the constant E-modulus is indeed correct.

And, finally, the effect of animal glue source material or the influence of (historic) additives remains an intriguing field of research.

Bibliography

[1] D. Achet and X. He. "Determination of the renaturation level in gelatin films". In: *Polymer* 36.4 (Jan. 1995), pp. 787–791. DOI: 10.1016/0032-3861(95)93109-y.

[2] ASTM International. *ASTM D882-12: Standard Test Method for Tensile Properties of Thin Plastic Sheeting*. 2012.

[3] Betawerk and Auteursgroep 10voorBiologie. *10voorbiologie - biologieonderwijs voor de toekomst*. Accessed on 2017-08-30. 2017. URL: www.10voorbiologie.nl/index.php?cat=9&id=370&par=376&sub=380.

[4] A. Bigi, S. Panzavolta, and K. Rubini. "Relationship between Triple-Helix Content and Mechanical Properties of Gelatin Films". In: *Biomaterials* 25 (2004), pp. 5675–5680.

[5] L. Bratasz. "Allowable Microclimatic Variations in Museums and Historic Buildings: Reviewing the Guidelines". In: *Climate for Collections: Standards and Uncertainties*. Ed. by J. Ashley-Smith, A. Burmester, and M. Eibl. Doerner Institut. 1 Birdcage Walk, London SW1H 9JJ: Archetype Publications Ltd. in association with Doerner Institut, Munich, 2013, pp. 11–19.

[6] A. Cannon. "The age of animal glue". In: *ICOM-CC 17th Triennial Conference Preprints, Melbourne, 15–19 September 2014*. Ed. by J. Bridgland. Paris: International Council of Museums, 2014, p. 8.

[7] C. Cennini. *Het handboek van de kunstenaar*. Trans. by H. V. den Bossche and H. Theuns. Contact, 2001.

[8] A. Coerdt. "Zum Leimen zu gebrauchen: Untersuchungen zu kaltflüssigen Glutinleimen, Teil 1". In: *Restauro: Forum für Restauratoren, Konservatoren und Denkmalpfleger* 113.1 (2007), pp. 32–38.

[9] F. Dawidowsky. *Die Leim- und Gelatine-Fabrikation : eine Darstellung dieses Industriezweiges in seinem ganzen Umfange, mit besonderer Berücksichtigung der Erzeugung von Tischlerleim, von Gelatine, von elastischem und flüssigem Leim, von Kleber-, Eiweiss-, Pflanzen- und Kaseinleim*. Fünfte, vollständig umgearbeitete Auflage. Vol. 15. A. Hartleben's chemisch-technische Bibliothek. A. Hartlebens Verlag, 1919.

[10] R. M. Deurenberg-Wilkinson. "Choosing an Adhesive for Exterior Woodwork through Mechanical Testing". In: *Journal of the American Institute for Conservation* 54.2 (2015), pp. 74–90.

[11] T. Dirks. *Monsters voor onderzoek naar dierlijke lijmen*. Personal Communication. Letter. Jan. 18, 2017.

[12] T. Dirks. *RE: Master thesis animal glue*. Personal communication. E-mail. June 7, 2017.

[13] M. Djabourov. "Architecture of gelatin gels". In: *Contemporary Physics* 29.3 (1988), pp. 273–297.

[14] P. van Duin. “What real museum objects can teach us about the influence of climate conditions”. In: *Climate for Collections: Standards and Uncertainties*. Ed. by J. Ashley-Smith, A. Burmester, and M. Eibl. Doerner Institut. 1 Birdcage Walk, London SW1H 9JJ: Archetype Publications Ltd. in association with Doerner Institut, Munich, 2013, pp. 271–281.

[15] S. Ekelund et al. “The Museum Study of the Climate4Wood research Project”. In: *Heritage Wood: Research & Conservation in the 21st Century*. Ed. by A. Nevin, M. Sawicki, and K. Seymour. 2013.

[16] European Committee for Standardization. *NEN-EN-ISO 9665: Lijmen - Dierlijke lijmen - Methoden voor monsterneming en beproeving*. 2000.

[17] J. M. Greber and E. Lehmann. *Die tierischen Leime: Geschichte, Herstellung, Untersuchung, Verwendung, Patentübersicht*. Th. Schäfer, 2003.

[18] A. Haly and J. Snaith. “Calorimetry of Hat Tail Tendoil Collagen before and after Denaturation: The Heat of Fusion of its Absorbed Water”. In: *Biopolymers* 10 (1971), pp. 1681–1699.

[19] F. W. Kotch, I. A. Guzei, and R. T. Raines. “Stabilization of the collagen triple helix by O-methylation of hydroxyproline residues”. In: *Journal of the American Chemical Society* 130.10 (2008), pp. 2952–2953.

[20] P. Kozlov and G. Burdygina. “The Structure and Properties of Solid Gelatin and the Principles of their Modification”. In: *Polymer* 24 (June 1983), pp. 651–666.

[21] Lexilogos. *L’Encyclopédie ou Dictionnaire raisonné des sciences, des arts et des métiers. dirigée par Diderot & d’Alembert (1751-1772)*. Accessed on 2016-10-05. 2016. URL: `http://www.lexilogos.com/encyclopedie_diderot_alembert.htm`.

[22] J. Maquet et al. “State of Water in Gelatin Solutions and Gels: An H n.m.r. Investigation”. In: *Polymer* 27 (July 1986), pp. 1103–1110.

[23] D. du Monceau. *The Art of Making Various Kinds of Glues*. Trans. by A. Heginbotham. l’Académie Royale des Sciences, 1771.

[24] S. Nijhuis. “Onderzoek naar de toepassing van dierlijke lijm en gelatine voor de restauratie van gefineerde meubelen”. MA thesis. Instituut Collectie Nederland, 2005.

[25] Nitta Gelatin Inc. *Business Activities*. Accessed on 2017-08-30. 2017. URL: `www.nitta-gelatin.co.jp/english/company/business.html`.

[26] T. Presbyter. *Schedula Diversarum Artium*. Trans. by A. Ilg. Vol. VII. Quellenschriften für Kunstgeschichte und Kunsttechnik des Mittelalters und der Renaissance. Otto Zeller Verlag, 1970.

[27] E. Sauer. *Chemie und Fabrikation der tierischen Leime und Gelatine*. Springer-Verlag OHG, 1958.

[28] N. C. Schellmann. “Animal Glues: a Review of their Key Properties Relevant to Conservation”. In: *Studies in Conservation* 52.1 (2007), pp. 55–66.

[29] M. M. Schmidt et al. “Collagen extraction process”. In: *International Food Research Journal* 23.3 (2016), pp. 913–922.

[30] R. Schrieber and H. Gareis. *Gelatine handbook: theory and industrial practice*. John Wiley & Sons, 2007.

[31] T. F. da Silva and A. L. B. Penna. “Colágeno: Características químicas e propriedades funcionais”. In: *Revista do Instituto Adolfo Lutz* 71.3 (2012), pp. 530–539.

[32] B. Skans and P. Michelsen. “Die Bedeutung von Fett in Tierleim für Malzwecke”. In: *Maltechnik-Restauro* 92.2 (1986), pp. 63–71.

[33] I. Yakimets et al. “Mechanical Properties with respect to Water Content of Gelatin Films in Glassy State”. In: *Polymer* 46 (2005), pp. 12577–12585.

[34] C. Young et al. “The mechanical behaviour of adhesives and gap fillers for re-joining panel paintings”. In: *National Gallery technical bulletin* 23 (2002), pp. 83–96.

Appendix A

MERGAL KM90

This appendix includes the Material Safety Data Sheet of the pesticide used to prevent moulding of the glue. The Pesticide was used in a 0.1v% concentration to the water used in the production of the casting solutions, leading to a concentration of 1w% with respect to the dry gelatin weight.

VEILIGHEIDSINFORMATIEBLAD

MERGAL KM90

RUBRIEK 1: Identificatie van de stof of het mengsel en van de vennootschap/onderneming

1.1 Productidentificatie

Productnaam : MERGAL KM90

Productbeschrijving : Niet beschikbaar.

Producttype : Vloeistof.

Overige middelen ter identificatie : Niet beschikbaar.

1.2 Relevant geïdentificeerd gebruik van de stof of het mengsel en ontraden gebruik

Bus-beschermingsmiddel

1.3 Details betreffende de verstrekker van het veiligheidsinformatieblad

e-mail adres van de verantwoordelijke voor dit : B.J. Vernooij, SDS Specialist (vernooib@troycorp.com)

1.4 Telefoonnummer voor noodgevallen

Telefoonnummer voor noodgevallen : +32 (0) 14 58 45 45

Nationaal adviesorgaan/Vergiftigingencentrum

Oostenrijk: Vergiftungsinformationszentrale, 01/406 43 43	België: Antigiftcentrum 070 245245	Tsjechië: 1.7 Nouzové telefonní číslo: Toxikologické informační středisko, Na Bojišti 1, 128 08 Praha 2: telefon (24 hodin/den) 224919293, 224915402, 224914575	Denemarken: Giftinformation: +45 35 31 60 60	Estland: Mürgistusteabekeskus: 16662	Finland: Myrkytyskeskus 09-471977 or 09 4711
Frankrijk: BNCP +33383852192	Duitsland: Giftnotrufzentrale Berlin: +49 030 - 192 40	Hongarije: Egészségügyi Toxikológiai Tájékoztató Szolgálat (ETTSZ) 1096 Budapest, Nagyvárad tér 2. +36-80-201199 (ingyenes, éjjel-nappal) +36-1-4766464	Ierland: Niet beschikbaar.	Italië: Ospedale Niguarda Cà Granda, Milan 0266101029	Litouwen: Poison centre: 236 20 52
Nederland: NVIC: Tel: 030-2748888	Noorwegen: Norwegian poison information center: 22 59 13 00	Polen: Niet beschikbaar.	Slovakije: Toxikologické informačné centrum Limbova 5 833 05 Bratislava Tel. 02/5477 4166, 02/5477 4605	Slovenië: Center za obveščanje 112	Portugal: CIAV 808 250 143
Zweden: 112	Zwitserland: Schweizerisches Toxikologisches Informationszentrum: +41 - 1-145	Turkije: Niet beschikbaar.	Verenigd Koninkrijk (GB): NPIS 0870 600 6266	Spanje: INSTITUTO NACIONAL DE TOXICOLOGÍA 91 562 04 20	Griekenland: Children's hospital "P.Kyriakou", Thivon & Levadias 1, GR 11527, Goudi, Athens Tel. +30 210 7793 777
Letland: Valsts ugunsdzēsības un glābšanas dienests – 112, Saindēšanās un zāļu informācijas centrs - +371 67042473	Kroatië: - Broj telefona službe za izvanredna stanja: 112 - Broj telefona za medicinske informacije: 00-385-(0)1-23-48-342	Serbia: Broj telefona Nacionalnog centra za kontrola trovanja: ++381 11-662 381 (24 sata)			

Leverancier

TROY CHEMICAL COMPANY BV
Uiverlaan 12e
PO Box 132
3145 XN Maassluis
The Netherlands
Phone: + 31 (0) 10 592-7494
Fax: +31 (0) 10 592-8877

Openingstijden : Maandag - Vrijdag: 08.30 - 17.00 (CET)

RUBRIEK 2: Identificatie van de gevaren

2.1 Indeling van de stof of het mengsel

Productomschrijving : Mengsel

Indeling overeenkomstig Richtlijn 1999/45/EG [Richtlijn gevaarlijke preparaten]

Het product is geklasseerd als gevaarlijk volgens richtlijn 1999/45/EG en zijn wijzigingen.

Classificatie : C; R35
Xi; R37
R43
N; R50

Risico's voor de gezondheid : Veroorzaakt ernstige brandwonden. Irriterend voor de ademhalingswegen. Kan overgevoeligheid veroorzaken bij contact met de huid.

Milieugevaren : Zeer vergiftig voor in het water levende organismen.

Zie Rubriek 16 voor de volledige tekst van de R- of S-zinnen die hierboven staan vermeld.

Zie rubriek 11 voor meer informatie over gezondheidseffecten en symptomen.

2.2 Etiketteringselementen

Gevarensymbool of gevarensymbolen :

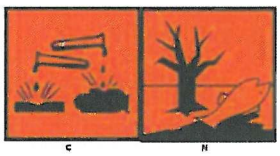

Gevaarindicatie : Bijtend, Milieugevaarlijk

Waarschuwingszinnen : R35- Veroorzaakt ernstige brandwonden.
R37- Irriterend voor de ademhalingswegen.
R43- Kan overgevoeligheid veroorzaken bij contact met de huid.
R50- Zeer vergiftig voor in het water levende organismen.

Veiligheidsaanbevelingen : S23- Damp niet inademen.
S26- Bij aanraking met de ogen onmiddellijk met overvloedig water afspoelen en deskundig medisch advies inwinnen.
S36/37/39- Draag geschikte beschermende kleding, handschoenen en een beschermingsmiddel voor de ogen/het gezicht.
S45- Bij een ongeval of indien men zich onwel voelt, onmiddellijk een arts raadplegen (indien mogelijk hem dit etiket tonen).
S57- Neem passende maatregelen om verspreiding in het milieu te voorkomen.
S61- Voorkom lozing in het milieu. Vraag om speciale instructies/veiligheidskaart.

Gevaarlijke bestanddelen : kaliumhydroxide
1,2-benzisothiazool-3(2H)-on
natriumhydroxide

Aanvullende etiketonderdelen : Niet van toepassing.

Speciale verpakkingseisen

Recipiënten die van een kinderveilige sluiting moeten zijn voorzien : Niet van toepassing.

Voelbare gevaarsaanduiding : Niet van toepassing.

2.3 Andere gevaren

Overige gevaren die niet leiden tot classificatie : Niet van toepassing

RUBRIEK 3: Samenstelling en informatie over de bestanddelen

Stof/preparaat : Mengsel

Product-/ingrediëntennaam	Identificatiemogelijkheden	%	Classificatie 67/548/EEG	Classificatie Verordening (EG) nr. 1272/2008 [CLP]	Type
bifenyl-2-ol	EG: 201-993-5 CAS-nummer: 90-43-7 Index: 604-020-00-6	32.6	Xi; R36/37/38 N; R50	Skin Irrit. 2, H315 Eye Irrit. 2, H319 STOT SE 3, H335 Aquatic Acute 1, H400	[1]
propaan-1,2-diol	EG: 200-338-0 CAS-nummer: 57-55-6	7 - 10	Niet geclassificeerd.	Niet geclassificeerd.	[2]
kaliumhydroxide	EG: 215-181-3 CAS-nummer: 1310-58-3 Index: 019-002-00-8	5 -7	Xn; R22 C; R35	Met. Corr. 1, H290 Acute Tox. 3, H301 Skin Corr. 1A, H314 Eye Dam. 1, H318	[1] [2]
1,2-benzisothiazool-3(2H)-on	EG: 220-120-9 CAS-nummer: 2634-33-5 Index: 613-088-00-6	4.9	Xn; R22 Xi; R41, R38 R43 N; R50	Acute Tox. 4, H302 Skin Irrit. 2, H315 Eye Dam. 1, H318 Skin Sens. 1, H317 Aquatic Acute 1, H400	[1]
natriumhydroxide	EG: 215-185-5 CAS-nummer: 1310-73-2 Index: 011-002-00-6	3 - 5	C; R35 **Zie rubriek 16 voor de volledige tekst van de R-zinnen die hierboven worden vermeld**	Met. Corr. 1, H290 Skin Corr. 1A, H314 Eye Dam. 1, H318 **Zie Rubriek 16 voor de volledige tekst van de S-zinnen die hierboven staan vermeld.**	[1] [2]

Er zijn geen additionele ingrediënten aanwezig die, voor zover op dit moment aan leverancier bekend is en in de van toepassing zijnde concentraties, geclassificeerd zijn als schadelijk voor de gezondheid of voor het milieu en op grond daarvan in deze sectie moeten worden vermeld.

Type

[1] Stof ingedeeld met een gezondheids- of milieugevaar
[2] Stof met een werkplaats blootstellingslimiet
[3] Stof voldoet aan criteria voor PBT overeenkomstig Verordening (EG) nr. 1207/2006, Bijlage XIII
[4] Stof voldoet aan criteria voor zPzB overeenkomstig Verordening (EG) nr. 1207/2006, Bijlage XIII

Ci ige gevaren die niet leiden tot classificatie

RUBRIEK 4: Eerstehulpmaatregelen

4.1 Beschrijving van de eerstehulpmaatregelen

Oogcontact : Raadpleeg onmiddellijk een arts. Spoel de ogen onmiddellijk met ruime hoeveelheden water, waarbij u de boven- en onderoogleden zo nu en dan oplicht. Ga aanwezigheid van contactlenzen na en verwijder ze. Blijf ten minste 10 minuten spoelen. Brandwonden door chemicaliën moeten onmiddellijk door een arts worden behandeld.

Inademing : Raadpleeg onmiddellijk een arts. Het slachtoffer in de frisse lucht brengen en laten rusten in een houding die het ademen vergemakkelijkt. Als vermoed wordt dat nog steeds dampen aanwezig zijn moet de reddingswerker een geschikt masker of onafhankelijke ademhalingsapparatuur dragen. Als de patiënt niet ademt, onregelmatig ademt, of als zich ademhalingsstilstand voordoet, dient kunstmatige beademing of zuurstof te worden toegediend door getraind personeel. Dit kan gevaarlijk zijn voor degene die mond-op-mondbeademing toepast. Plaats in stabiele zijligging en roep onmiddelijk medische hulp in, indien de persoon bewusteloos is. Zorg dat luchtwegen vrij blijven. Maak strakzittende kleding los, zoals een overhemdboord, das, riem of ceintuur. Na inhalatie van afbraakproducten in geval van brand kunnen symptomen met vertraging optreden. Het slachtoffer moet mogelijk 48 uur lang onder medisch toezicht blijven.

RUBRIEK 4: Eerstehulpmaatregelen

Huidcontact : Raadpleeg onmiddellijk een arts. Spoel verontreinigde huid met grote hoeveelheid water. Verwijder verontreinigde kleding en schoenen. Was verontreinigde kleding grondig met water voordat u die uittrekt of draag handschoenen. Blijf ten minste 10 minuten spoelen. Brandwonden door chemicaliën moeten onmiddellijk door een arts worden behandeld. Vermijdt verdere blootstelling wanneer er klachten of symptomen van welke aard dan ook zijn. Was kleding alvorens ze opnieuw te gebruiken. Maak schoenen grondig schoon voor hergebruik.

Inslikken : Raadpleeg onmiddellijk een arts. Spoel de mond met water. Kunstgebit indien aanwezig verwijderen. Het slachtoffer in de frisse lucht brengen en laten rusten in een houding die het ademen vergemakkelijkt. Als het slachtoffer het materiaal heeft doorgeslikt en bij bewustzijn is, laat u het slachtoffer kleine hoeveelheden water drinken. Stop hiermee als het slachtoffer misselijk wordt, omdat overgeven gevaarlijk kan zijn. Zet niet aan tot braken tenzij medisch personeel aangeeft dat dit wel moet. Indien de persoon moet braken, houdt het hoofd dan laag om te voorkomen dat er braaksel in de longen komt. Brandwonden door chemicaliën moeten onmiddellijk door een arts worden behandeld. Geef een bewusteloos iemand nooit iets via de mond. Plaats in stabiele zijligging en roep onmiddelijk medische hulp in, indien de persoon bewusteloos is. Zorg dat luchtwegen vrij blijven. Maak strakzittende kleding los, zoals een overhemdboord, das, riem of ceintuur.

Bescherming van eerste-hulpverleners : Er mag geen actie worden ondernomen als er kans is op persoonlijke ongelukken of in geval van onvoldoende training. Als vermoed wordt dat nog steeds dampen aanwezig zijn moet de reddingswerker een geschikt masker of onafhankelijke ademhalingsapparatuur dragen. Dit kan gevaarlijk zijn voor degene die mond-op-mondbeademing toepast. Was verontreinigde kleding grondig met water voordat u die uittrekt of draag handschoenen.

4.2 Belangrijkste acute en uitgestelde symptomen en effecten

Mogelijke acute gevolgen voor de gezondheid

Oogcontact : Zeer corrosief voor de ogen. Veroorzaakt ernstige brandwonden.

Inademing : Irriterend voor de ademhalingswegen. Blootstelling aan ontledingsproducten kan gevaar voor de gezondheid opleveren. Na blootstelling kunnen ernstige gevolgen met vertraging optreden.

Huidcontact : Zeer corrosief voor de huid. Veroorzaakt ernstige brandwonden. Kan overgevoeligheid veroorzaken bij contact met de huid.

Inslikken : Kan brandwonden aan mond, keel en maag veroorzaken.

Tekenen/symptomen van overmatige blootstelling

Oogcontact : Ongewenste symptomen kunnen de volgende zijn:
pijn
tranenvloed
roodheid

Inademing : Ongewenste symptomen kunnen de volgende zijn:
irritatie van de luchtwegen
hoesten

Huidcontact : Ongewenste symptomen kunnen de volgende zijn:
pijn of irritatie
roodheid
blaarvorming kan voorkomen

Inslikken : Ongewenste symptomen kunnen de volgende zijn:
maagpijnen

4.3 Vermelding van de vereiste onmiddellijke medische verzorging en speciale behandeling

Opmerkingen voor arts : Na inhalatie van afbraakproducten in geval van brand kunnen symptomen met vertraging optreden. Het slachtoffer moet mogelijk 48 uur lang onder medisch toezicht blijven.

Specifieke behandelingen : Geen specifieke behandeling.

RUBRIEK 5: Brandbestrijdingsmaatregelen

5.1 Blusmiddelen

Geschikte blusmiddelen : Gebruik een blusmiddel dat geschikt is voor de ontstane brand.

Ongeschikte blusmiddelen : Geen bekend.

5.2 Speciale gevaren die door de stof of het mengsel worden veroorzaakt

Risico's van de stof of het mengsel : Bij brand of verhitting loopt de druk op en kan de houder barsten.

Gevaarlijke verbrandingsproducten : Afbraakproducten kunnen onder meer zijn:
kooldioxide
koolmonoxide
stikstofoxiden
zwaveloxiden
metaaloxide(n)

5.3 Advies voor brandweerlieden

Speciale voorzorgsmaatregelen voor brandbestrijders : In geval van brand, isoleer het terrein direct door alle personen uit de buurt van het incident te verwijderen. Er mag geen actie worden ondernomen als er kans is op persoonlijke ongelukken of in geval van onvoldoende training. Dit materiaal is zeer giftig voor waterorganismen. Met dit materiaal verontreinigd bluswater dient te worden opgevangen, zodat het niet in het oppervlaktewater, riool of afvoer terechtkomt.

Speciale beschermende uitrusting voor brandweerlieden : Brandbestrijders dienen geschikte kleding te dragen en een onafhankelijk ademhalingstoestel (SCBA) dat een volledig gelaatsdeel heeft en met een overdrukmodus werkt. Kleding voor brandweerlieden (inclusief helmen, beschermende laarzen en handschoenen) overeenkomstig Europese norm EN 469 geeft een basis beschermingsniveau voor incidenten met chemische stoffen.

RUBRIEK 6: Maatregelen bij het accidenteel vrijkomen van de stof of het mengsel

6.1 Persoonlijke voorzorgsmaatregelen, beschermde uitrusting en noodprocedures

Voor andere personen dan de hulpdiensten : Er mag geen actie worden ondernomen als er kans is op persoonlijke ongelukken of in geval van onvoldoende training. Evacueer omringende gebieden. Zorg dat onbeschermd en overbodig personeel niet binnenkomt. Raak gemorst materiaal niet aan en loop er niet doorheen. Adem damp of mist niet in. Zorg voor voldoende ventilatie. Draag het daartoe geëigende ademhalingsmasker bij onvoldoende ventilatie. Draag geschikte persoonlijke beschermingsmiddelen.

Voor de hulpdiensten : Indien speciale kleding is vereist voor het hanteren van het gemorst product, lees dan ook de eventuele informatie in Rubriek 8 over geschikte en ongeschikte materialen. Zie ook Rubriek 8 voor aanvullende informatie over hygiënische maatregelen.

6.2 Milieuvoorzorgsmaatregelen : Vermijd verspreiding van gemorst materiaal en afvalmateriaal en voorkom dat dit in contact komt met bodem, waterwegen, afvoerleidingen en riool. Informeer de betreffende autoriteiten wanneer het product het milieu heeft vervuild (riolering, waterwegen, bodem of lucht) Watervervuilend materiaal. Dit product kan schadelijk zijn voor het milieu wanneer het in grote hoeveelheden vrijkomt.

6.3 Insluitings- en reinigingsmethoden en -materiaal

Gering morsen : Dicht het lek als dat zonder risico kan. Verwijder verpakkingen uit het gebied waar gemorst is. Verdun met water en opmoppen indien wateroplosbaar. Alternatief, of indien water-onoplosbaar, absorbeer met inert droog materiaal en plaats in een toepasbare afvalcontainer. Af laten voeren door een vergunninghoudend afvalverwerkingsbedrijf.

RUBRIEK 6: Maatregelen bij het accidenteel vrijkomen van de stof of het mengsel

Uitgebreid morsen : Dicht het lek als dat zonder risico kan. Verwijder verpakkingen uit het gebied waar gemorst is. Benader de uitstoot met de wind in de rug. Vermijd toegang tot riolen, waterwegen, kelders of gesloten ruimten. Voer weggelekt materiaal af naar een afvalwaterzuiveringsinstallatie of handel als volgt. Neem gemorst preparaat op met niet-brandbare absorberende materialen, bijvoorbeeld zand, aarde, vermiculiet of diatomeeënaarde en doe dit in een afvoercontainer in overeenstemming met de plaatselijke voorschriften. Af laten voeren door een vergunninghoudend afvalverwerkingsbedrijf. Vervuild absorberend materiaal kan dezelfde risico's met zich meebrengen als het gemorste product.

6.4 Verwijzing naar andere rubrieken : Zie Rubriek 1 voor contactgegevens voor noodgevallen.
Zie Rubriek 8 voor informatie over geschikte persoonlijke beschermingsmiddelen.
Zie Rubriek 13 voor aanvullende informatie over afvalbehandeling.

RUBRIEK 7: Hantering en opslag

De informatie in deze rubriek bevat algemene adviezen en richtlijnen. De lijst van Aanbevolen toepassingen in Rubriek 1 moet worden geraadpleegd voor eventueel beschikbare gebruikspecifieke informatie die gegeven wordt in de Blootstellingscenario('s). Van toepassing wanneer blootstellingsscenario beschikbaar is.

7.1 Voorzorgsmaatregelen voor het veilig hanteren van de stof of het mengsel

Beschermende maatregelen : Trek van toepassing zijnde persoonlijke beschermingsmiddelen aan (zie rubriek 8). Personen die in het verleden last hebben gehad van sensibilisatie van de huid mogen niet worden ingezet bij enig proces waarbij dit produkt wordt gebruikt. Zorg dat het product niet in de ogen of op de huid of kleding terecht komt. Adem damp of mist niet in. Niet innemen. Voorkom lozing in het milieu. Vraag om speciale instructies/veiligheidskaart. Alleen gebruiken bij voldoende ventilatie. Draag het daartoe geëigende ademhalingsmasker bij onvoldoende ventilatie. Bewaren in de originele verpakking, of in een goedgekeurd alternatief dat is gemaakt van compatibel materiaal; goed gesloten houden wanneer het niet in gebruik is. Gescheiden houden van zuren. Lege verpakkingen bevatten restproduct en kunnen gevaarlijk zijn. Vat niet hergebruiken.

Advies inzake algemene arbeidshygiëne : In de ruimte waar dit materiaal wordt gebruikt, opgeslagen of verwerkt, moet eten, drinken en roken verboden worden. Werknemers moeten hun handen en gezicht wassen alvorens te eten, drinken en roken. Verwijder verontreinigde kleding en beschermingsmiddelen voordat u kantines, e.d. binnengaat. Zie ook Rubriek 8 voor aanvullende informatie over hygiënische maatregelen.

7.2 Voorwaarden voor een veilige opslag, met inbegrip van incompatibele producten : Opslaan in overeenstemming met de plaatselijke regelgeving. Opslaan in oorspronkelijke verpakking, beschermd tegen direct zonlicht, op een droge, koele, goed geventileerde plaats, verwijderd van materiaal waarmee contact vermeden dient te worden (zie rubriek 10) en voedsel en drank. Gescheiden houden van zuren. Bewaar de verpakking goed afgesloten en verzegeld tot aan gebruik. Geopende verpakkingen dienen zorgvuldig opnieuw te worden afgesloten en dienen rechtop te worden bewaard om lekkage te voorkomen. Niet opslaan in verpakkingen zonder etiket. Neem passende maatregelen om verspreiding in het milieu te voorkomen.

7.3 Specifiek eindgebruik

Aanbevelingen : Niet beschikbaar.

Oplossingen specifiek voor de industriële sector : Niet beschikbaar.

RUBRIEK 8: Maatregelen ter beheersing van blootstelling/persoonlijke bescherming

De informatie in deze rubriek bevat algemene adviezen en richtlijnen. De lijst van Aanbevolen toepassingen in Rubriek 1 moet worden geraadpleegd voor eventueel beschikbare gebruikspecifieke informatie die gegeven wordt in de Blootstellingscenario('s). Van toepassing wanneer blootstellingsscenario beschikbaar is.

8.1 Controleparameters

Beroepsmatige blootstellingslimieten

RUBRIEK 8: Maatregelen ter beheersing van blootstelling/persoonlijke bescherming

Product- /ingrediëntennaam	Grenswaarden voor blootstelling
Europa	
kaliumhydroxide	**ACGIH TLV (Verenigde Staten, 1/2009).** C: 2 mg/m³
natriumhydroxide	**ACGIH TLV (Verenigde Staten, 1/2009).** C: 2 mg/m³
Oostenrijk	
kaliumhydroxide	**GKV_MAK (Oostenrijk, 9/2007).** TWA: 2 mg/m³ 8 uur. Vorm: inhalable fraction
natriumhydroxide	**GKV_MAK (Oostenrijk, 9/2007).** TWA: 2 mg/m³ 8 uur. Vorm: inhalable fraction PEAK: 4 mg/m³, 8 maal per dienst, 5 minuut/minuten. Vorm: inhalable fraction
België	
kaliumhydroxide	**Lijst Grenswaarden / Valeurs Limites (België, 6/2009).** M: 2 mg/m³
natriumhydroxide	**Lijst Grenswaarden / Valeurs Limites (België, 6/2009).** M: 2 mg/m³
Bulgarije	
kaliumhydroxide	**РБ МТСП и МЗ Наредба №13/2003 (Bulgarije, 8/2007).** Limit value 8 hours: 2 mg/m³ 8 uur.
natriumhydroxide	**РБ МТСП и МЗ Наредба №13/2003 (Bulgarije, 8/2007).** Limit value 8 hours: 2 mg/m³ 8 uur. Vorm: aerosols
Tsjechië	
kaliumhydroxide	**178/2001 (Tsjechië, 12/2007).** TWA: 1 mg/m³ 8 uur. STEL: 2 mg/m³ 15 minuut/minuten.
natriumhydroxide	**178/2001 (Tsjechië, 12/2007).** TWA: 1 mg/m³ 8 uur. STEL: 2 mg/m³ 15 minuut/minuten.
Denemarken	
kaliumhydroxide	**Arbejdstilsynet (Denemarken, 3/2008).** CEIL: 2 mg/m³
natriumhydroxide	**Arbejdstilsynet (Denemarken, 3/2008).** CEIL: 2 mg/m³
Estland	
kaliumhydroxide	**Sotsiaalminister (Estland, 10/2007).** TWA: 2 mg/m³ 8 uur.
natriumhydroxide	**Sotsiaalminister (Estland, 10/2007).** TWA: 1 mg/m³ 8 uur. *: 2 mg/m³
Finland	
kaliumhydroxide	**Työterveyslaitos, Sosiaali- ja terveysministeriö (Finland, 7/2009).** CEIL: 2 mg/m³
natriumhydroxide	**Työterveyslaitos, Sosiaali- ja terveysministeriö (Finland, 7/2009).** CEIL: 2 mg/m³
Frankrijk	
kaliumhydroxide	**INRS (Frankrijk, 12/2007). Opmerkingen: indicative exposure limits** STEL: 2 mg/m³ 15 minuut/minuten.
natriumhydroxide	**INRS (Frankrijk, 12/2007). Opmerkingen: indicative exposure limits** TWA: 2 mg/m³ 8 uur.
Griekenland	

RUBRIEK 8: Maatregelen ter beheersing van blootstelling/persoonlijke bescherming

kaliumhydroxide	**PD 90/1999 (Griekenland, 8/2007).** TWA: 2 mg/m³ 8 uur. STEL: 2 mg/m³ 15 minuut/minuten.
natriumhydroxide	**PD 90/1999 (Griekenland, 8/2007).** TWA: 2 mg/m³ 8 uur. STEL: 2 mg/m³ 15 minuut/minuten.
Hongarije	
kaliumhydroxide	**EüM-SzCsM (Hongarije, 12/2007).** TWA: 2 mg/m³ 8 uur. PEAK: 2 mg/m³ 15 minuut/minuten.
natriumhydroxide	**EüM-SzCsM (Hongarije, 12/2007).** TWA: 2 mg/m³ 8 uur.
Ierland	
propaan-1,2-diol	**NAOSH (Ierland, 5/2010).** OELV-8hr: 10 mg/m³ 8 uur. Vorm: particulate OELV-8hr: 470 mg/m³ 8 uur. Vorm: vapour and particulates OELV-8hr: 150 ppm 8 uur. Vorm: vapour and particulates
kaliumhydroxide	**NAOSH (Ierland, 8/2007).** OELV-15min: 2 mg/m³ 15 minuut/minuten.
natriumhydroxide	**NAOSH (Ierland, 8/2007).** OELV-15min: 2 mg/m³ 15 minuut/minuten.
Italië	
kaliumhydroxide	**ACGIH TLV (Verenigde Staten, 1/2009).** C: 2 mg/m³
natriumhydroxide	**ACGIH TLV (Verenigde Staten, 1/2009).** C: 2 mg/m³
Letland	
propaan-1,2-diol	**LV Nat. Standardisation and Meterological Centre (Letland, 5/2007).** TWA: 7 mg/m³ 8 uur.
natriumhydroxide	**LV Nat. Standardisation and Meterological Centre (Letland, 5/2007).** TWA: 0.5 mg/m³ 8 uur.
Litouwen	
propaan-1,2-diol	**Del Lietuvos Higienos Normos (Litouwen, 10/2007).** TWA: 7 mg/m³ 8 uur.
natriumhydroxide	**Del Lietuvos Higienos Normos (Litouwen, 10/2007).** CEIL: 2 mg/m³
Noorwegen	
propaan-1,2-diol	**Arbeidstilsynet (Noorwegen, 3/2009).** TWA: 79 mg/m³ 8 uur. TWA: 25 ppm 8 uur.
kaliumhydroxide	**Arbeidstilsynet (Noorwegen, 3/2009).** CEIL: 2 mg/m³
natriumhydroxide	**Arbeidstilsynet (Noorwegen, 3/2009).** CEIL: 2 mg/m³
Polen	
kaliumhydroxide	**Ministra Pracy i Polityki Społecznej (Polen, 7/2009).** TWA: 0.5 mg/m³ 8 uur. STEL: 1 mg/m³ 15 minuut/minuten.
natriumhydroxide	**Ministra Pracy i Polityki Społecznej (Polen, 7/2009).** TWA: 0.5 mg/m³ 8 uur. STEL: 1 mg/m³ 15 minuut/minuten.
Portugal	
kaliumhydroxide	**Instituto Português da Qualidade (Portugal, 3/2007).** CEIL: 2 mg/m³
natriumhydroxide	**Instituto Português da Qualidade (Portugal, 3/2007).** CEIL: 2 mg/m³
Roemenië	

RUBRIEK 8: Maatregelen ter beheersing van blootstelling/persoonlijke bescherming

kaliumhydroxide	**Ministry of Social Assistance and Family Policies and Ministry of Public Health (Roemenië, 10/2006).** VLA: 1 mg/m³, (expressed as sodium hydroxide) 8 uur. Short term: 3 mg/m³, (expressed as sodium hydroxide) 15 minuut/minuten.
natriumhydroxide	**Ministry of Social Assistance and Family Policies and Ministry of Public Health (Roemenië, 10/2006).** VLA: 1 mg/m³, (expressed as sodium hydroxide) 8 uur. Short term: 3 mg/m³, (expressed as sodium hydroxide) 15 minuut/minuten.
Slovakije	
natriumhydroxide	**Nariadenie Vlády Slovenskej republiky (Slovakije, 6/2007).** TWA: 2 mg/m³ 8 uur.
Slovenië	
natriumhydroxide	**Uradni list Republike Slovenije (Slovenië, 6/2007).** TWA: 2 mg/m³ 8 uur. Vorm: inhalable fraction
Spanje	
kaliumhydroxide	**INSHT (Spanje, 2/2009).** STEL: 2 mg/m³ 15 minuut/minuten.
natriumhydroxide	**INSHT (Spanje, 2/2009).** STEL: 2 mg/m³ 15 minuut/minuten.
Zweden	
kaliumhydroxide	**AFS 2005:17 (Zweden, 6/2007).** TWA: 1 mg/m³ 8 uur. Vorm: Inhalable dust CEIL: 2 mg/m³ Vorm: Inhalable dust
natriumhydroxide	**AFS 2005:17 (Zweden, 6/2007).** CEIL: 2 mg/m³ Vorm: Inhalable dust TWA: 1 mg/m³ 8 uur. Vorm: Inhalable dust
Zwitserland	
kaliumhydroxide	**SUVA (Zwitserland, 1/2009).** TWA: 2 mg/m³ 8 uur. Vorm: inhalable fraction
natriumhydroxide	**SUVA (Zwitserland, 1/2009).** TWA: 2 mg/m³ 8 uur. Vorm: inhalable fraction STEL: 2 mg/m³ 15 minuut/minuten. Vorm: inhalable fraction
Turkije	
kaliumhydroxide	**NIOSH REL (Verenigde Staten, 6/2009).** TWA: 2 mg/m³ 10 uur.
natriumhydroxide	**NIOSH REL (Verenigde Staten, 6/2009).** CEIL: 2 mg/m³
Verenigd Koninkrijk (GB)	
propaan-1,2-diol	**EH40/2005 WELs (Verenigd Koninkrijk (GB), 8/2007).** TWA: 10 mg/m³ 8 uur. Vorm: Particulate TWA: 150 ppm 8 uur. Vorm: Sum of vapour and particulates TWA: 474 mg/m³ 8 uur. Vorm: Sum of vapour and particulates
kaliumhydroxide	**EH40/2005 WELs (Verenigd Koninkrijk (GB), 8/2007).** STEL: 2 mg/m³ 15 minuut/minuten.
natriumhydroxide	**EH40/2005 WELs (Verenigd Koninkrijk (GB), 8/2007).** STEL: 2 mg/m³ 15 minuut/minuten.

Aanbevolen monitoring procedures : Wanneer dit product ingrediënten bevat met blootstellingslimieten, kan monitoring van personen, van werkplaatsomgeving of biologisch monitoren vereist zijn om de effectiviteit van de ventilatie of van andere controlemaatregelen en/of de noodzaak van het gebruik van ademhalingsbeschermingsmiddelen te bepalen. Voor methoden om de blootstelling aan chemische stoffen door inademing te bepalen en nationale richtlijnen voor de bepaling van gevaarlijke stoffen dient u de Europese Norm EN 689 te raadplegen.

DEL's (Derived Effect Levels; afgeleide effectdoses)

Geen DEL's beschikbaar.

RUBRIEK 8: Maatregelen ter beheersing van blootstelling/persoonlijke bescherming

PEC's (Predicted Effect Concentrations; voorspelde effectconcentraties)

Geen PEC's beschikbaar.

8.2 Maatregelen ter beheersing van blootstelling

Geschikte technische beheersmaatregelen : Alleen gebruiken bij voldoende ventilatie. Wanneer door de handelingen van de gebruiker stof, rook, gas, damp of nevel ontstaat, gebruik dan een gesloten installatie, lokale afzuiging of andere technische controlemiddelen om beroepsmatige blootstelling beneden alle aanbevolen of wettelijke grenswaarden te houden.

Individuele beschermingsmaatregelen

Hygiënische maatregelen : Was na het hanteren van chemische producten uw handen, onderarmen en gezicht grondig voordat u eet, drinkt of naar het toilet gaat en aan het eind van de werkdag. Toepasselijke technieken moeten gebruikt worden om mogelijk verontreinigde kleding te verwijderen. Verontreinigde werkkleding mag de werkruimte niet verlaten. Was verontreinigde kleding alvorens die opnieuw te gebruiken. Zorg ervoor dat de oogwasstations en veiligheidsdouches zich dicht bij de werkplek bevinden.

Bescherming van de ogen/het gezicht : Wanneer een risicoanalyse aangeeft dat dit noodzakelijk is om blootstelling aan spatten, nevel of stof te vermijden, dient een veiligheidsbescherming voor de ogen te worden gedragen die voldoet aan een goedgekeurde standaard.

Bescherming van de huid

Bescherming van de handen : Wanneer een risicoanalyse aangeeft dat dit noodzakelijk is, dienen bij het hanteren van chemische producten ondoorlaatbare handschoenen te worden gedragen die resistent zijn tegen chemicaliën en die voldoen aan een goedgekeurde norm.

for example KCL (Material: article number (thickness in mm)):
neopreen (Polychloropene): 0720 (0.65)
Butyl: 0898 (0.7)
Butyl II: 0897 (-)
Viton: 0890 (0.7)
The above mentioned breakthrough times are based on KCL laboratory test results according to EN374 and are only applicable for these KCL gloves.

This recommendation is only for the product delivered by us and for its intended purpose. Should the worker be exposed to mixtures of the product with other ingredients or to other products, safety advice on gloves can be obtained with the supplier of CE-approved gloves (i.e. KCL GmbH, D-36124 Eichenzell, Tel. ++49 (0) 6659 87300, Fax: ++49 (0) 6659 87155, e-mail vertrieb@kcl.de).

Lichaamsbescherming : Persoonlijke lichaamsbeschermende middelen dienen te worden gekozen op basis van de uit te voeren taak, de daarbij behorende risico's en dient door een specialist te worden goedgekeurd voordat het product wordt gebruikt.

Overige huidbescherming : Geschikt schoeisel en eventuele aanvullende huidbeschermingsmaatregelen moeten worden geselecteerd op basis van de taak die wordt uitgevoerd en de risico's die daarmee gepaard gaan. Deze moeten worden goedgekeurd door een deskundige voorafgaand aan de hantering van dit product.

Bescherming van de ademhalingswegen : Wanneer een risicoanalyse aangeeft dat dit noodzakelijk is, dient u een goed passend, luchtzuiverend of luchttoevoerend ademhalingstoestel te gebruiken dat voldoet aan een goedgekeurde standaard. De keuze van een masker moet gebaseerd worden op verwachte blootstellingslimieten, de gevaren van het product en de limieten voor veilig werken van het type masker.

Beheersing van milieublootstelling : Uitstoot van ventilatie of bewerkingsapparatuur moet worden gecontroleerd om er zeker van te zijn dat deze voldoet aan de eisen van de milieubeschermingswetgeving. In sommige gevallen zijn gaswassers, filters of technische modificaties van de procesapparatuur nodig om de emissie terug te brengen tot een aanvaardbaar niveau.

RUBRIEK 9: Fysische en chemische eigenschappen

9.1 Informatie over fysische en chemische basiseigenschappen

Voorkomen

Fysische toestand	:	Vloeistof.
Kleur	:	Helder. Bruin.
Geur	:	Phenolachtig.
Geurdrempel	:	Niet beschikbaar.
pH	:	11 tot 13
Smeltpunt/vriespunt	:	<0°C
Initieel kookpunt en kookbereik	:	>100°C
Vlampunt	:	Gesloten kroes: >100°C
Verdampingssnelheid	:	Niet beschikbaar.
Ontvlambaarheid (vast, gas)	:	Niet beschikbaar.
Verbrandingstijd	:	Niet van toepassing.
Verbrandingssnelheid	:	Niet van toepassing.
Bovenste/onderste ontvlambaarheids- of explosiegrenzen	:	Niet beschikbaar.
Dampspanning	:	Niet beschikbaar.
Dampdichtheid	:	Niet beschikbaar.
Relatieve dichtheid	:	1.1
Oplosbaarheid	:	Niet beschikbaar.
Octanol/water verdelingscoëfficiënt	:	Niet beschikbaar.
Zelfontbrandingstemperatuur	:	Niet beschikbaar.
Ontledingstemperatuur	:	Niet beschikbaar.
Viscositeit	:	Niet beschikbaar.
Ontploffingseigenschappen	:	Niet explosief in aanwezigheid van de volgende materialen of condities: open vuur, vonken en statische ontlading, hitte, schokken en mechanische inwerkingen, oxyderende stoffen, reducerende stoffen, brandbare materialen, organische materialen, metalen, zuren, alkaliën en vocht.
Oxyderende eigenschappen	:	Niet beschikbaar.

9.2 Overige informatie

Geen aanvullende informatie.

RUBRIEK 10: Stabiliteit en reactiviteit

10.1 Reactiviteit	:	Er zijn voor dit product of de bestanddelen ervan geen specifieke testgegevens beschikbaar met betrekking tot de reactiviteit.
10.2 Chemische stabiliteit	:	Het product is stabiel.
10.3 Mogelijke gevaarlijke reacties	:	Onder normale opslagomstandigheden en bij normaal gebruik zullen geen gevaarlijke reacties optreden.
10.4 Te vermijden omstandigheden	:	Geen specifieke gegevens.
10.5 Chemisch op elkaar inwerkende materialen	:	Reactief of niet verenigbaar met de volgende materialen: zuren
10.6 Gevaarlijke ontledingsproducten	:	Onder normale omstandigheden van opslag en gebruik worden normaal geen gevaarlijke afvalproducten gevormd.

RUBRIEK 11: Toxicologische informatie

11.1 Informatie over toxicologische effecten

Acute toxiciteit

Product-/ingrediëntennaam	Resultaat	Soorten	Dosis	Blootstelling
MERGAL KM90	LD50 Dermaal	Rat	>2000 mg/kg	-
	LD50 Oraal	Rat	>2000 mg/kg	-
bifenyl-2-ol	LC50 Inademing Stof en nevels	Rat	>949 mg/m³	1 uren
	LC50 Inademing Stof en nevels	Rat	>36 mg/m3	4 uren
	LD50 Dermaal	Konijn	>5000 mg/kg	-
	LD50 Dermaal	Rat	>2000 mg/kg	-
	LD50 Dermaal	Rat	>2000 mg/kg	-
	LD50 Oraal	Kat	500 mg/kg	-
	LD50 Oraal	Muis	1050 mg/kg	-
	LD50 Oraal	Rat	2 g/kg	-
	LD50 Oraal	Rat	2980 mg/kg	-
kaliumhydroxide	LD50 Oraal	Rat	273 mg/kg	-
1,2-benzisothiazool-3(2H)-on	LD50 Dermaal	Rat	>2000 mg/kg	-
	LD50 Oraal	Muis	1150 mg/kg	-
	LD50 Oraal	Rat	597 mg/kg	-
natriumhydroxide	LD50 Dermaal	Konijn	1350 mg/kg	-
	LD50 Oraal	Rat	2000 mg/kg	-
	LDLo Oraal	Konijn	500 mg/kg	-

Conclusie/Samenvatting : Niet beschikbaar.

Irritatie/corrosie

Product-/ingrediëntennaam	Resultaat	Soorten	Score	Blootstelling	Observatie
1,2-benzisothiazool-3(2H)-on	Ogen - Ernstig irriterend	Rat	-	-	-
	Huid - Gematigd irriterend	Konijn	-	-	-

Conclusie/Samenvatting : Niet beschikbaar.

Overgevoeligheid veroorzakend

Product-/ingrediëntennaam	Wijze van blootstelling	Soorten	Resultaat
MERGAL KM90	huid	Cavia (Guinese big)	Sensibiliserend
1,2-benzisothiazool-3(2H)-on	huid	Konijn	Sensibiliserend

Conclusie/Samenvatting

Huid : Overgevoeligheid: maximaliseringstest (OECD 406, EU B.6)

Mutageniciteit

Conclusie/Samenvatting : Niet beschikbaar.

Carcinogeniciteit

Conclusie/Samenvatting : Niet beschikbaar.

Toxiciteit voor de voortplanting

Conclusie/Samenvatting : Niet beschikbaar.

Teratogeniciteit

Conclusie/Samenvatting : Niet beschikbaar.

Informatie over de meest waarschijnlijke blootstellingsroutes : Niet beschikbaar.

Mogelijke acute gevolgen voor de gezondheid

Inademing : Irriterend voor de ademhalingswegen. Blootstelling aan ontledingsproducten kan gevaar voor de gezondheid opleveren. Na blootstelling kunnen ernstige gevolgen met vertraging optreden.

Inslikken : Kan brandwonden aan mond, keel en maag veroorzaken.

Huidcontact : Zeer corrosief voor de huid. Veroorzaakt ernstige brandwonden. Kan overgevoeligheid veroorzaken bij contact met de huid.

Oogcontact : Zeer corrosief voor de ogen. Veroorzaakt ernstige brandwonden.

RUBRIEK 11: Toxicologische informatie

Symptomen met betrekking tot de fysische, chemische en toxicologische eigenschappen

Inademing : Ongewenste symptomen kunnen de volgende zijn:
irritatie van de luchtwegen
hoesten

Inslikken : Ongewenste symptomen kunnen de volgende zijn:
maagpijnen

Huidcontact : Ongewenste symptomen kunnen de volgende zijn:
pijn of irritatie
roodheid
blaarvorming kan voorkomen

Oogcontact : Ongewenste symptomen kunnen de volgende zijn:
pijn
tranenvloed
roodheid

Vertraagd optredende en directe effecten en ook chronische effecten als gevolg van kortdurende en langdurige blootstelling

Kortdurende blootstelling

Mogelijke directe effecten : Niet beschikbaar.

Mogelijke vertraagde effecten : Niet beschikbaar.

Langdurige blootstelling

Mogelijke directe effecten : Niet beschikbaar.

Mogelijke vertraagde effecten : Niet beschikbaar.

Mogelijke chronische gevolgen voor de gezondheid

Niet beschikbaar.

Conclusie/Samenvatting : Niet beschikbaar.

Algemeen : Bij personen die eenmaal zijn gesensibiliseerd, kan daarna bij blootstelling aan zeer lage concentraties een ernstige allergische reactie plaatsvinden.

Carcinogeniciteit : Significante effecten of kritische gevaren zijn niet bekend.

Mutageniciteit : Significante effecten of kritische gevaren zijn niet bekend.

Teratogeniciteit : Significante effecten of kritische gevaren zijn niet bekend.

Effecten op de ontwikkeling : Significante effecten of kritische gevaren zijn niet bekend.

Effecten op de vruchtbaarheid : Significante effecten of kritische gevaren zijn niet bekend.

Overige informatie : Niet beschikbaar.

RUBRIEK 12: Ecologische informatie

12.1 Toxiciteit

Product-/ingrediëntennaam	Resultaat	Soorten	Blootstelling
bifenyl-2-ol	Acuut EC50 0.85 mg/L	Algen	72 uren
	Acuut EC50 1.5 mg/L	Daphnia	24 uren
	Acuut LC50 710 ug/L Zoetwater	Daphnia - Daphnia magna - <24 uren	48 uren
	Acuut LC50 2.3 mg/L	Vis	96 uren
	Acuut LC50 20 mg/L	Vis	96 uren
kaliumhydroxide	Acuut LC50 80 mg/L	Vis	24 uren
	Acuut LC50 80000 ug/L Zoetwater	Vis - Gambusia affinis - Adult	96 uren
1,2-benzisothiazool-3(2H)-on	Acuut EC50 2.44 mg/l	Daphnia - Daphnia magna	48 uren
	Acuut LC50 0.74 mg/l	Vis	96 uren
natriumhydroxide	Acuut EC50 76 mg/l	Daphnia	24 uren
	Acuut EC50 40.38 mg/L Zoetwater	Daphnia - Ceriodaphnia dubia - Neonate - <24 uren	48 uren

RUBRIEK 12: Ecologische informatie

	Acuut LC50 33000 tot 100000 ug/L Zeewater	Crustaceeën - Crangon crangon - Adult	48 uren
	Acuut LC50 99 mg/l	Vis - Lepomis macrochirus	48 uren
	Acuut LC50 45.5 mg/l	Vis - Oncorhynchus mykiss	96 uren
	Chronisch NOEC 56 mg/L Zeewater	Vis - Poecilia reticulata - Young - 3 tot 4 weken	96 uren

Conclusie/Samenvatting : Niet beschikbaar.

12.2 Persistentie en afbreekbaarheid

Conclusie/Samenvatting : Niet beschikbaar.

Product-/ingrediëntennaam	Halfwaardetijd in water	Fotolyse	Biologische afbreekbaarheid
bifenyl-2-ol	-	-	Gemakkelijk

Product- /ingrediëntennaam	BOD_5	COD	ThOD
bifenyl-2-ol	62.2 mg/l	-	-

12.3 Bioaccumulatie

Product-/ingrediëntennaam	$LogP_{ow}$	BCF	Potentieel
bifenyl-2-ol	3.18	-	hoog
1,2-benzisothiazool-3(2H)-on	0.4	-	laag

12.4 Mobiliteit in de bodem

Scheidingscoëfficiënt aarde/water (K_{OC}) : Niet van toepassing.

Mobiliteit : Niet beschikbaar.

12.5 Resultaten van PBT- en zPzB-beoordeling

PBT : Niet van toepassing.

zPzB : Niet van toepassing.

12.6 Andere schadelijke effecten : Significante effecten of kritische gevaren zijn niet bekend.

RUBRIEK 13: Instructies voor verwijdering

De informatie in deze rubriek bevat algemene adviezen en richtlijnen. De lijst van Aanbevolen toepassingen in Rubriek 1 moet worden geraadpleegd voor eventueel beschikbare gebruikspecifieke informatie die gegeven wordt in de Blootstellingscenario('s).

13.1 Afvalverwerkingsmethoden

Product

Verwijderingsmethoden : Het produceren van afval dient altijd voor zover mogelijk te worden vermeden of tot een minimum te worden beperkt. Lege vaten of binnenzak kunnen enig restproduct bevatten. Deze stof en de verpakking op veilige wijze afvoeren. Grote hoeveelheden productresten mogen niet via het riool worden afgevoerd, maar moeten worden verwerkt in een geschikte afvalwaterbehandelingsinstallatie. Laat overtollige en niet te recycleren producten afvoeren door een vergunninghoudend afvalverwerkingsbedrijf. Het afvoeren van dit product, oplossingen en alle bijproducten dient altijd te geschieden in overeenstemming met de geldende wetgeving op het gebied van milieubescherming en afvalverwerking en met alle andere regionaal of plaatselijk geldende reglementeringen. Vermijd verspreiding van gemorst materiaal en afvalmateriaal en voorkom dat dit in contact komt met bodem, waterwegen, afvoerleidingen en riool.

Gevaarlijke Afvalstoffen : Ja.

Europese Afvalcatalogus (EAK)

RUBRIEK 13: Instructies voor verwijdering

Afvalcode	Afvalnotatie
07 04 99	niet elders genoemd afval

Verpakking

Verwijderingsmethoden : Het produceren van afval dient altijd voor zover mogelijk te worden vermeden of tot een minimum te worden beperkt. De lege verpakking moet worden gerecycled. Verbranding of storten moet alleen worden overwogen wanneer recycling niet mogelijk is.

Speciale voorzorgsmaatregelen : Deze stof en de verpakking op veilige wijze afvoeren. Wees voorzichtig met het hanteren van lege verpakkingen/containers die nog niet zijn schoongemaakt of omgespoeld. Lege vaten of binnenzak kunnen enig restproduct bevatten. Vermijd verspreiding van gemorst materiaal en afvalmateriaal en voorkom dat dit in contact komt met bodem, waterwegen, afvoerleidingen en riool.

RUBRIEK 14: Informatie met betrekking tot het vervoer

	ADR/RID	IMDG	IATA
14.1 UN-nummer	UN3266	UN3266	UN3266
14.2 Juiste ladingnaam overeenkomstig de modelreglementen van de VN	Bijtende basische anorganische vloeistof, n.e.g. (Bevat: kaliumhydroxide, bifenyl-2-ol)	Corrosive liquid, basic, inorganic, n.o.s. (Contains: Potassium hydroxide, 2-phenylphenol (ISO))	Corrosive liquid, basic, inorganic, n.o.s. (Contains: Potassium hydroxide, 2-phenylphenol (ISO))
14.3 Transportgevarenklasse(n)	8 C5 	8 	8 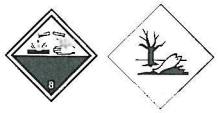
14.4 Verpakkingsgroep	III	III	III
14.5 Milieugevaren	Ja.	Yes.	Yes.
14.6 Bijzondere voorzorgen voor de gebruiker	Niet beschikbaar.	Niet beschikbaar.	Niet beschikbaar.
Extra informatie	-	**Emergency schedules (EmS)** F-A, S-B Marine pollutant	-

14.7 Vervoer in bulk overeenkomstig bijlage II bij MARPOL 73/78 en de IBC-code : Niet beschikbaar.

RUBRIEK 15: Regelgeving

15.1 Specifieke veiligheids-, gezondheids- en milieureglementen en -wetgeving voor de stof of het mengsel

EU Verordening (EG) nr. 1907/2006 (REACH)

Bijlage XIV - Lijst van stoffen die aan toestemming zijn onderworpen

Zeer zorgwekkende stoffen

Geen van de bestanddelen zijn gereguleerd.

RUBRIEK 15: Regelgeving

Bijlage XVII - Beperkingen met betrekking tot de productie, het op de markt brengen en het gebruik van bepaalde gevaarlijke stoffen, mengsels en producten : Niet van toepassing.

Overige EU-regelgeving

Europese inventaris : Alle bestanddelen worden vermeld tenzij ze daarvan zijn vrijgesteld.

Zwarte lijst van stoffen : Niet vermeld

Lijst van prioritaire stoffen : In lijst opgenomen

Lijst geïntegreerde preventie en bestrijding van verontreiniging (IPPC) - Lucht : Niet vermeld

Lijst geïntegreerde preventie en bestrijding van verontreiniging (IPPC) - Water : Niet vermeld

Nationale regelgeving

Productregistratie : **Australische inventaris (AICS)**: Alle bestanddelen worden vermeld tenzij ze daarvan zijn vrijgesteld.
Chinese inventaris (IECSC): Alle bestanddelen worden vermeld tenzij ze daarvan zijn vrijgesteld.
Japanse inventaris: Alle bestanddelen worden vermeld tenzij ze daarvan zijn vrijgesteld.
Koreaanse inventaris: Alle bestanddelen worden vermeld tenzij ze daarvan zijn vrijgesteld.
Nieuw Zeelandse lijst van chemische stoffen (NZIoC): Alle bestanddelen worden vermeld tenzij ze daarvan zijn vrijgesteld.
Lijst Chemische stoffen op de Filippijnen (PICCS): Alle bestanddelen worden vermeld tenzij ze daarvan zijn vrijgesteld.
V.S. Inventaris (TSCA 8b): Alle bestanddelen worden vermeld tenzij ze daarvan zijn vrijgesteld.
Europese inventaris: Alle bestanddelen worden vermeld tenzij ze daarvan zijn vrijgesteld.
Canadese inventaris: Alle bestanddelen worden vermeld tenzij ze daarvan zijn vrijgesteld.

Productregistratienummer

Noorwegen : P-200424

Denemarken : 16655552

Zweden : 416497-6

Zwitserland : 61317

Denemarken

MAL-code : 00-4

Duitsland

Risikoklasse voor water : 2 Aanhangsel 4

Internationale regelgeving

Chemische Wapens Conventie Bijlage I stoffen : Niet vermeld

Chemische Wapens Conventie Bijlage II stoffen : Niet vermeld

Chemische Wapens Conventie Bijlage III stoffen : Niet vermeld

RUBRIEK 15: Regelgeving

15.2 Chemischeveiligheidsbeoordeling : Dit product bevat bestanddelen waarvoor chemische veiligheidsbeoordelingen vereist zijn.

RUBRIEK 16: Overige informatie

Geeft informatie aan die gewijzigd is sinds de voorgaande uitgave.

Afkortingen en acroniemen : ATE = Acuut toxiciteitsschatting
CLP = Indeling, etikettering en verpakking van stoffen en mengsels [Verordening (EG) No. 1272/2008]
DNEL = De afgeleide dosis zonder effect
EUH zin = CLP-specifieke gevaarszin
PNEC = Voorspelde geen effect concentratie
RRN = REACH registratie nummer

Classificatie volgens de Regelgeving (EG) 1272/2008 [CLP/GHS]

Skin Corr. 1A, H314
Eye Dam. 1, H318
Skin Sens. 1, H317
STOT SE 3, H335i
Aquatic Acute 1, H400

Procedure gebruikt voor het afleiden van de indeling in overeenstemming met Verordening (EG) nr.1272/2008 [CLP/GHS]

Classificatie	Rechtvaardiging
Skin Corr. 1A, H314	Beoordeling door deskundige
Eye Dam. 1, H318	Beoordeling door deskundige
Skin Sens. 1, H317	Beoordeling door deskundige
STOT SE 3, H335i	Beoordeling door deskundige
Aquatic Acute 1, H400	Beoordeling door deskundige

Volledige tekst van afgekorte S-zinnen :

H290	Kan bijtend zijn voor metalen.
H301	Giftig bij inslikken.
H302	Schadelijk bij inslikken.
H314	Veroorzaakt ernstige brandwonden en oogletsel.
H315	Veroorzaakt huidirritatie.
H317	Kan een allergische huidreactie veroorzaken.
H318	Veroorzaakt ernstig oogletsel.
H319	Veroorzaakt ernstige oogirritatie.
H335	Kan irritatie van de luchtwegen veroorzaken.
H335i	Kan irritatie van de luchtwegen veroorzaken.
H400	Zeer giftig voor in het water levende organismen.

Volledige tekst van indelingen [CLP/GHS] :

Acute Tox. 3, H301	ACUTE TOXICITEIT: ORAAL - Categorie 3
Acute Tox. 4, H302	ACUTE TOXICITEIT: ORAAL - Categorie 4
Aquatic Acute 1, H400	ACUTE AQUATISCHE TOXICITEIT - Categorie 1
Eye Dam. 1, H318	ERNSTIG OOGLETSEL/OOGIRRITATIE - Categorie 1
Eye Irrit. 2, H319	ERNSTIG OOGLETSEL/OOGIRRITATIE - Categorie 2
Met. Corr. 1, H290	BIJTEND VOOR METALEN - Categorie 1
Skin Corr. 1A, H314	HUIDCORROSIE/-IRRITATIE - Categorie 1A
Skin Irrit. 2, H315	HUIDCORROSIE/-IRRITATIE - Categorie 2
Skin Sens. 1, H317	HUIDALLERGEEN - Categorie 1
STOT SE 3, H335	SPECIFIEKE DOELORGAANTOXICITEIT BIJ EENMALIGE BLOOTSTELLING [Irritatie van de luchtwegen] - Categorie 3
STOT SE 3, H335i	SPECIFIEKE DOELORGAANTOXICITEIT BIJ EENMALIGE BLOOTSTELLING: INADEMING [Irritatie van de luchtwegen] - Categorie 3

Volledige tekst van afgekorte R-zinnen : R22- Schadelijk bij opname door de mond.
R35- Veroorzaakt ernstige brandwonden.
R41- Gevaar voor ernstig oogletsel.
R37- Irriterend voor de ademhalingswegen.
R38- Irriterend voor de huid.
R36/37/38- Irriterend voor de ogen, de ademhalingswegen en de huid.
R43- Kan overgevoeligheid veroorzaken bij contact met de huid.

RUBRIEK 16: Overige informatie

R50- Zeer vergiftig voor in het water levende organismen.

Volledige tekst van indelingen [Richtlijn gevaarlijke stoffen/Richtlijn gevaarlijke preparaten]	:	C - Bijtend Xn - Schadelijk Xi - Irriterend N - Milieugevaarlijk
Gedrukt op	:	juli 03, 2012.
Datum van uitgave/ Revisie datum	:	juni 06, 2012.
Datum vorige uitgave	:	mei 22, 2012.
Versie	:	6.01

Kennisgeving aan de lezer

Naar ons beste weten is de hierin ingesloten informatie juist. Noch bovengenoemde leverancier, noch enige dochtermaatschappij ervan, aanvaardt echter ook maar enige aansprakelijkheid voor de juistheid en volledigheid van de hierin besloten informatie. De gebruiker is als enige verantwoordelijk voor de uiteindelijke beslissing of een bepaald materiaal al dan niet geschikt is. Elk van de materialen kan onbekende risico's met zich meebrengen. In het gebruik ervan moet daarom grote zorgvuldigheid betracht worden. Ofschoon sommige risico's in dit gevarendocument worden beschreven, kunnen wij niet garanderen dat dit de enige bestaande risico's zijn.

Appendix B

Overview of Sample Production Procedures

This appendix gives an overview of the casting and drying procedures described in Chapter 4 and used in Chapter 6.

Table B.1: Comparison of the two film casting methods.

	Method 1	Method 2
Mould	I	II
Size	1.0x1.0 m	0.49x0.49 m
Materials	MDF, Perspex, Teflon	MDF, Perspex, Polyethylene
Glue	75 g	30 g
Water	1500 ml	300 ml
Preservatives	None	0.1 v%
Soaking time	>1 h	>1 h
Casting temperature	55-60 °C	55-60 °C

Table B.2: Comparison of the three film drying methods.

	Method 1	Method 2	Method 3
Mould	2xI	2xII	2xII
Location	Isolated room AG	(1) Isolated room AG (2) Conservation studio AG	*Weiss SB11 300 40* Delft
Dessicants	None	200 g	None
Climate	Logged	(1) Logged (2) 55% RH & 21 °C	(1) 48h 70% RH & 18 °C (2) 24h 55% RH & 21 °C

Appendix C

Climate Logs of the Animal Glue Films made at the Atelier Gebouw

The following graphs show the climates measured for the glues made in the AG. Except for Figure C.5, all nicely follow the profile used in the climate chamber in Delft. The explanation for the different behaviour of the data in Figure C.5 is trivial. The RH/T-Logger was accidentally left in the climate chamber of the AG when the moulds were taken up to the furniture conservation studio.

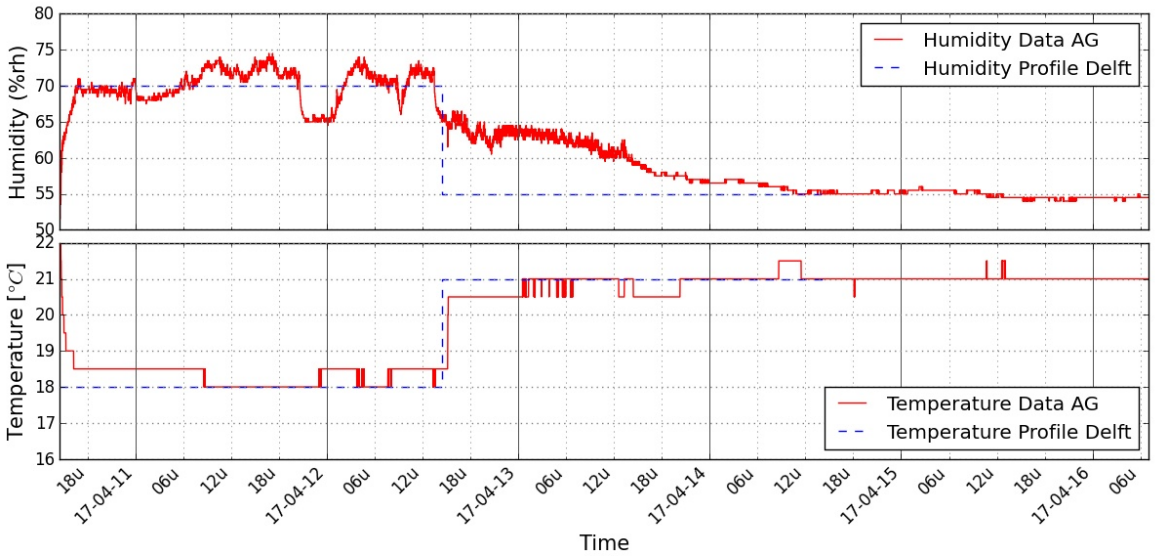

Figure C.1: Logged humidity and temperature for G240RMA1 and G180RMA1 compared to the profile used in the climate chamber in Delft.

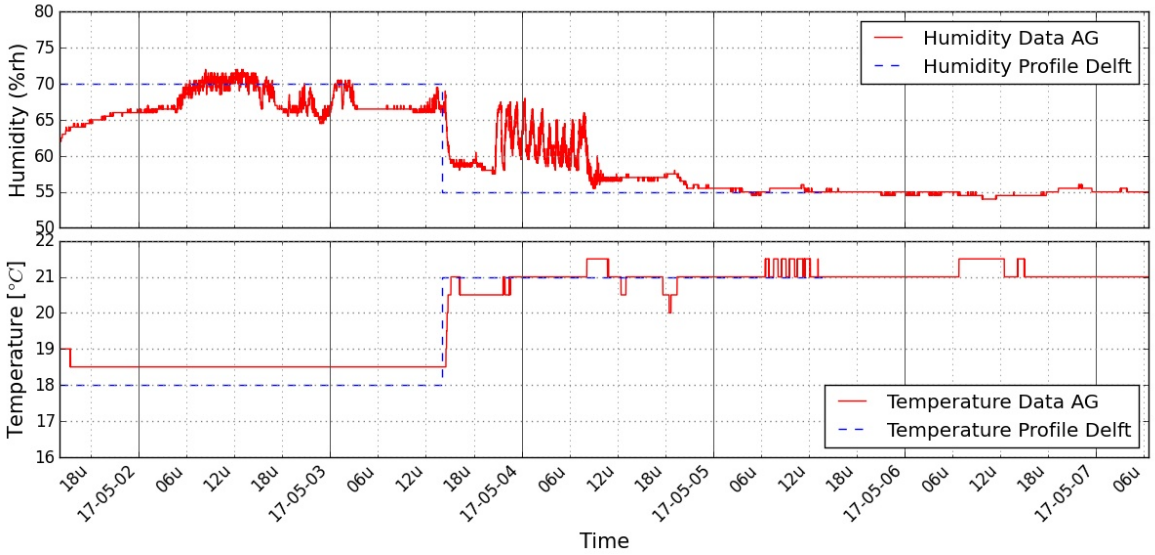

Figure C.2: Logged humidity and temperature for G120RMA1 and L330RMA1 compared to the profile used in the climate chamber in Delft.

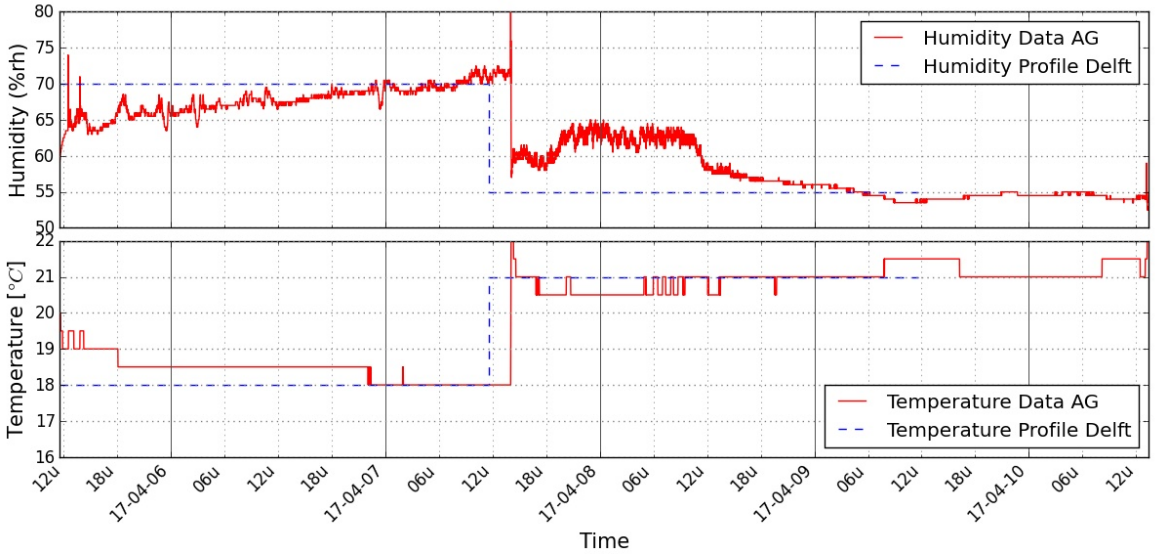

Figure C.3: Logged humidity and temperature for L180RMA1 and G240RMA2 compared to the profile used in the climate chamber in Delft.

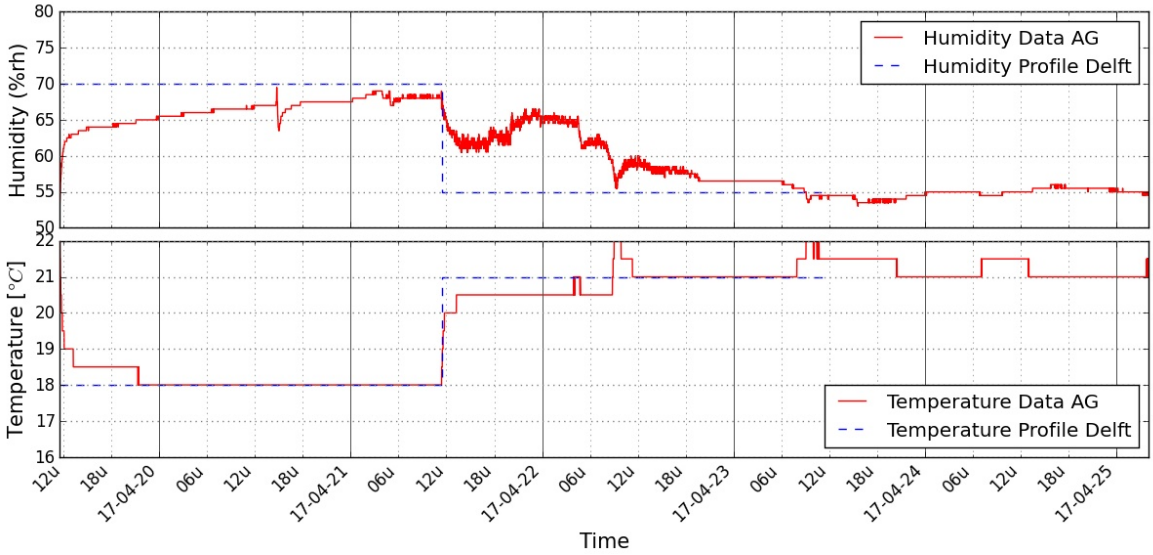

Figure C.4: Logged humidity and temperature for G180RMA2 and G120RMA2 compared to the profile used in the climate chamber in Delft.

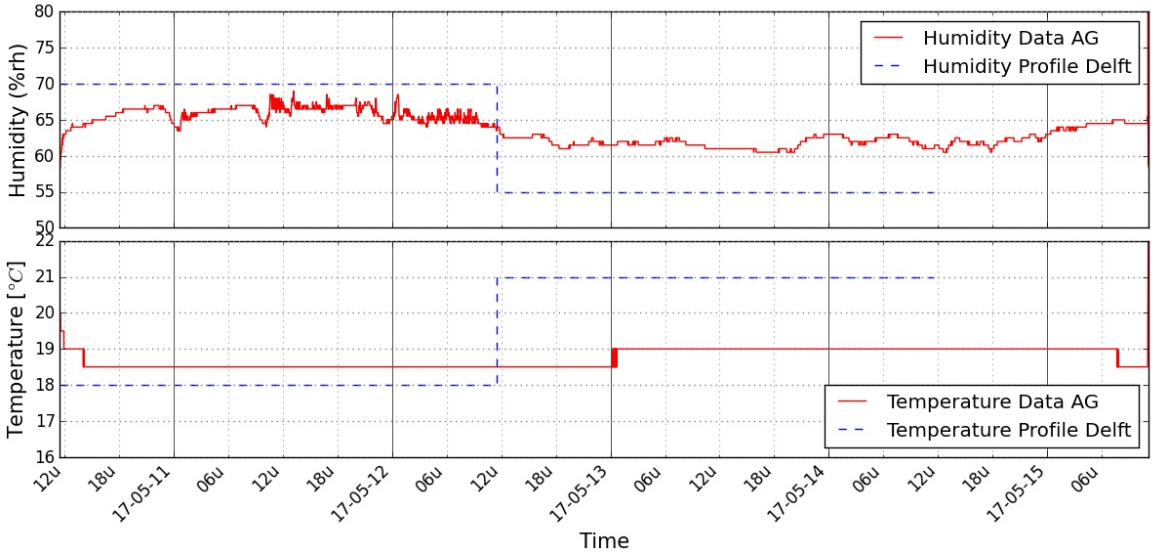

Figure C.5: Logged humidity and temperature for L330RMA2 and L180RMA2 compared to the profile used in the climate chamber in Delft.

Appendix D

Results of the Tensile Tests

This appendix shows the data of all 200 tensile tests. First a series of tables show a summary of the data, followed by the stress-strain curves of the tests, grouped per five tests.

For Table D.1 till D.5 the following remarks hold: Two entries do not have a value for E. For G240RMA1-6 the reason was that the extensometer was not connected, however, for L330RMA1-8 the reason is not exactly known.

E, $F_{\max}$, and $\epsilon_{F\max}$ were measured by the tensile testing machine. The latter variable is not particular accurate as several entries have been influenced by slippage as can be seen from the stress strain curves in this appendix.

The M was determined using a balance and the thicknesses t_1-t_3 were measured using an analogue micrometer. t_1 was measured at the top of the sample, t_2 halfway along its length, and t_3 at the bottom. The t_{avg} used in the calculation of $\sigma_{\max}$ is the average of the three values, rounded to 0.01 mm.

An estimate of estimate of ρ was made using M and an estimate of V. The estimate of V was calculated via the formula:

$$V_{\text{est}} = \text{length} \cdot \text{width} \cdot (t_2 + \frac{1}{2}(t_1 - t_2) + \frac{1}{2}(t_3 - t_2))$$

Finally, the factor K_{vq} is a factor describing the amount of visible damage to the samples. The factor ranges from 1-4, with 1 being no damage and 4 being severe damage such as wrinkles with decreased thickness etc.

The graphs show the force-strain curves of all the tests. These curves are the most unprocessed forms of the data. The graphs include the results found from tests that have been discarded in the analysis of the results. They have been included here for sake of completeness. All graphs have the same scale to allow for easy comparison.

The most obvious flaw can be found in Figure D.2. Sample G240RMA1-6 shows no strain as the load increases. This was due to the fact that the extensometer was not connected during that specific run.

Other flaws that are clearly visible are results of slippage of the extensometer. In most cases it shows up as an increase in load without an increase in strain, or even a decrease in strain. This is for example visible in Figure D.3, for the samples G240RMA2-3 and G240RMA2-5.

Table D.1: Summary of the tensile data of the G240 films

Sample ID	E [GPa]	F_{max} [N]	σ_{max} [MPa]	$\varepsilon_{F_{max}}$ [%]	M [mg]	t_1 [mm]	t_2 [mm]	t_3 [mm]	K_{vq} [-]	V [mm^3]	ρ [$\frac{mg}{mm^3}$]
G240-RMA-1-1	4.7	216	83	2.1	581.7	0.13	0.13	0.14	2	$4.6{\cdot}10^2$	1.3
G240-RMA-1-2	4.7	249	96	4.2	583.7	0.13	0.13	0.14	2	$4.6{\cdot}10^2$	1.3
G240-RMA-1-3	4.6	239	92	3.1	575.5	0.13	0.13	0.14	2	$4.6{\cdot}10^2$	1.2
G240-RMA-1-4	4.2	245	94	4.2	577.4	0.13	0.13	0.13	2	$4.5{\cdot}10^2$	1.3
G240-RMA-1-5	4.8	235	90	2.8	577.9	0.13	0.13	0.13	2	$4.5{\cdot}10^2$	1.3
G240-RMA-1-6		237	91	0.0	572.3	0.13	0.13	0.13	2	$4.5{\cdot}10^2$	1.3
G240-RMA-1-7	4.6	152	59	1.4	576.6	0.13	0.13	0.13	2	$4.5{\cdot}10^2$	1.3
G240-RMA-1-8	4.7	232	89	2.9	585.4	0.13	0.14	0.13	2	$4.7{\cdot}10^2$	1.2
G240-RMA-1-9	5.0	247	95	4.0	582.7	0.13	0.14	0.13	2	$4.7{\cdot}10^2$	1.2
G240-RMA-1-10	4.7	249	96	5.8	579.4	0.13	0.13	0.13	2	$4.5{\cdot}10^2$	1.3
G240-RMA-2-1	4.3	233	83	3.5	590.8	0.14	0.14	0.14	2	$4.9{\cdot}10^2$	1.2
G240-RMA-2-2	4.5	229	82	2.4	595.4	0.13	0.14	0.14	2	$4.8{\cdot}10^2$	1.2
G240-RMA-2-3	4.4	234	83	1.5	604.6	0.14	0.14	0.14	2	$4.9{\cdot}10^2$	1.2
G240-RMA-2-4	4.7	236	84	2.1	610.1	0.14	0.14	0.14	2	$4.9{\cdot}10^2$	1.3
G240-RMA-2-5	4.6	187	67	1.4	608.2	0.15	0.14	0.14	3	$5.0{\cdot}10^2$	1.2
G240-RMA-2-6	4.6	155	55	1.3	607.8	0.14	0.14	0.14	3	$4.9{\cdot}10^2$	1.2
G240-RMA-2-7	4.8	224	80	1.9	618.6	0.14	0.14	0.15	3	$5.0{\cdot}10^2$	1.2
G240-RMA-2-8	5.2	216	83	2.5	583.0	0.13	0.13	0.13	2	$4.5{\cdot}10^2$	1.3
G240-RMA-2-9	4.3	231	83	3.1	591.8	0.14	0.13	0.14	2	$4.7{\cdot}10^2$	1.3
G240-RMA-2-10	5.0	164	63	1.5	597.3	0.13	0.13	0.13	2	$4.5{\cdot}10^2$	1.3
G240-D-1-1	4.6	156	78	2.5	405.8	0.10	0.10	0.09	2	$3.4{\cdot}10^2$	1.2
G240-D-1-2	4.5	141	70	1.7	426.0	0.10	0.10	0.09	2	$3.4{\cdot}10^2$	1.3
G240-D-1-3	4.8	182	83	2.4	454.9	0.11	0.11	0.10	2	$3.8{\cdot}10^2$	1.2
G240-D-1-4	5.3	188	85	2.4	461.7	0.11	0.11	0.10	2	$3.8{\cdot}10^2$	1.2
G240-D-1-5	4.8	205	93	2.9	492.8	0.11	0.11	0.11	2	$3.9{\cdot}10^2$	1.3
G240-D-1-6	4.3	194	81	2.9	481.8	0.12	0.11	0.12	2	$4.0{\cdot}10^2$	1.2
G240-D-1-7	5.1	155	86	2.1	394.9	0.09	0.09	0.09	2	$3.1{\cdot}10^2$	1.3
G240-D-1-8	4.4	154	77	2.2	462.2	0.10	0.09	0.10	3	$3.3{\cdot}10^2$	1.4
G240-D-1-9	3.8	181	82	3.4	450.7	0.11	0.10	0.11	2	$3.7{\cdot}10^2$	1.2
G240-D-1-10	4.8	228	95	3.3	545.9	0.13	0.12	0.12	3	$4.3{\cdot}10^2$	1.3
G240-D-2-1	5.3	236	98	2.8	588.9	0.13	0.14	0.14	2	$4.8{\cdot}10^2$	1.2
G240-D-2-2	4.9	238	92	3.4	578.7	0.12	0.13	0.14	2	$4.5{\cdot}10^2$	1.3
G240-D-2-3	4.4	231	89	3.0	577.7	0.12	0.13	0.14	2	$4.5{\cdot}10^2$	1.3
G240-D-2-4	4.9	232	89	1.9	569.0	0.11	0.13	0.14	2	$4.5{\cdot}10^2$	1.3
G240-D-2-5	4.5	242	87	2.8	621.3	0.14	0.14	0.14	2	$4.9{\cdot}10^2$	1.3
G240-D-2-6	5.3	221	85	2.2	602.8	0.13	0.13	0.14	2	$4.6{\cdot}10^2$	1.3
G240-D-2-7	4.6	236	84	1.6	602.8	0.14	0.13	0.14	2	$4.7{\cdot}10^2$	1.3
G240-D-2-8	4.5	220	85	2.2	587.4	0.13	0.13	0.14	2	$4.6{\cdot}10^2$	1.3
G240-D-2-9	4.7	200	77	1.7	546.2	0.13	0.12	0.13	2	$4.4{\cdot}10^2$	1.3
G240-D-2-10	4.9	250	83	2.1	662.8	0.15	0.15	0.15	2	$5.3{\cdot}10^2$	1.3

Table D.2: Summary of the tensile data of the G180 films

Sample ID	E [GPa]	F_{max} [N]	σ_{max} [MPa]	$\varepsilon_{F_{max}}$ [%]	M [mg]	t_1 [mm]	t_2 [mm]	t_3 [mm]	K_{vq} [-]	V [mm^3]	ρ [$\frac{mg}{mm^3}$]
G180-RMA-1-1	4.7	230	89	2.5	588.9	0.14	0.13	0.13	2	$4.6{\cdot}10^2$	1.3
G180-RMA-1-2	4.7	209	81	2.1	591.3	0.14	0.13	0.13	2	$4.6{\cdot}10^2$	1.3
G180-RMA-1-3	4.5	199	77	1.8	579.3	0.13	0.13	0.13	2	$4.5{\cdot}10^2$	1.3
G180-RMA-1-4	4.4	225	87	2.5	574.8	0.13	0.13	0.13	2	$4.5{\cdot}10^2$	1.3
G180-RMA-1-5	4.3	230	89	3.2	570.9	0.13	0.13	0.13	2	$4.5{\cdot}10^2$	1.3
G180-RMA-1-6	4.7	224	93	1.6	560.7	0.13	0.12	0.12	2	$4.3{\cdot}10^2$	1.3
G180-RMA-1-7	4.5	182	70	1.6	554.7	0.13	0.13	0.12	2	$4.5{\cdot}10^2$	1.2
G180-RMA-1-8	4.5	188	67	1.7	621.0	0.14	0.13	0.14	3	$4.7{\cdot}10^2$	1.3
G180-RMA-1-9	4.8	150	54	1.0	619.9	0.14	0.14	0.14	3	$4.9{\cdot}10^2$	1.3
G180-RMA-1-10	4.8	229	82	1.5	616.1	0.14	0.14	0.14	2	$4.9{\cdot}10^2$	1.3
G180-RMA-2-1	4.1	221	74	2.6	638.0	0.15	0.15	0.14	3	$5.2{\cdot}10^2$	1.2
G180-RMA-2-2	4.3	190	68	2.0	626.0	0.14	0.14	0.13	3	$4.8{\cdot}10^2$	1.3
G180-RMA-2-3	4.0	151	50	1.4	634.3	0.15	0.15	0.14	3	$5.2{\cdot}10^2$	1.2
G180-RMA-2-4	3.6	71	25	0.7	622.7	0.15	0.14	0.14	3	$5.0{\cdot}10^2$	1.3
G180-RMA-2-5	3.6	89	32	0.8	587.2	0.15	0.14	0.12	3	$4.8{\cdot}10^2$	1.2
G180-RMA-2-6	4.1	147	57	1.8	585.5	0.13	0.13	0.14	3	$4.6{\cdot}10^2$	1.3
G180-RMA-2-7	4.0	143	55	1.6	572.4	0.13	0.12	0.14	3	$4.5{\cdot}10^2$	1.3
G180-RMA-2-8	4.0	143	55	1.7	529.2	0.13	0.13	0.13	3	$4.5{\cdot}10^2$	1.2
G180-RMA-2-9	4.4	185	66	1.9	589.1	0.13	0.14	0.14	3	$4.8{\cdot}10^2$	1.2
G180-RMA-2-10	4.0	147	52	1.4	617.0	0.13	0.14	0.14	3	$4.8{\cdot}10^2$	1.3
G180-D-1-1	4.4	168	70	1.2	467.4	0.12	0.11	0.13	2	$4.1{\cdot}10^2$	1.1
G180-D-1-2	5.0	143	65	1.1	499.5	0.12	0.11	0.10	3	$3.9{\cdot}10^2$	1.3
G180-D-1-3	5.1	181	82	1.8	512.0	0.13	0.11	0.10	3	$3.9{\cdot}10^2$	1.3
G180-D-1-4	5.3	201	84	0.6	528.3	0.13	0.12	0.11	2	$4.2{\cdot}10^2$	1.3
G180-D-1-5	5.0	219	91	2.8	545.4	0.13	0.12	0.11	2	$4.2{\cdot}10^2$	1.3
G180-D-1-6	4.4	138	63	1.2	459.7	0.11	0.11	0.10	2	$3.8{\cdot}10^2$	1.2
G180-D-1-7	4.7	191	87	1.3	482.6	0.11	0.11	0.11	2	$3.9{\cdot}10^2$	1.3
G180-D-1-8	4.9	206	94	2.9	502.6	0.12	0.11	0.11	2	$3.9{\cdot}10^2$	1.3
G180-D-1-9	4.7	216	90	3.3	526.8	0.13	0.12	0.11	2	$4.2{\cdot}10^2$	1.3
G180-D-1-10	5.2	212	88	2.2	554.0	0.13	0.12	0.12	2	$4.3{\cdot}10^2$	1.3
G180-D-2-1	4.4	171	61	1.3	600.8	0.13	0.14	0.14	3	$4.8{\cdot}10^2$	1.3
G180-D-2-2	5.7	80	33	0.6	605.3	0.15	0.14	0.13	3	$4.9{\cdot}10^2$	1.2
G180-D-2-3	4.5	155	55	1.3	603.9	0.14	0.14	0.14	3	$4.9{\cdot}10^2$	1.2
G180-D-2-4	4.5	165	64	1.6	593.0	0.13	0.14	0.13	3	$4.7{\cdot}10^2$	1.3
G180-D-2-5	4.8	155	59	1.3	543.4	0.13	0.13	0.15	3	$4.7{\cdot}10^2$	1.1
G180-D-2-6	3.5	77	28	0.8	604.9	0.13	0.14	0.13	3	$4.7{\cdot}10^2$	1.3
G180-D-2-7	4.1	174	67	1.6	590.2	0.14	0.14	0.14	4	$4.9{\cdot}10^2$	1.2
G180-D-2-8	3.2	158	56	1.5	569.2	0.15	0.12	0.11	3	$4.4{\cdot}10^2$	1.3
G180-D-2-9	3.9	198	76	1.9	570.9	0.13	0.14	0.14	4	$4.8{\cdot}10^2$	1.2
G180-D-2-10	2.9	93	33	1.0	561.7	0.11	0.13	0.14	4	$4.5{\cdot}10^2$	1.3

Table D.3: Summary of the tensile data of the G120 films

Sample ID	E [GPa]	F_{max} [N]	σ_{max} [MPa]	$\varepsilon_{F_{max}}$ [%]	M [mg]	t_1 [mm]	t_2 [mm]	t_3 [mm]	K_{vq} [-]	V [mm^3]	ρ [$\frac{mg}{mm^3}$]
G120-RMA-1-1	4.3	123	44	1.0	599.6	0.14	0.14	0.14	3	$4.9{\cdot}10^2$	1.2
G120-RMA-1-2	4.3	72	26	0.6	603.2	0.14	0.14	0.14	3	$4.9{\cdot}10^2$	1.2
G120-RMA-1-3	4.6	174	62	0.9	603.3	0.14	0.14	0.14	3	$4.9{\cdot}10^2$	1.2
G120-RMA-1-4	4.3	133	47	1.1	606.7	0.14	0.14	0.14	3	$4.9{\cdot}10^2$	1.2
G120-RMA-1-5	4.7	157	56	1.3	614.9	0.14	0.14	0.14	4	$4.9{\cdot}10^2$	1.3
G120-RMA-1-6	4.3	65	23	0.5	616.9	0.14	0.14	0.15	4	$5.0{\cdot}10^2$	1.2
G120-RMA-1-7	4.3	226	81	2.6	608.4	0.14	0.14	0.14	3	$4.9{\cdot}10^2$	1.2
G120-RMA-1-8	4.1	176	63	0.8	571.3	0.14	0.14	0.14	4	$4.9{\cdot}10^2$	1.2
G120-RMA-1-9	4.4	219	78	2.0	611.5	0.14	0.13	0.15	3	$4.8{\cdot}10^2$	1.3
G120-D-1-1	4.8	127	42	0.9	658.7	0.15	0.15	0.15	4	$5.3{\cdot}10^2$	1.3
G120-RMA-1-10	5.1	200	67	1.7	614.2	0.15	0.14	0.10	2	$4.6{\cdot}10^2$	1.3
G120-RMA-2-1	4.5	196	75	2.1	627.6	0.16	0.14	0.10	2	$4.7{\cdot}10^2$	1.3
G120-RMA-2-2	5.2	193	74	1.8	644.3	0.16	0.16	0.12	2	$5.3{\cdot}10^2$	1.2
G120-RMA-2-3	4.8	203	68	1.9	643.2	0.16	0.15	0.12	2	$5.1{\cdot}10^2$	1.3
G120-RMA-2-4	5.4	209	75	1.9	659.8	0.16	0.16	0.12	2	$5.3{\cdot}10^2$	1.3
G120-RMA-2-5	4.6	217	78	2.1	679.1	0.16	0.16	0.14	2	$5.4{\cdot}10^2$	1.3
G120-RMA-2-6	4.3	244	81	2.7	624.5	0.15	0.13	0.13	2	$4.7{\cdot}10^2$	1.3
G120-RMA-2-7	4.3	219	78	2.8	669.9	0.16	0.15	0.14	3	$5.3{\cdot}10^2$	1.3
G120-RMA-2-8	4.4	214	71	2.0	690.7	0.16	0.15	0.15	3	$5.3{\cdot}10^2$	1.3
G120-RMA-2-9	4.2	224	75	2.1	706.0	0.15	0.16	0.16	2	$5.5{\cdot}10^2$	1.3
G120-RMA-2-10	5.7	210	66	1.7	641.5	0.13	0.15	0.16	2	$5.2{\cdot}10^2$	1.2
G120-D-1-2	4.8	255	85	2.5	647.7	0.14	0.15	0.16	2	$5.3{\cdot}10^2$	1.2
G120-D-1-3	4.2	160	53	1.2	628.1	0.14	0.14	0.16	2	$5.1{\cdot}10^2$	1.2
G120-D-1-4	4.6	225	80	2.2	606.8	0.13	0.14	0.15	2	$4.9{\cdot}10^2$	1.2
G120-D-1-5	4.1	204	73	2.1	576.7	0.13	0.14	0.14	2	$4.8{\cdot}10^2$	1.2
G120-D-1-6	4.6	196	55	1.3	739.9	0.17	0.18	0.18	3	$6.2{\cdot}10^2$	1.2
G120-D-1-7	4.9	245	76	2.0	723.3	0.16	0.17	0.16	2	$5.8{\cdot}10^2$	1.3
G120-D-1-8	4.7	234	69	1.8	765.3	0.16	0.17	0.17	2	$5.9{\cdot}10^2$	1.3
G120-D-1-9	4.7	210	66	1.6	681.9	0.15	0.16	0.17	2	$5.6{\cdot}10^2$	1.2
G120-D-1-10	4.0	215	67	2.0	673.0	0.15	0.16	0.17	3	$5.6{\cdot}10^2$	1.2
G120-D-2-1	4.3	217	78	2.2	607.0	0.14	0.13	0.14	2	$4.7{\cdot}10^2$	1.3
G120-D-2-2	4.8	139	53	1.2	586.0	0.11	0.13	0.14	2	$4.5{\cdot}10^2$	1.3
G120-D-2-3	4.8	160	62	1.5	579.0	0.14	0.12	0.13	2	$4.5{\cdot}10^2$	1.3
G120-D-2-4	4.7	174	67	1.5	562.4	0.14	0.13	0.14	2	$4.7{\cdot}10^2$	1.2
G120-D-2-5	5.0	175	73	1.9	522.4	0.12	0.13	0.12	2	$4.4{\cdot}10^2$	1.2
G120-D-2-6	5.2	177	63	1.5	596.2	0.12	0.14	0.15	3	$4.8{\cdot}10^2$	1.2
G120-D-2-7	4.7	218	73	1.9	618.8	0.15	0.15	0.14	2	$5.2{\cdot}10^2$	1.2
G120-D-2-8	4.9	227	81	2.1	618.6	0.14	0.15	0.13	2	$5.0{\cdot}10^2$	1.2
G120-D-2-9	5.2	242	87	2.7	607.3	0.14	0.13	0.14	2	$4.7{\cdot}10^2$	1.3
G120-D-2-10	4.2	217	78	2.3	595.9	0.15	0.13	0.14	2	$4.8{\cdot}10^2$	1.2

Table D.4: Summary of the tensile data of the L330 films

Sample ID	E [GPa]	F_{max} [N]	σ_{max} [MPa]	$\varepsilon_{F_{max}}$ [%]	M [mg]	t_1 [mm]	t_2 [mm]	t_3 [mm]	K_{vq} [-]	V [mm^3]	ρ [$\frac{mg}{mm^3}$]
L330-RMA-1-1	4.4	109	39	0.8	605.0	0.14	0.14	0.14	3	$4.9{\cdot}10^2$	1.2
L330-RMA-1-2	4.6	132	47	1.1	575.8	0.14	0.14	0.14	4	$4.9{\cdot}10^2$	1.2
L330-RMA-1-3	5.3	115	44	0.9	557.4	0.13	0.14	0.13	3	$4.7{\cdot}10^2$	1.2
L330-RMA-1-4	5.0	112	43	0.9	587.3	0.13	0.13	0.13	2	$4.5{\cdot}10^2$	1.3
L330-RMA-1-5	5.1	91	35	0.8	534.9	0.14	0.13	0.13	4	$4.6{\cdot}10^2$	1.1
L330-RMA-1-6	4.5	131	47	1.0	593.6	0.14	0.14	0.14	3	$4.9{\cdot}10^2$	1.2
L330-RMA-1-7	4.7	191	68	1.5	586.8	0.14	0.14	0.14	3	$4.9{\cdot}10^2$	1.2
L330-RMA-1-8		35	14	0.2	571.2	0.13	0.13	0.13	3	$4.5{\cdot}10^2$	1.3
L330-RMA-1-9	4.7	107	41	0.9	565.8	0.13	0.13	0.13	3	$4.5{\cdot}10^2$	1.2
L330-RMA-1-10	5.2	187	72	1.6	595.3	0.13	0.13	0.13	2	$4.5{\cdot}10^2$	1.3
L330-RMA-2-1	4.9	188	63	1.2	696.3	0.18	0.16	0.11	3	$5.3{\cdot}10^2$	1.3
L330-RMA-2-2	4.9	180	60	1.2	687.2	0.18	0.16	0.11	3	$5.3{\cdot}10^2$	1.3
L330-RMA-2-3	4.3	242	76	1.9	709.9	0.19	0.16	0.12	3	$5.5{\cdot}10^2$	1.3
L330-RMA-2-4	4.2	175	55	1.2	713.2	0.19	0.17	0.12	3	$5.7{\cdot}10^2$	1.3
L330-RMA-2-5	4.0	220	65	1.5	771.2	0.18	0.17	0.15	3	$5.9{\cdot}10^2$	1.3
L330-RMA-2-6	3.4	137	38	1.0	786.3	0.18	0.19	0.18	3	$6.5{\cdot}10^2$	1.2
L330-RMA-2-7	4.4	247	73	1.6	779.7	0.18	0.18	0.15	3	$6.0{\cdot}10^2$	1.3
L330-RMA-2-8	3.8	177	49	1.3	760.9	0.18	0.18	0.17	3	$6.2{\cdot}10^2$	1.2
L330-RMA-2-9	4.4	203	60	1.3	742.7	0.19	0.17	0.16	2	$6.0{\cdot}10^2$	1.2
L330-RMA-2-10	4.2	223	70	1.6	724.3	0.18	0.16	0.15	2	$5.7{\cdot}10^2$	1.3
L330-D-1-1	4.9	122	47	1.0	564.3	0.13	0.14	0.13	3	$4.7{\cdot}10^2$	1.2
L330-D-1-2	4.8	172	66	1.5	577.2	0.14	0.13	0.13	2	$4.6{\cdot}10^2$	1.2
L330-D-1-3	4.5	183	65	1.7	554.6	0.14	0.14	0.13	2	$4.8{\cdot}10^2$	1.1
L330-D-1-4	4.0	151	54	1.3	550.6	0.13	0.14	0.14	3	$4.8{\cdot}10^2$	1.1
L330-D-1-5	5.0	156	60	1.3	550.7	0.14	0.14	0.12	3	$4.7{\cdot}10^2$	1.2
L330-D-1-6	4.5	159	57	1.3	550.0	0.14	0.14	0.14	2	$4.9{\cdot}10^2$	1.1
L330-D-1-7	4.7	86	31	0.6	555.8	0.13	0.14	0.14	3	$4.8{\cdot}10^2$	1.1
L330-D-1-8	4.8	148	57	1.1	538.6	0.13	0.14	0.13	2	$4.7{\cdot}10^2$	1.1
L330-D-1-9	4.9	98	41	0.9	507.9	0.13	0.12	0.12	2	$4.3{\cdot}10^2$	1.2
L330-D-1-10	5.5	108	45	0.9	527.4	0.13	0.13	0.11	2	$4.4{\cdot}10^2$	1.2
L330-D-2-1	4.6	158	53	1.2	668.5	0.15	0.16	0.15	3	$5.4{\cdot}10^2$	1.2
L330-D-2-2	4.0	124	39	0.9	679.7	0.16	0.17	0.15	4	$5.7{\cdot}10^2$	1.2
L330-D-2-3	4.2	156	52	1.2	674.1	0.15	0.15	0.15	4	$5.3{\cdot}10^2$	1.3
L330-D-2-4	4.4	159	53	1.1	665.1	0.16	0.16	0.14	3	$5.4{\cdot}10^2$	1.2
L330-D-2-5	4.8	186	62	1.4	678.4	0.16	0.14	0.16	3	$5.3{\cdot}10^2$	1.3
L330-D-2-6	4.4	167	56	1.2	670.8	0.15	0.14	0.15	3	$5.1{\cdot}10^2$	1.3
L330-D-2-7	5.0	161	62	1.4	611.3	0.14	0.14	0.12	2	$4.7{\cdot}10^2$	1.3
L330-D-2-8	4.7	148	53	1.3	619.8	0.14	0.14	0.14	3	$4.9{\cdot}10^2$	1.3
L330-D-2-9	4.4	93	39	0.9	561.6	0.11	0.13	0.13	4	$4.4{\cdot}10^2$	1.3
L330-D-2-10	4.7	141	54	1.3	603.4	0.14	0.12	0.14	3	$4.5{\cdot}10^2$	1.3

Table D.5: Summary of the tensile data of the L180 films

Sample ID	E [GPa]	F_{max} [N]	σ_{max} [MPa]	$\varepsilon_{F_{max}}$ [%]	M [mg]	t_1 [mm]	t_2 [mm]	t_3 [mm]	K_{vq} [-]	V [mm^3]	ρ [$\frac{mg}{mm^3}$]
L180-RMA-1-1	4.1	76	29	0.7	575.3	0.13	0.13	0.14	3	$4.6 \cdot 10^2$	1.2
L180-RMA-1-2	4.9	146	56	1.3	563.2	0.13	0.13	0.13	4	$4.5 \cdot 10^2$	1.2
L180-RMA-1-3	5.4	155	65	1.0	561.6	0.11	0.13	0.13	3	$4.4 \cdot 10^2$	1.3
L180-RMA-1-4	5.4	105	44	0.6	553.9	0.11	0.12	0.14	4	$4.3 \cdot 10^2$	1.3
L180-RMA-1-5	5.4	126	52	0.9	553.1	0.11	0.13	0.12	3	$4.3 \cdot 10^2$	1.3
L180-RMA-1-6	5.4	215	83	1.0	558.1	0.14	0.13	0.14	2	$4.7 \cdot 10^2$	1.2
L180-RMA-1-7	5.7	156	60	0.2	594.3	0.12	0.13	0.14	2	$4.5 \cdot 10^2$	1.3
L180-RMA-1-8	5.2	119	46	0.2	562.2	0.12	0.12	0.14	2	$4.4 \cdot 10^2$	1.3
L180-RMA-1-9	5.7	178	74	0.6	568.9	0.13	0.12	0.12	2	$4.3 \cdot 10^2$	1.3
L180-RMA-1-10	4.6	101	39	0.8	567.3	0.13	0.13	0.13	2	$4.5 \cdot 10^2$	1.3
L180-RMA-2-1	4.1	103	37	0.9	588.2	0.16	0.13	0.13	4	$4.8 \cdot 10^2$	1.2
L180-RMA-2-2	6.4	137	53	1.1	593.7	0.14	0.13	0.13	4	$4.6 \cdot 10^2$	1.3
L180-RMA-2-3	4.0	101	36	0.9	558.5	0.14	0.14	0.13	4	$4.8 \cdot 10^2$	1.2
L180-RMA-2-4	4.8	114	44	0.9	566.7	0.14	0.13	0.13	4	$4.6 \cdot 10^2$	1.2
L180-RMA-2-5	5.2	158	56	1.4	581.3	0.14	0.13	0.14	3	$4.7 \cdot 10^2$	1.2
L180-RMA-2-6	3.7	94	36	0.9	548.3	0.13	0.13	0.13	3	$4.5 \cdot 10^2$	1.2
L180-RMA-2-7	5.8	197	76	2.0	579.3	0.15	0.13	0.12	3	$4.6 \cdot 10^2$	1.3
L180-RMA-2-8	4.1	166	64	1.7	566.1	0.14	0.13	0.13	3	$4.6 \cdot 10^2$	1.2
L180-RMA-2-9	4.8	97	40	0.8	549.4	0.13	0.11	0.13	2	$4.2 \cdot 10^2$	1.3
L180-RMA-2-10	5.1	145	56	1.5	522.6	0.13	0.12	0.13	3	$4.4 \cdot 10^2$	1.2
L180-D-1-1	4.7	110	42	0.8	545.8	0.14	0.13	0.12	3	$4.5 \cdot 10^2$	1.2
L180-D-1-2	4.6	102	39	0.9	539.3	0.14	0.13	0.11	3	$4.5 \cdot 10^2$	1.2
L180-D-1-3	4.5	142	55	0.9	535.9	0.14	0.12	0.12	3	$4.4 \cdot 10^2$	1.2
L180-D-1-4	4.6	50	21	0.4	505.2	0.14	0.12	0.10	3	$4.2 \cdot 10^2$	1.2
L180-D-1-5	4.9	99	45	0.4	466.1	0.13	0.11	0.09	3	$3.9 \cdot 10^2$	1.2
L180-D-1-6	5.1	75	34	0.6	490.0	0.13	0.11	0.09	2	$3.9 \cdot 10^2$	1.3
L180-D-1-7	5.5	169	65	0.8	612.8	0.14	0.14	0.12	2	$4.7 \cdot 10^2$	1.3
L180-D-1-8	4.9	110	39	0.8	608.5	0.14	0.14	0.13	3	$4.8 \cdot 10^2$	1.3
L180-D-1-9	4.9	108	39	0.8	631.2	0.14	0.14	0.14	3	$4.9 \cdot 10^2$	1.3
L180-D-1-10	5.0	107	38	0.8	633.8	0.14	0.14	0.14	3	$4.9 \cdot 10^2$	1.3
L180-D-2-1	5.1	124	52	1.1	589.9	0.13	0.13	0.11	3	$4.4 \cdot 10^2$	1.4
L180-D-2-2	4.2	102	42	1.0	530.8	0.12	0.13	0.12	3	$4.4 \cdot 10^2$	1.2
L180-D-2-3	3.8	72	30	0.7	515.2	0.12	0.13	0.12	4	$4.4 \cdot 10^2$	1.2
L180-D-2-4	4.2	120	50	1.3	499.1	0.12	0.12	0.11	2	$4.1 \cdot 10^2$	1.2
L180-D-2-5	4.7	102	46	1.0	516.9	0.11	0.12	0.10	2	$3.9 \cdot 10^2$	1.3
L180-D-2-6	4.3	102	46	1.1	472.7	0.11	0.11	0.11	3	$3.9 \cdot 10^2$	1.2
L180-D-2-7	4.4	77	39	0.9	445.2	0.11	0.10	0.10	2	$3.6 \cdot 10^2$	1.2
L180-D-2-8	4.5	63	35	0.8	424.3	0.11	0.08	0.09	2	$3.1 \cdot 10^2$	1.4
L180-D-2-9	3.8	87	43	1.1	448.8	0.12	0.09	0.10	2	$3.5 \cdot 10^2$	1.3
L180-D-2-10	3.7	91	46	1.1	451.2	0.11	0.11	0.09	3	$3.7 \cdot 10^2$	1.2

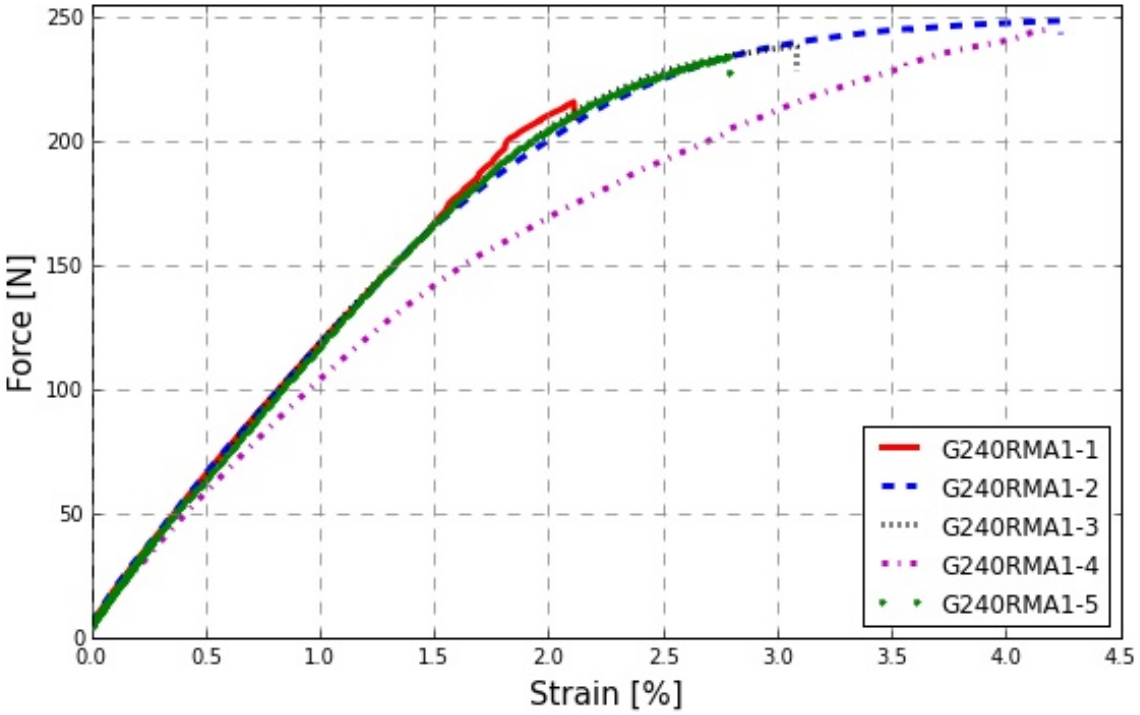

Figure D.1: Graphs of force versus strain measured for the samples 1-5 of G240-RMA-1.

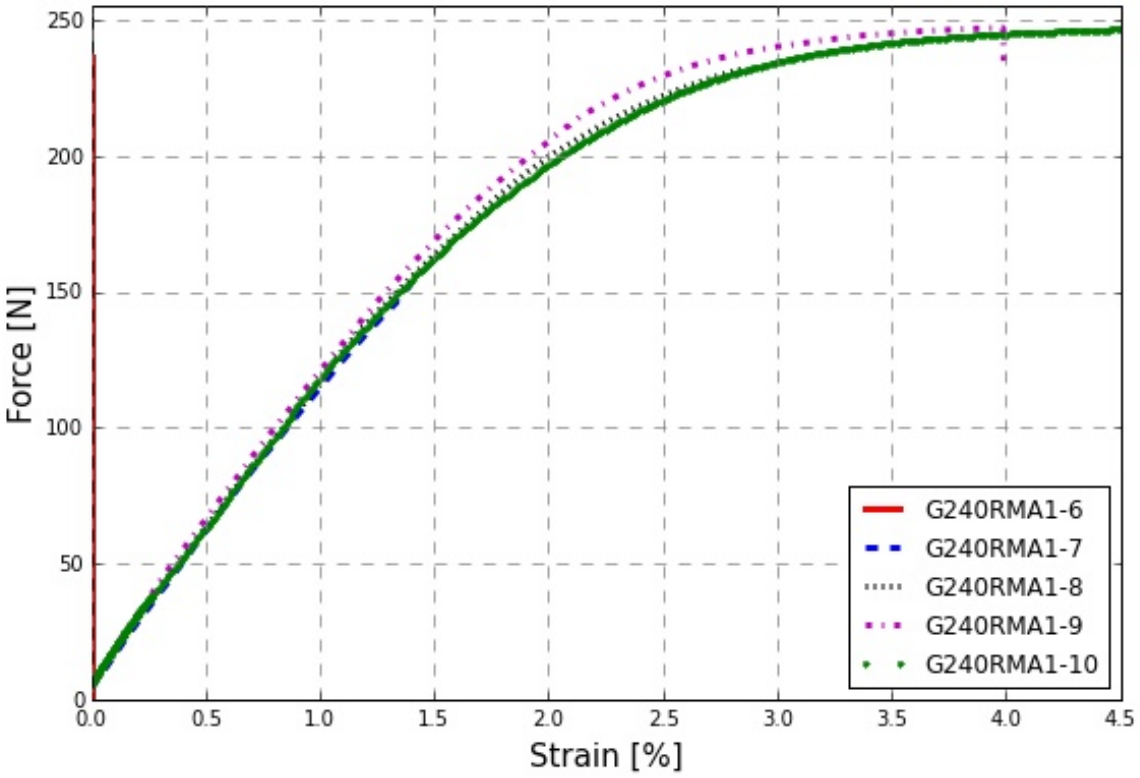

Figure D.2: Graphs of force versus strain measured for the samples 6-10 of G240-RMA-1.

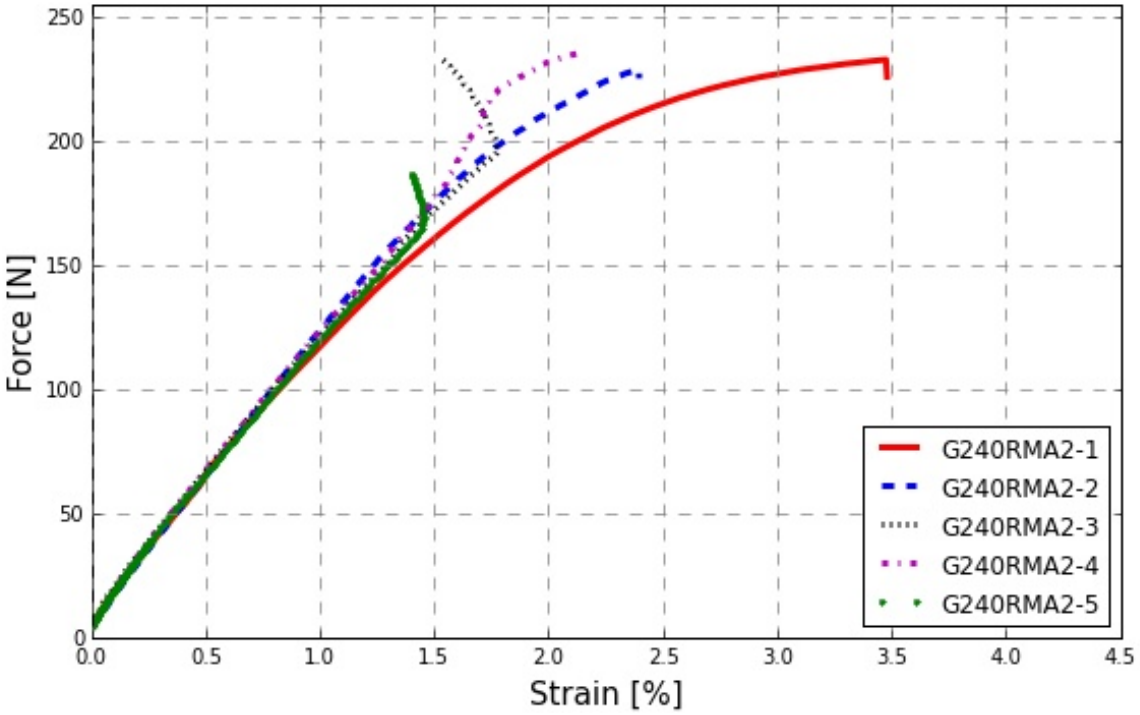

Figure D.3: Graphs of force versus strain measured for the samples 1-5 of G240-RMA-2.

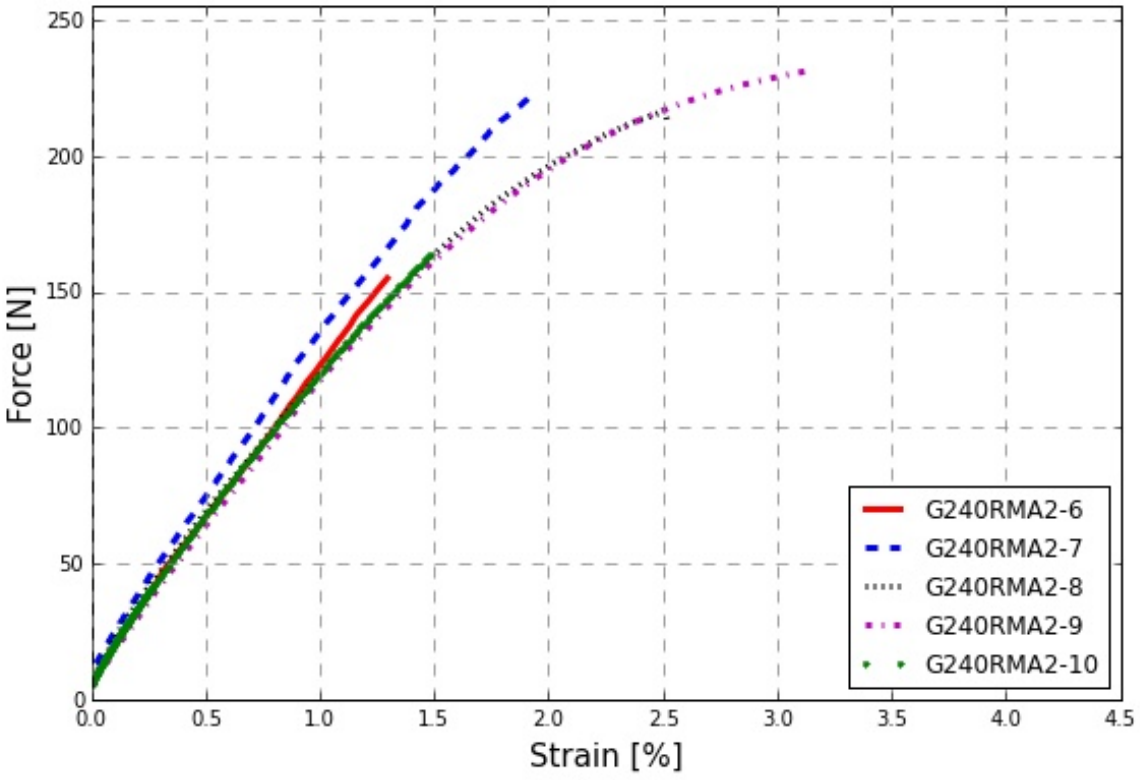

Figure D.4: Graphs of force versus strain measured for the samples 6-10 of G240-RMA-2.

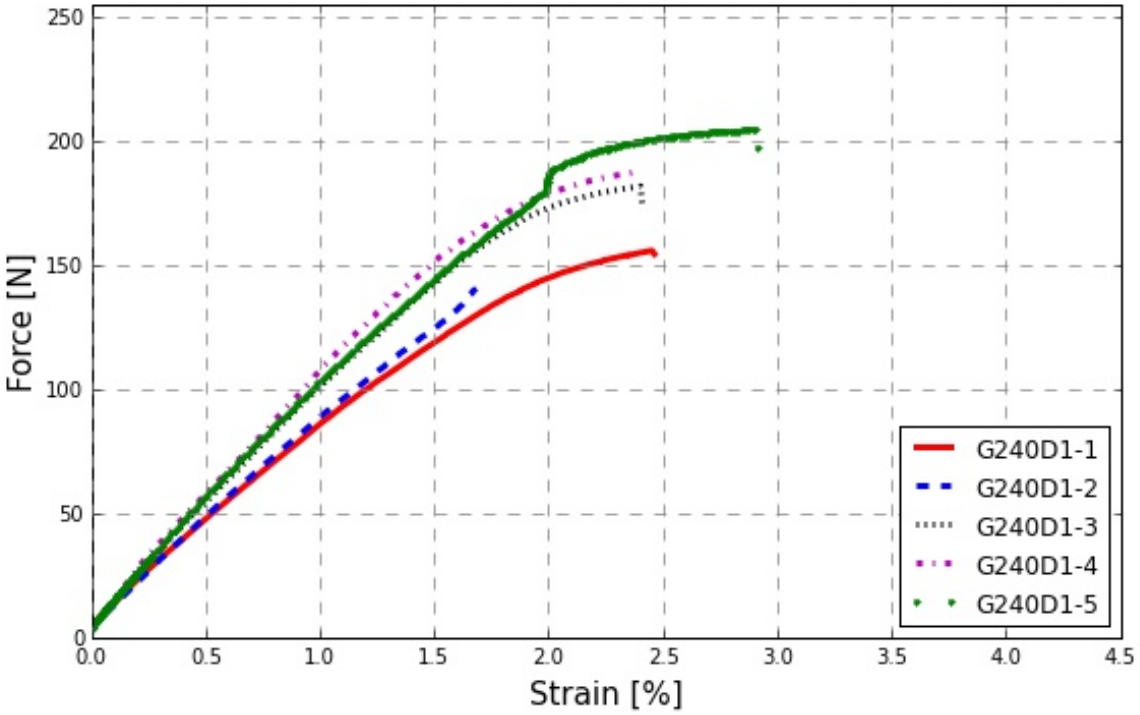

Figure D.5: Graphs of force versus strain measured for the samples 1-5 of G240-D-1.

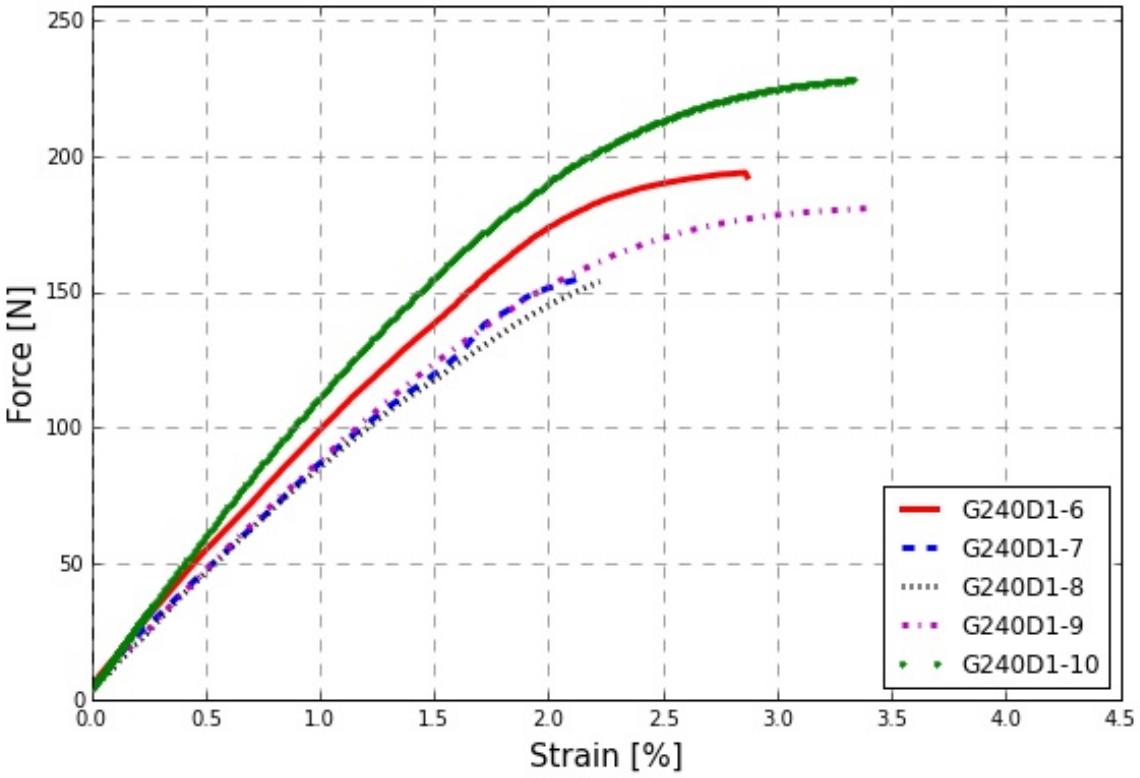

Figure D.6: Graphs of force versus strain measured for the samples 6-10 of G240-D-1.

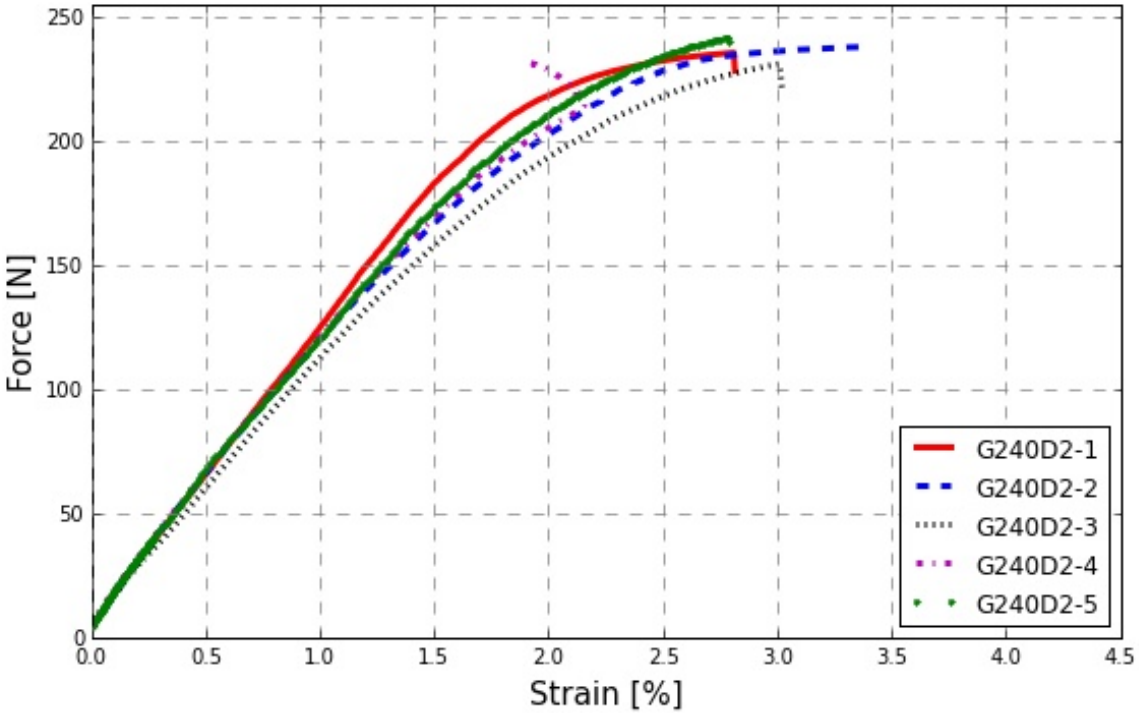

Figure D.7: Graphs of force versus strain measured for the samples 1-5 of G240-D-2.

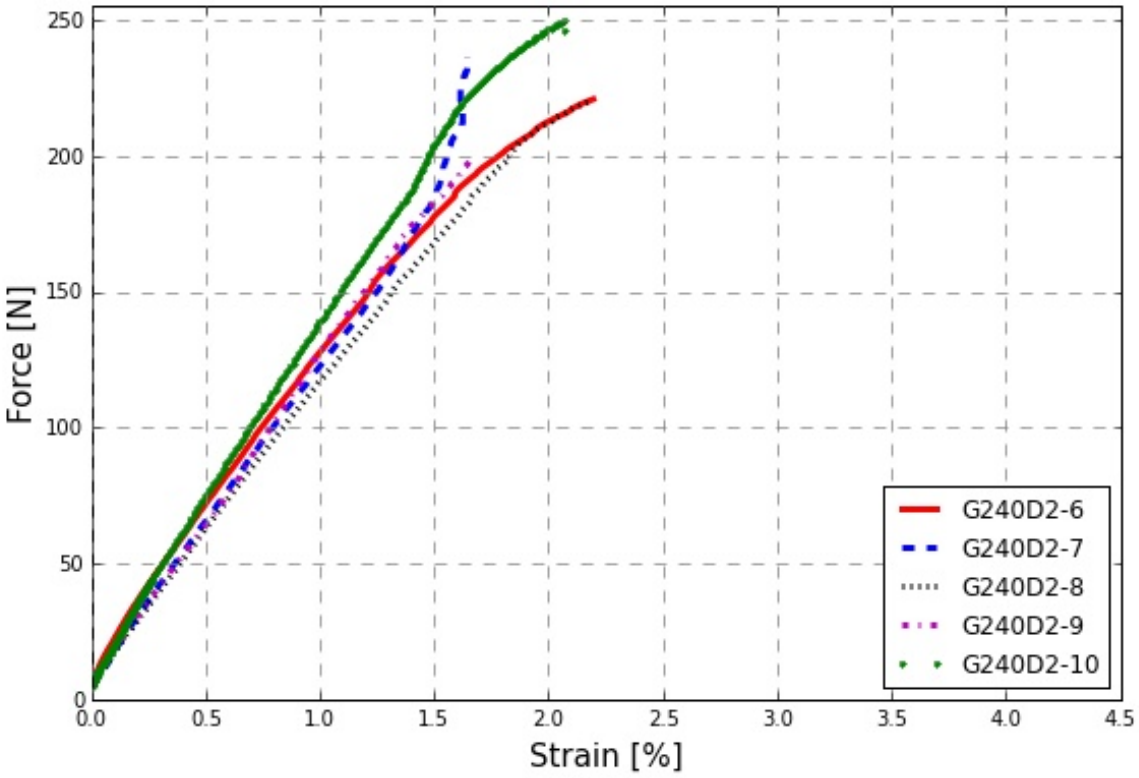

Figure D.8: Graphs of force versus strain measured for the samples 6-10 of G240-D-2.

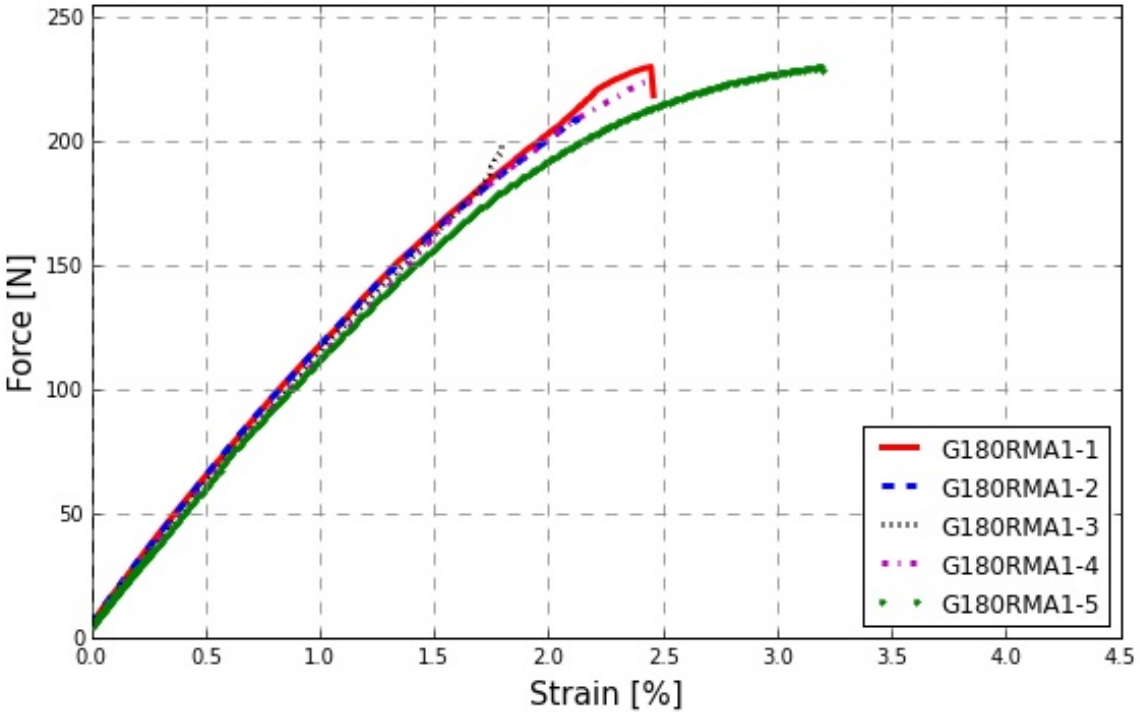

Figure D.9: Graphs of force versus strain measured for the samples 1-5 of G180-RMA-1.

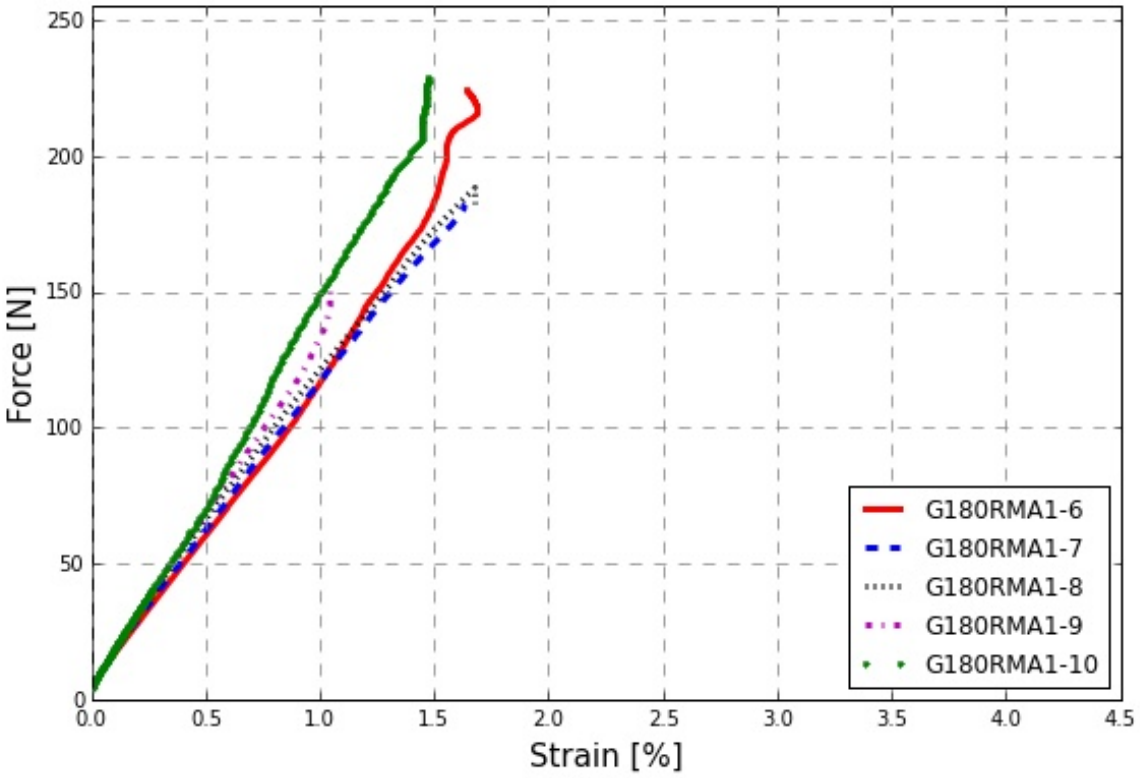

Figure D.10: Graphs of force versus strain measured for the samples 6-10 of G180-RMA-1.

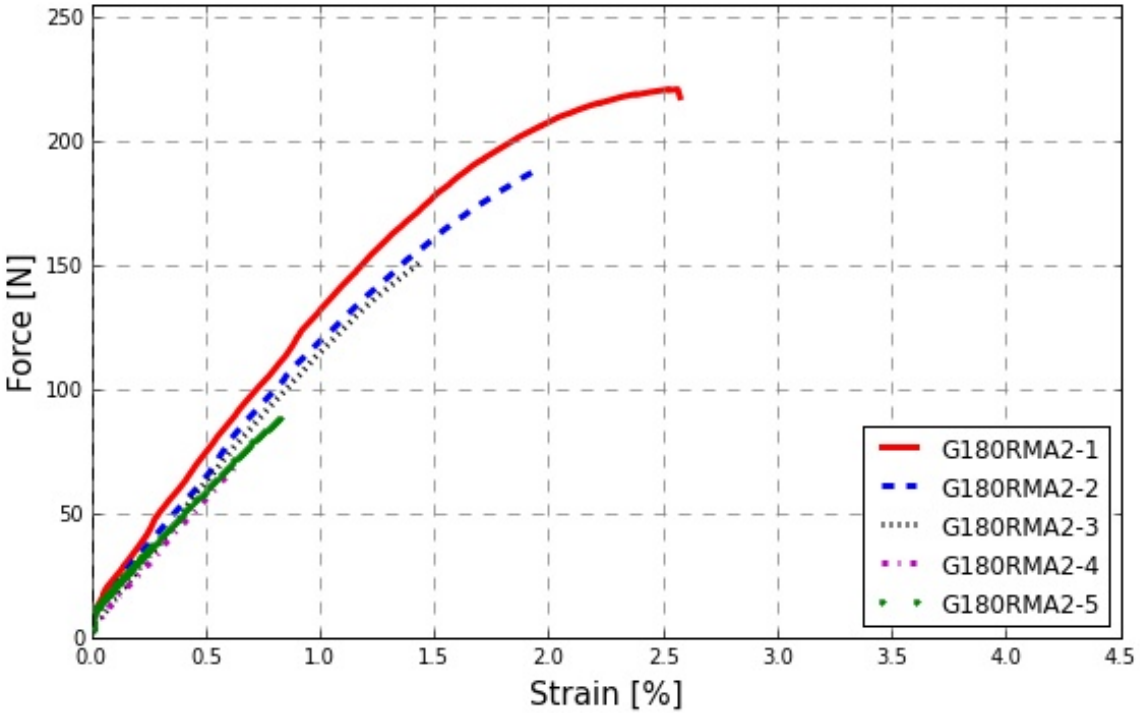

Figure D.11: Graphs of force versus strain measured for the samples 1-5 of G180-RMA-2.

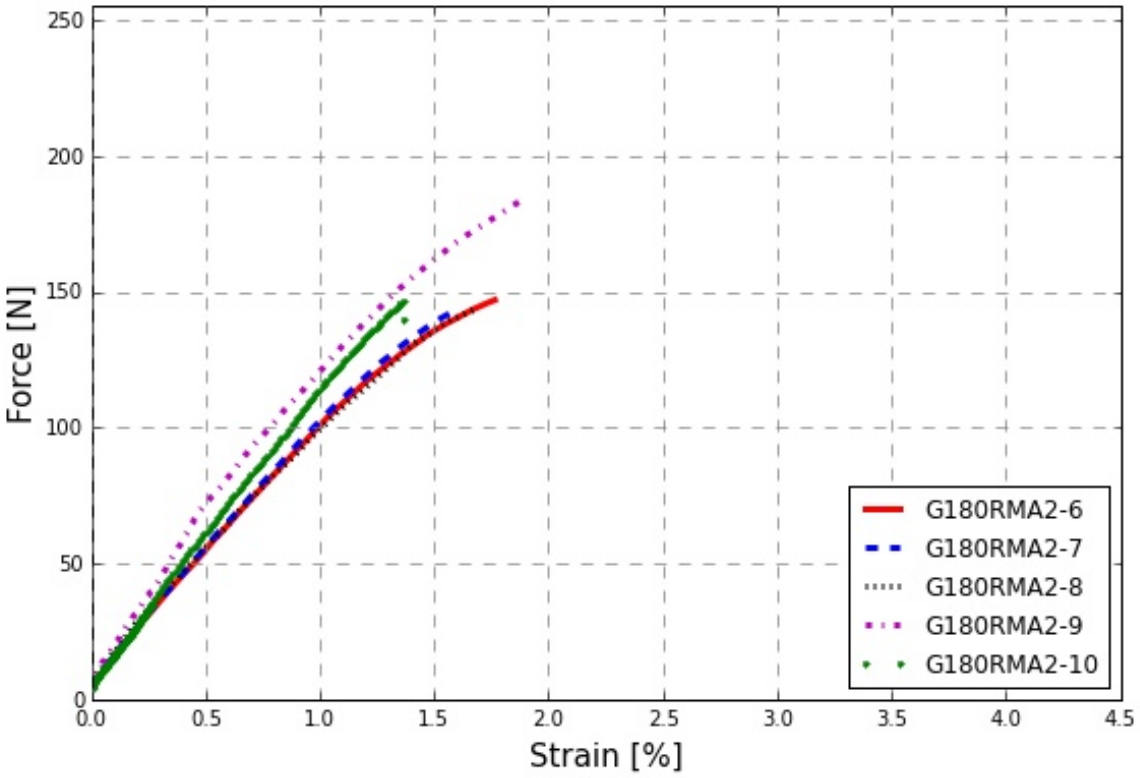

Figure D.12: Graphs of force versus strain measured for the samples 6-10 of G180-RMA-2.

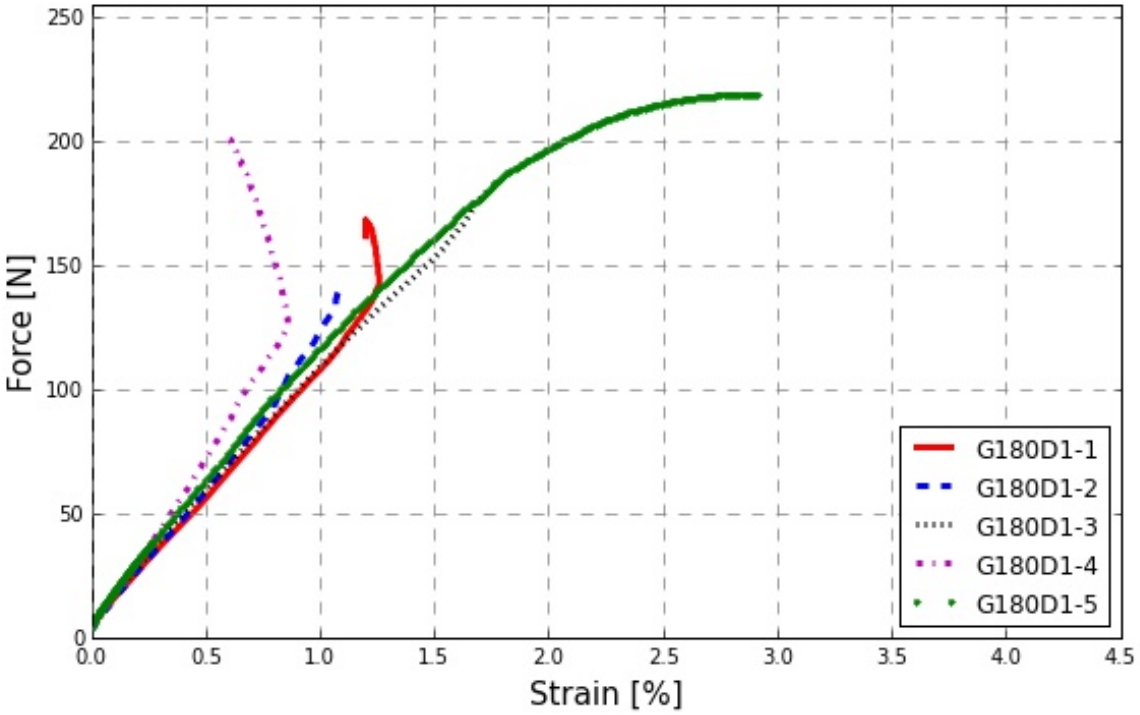

Figure D.13: Graphs of force versus strain measured for the samples 1-5 of G180-D-1.

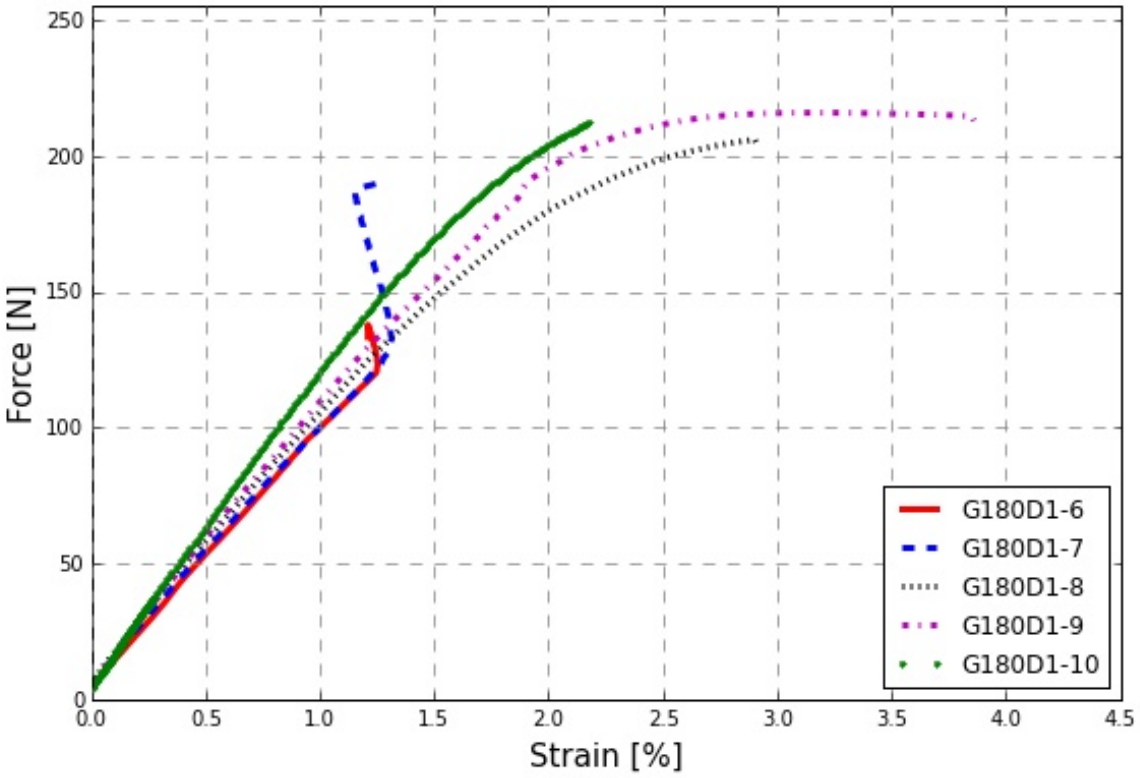

Figure D.14: Graphs of force versus strain measured for the samples 6-10 of G180-D-1.

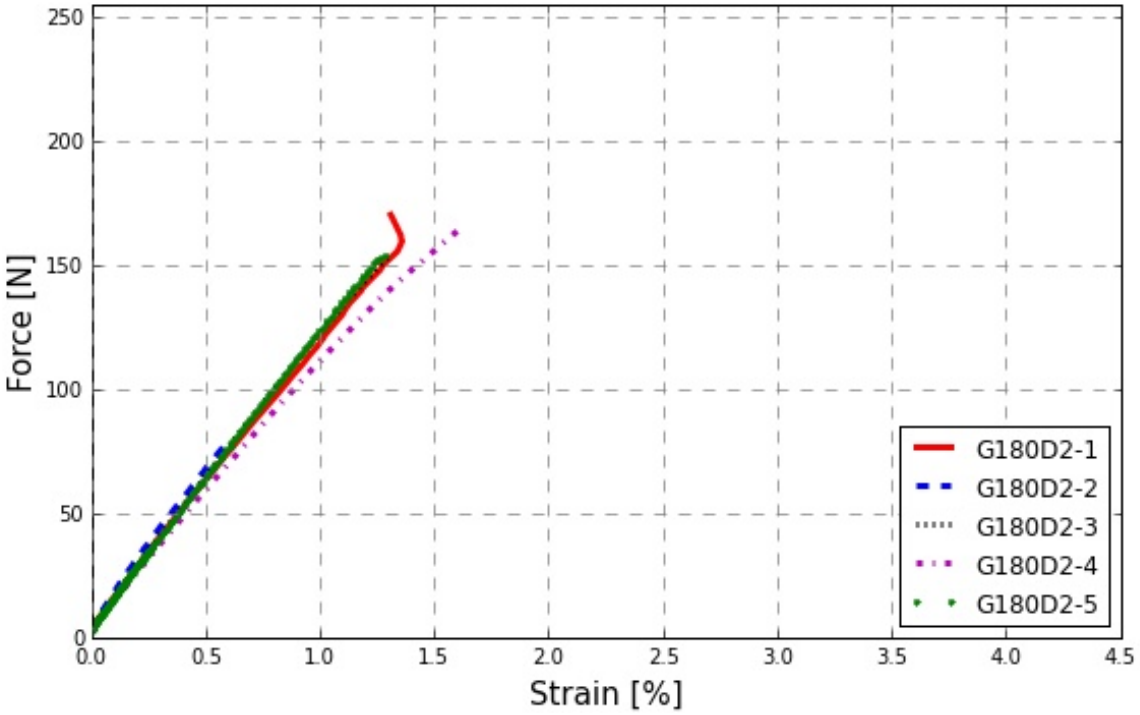

Figure D.15: Graphs of force versus strain measured for the samples 1-5 of G180-D-2.

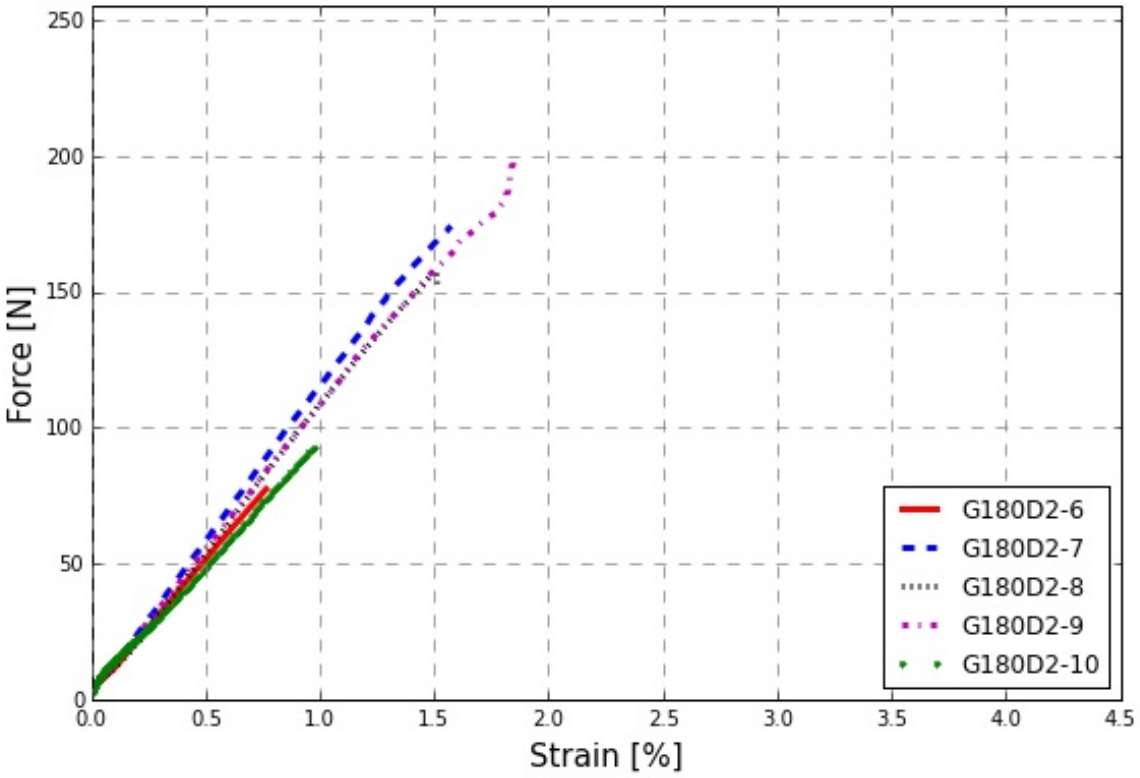

Figure D.16: Graphs of force versus strain measured for the samples 6-10 of G180-D-2.

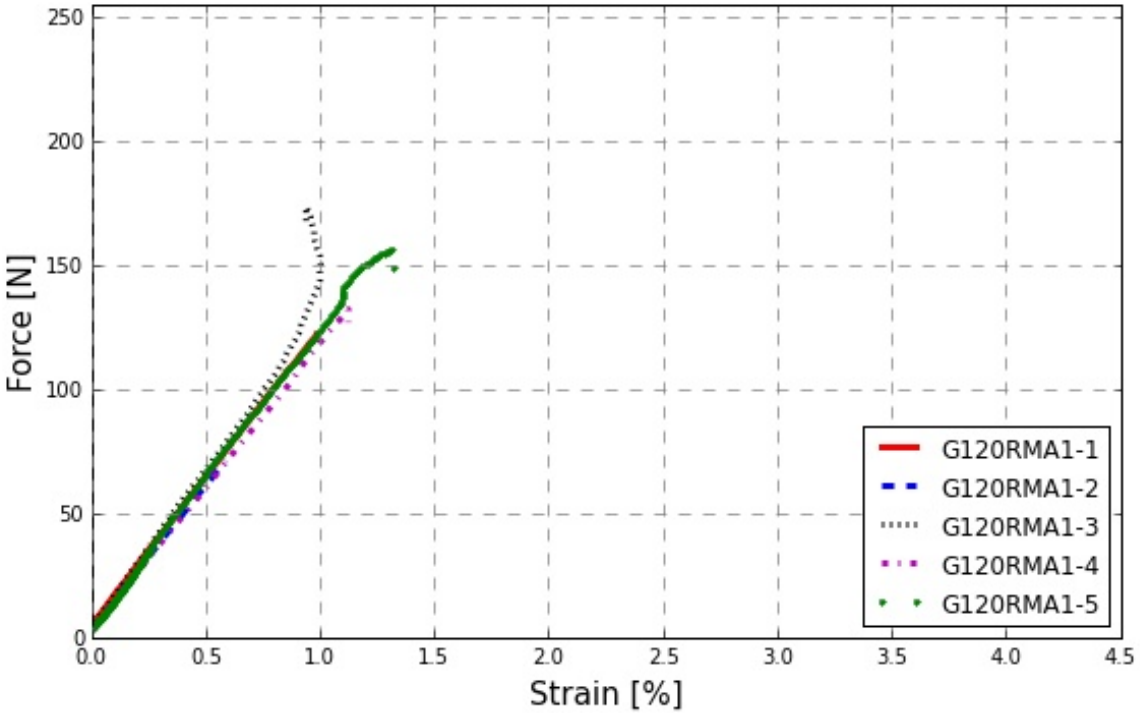

Figure D.17: Graphs of force versus strain measured for the samples 1-5 of G120-RMA-1.

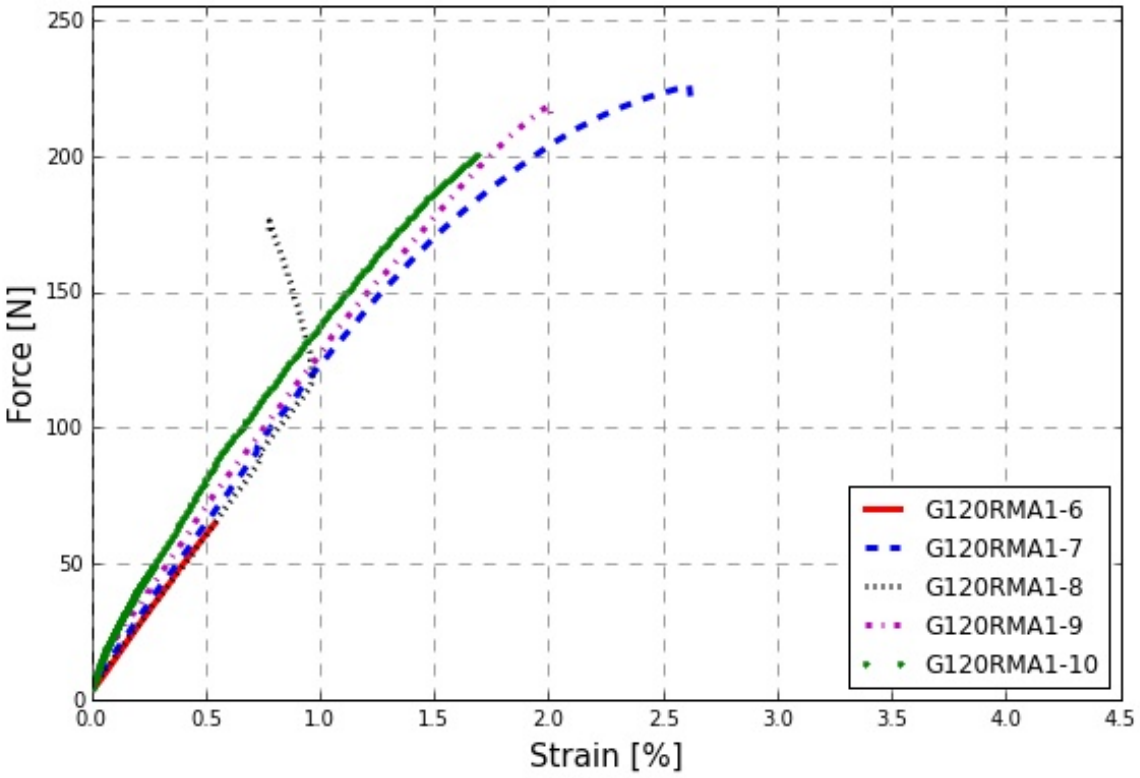

Figure D.18: Graphs of force versus strain measured for the samples 6-10 of G120-RMA-1.

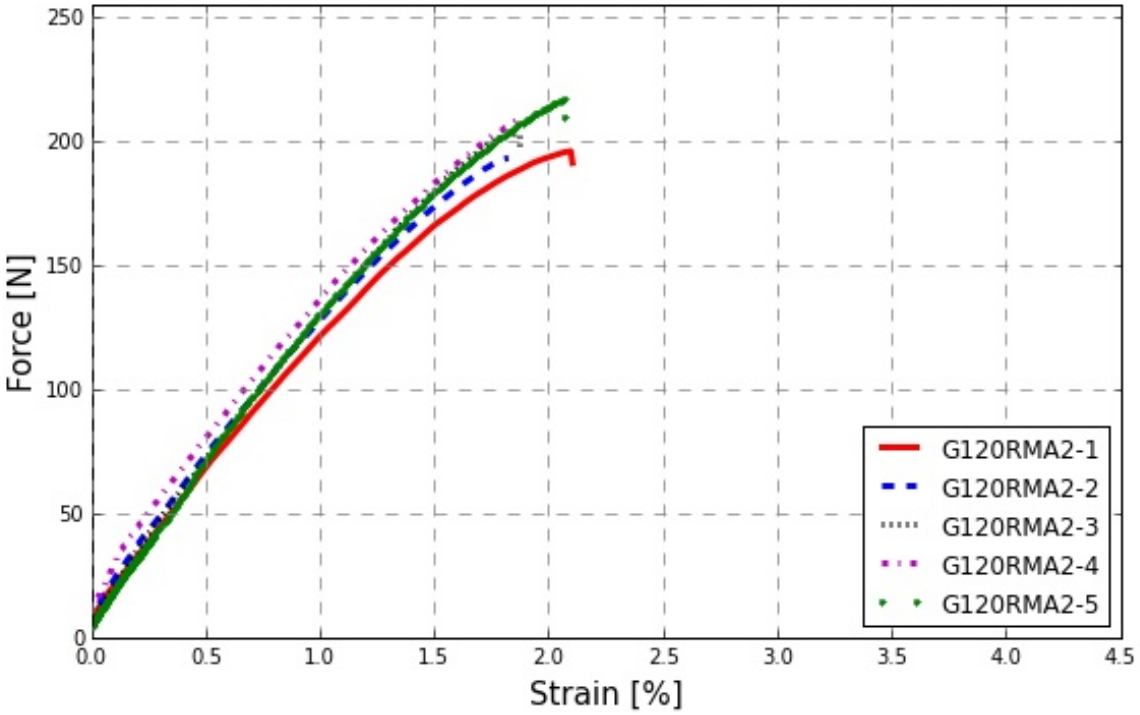

Figure D.19: Graphs of force versus strain measured for the samples 1-5 of G120-RMA-2.

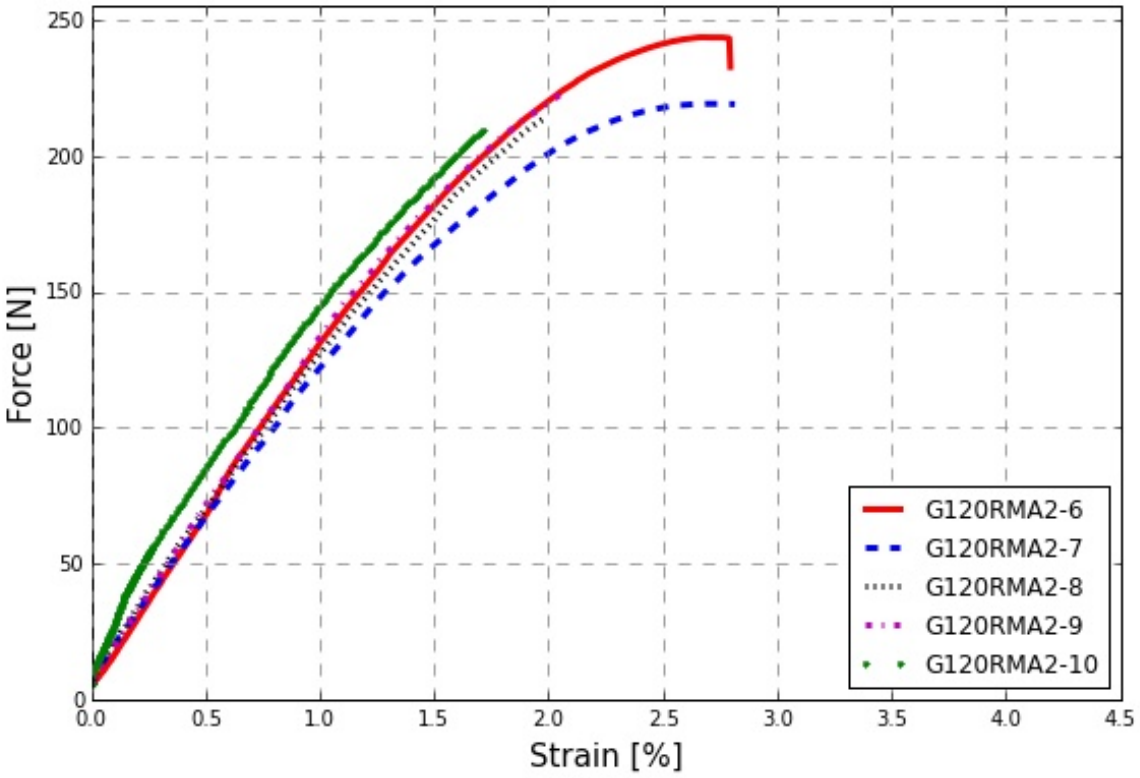

Figure D.20: Graphs of force versus strain measured for the samples 6-10 of G120-RMA-2.

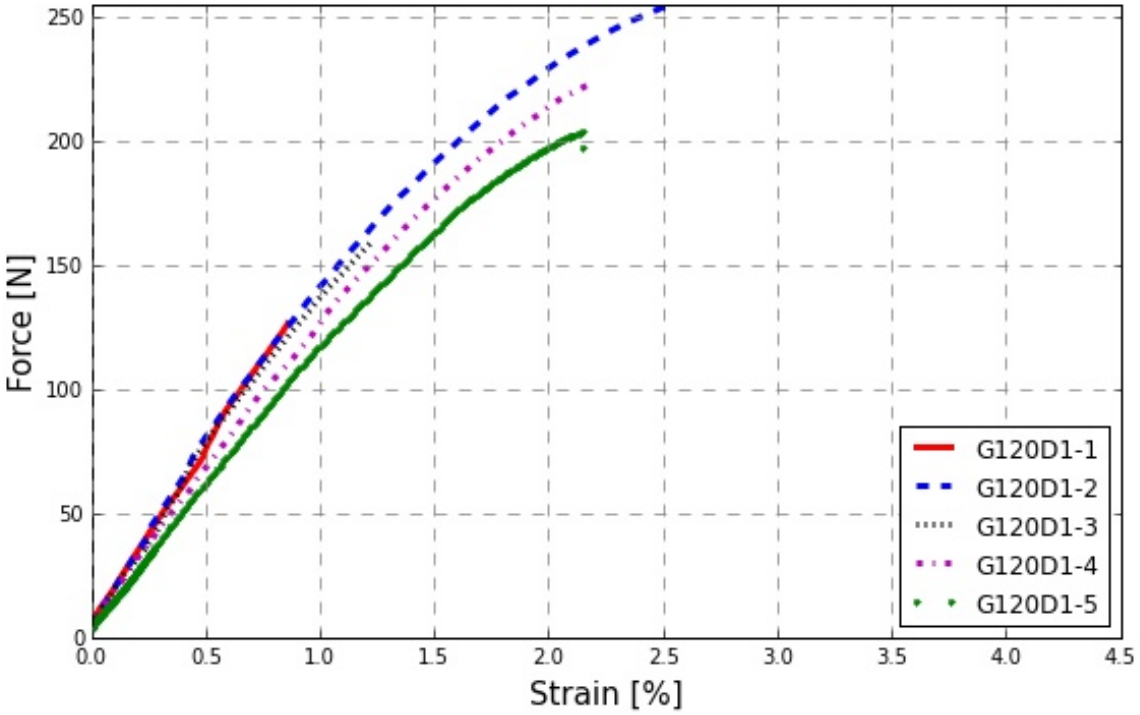

Figure D.21: Graphs of force versus strain measured for the samples 1-5 of G120-D-1.

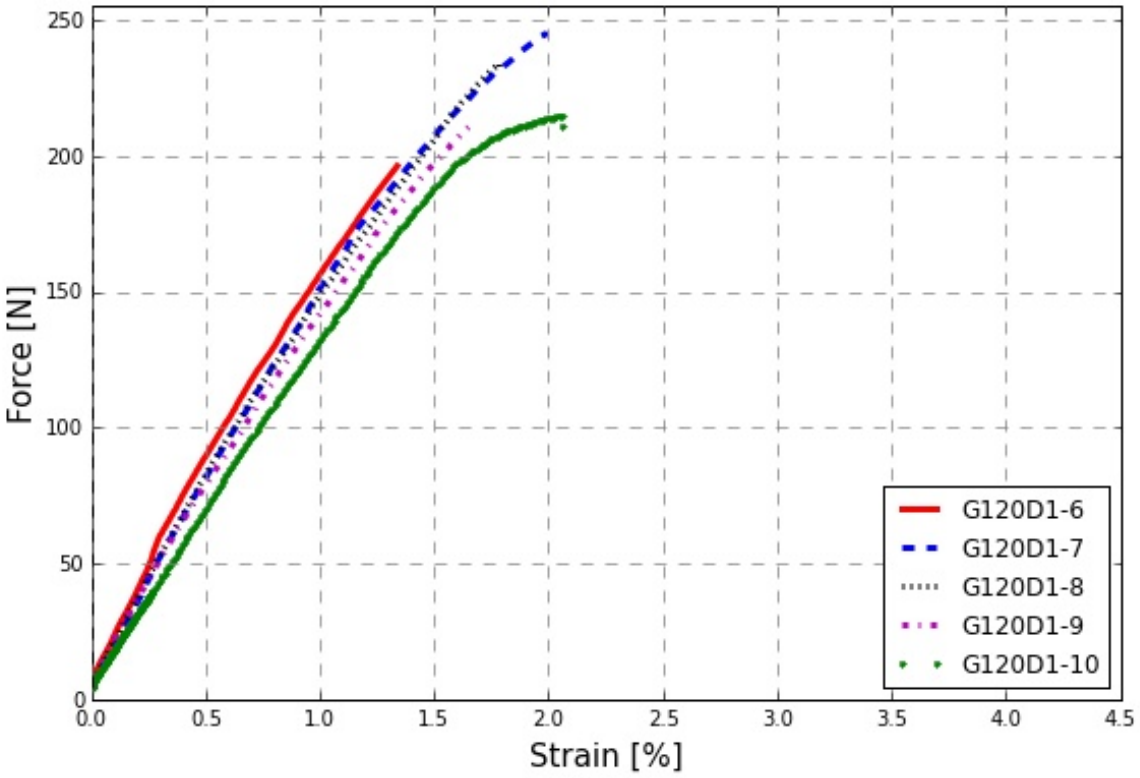

Figure D.22: Graphs of force versus strain measured for the samples 6-10 of G120-D-1.

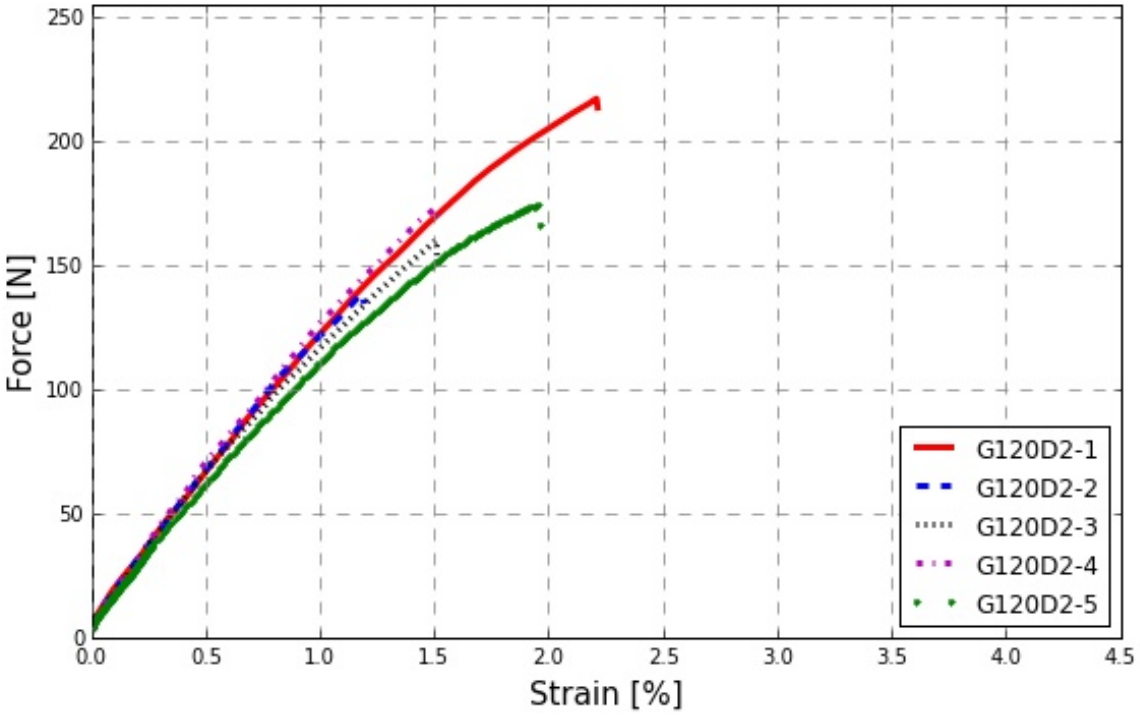

Figure D.23: Graphs of force versus strain measured for the samples 1-5 of G120-D-2.

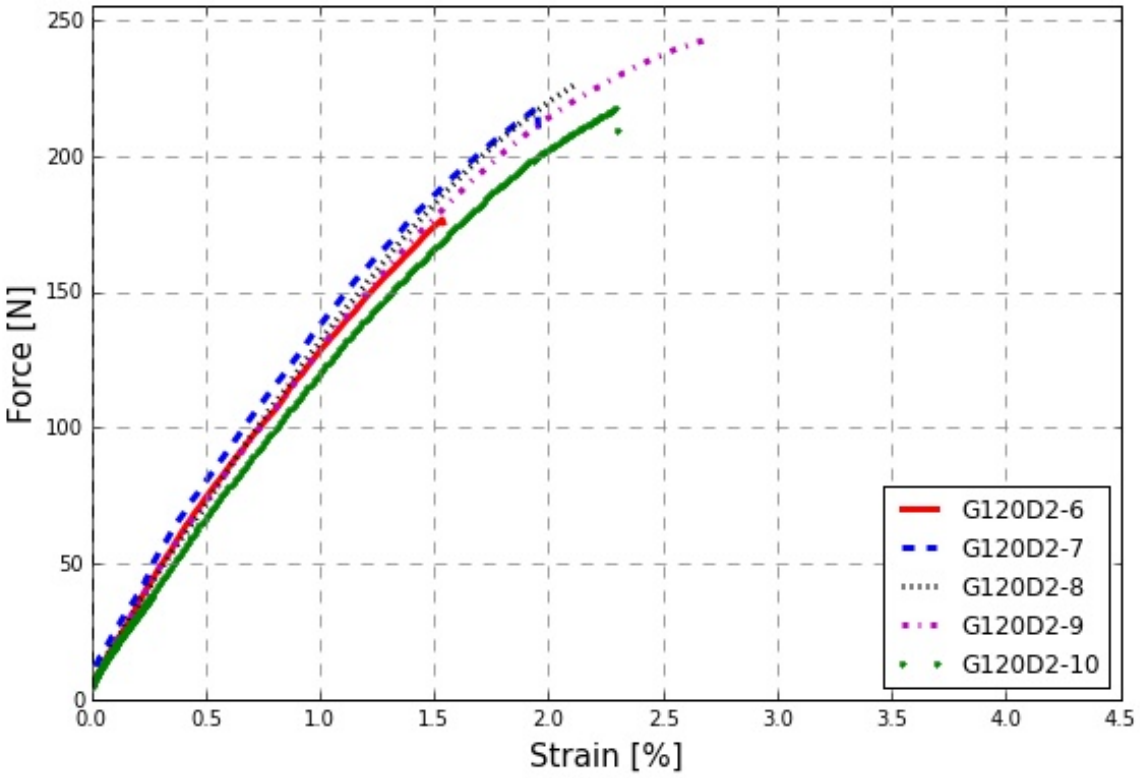

Figure D.24: Graphs of force versus strain measured for the samples 6-10 of G120-D-2.

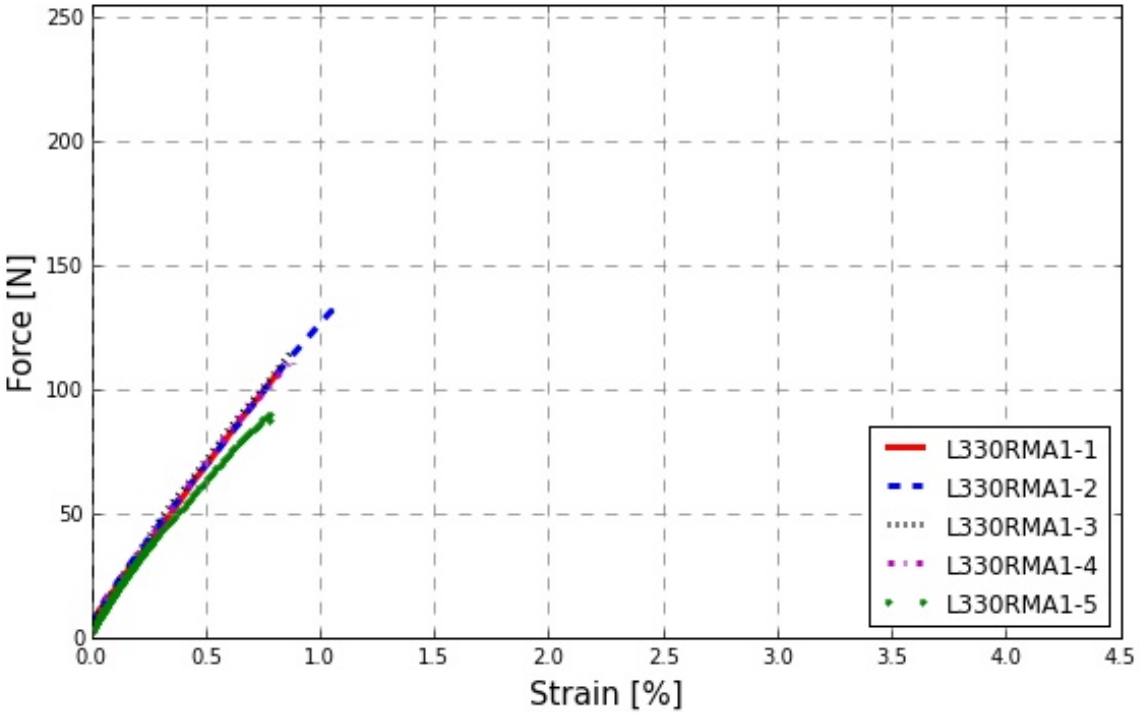

Figure D.25: Graphs of force versus strain measured for the samples 1-5 of L330-RMA-1.

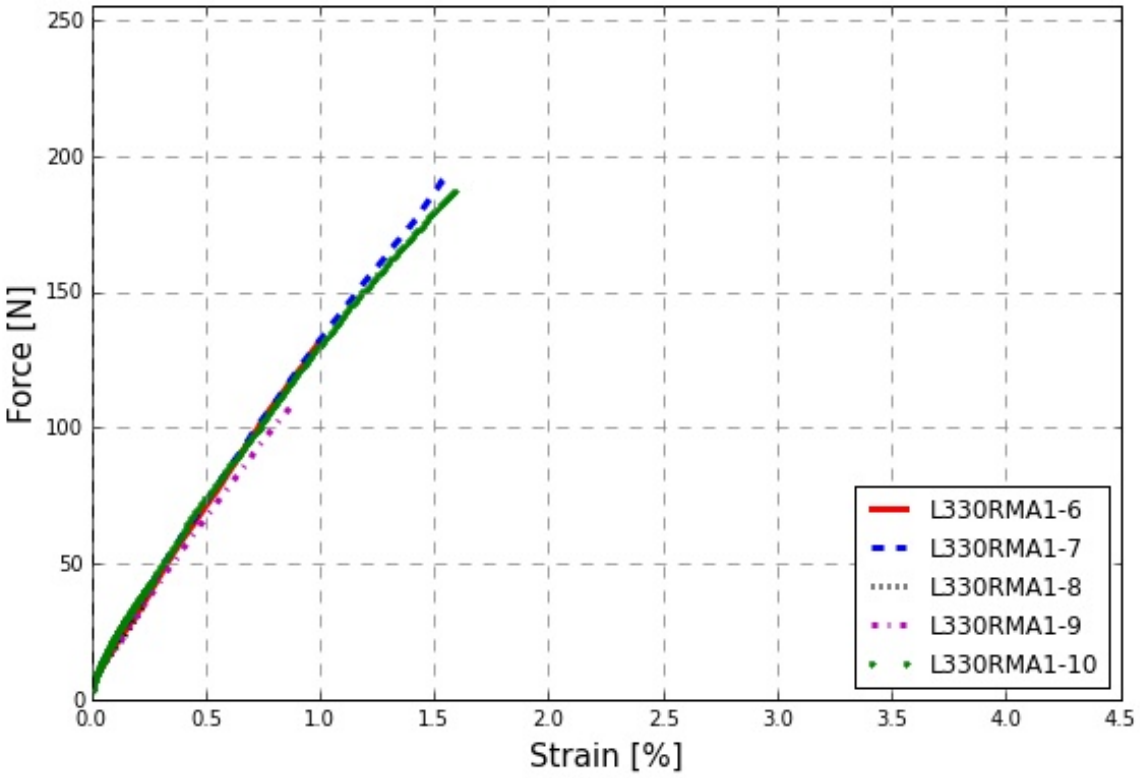

Figure D.26: Graphs of force versus strain measured for the samples 6-10 of L330-RMA-1.

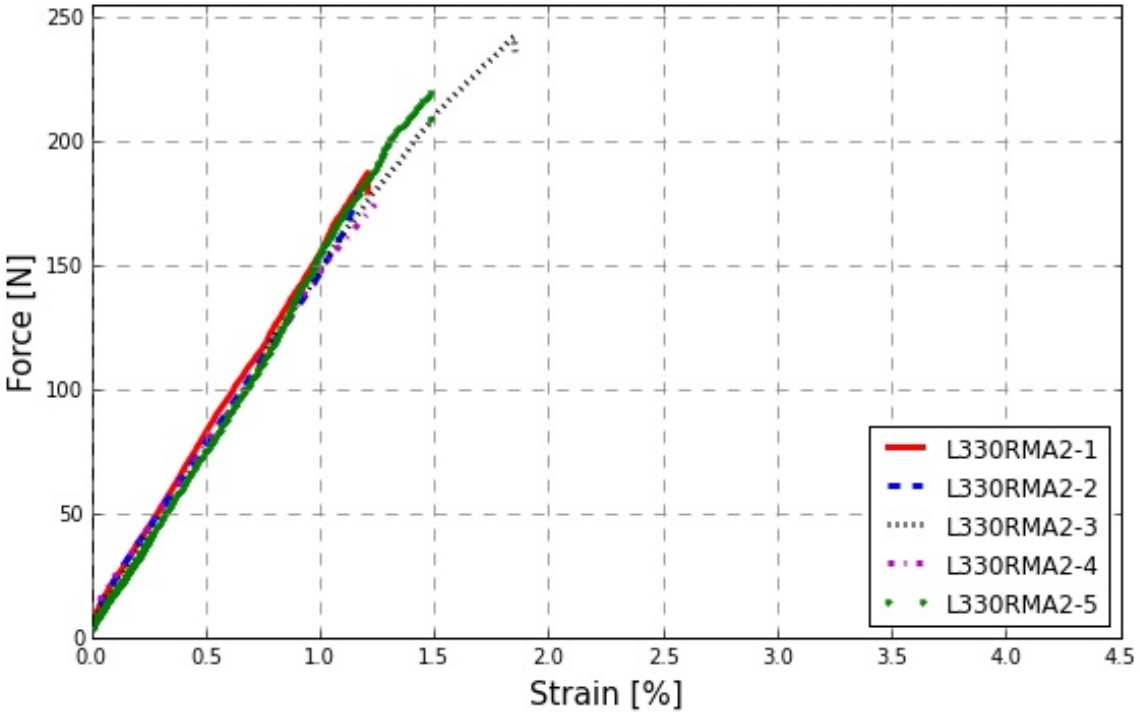

Figure D.27: Graphs of force versus strain measured for the samples 1-5 of L330-RMA-2.

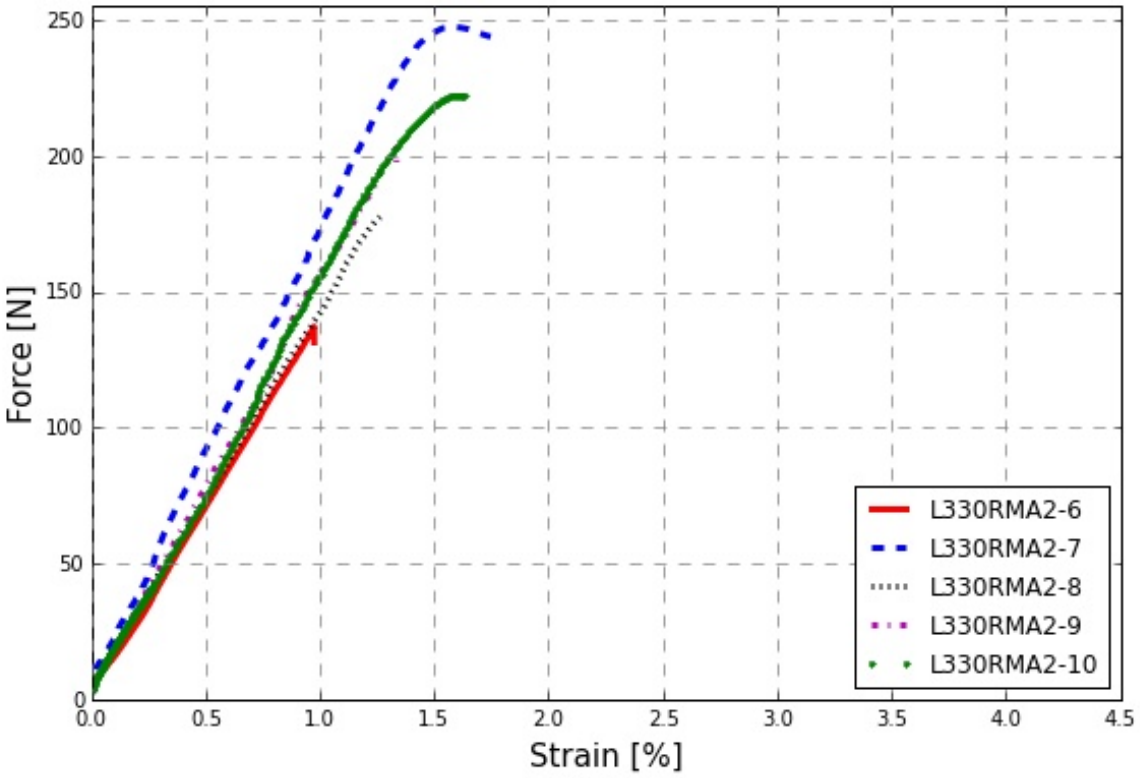

Figure D.28: Graphs of force versus strain measured for the samples 6-10 of L330-RMA-2.

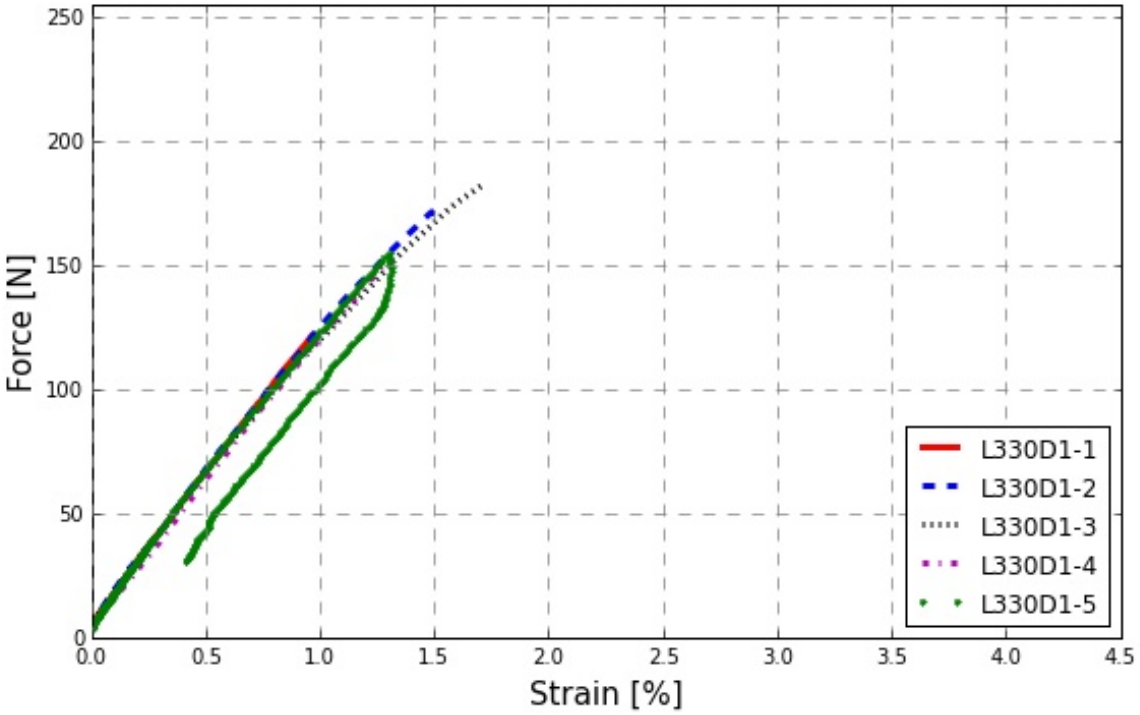

Figure D.29: Graphs of force versus strain measured for the samples 1-5 of L330-D-1.

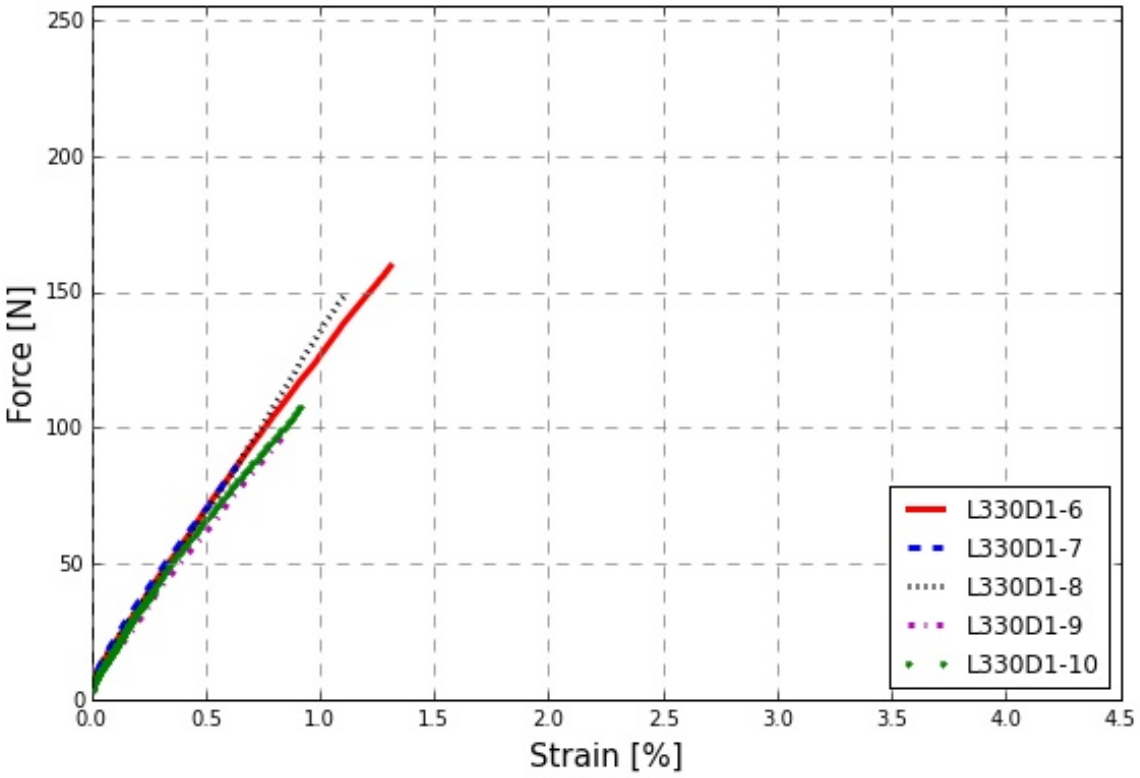

Figure D.30: Graphs of force versus strain measured for the samples 6-10 of L330-D-1.

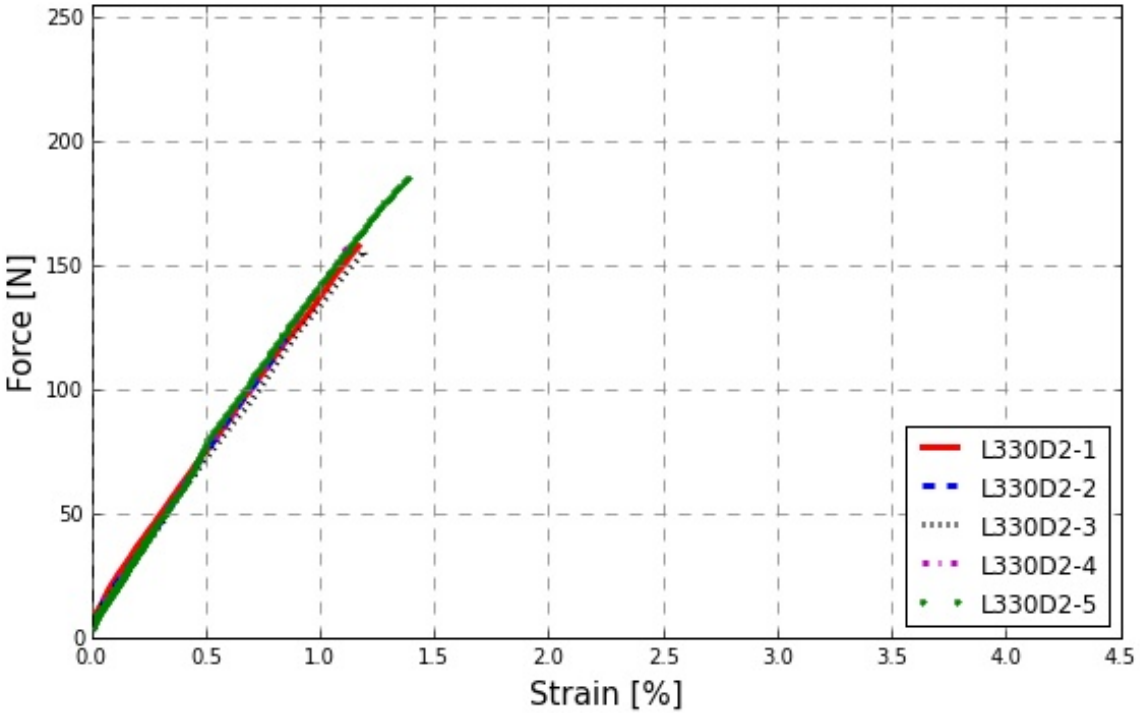

Figure D.31: Graphs of force versus strain measured for the samples 1-5 of L330-D-2.

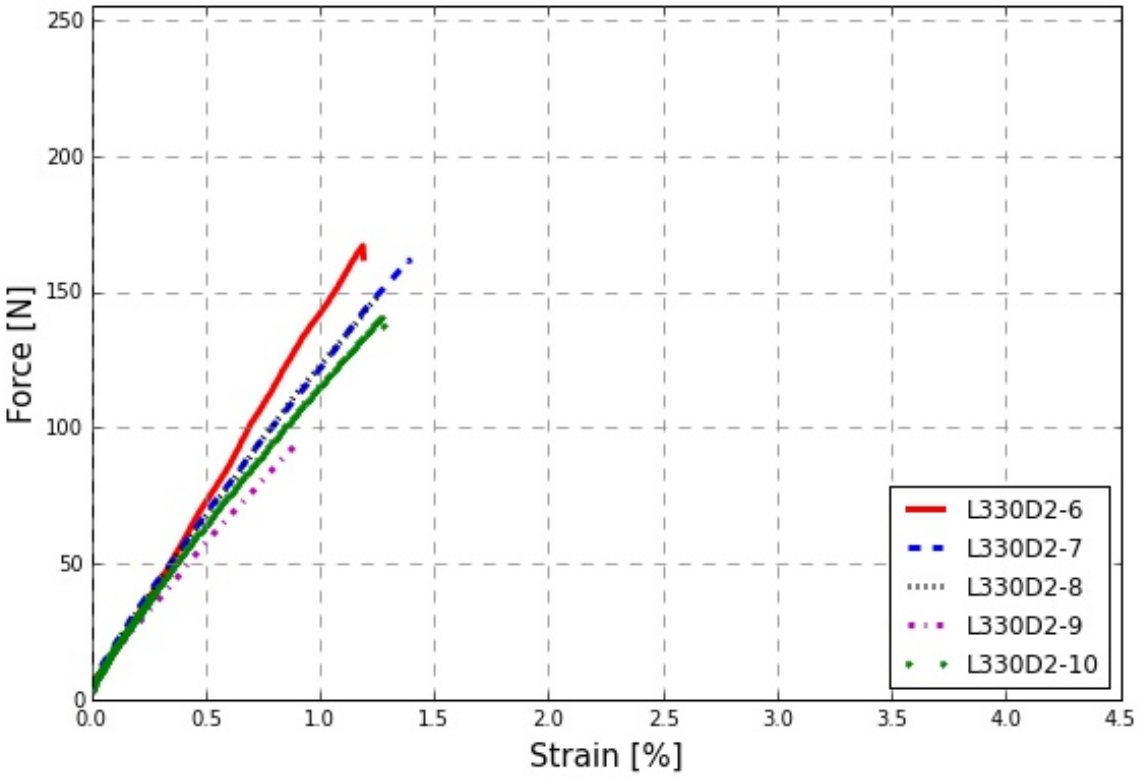

Figure D.32: Graphs of force versus strain measured for the samples 6-10 of L330-D-2.

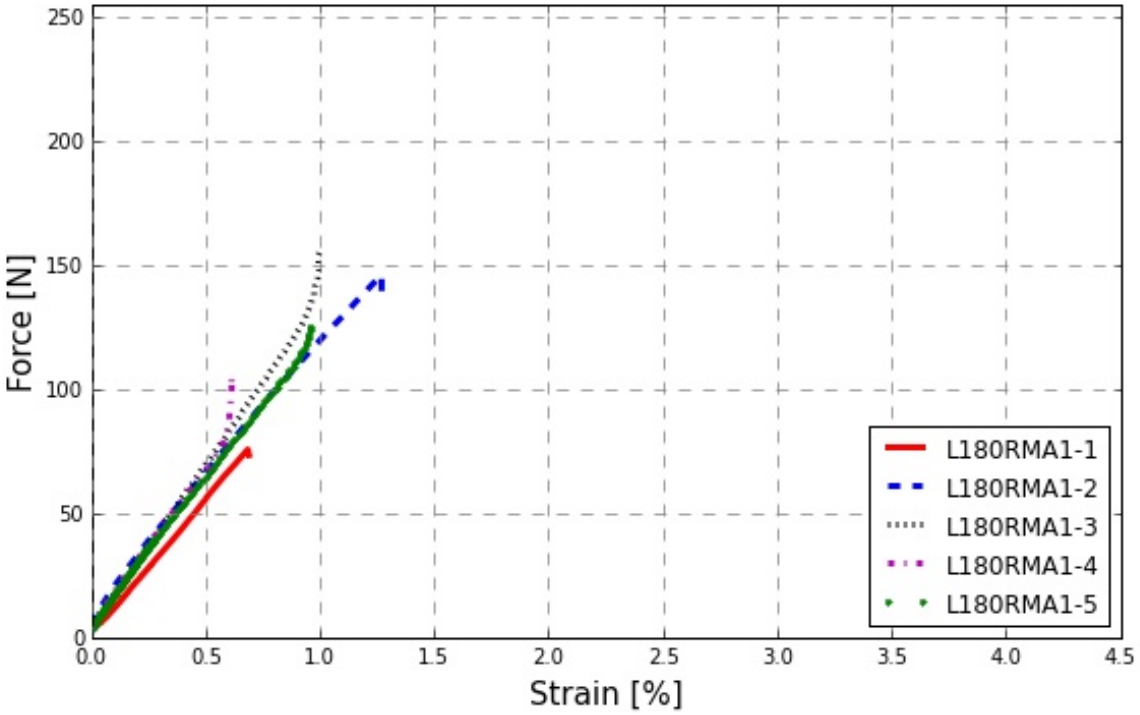

Figure D.33: Graphs of force versus strain measured for the samples 1-5 of L180-RMA-1.

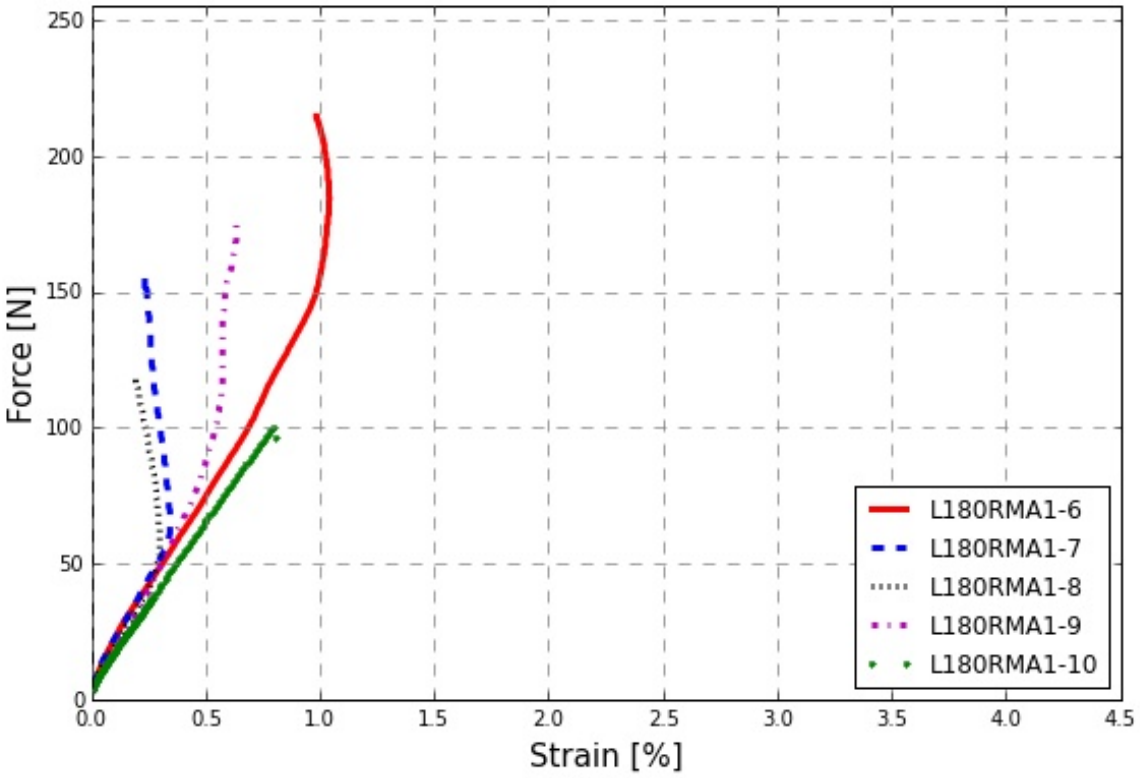

Figure D.34: Graphs of force versus strain measured for the samples 6-10 of L180-RMA-1.

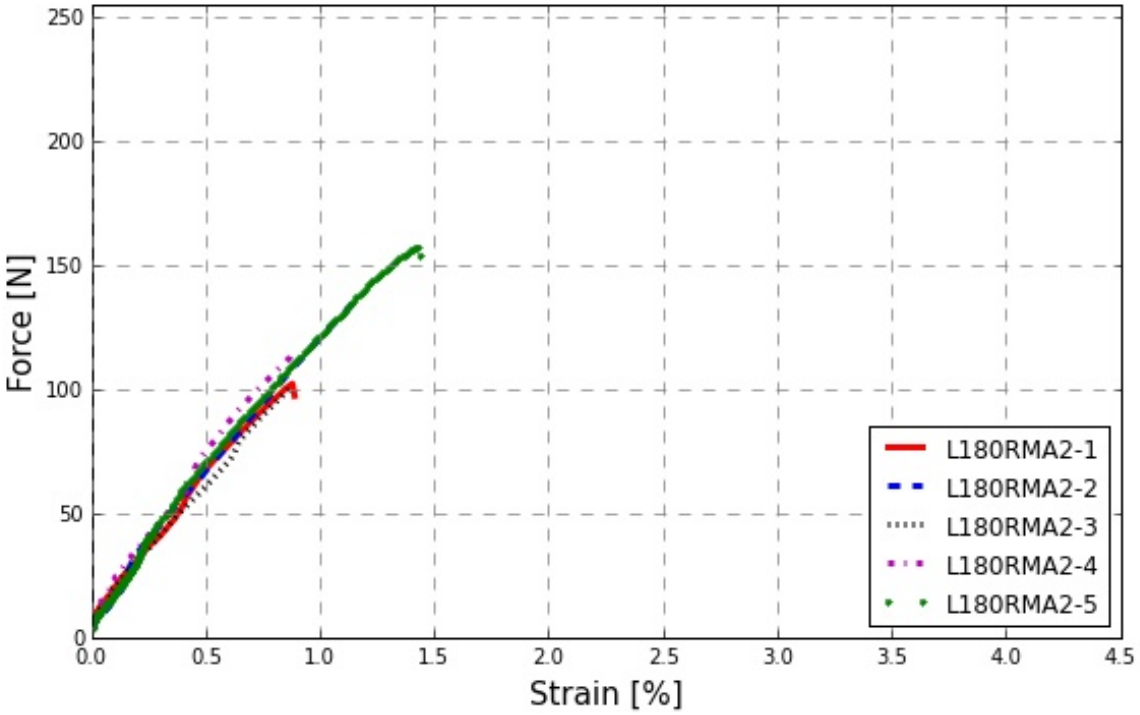

Figure D.35: Graphs of force versus strain measured for the samples 1-5 of L180-RMA-2.

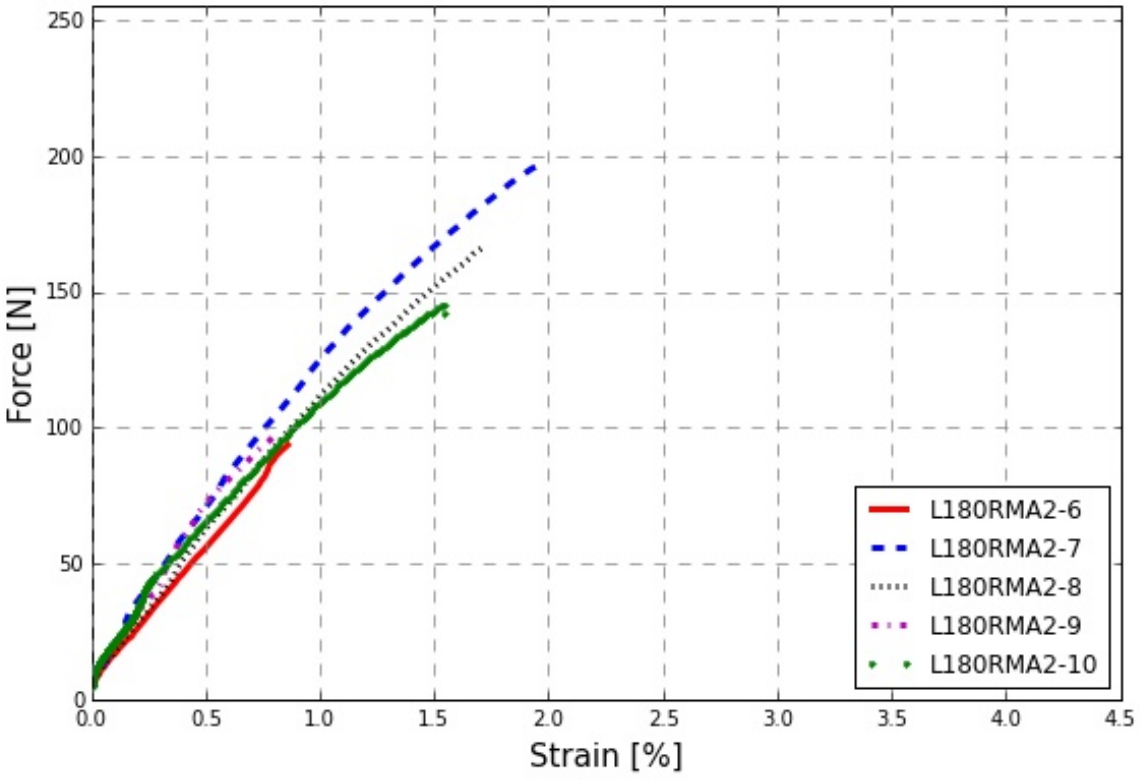

Figure D.36: Graphs of force versus strain measured for the samples 6-10 of L180-RMA-2.

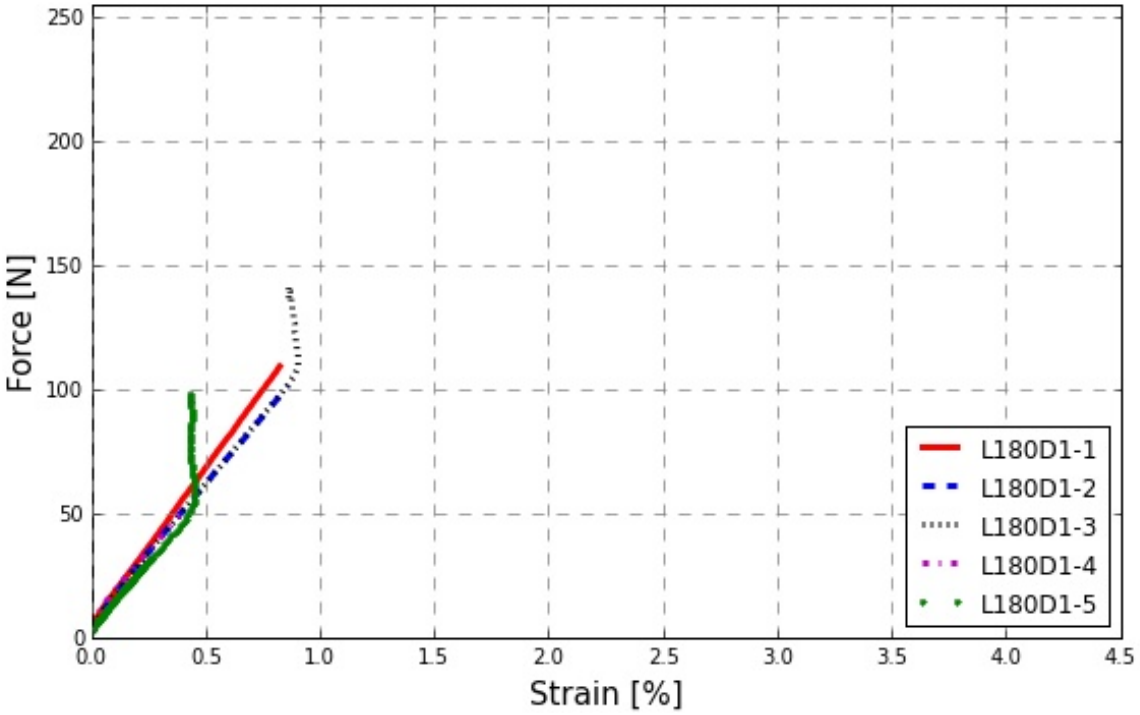

Figure D.37: Graphs of force versus strain measured for the samples 1-5 of L180-D-1.

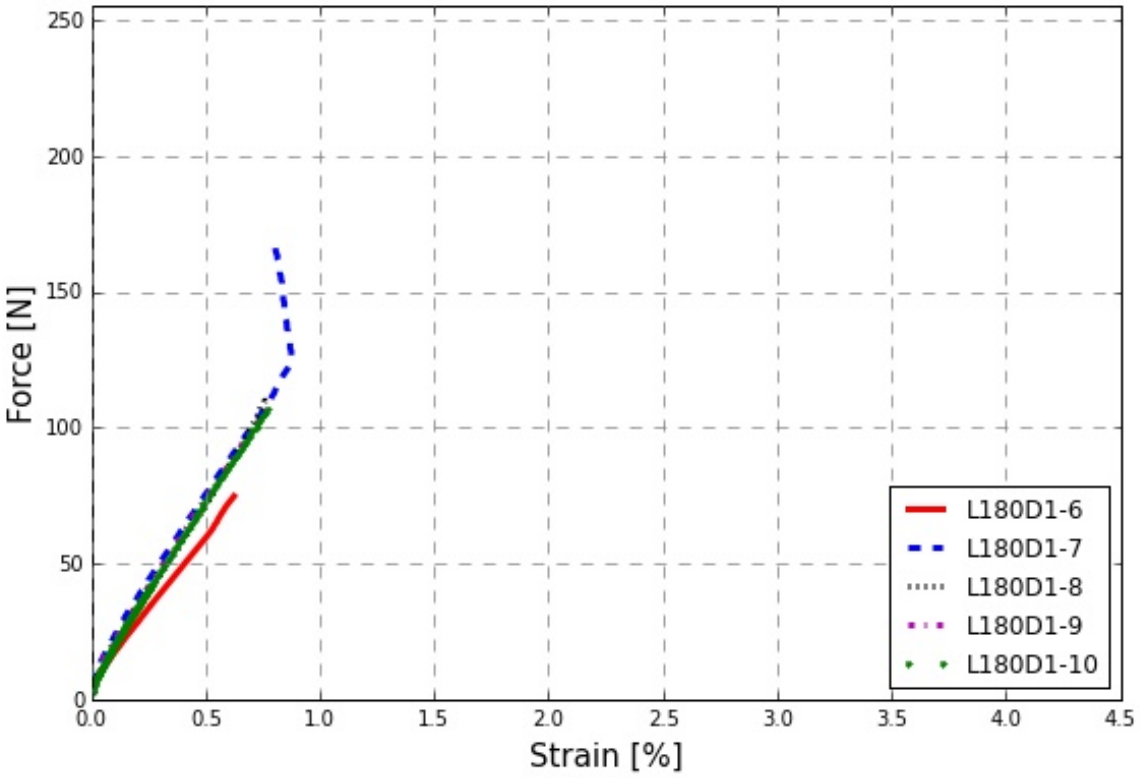

Figure D.38: Graphs of force versus strain measured for the samples 6-10 of L180-D-1.

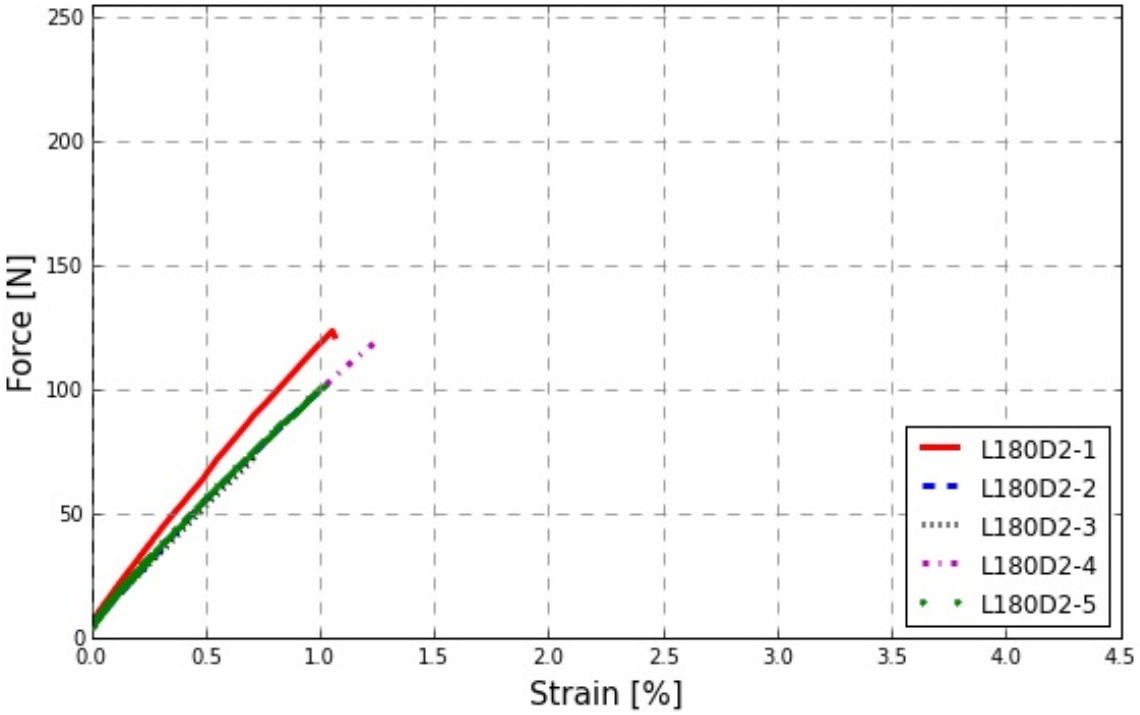

Figure D.39: Graphs of force versus strain measured for the samples 1-5 of L180-D-2.

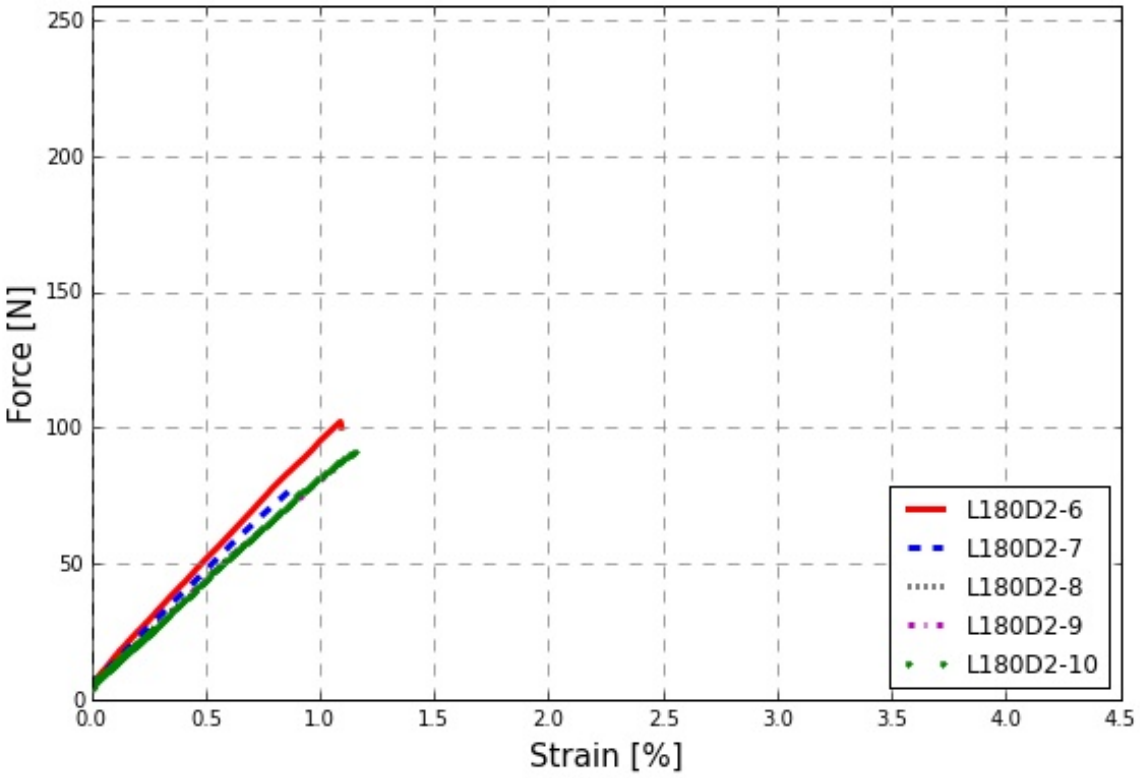

Figure D.40: Graphs of force versus strain measured for the samples 6-10 of L180-D-2.

Appendix E

Results of the DSC Analyses

All DSC data has been preprocessed. The original data was rotated to allow easier evaluation of the data. In order to do so a linear line was fit through the data at 50 °C and at 245 °C. This line was then subtracted from the data leading to a rotated graph. This transformation can be done as it does not influence onset temperatures or peak areas, the values of interest in this analysis.

Besides the original graphs this appendix shows the graphs of which the onset temperatures have been determined. These graphs show which points were taken to construct the onset and which value has been reported.

The graphs are shown in pairs based on the type of animal glue. Except for the first graph, which shows the DSC curves of the conditioned RMA1 curves.

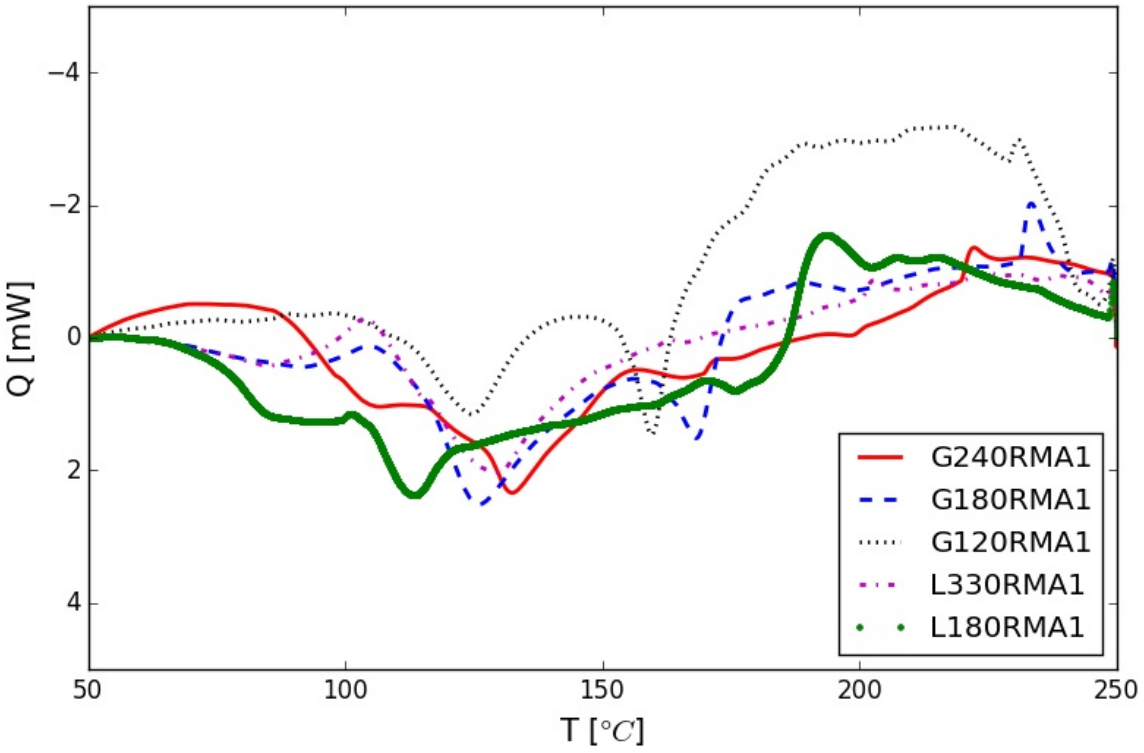

Figure E.1: DSC curves of the RMA1 sheets of the different types of animal glue after conditioning.

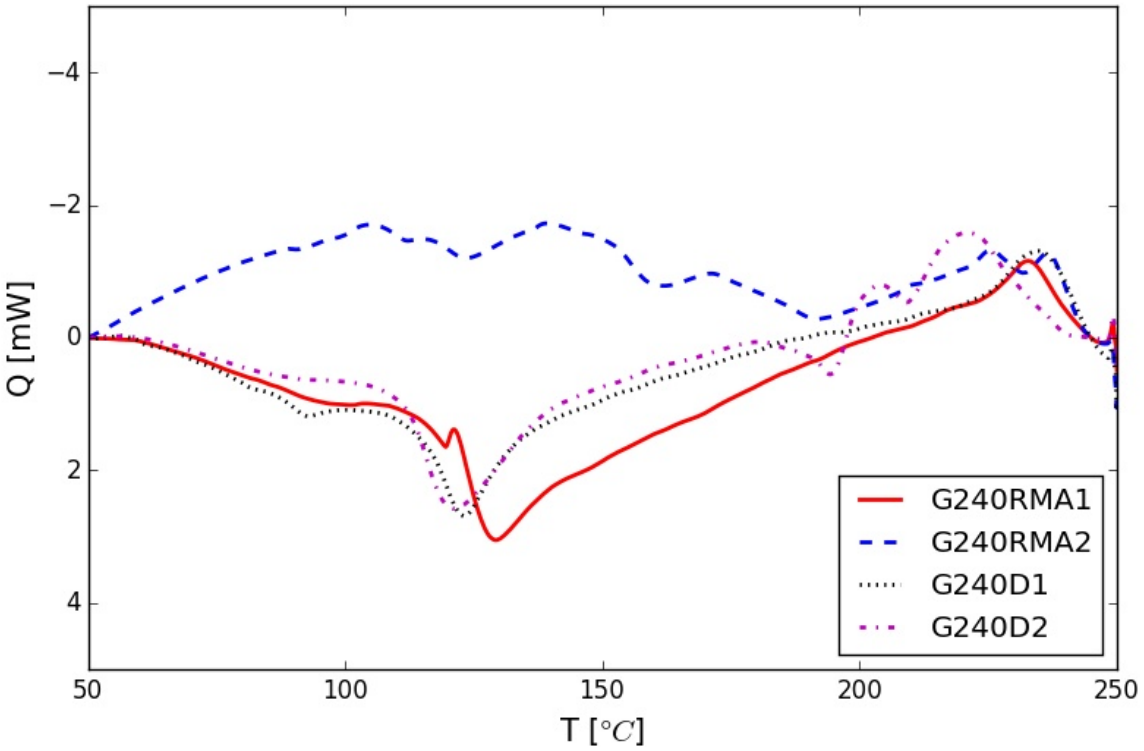

Figure E.2: Differential Scanning Calorimetry curves of the sheets of G240

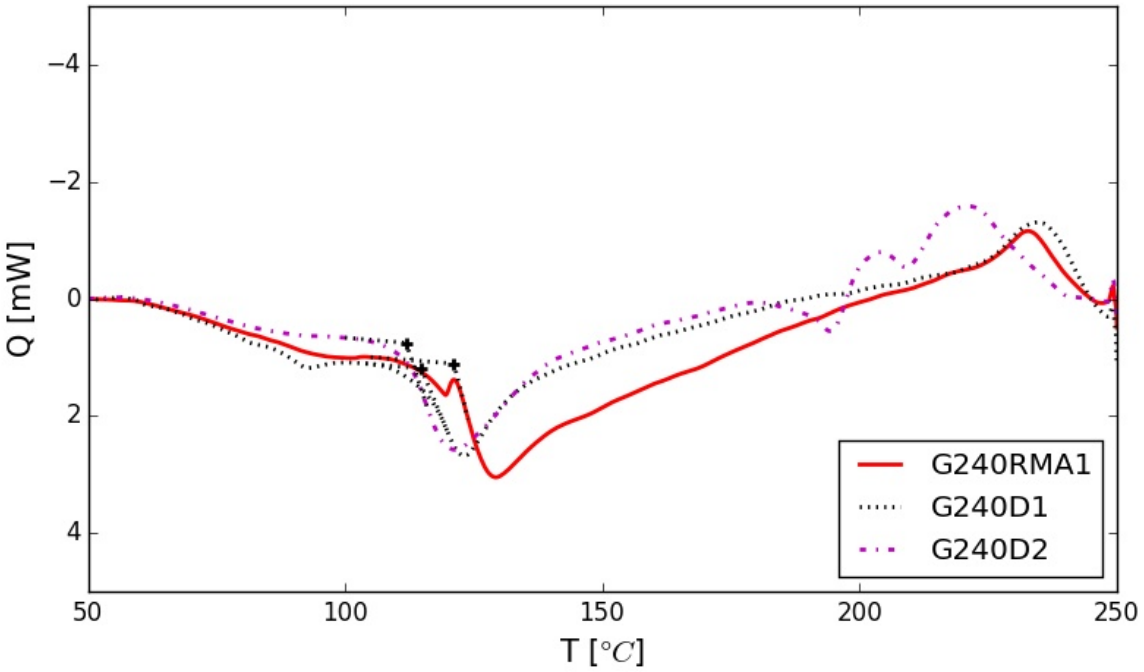

Figure E.3: DSC curves of the sheets of G240 with indication of the determined onset of the melting peak

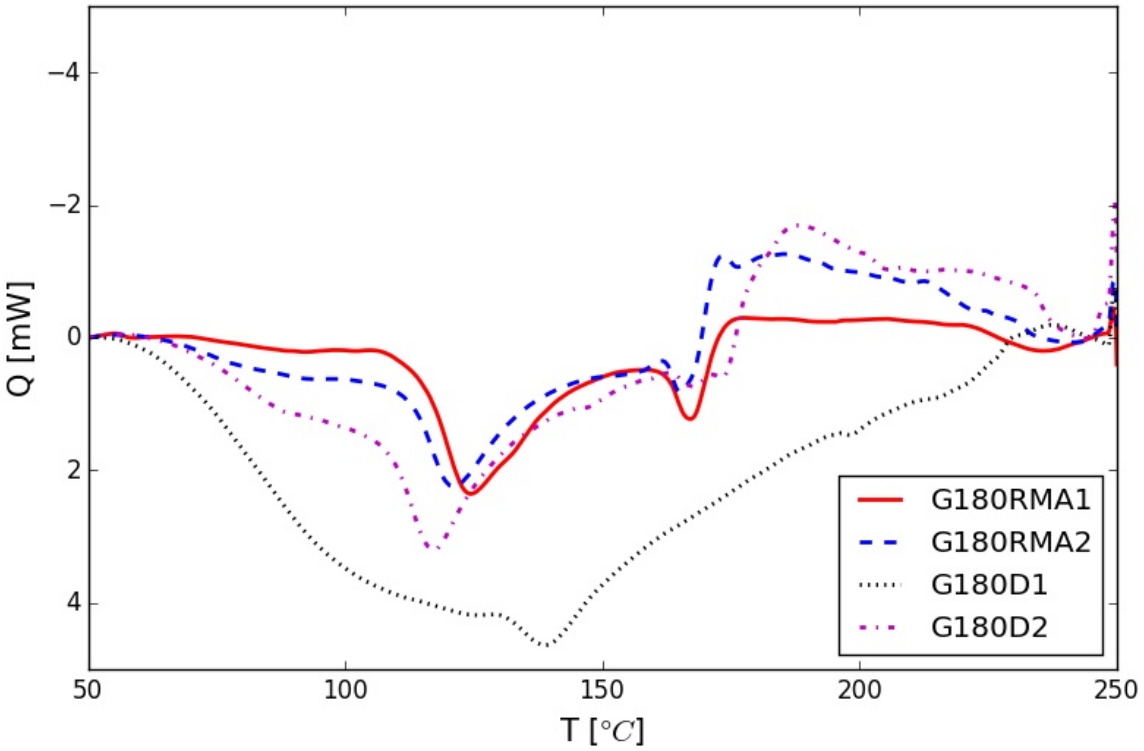

Figure E.4: DSC curves of the sheets of G180

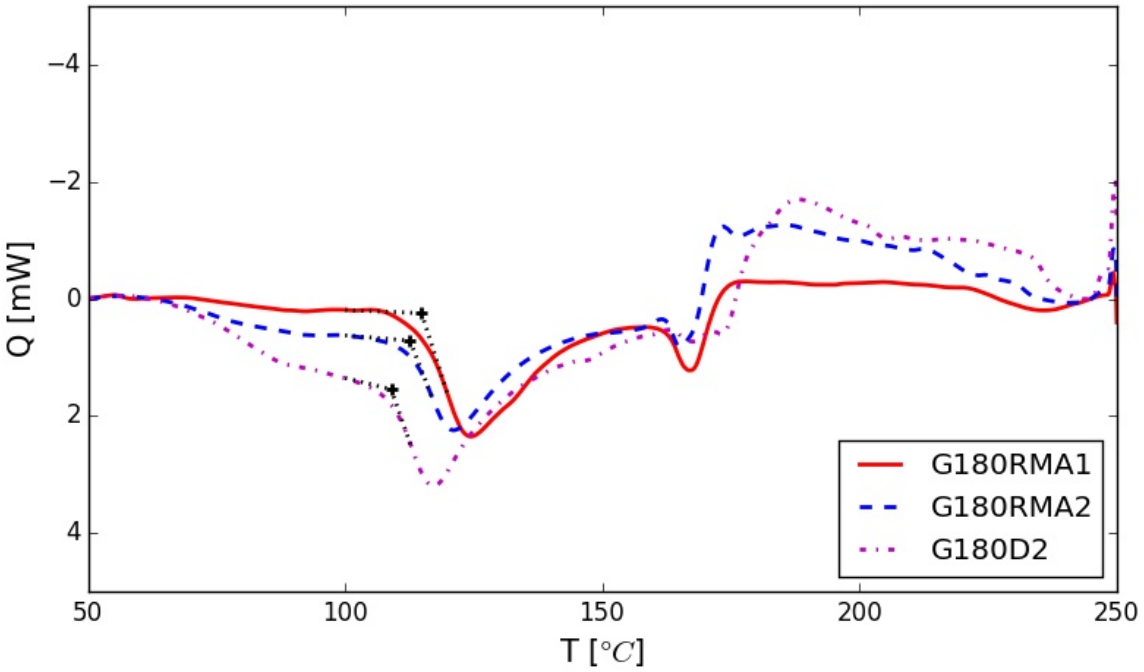

Figure E.5: DSC curves of the sheets of G180 with indication of the determined onset of the melting peak

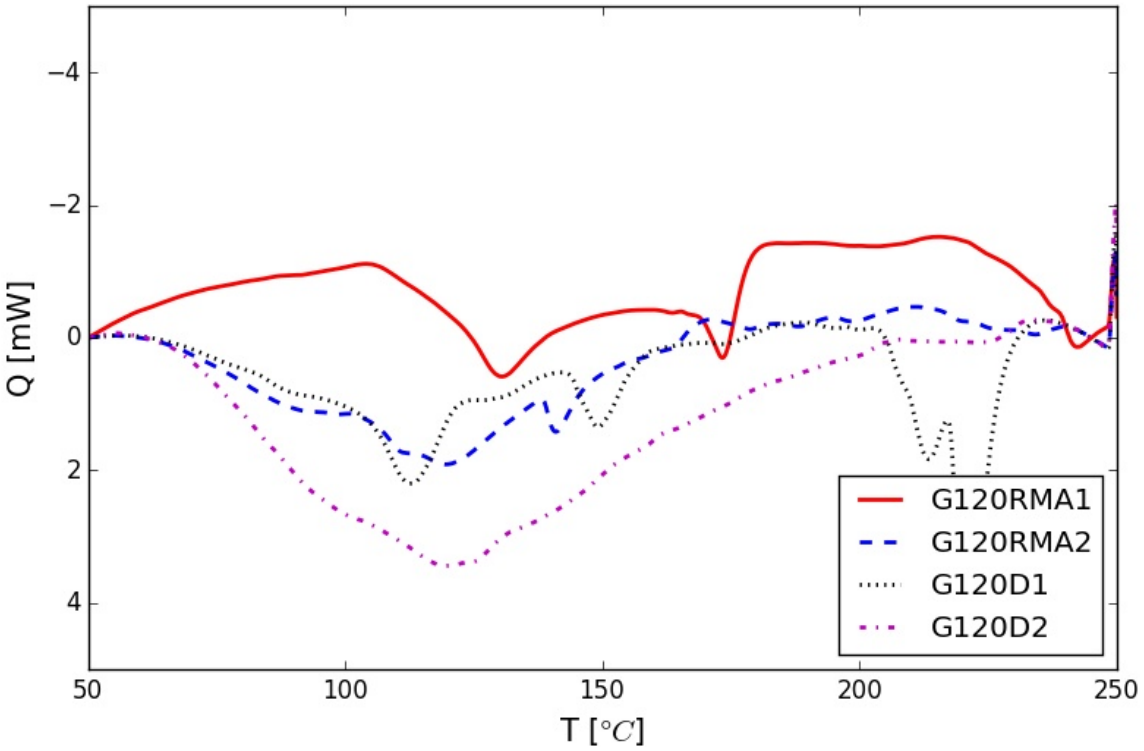

Figure E.6: DSC curves of the sheets of G120

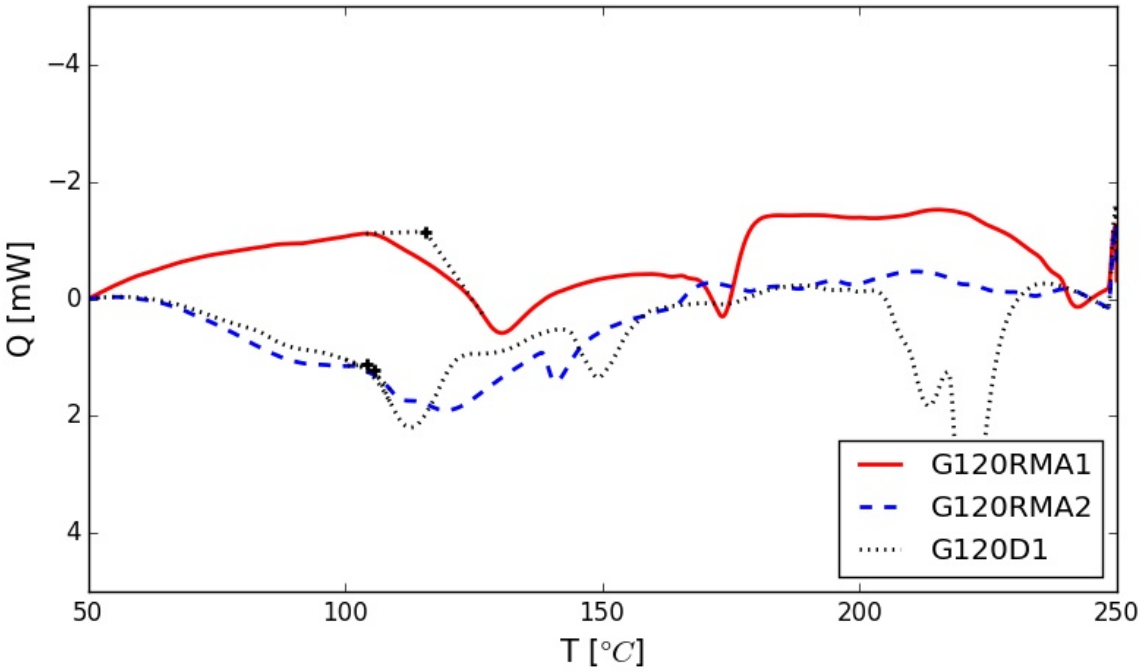

Figure E.7: DSC curves of the sheets of G120 with indication of the determined onset of the melting peak

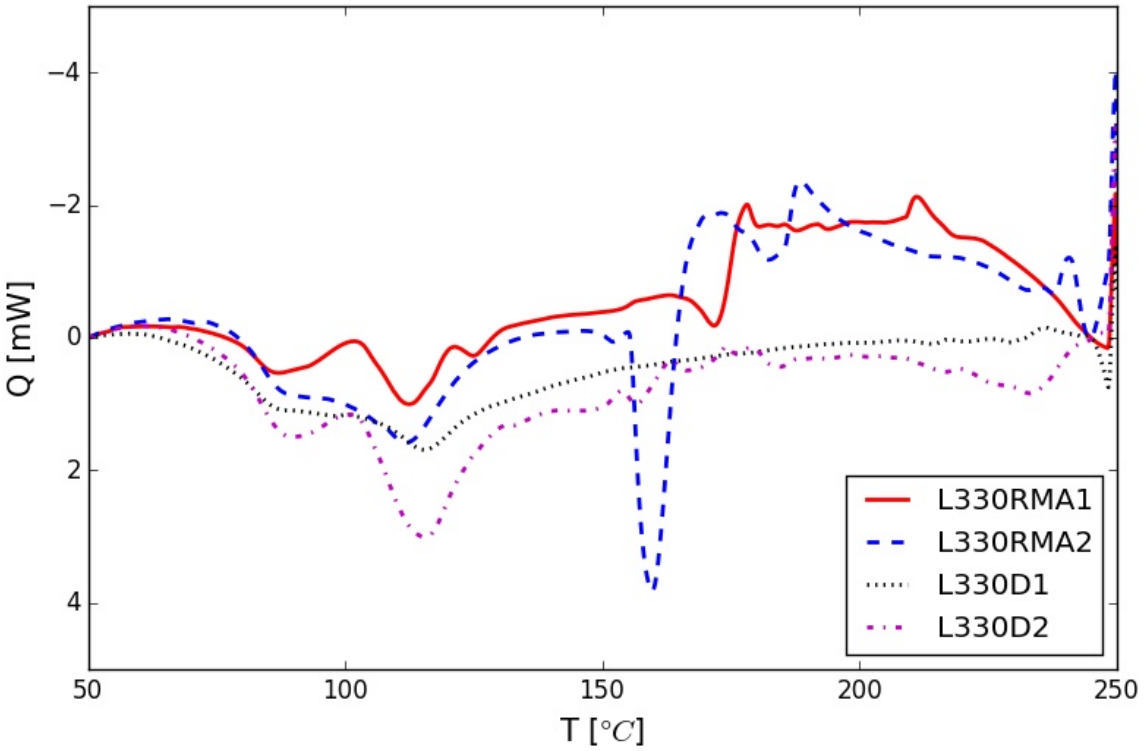

Figure E.8: DSC curves of the sheets of L330

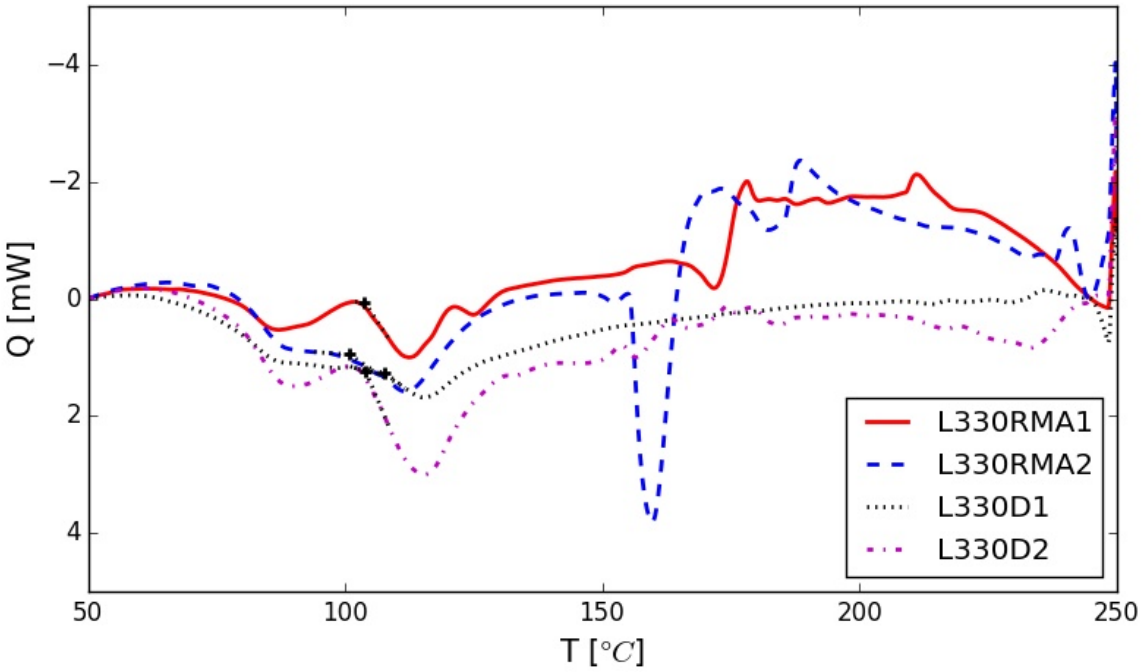

Figure E.9: DSC curves of the sheets of L330 with indication of the determined onset of the melting peak

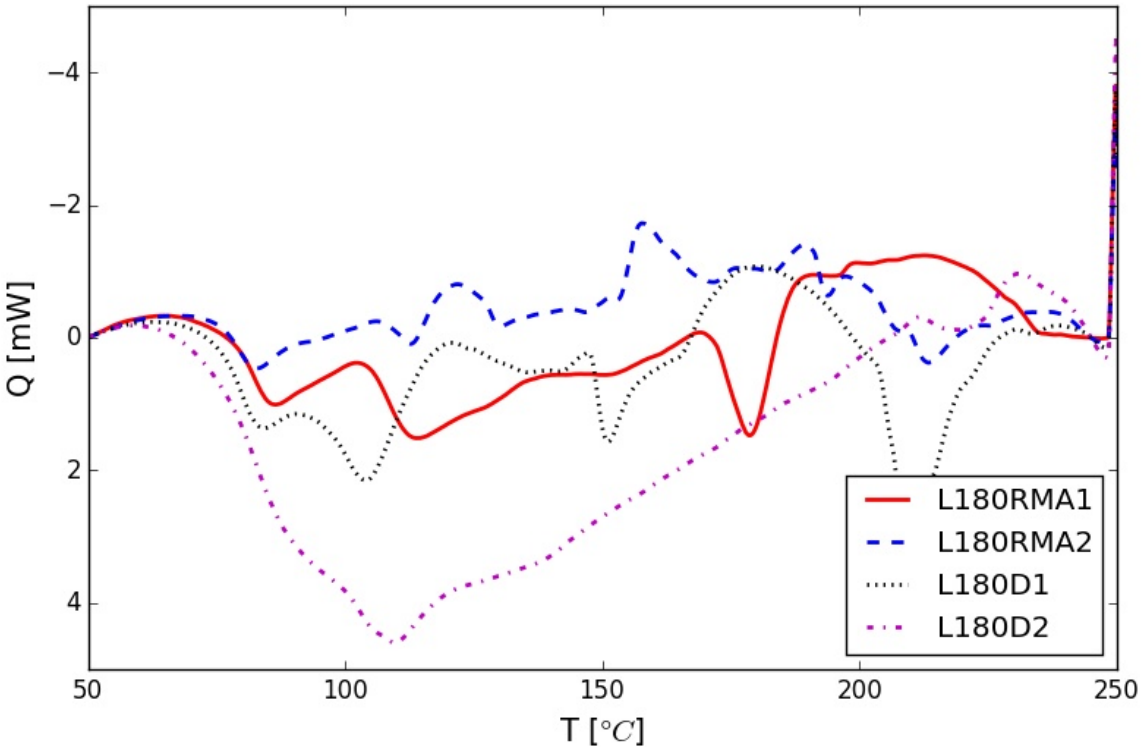

Figure E.10: DSC curves of the sheets of L180

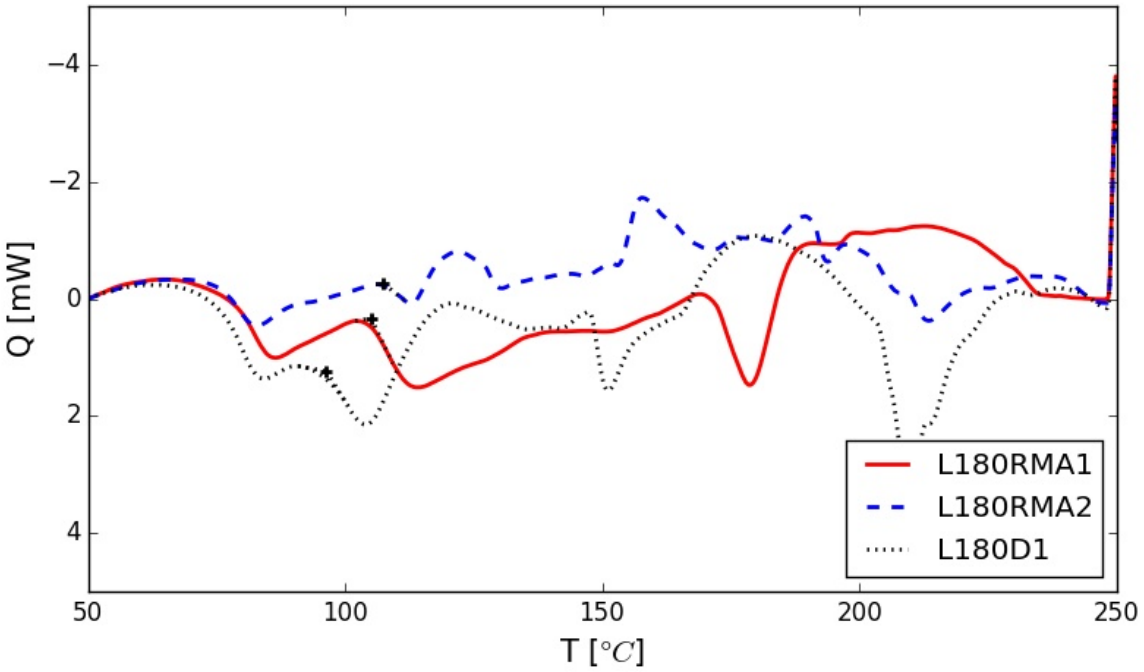

Figure E.11: DSC curves of the sheets of L180 with indication of the determined onset of the melting peak

Appendix F

Results of the XRD analyses

All data are presented as obtained from the XRD only smoothened using a rolling mean filter with a window of 5 data points. The effect of this is mostly a reduction of noise. The only exception is Figure F.1, of which only the raw data is presented.

Table F.1: Integrated intensities of the X-ray Diffraction diffractogram peak at 8 °2ϑ. The first column shows the results for the conditioned samples, both for the short and long domain.

Integrated Peak Intensity							
Conditioned		**Unconditioned**					
$G240RMA1_{cond}$	7060.85	G240RMA1	7610.57	G180D2	6632.62	L330D1	3086.86
$G180RMA1_{cond}$	6557.14	G240RMA2	7612.64	G120RMA1	4537.71	L330D2	1740.94
$G120RMA1_{cond}$	4348.98	G240D1	7334.9	G120RMA2	4489.42	L180RMA1	2301.28
$L330RMA1_{cond}$	2849.26	G240D2	7951.0	G120D1	2840.96	L180RMA2	2233.21
$L180RMA1_{cond}$	2254.09	G180RMA1	6835.54	G120D2	4281.84	L180D1	2447.4
$G240RMA1_{long}$	6987.96	G180RMA2	6888.86	L330RMA1	2967.85	L180D2	1379.34
$L180RMA1_{long}$	2221.50	G180D1	5543.88	L330RMA2	2242.22		

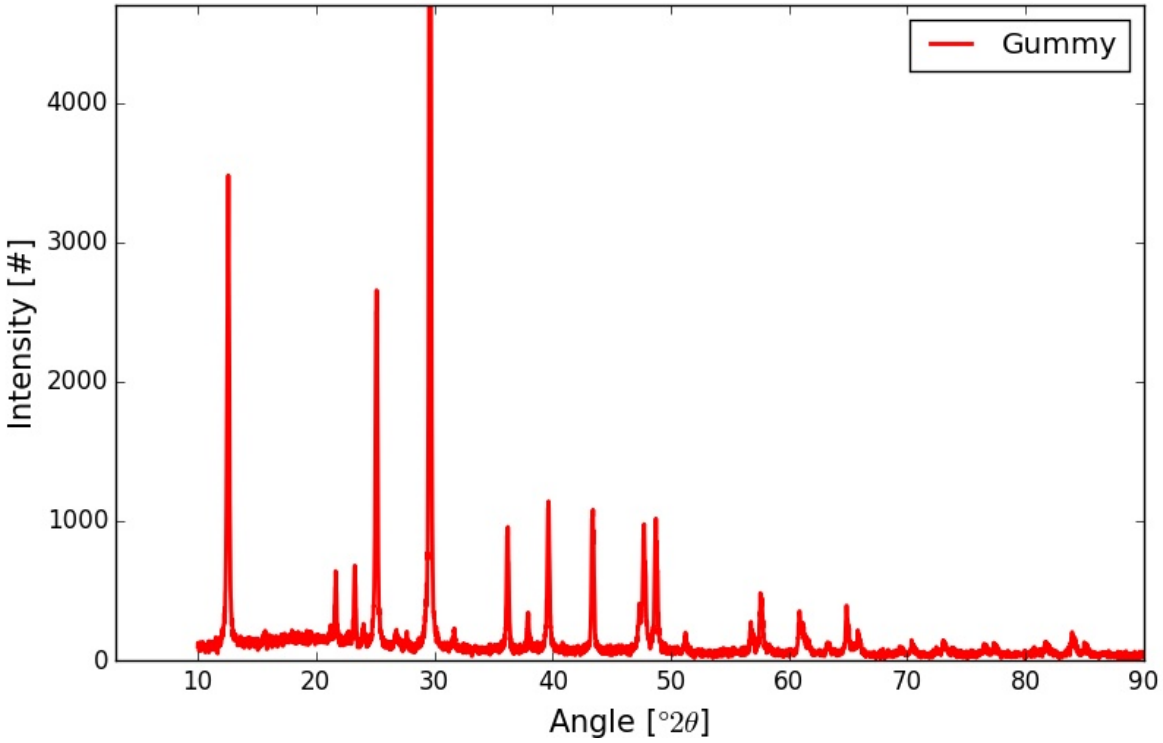

Figure F.1: Graph obtained by X-ray Diffraction analysis of the gummy used in sample placement. The peak at 29.62 °2ϑ has an intensity of 7630.

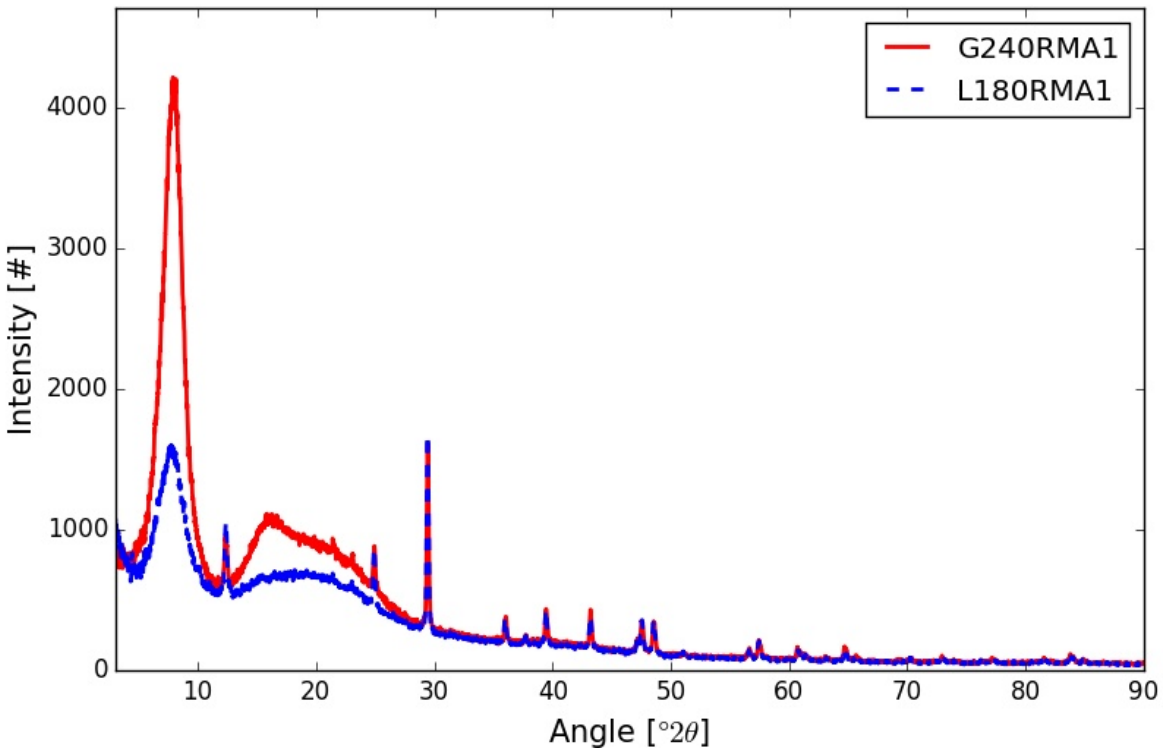

Figure F.2: Smoothened graph obtained by XRD analysis of the conditioned samples of G240RMA1 and L180RMA1.

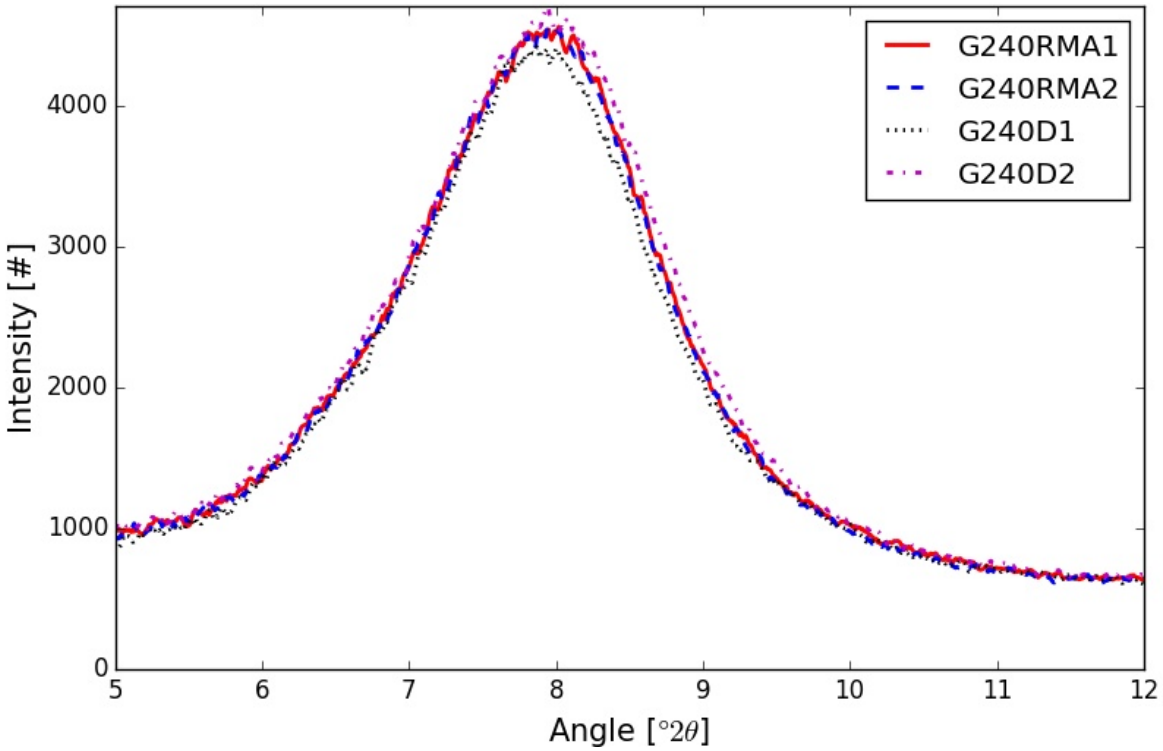

Figure F.3: Smoothened graph obtained by XRD analysis of the unconditioned films of G240.

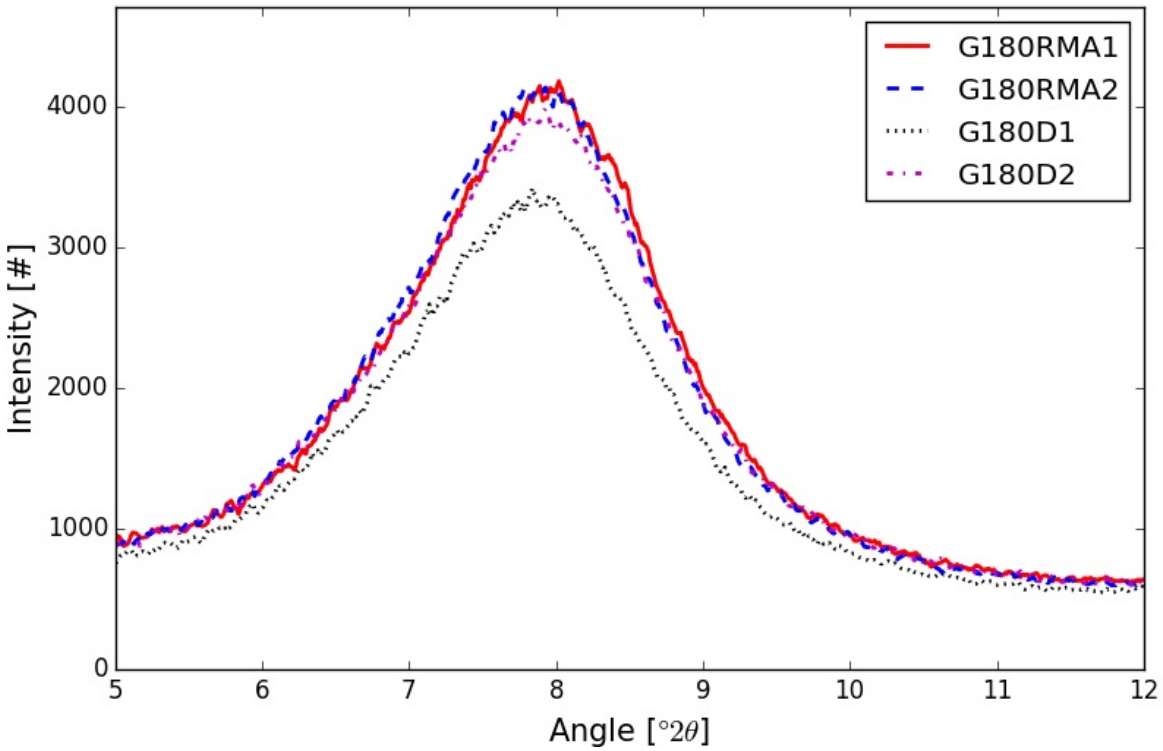

Figure F.4: Smoothened graph obtained by XRD analysis of the unconditioned films of G180.

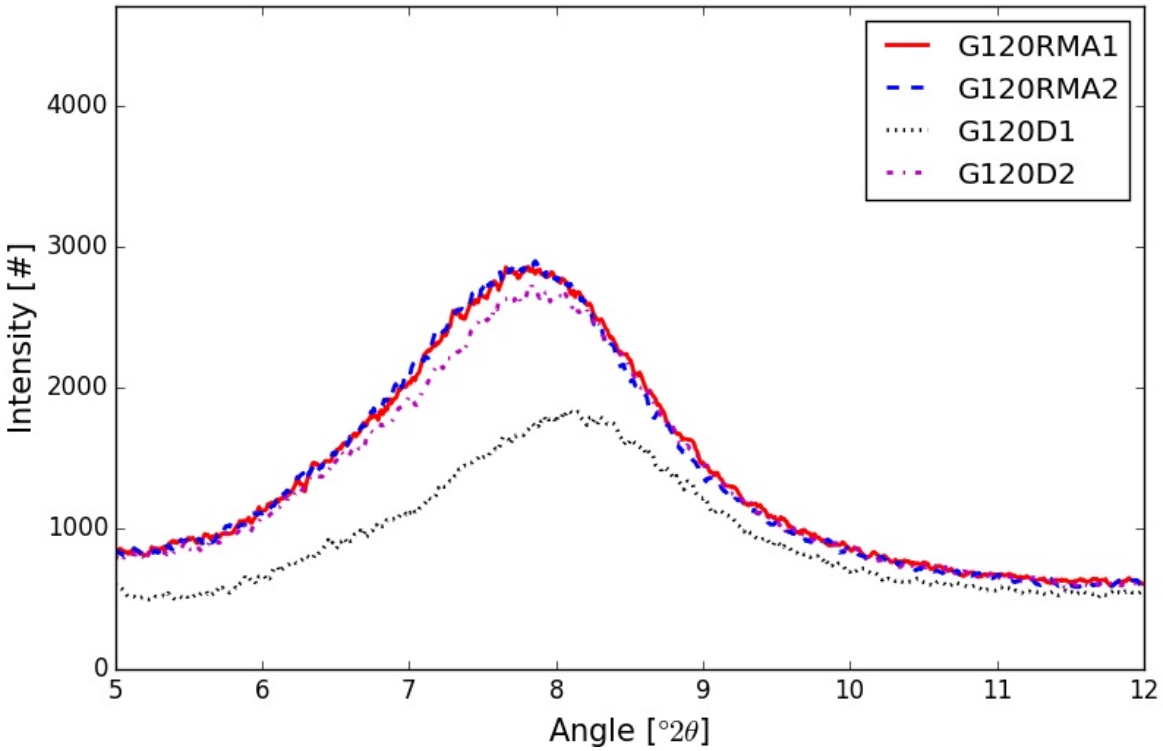

Figure F.5: Smoothened graph obtained by XRD analysis of the unconditioned films of G120.

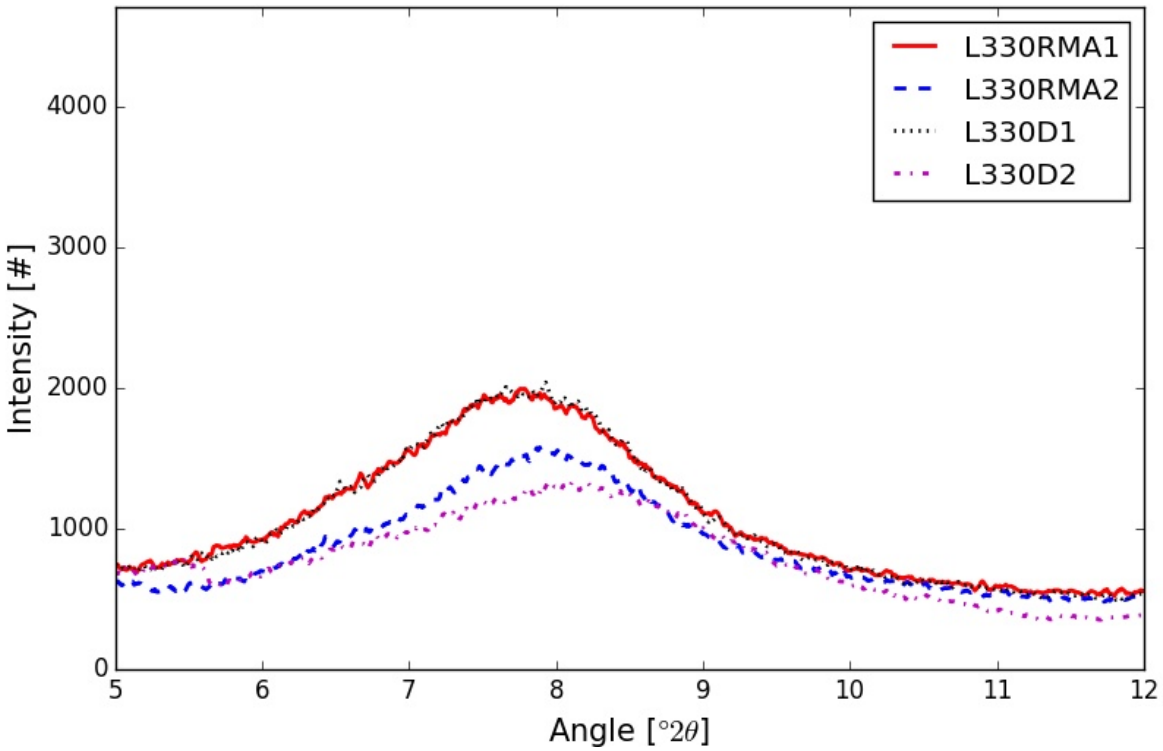

Figure F.6: Smoothened graph obtained by XRD analysis of the unconditioned films of L330.

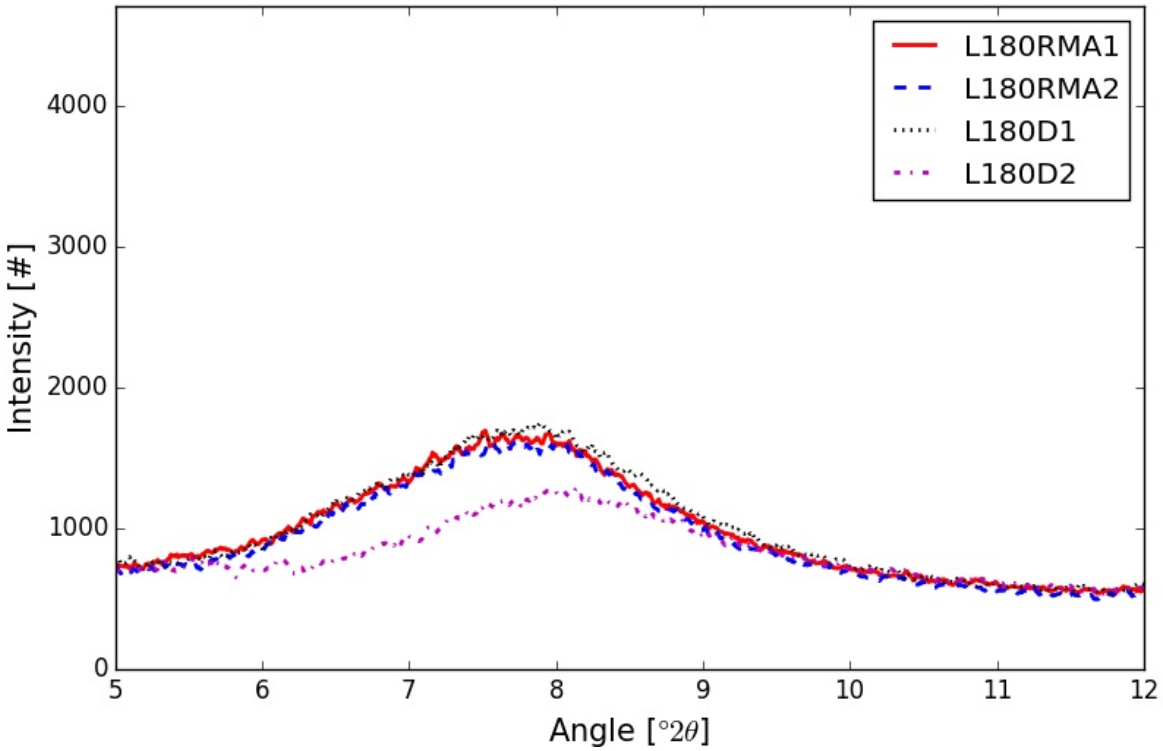

Figure F.7: Smoothened graph obtained by XRD analysis of the unconditioned films of L180.

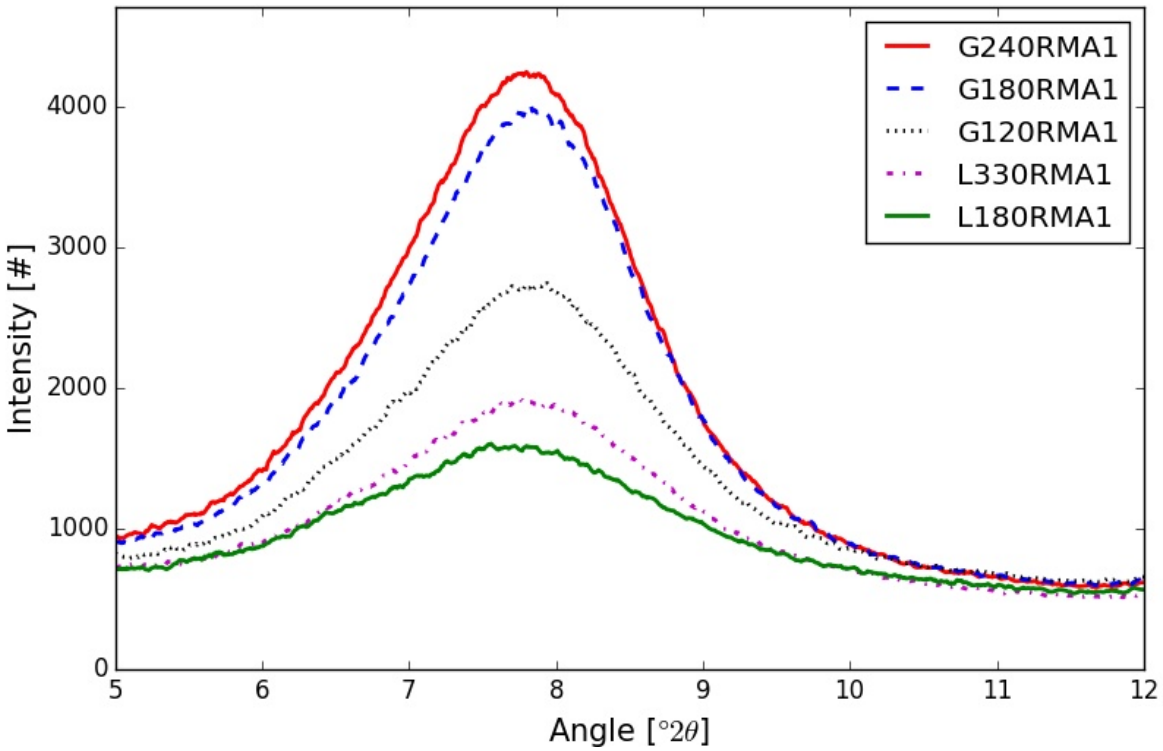

Figure F.8: Smoothened graph obtained by XRD analysis of the conditioned RMA1 sheets.

Appendix G

Results of the FTIR Analyses

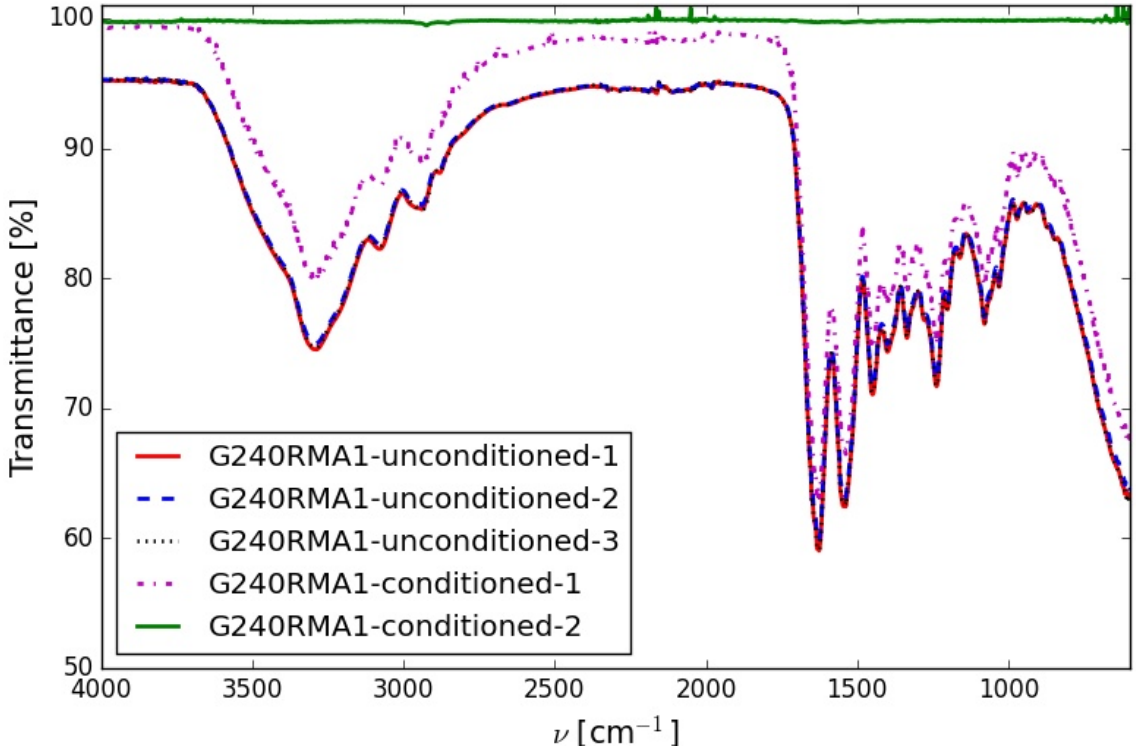

Figure G.1: Spectra obtained by FTIR analysis of G240RMA1

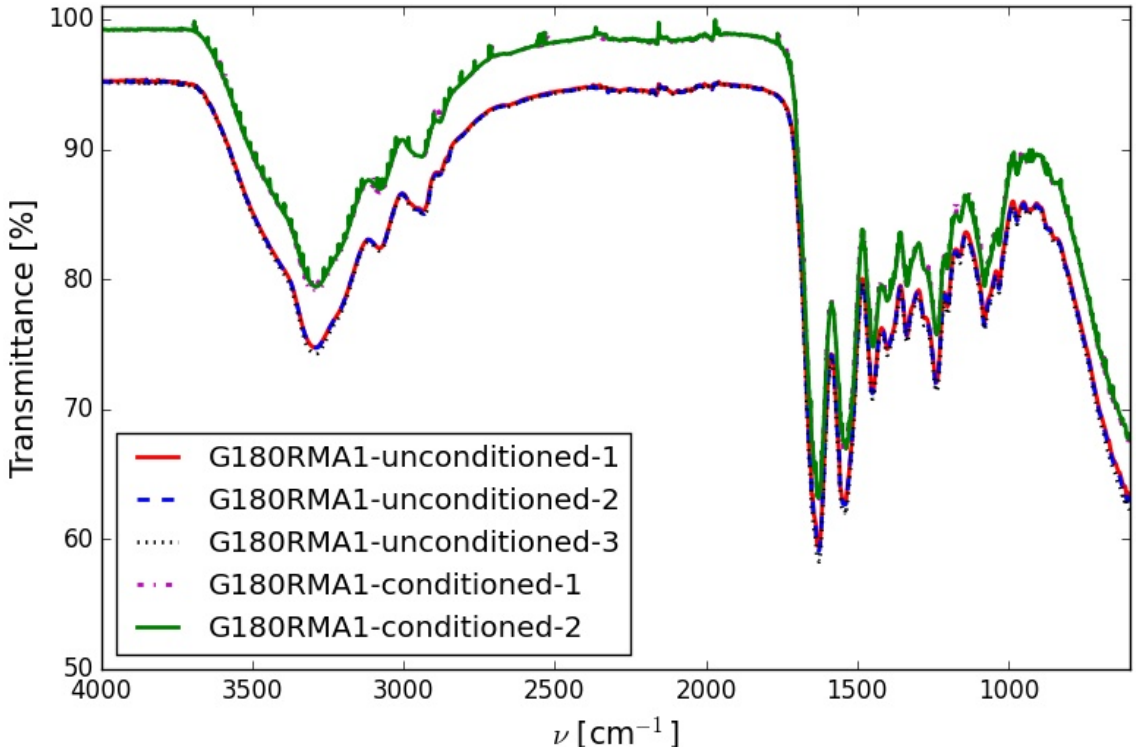

Figure G.2: Spectra obtained by FTIR analysis of G180RMA1

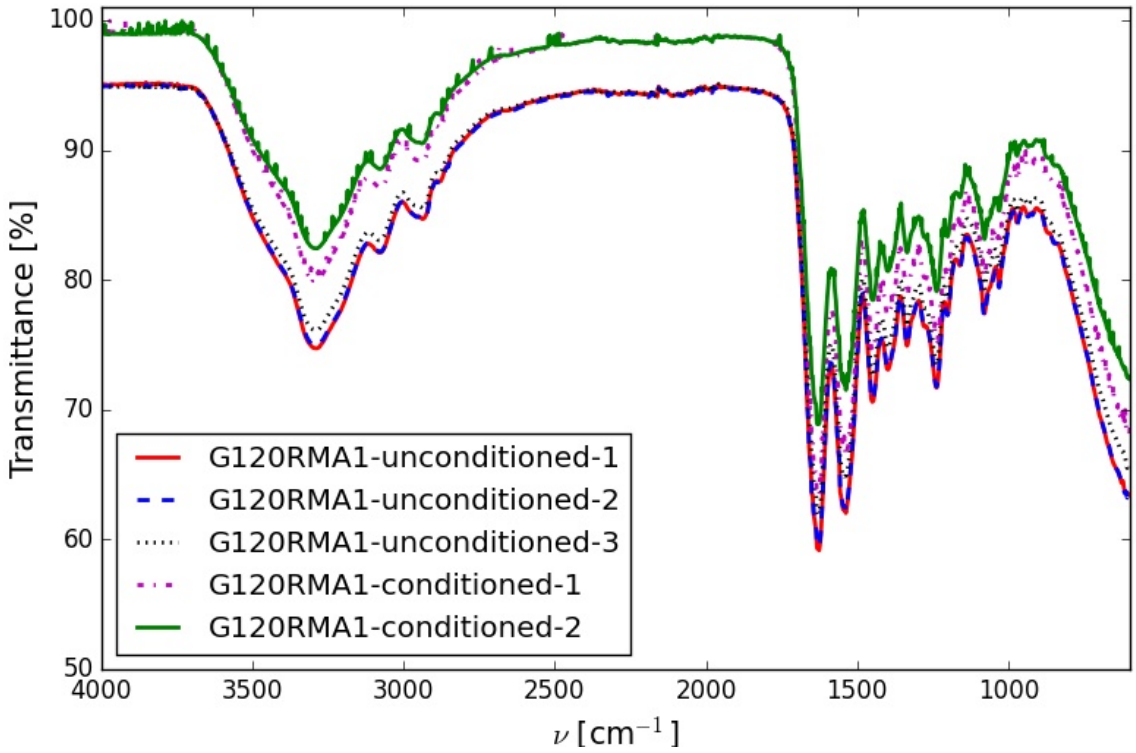

Figure G.3: Spectra obtained by FTIR analysis of G120RMA1

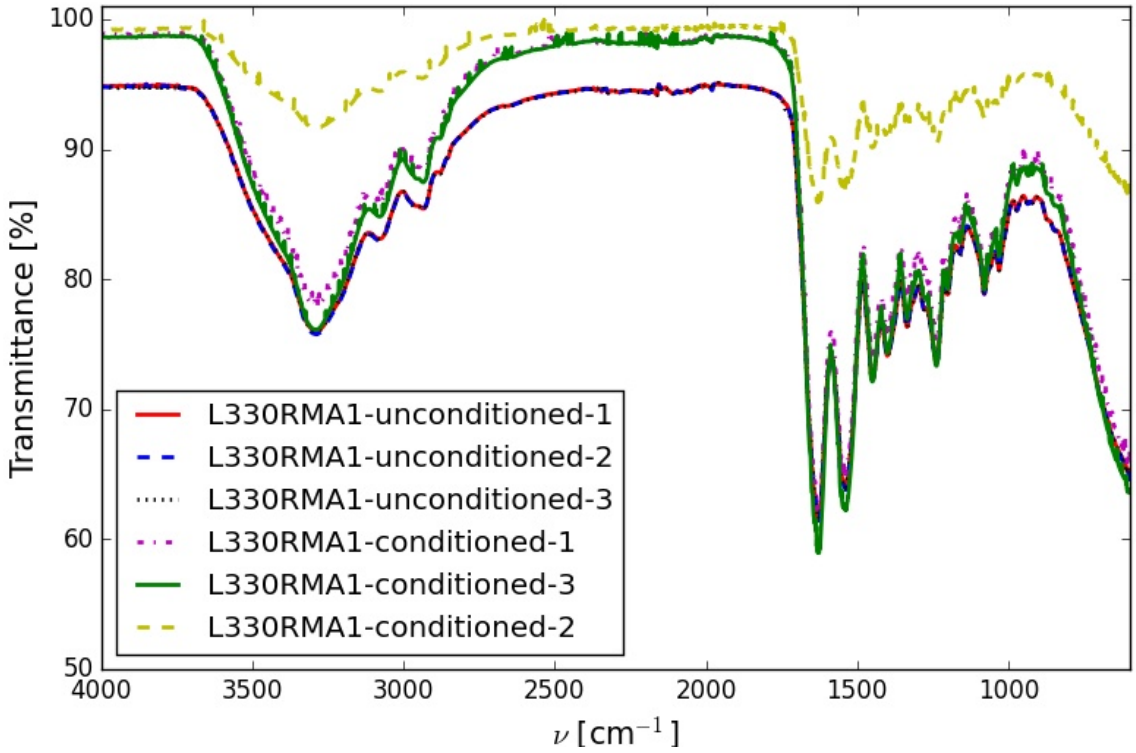

Figure G.4: Spectra obtained by FTIR analysis of L330RMA1

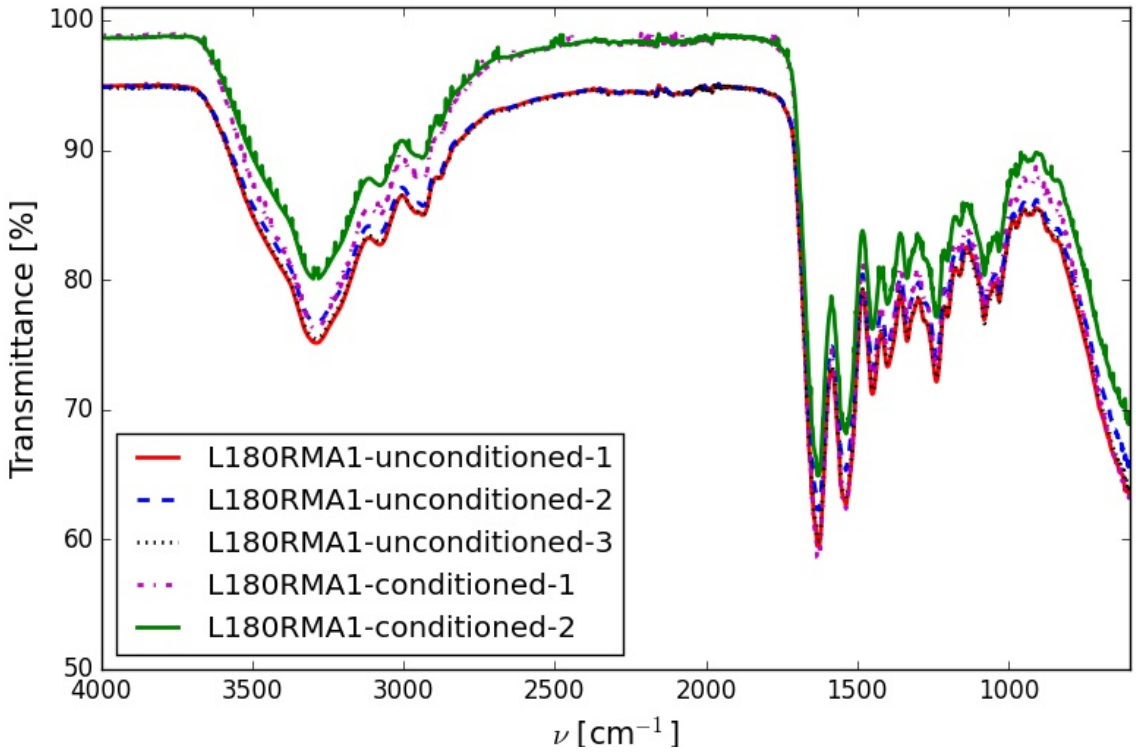

Figure G.5: Spectra obtained by FTIR analysis of L120RMA1